



<https://theses.gla.ac.uk/>

Theses Digitisation:

<https://www.gla.ac.uk/myglasgow/research/enlighten/theses/digitisation/>

This is a digitised version of the original print thesis.

Copyright and moral rights for this work are retained by the author

A copy can be downloaded for personal non-commercial research or study,
without prior permission or charge

This work cannot be reproduced or quoted extensively from without first
obtaining permission in writing from the author

The content must not be changed in any way or sold commercially in any
format or medium without the formal permission of the author

When referring to this work, full bibliographic details including the author,
title, awarding institution and date of the thesis must be given

Enlighten: Theses

<https://theses.gla.ac.uk/>
research-enlighten@glasgow.ac.uk

UNIVERSITY OF GLASGOW

**Prediction of Airborne Contamination in
Conventionally-Ventilated Cleanrooms**

MAHMOUD HEJAB (B.Sc., M.Sc.)

**Thesis submitted for the degree of Doctor of Philosophy in the
Building Services Research Unit of the Department of Mechanical
Engineering, University of Glasgow.**

© Mahmoud Hejab, 1992

January 1992

ProQuest Number: 10987099

All rights reserved

INFORMATION TO ALL USERS

The quality of this reproduction is dependent upon the quality of the copy submitted.

In the unlikely event that the author did not send a complete manuscript and there are missing pages, these will be noted. Also, if material had to be removed, a note will indicate the deletion.



ProQuest 10987099

Published by ProQuest LLC (2018). Copyright of the Dissertation is held by the Author.

All rights reserved.

This work is protected against unauthorized copying under Title 17, United States Code
Microform Edition © ProQuest LLC.

ProQuest LLC.
789 East Eisenhower Parkway
P.O. Box 1346
Ann Arbor, MI 48106 – 1346

ABSTRACT

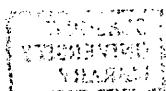
An important facet of designing cleanrooms is the prediction of the volume of air necessary to achieve the required airborne cleanliness in the room. Current experience shows that these predicted volumes are often too high and the air conditioning plant is consequently oversized. The design has traditionally been a matter of experience tempered with a little knowledge of fluid dynamics.

The main objective of this investigation was therefore to develop a mathematical model for assessing the volume of air required in conventionally-ventilated cleanrooms. The assumption of perfect mixing was used in the derivation of this model. However this assumption had to be verified and a substantial part of the research program was devoted to that problem.

The findings showed that the assumption of perfect mixing is reasonable for normal types of air terminal devices which entrain room air, but less reliable for air terminal devices in which the air is supplied unidirectionally as a jet. The effect of increasing the ventilation rate appeared to increase the amount of air mixing in the room until a critical value was reached. After this any increase in the ventilation rate reduced the amount of air mixing in the room.

To compute the airborne contaminant concentration in the room, data on the dispersal of airborne contaminants by male and female personnel, process equipment and typical outdoor airborne contaminant concentration was gathered. The results obtained for contaminant dispersion from people showed a great variability in the rate of dispersion.

The airborne contaminant concentration will be reduced due to deposition of the airborne particles on room surfaces. Therefore possible surface deposition mechanisms were investigated and a computational model was developed and verified experimentally so that the most important mechanisms could be included in the airborne contaminant concentration model. Agreement between theory and experiment was good considering the experimental difficulties.



The airborne contaminant concentration model derived initially was only valid for one discrete particle size. To comply with the current cleanroom standards, and so that the results can be compared with counts given by particle counters, the airborne particulate concentration at sizes greater than and equal to a particular particle size are required (usually $0.1\mu\text{m}$, $0.3\mu\text{m}$, $0.5\mu\text{m}$). By including particle size distributions it was possible to formulate a model for calculating the airborne contaminant concentration for the range of particle sizes normally encountered in cleanrooms. The model developed was then coded into a user-friendly software package to run on an IBM personal computer.

The validity of the model was examined by comparing the predicted airborne contaminant concentration with that found in industrial cleanrooms. Overall it was concluded that despite the dynamic and large fluctuations in the contaminant dispersion rates the expected airborne contaminant concentration can be computed with a good degree of precision.

A sensitivity analysis of the model to changes in input parameters showed that the release rate of contaminants and the volume of air supply are the key parameters, with ventilation effectiveness secondarily influencing the airborne contaminant concentration in the room. For perfect mixing the airborne contaminant concentration was found to be linearly proportional to the release rate but only approximately inversely proportional to the volumetric rate of air supply.

It has also been demonstrated that for a given supplied air volume and dispersion rate, the volume of the room has no bearing on the steady-state airborne contaminant concentration in the room. It is the volumetric flow rate of supplied air which controls and dilutes the airborne contamination within the room. This demonstrates the inaccuracy of various standards in specifying various grades of microbially controlled environments in terms of air change rates. It should be noted that the volume of the room will affect the rate of build-up as well as the decay rates of airborne contamination in the room.

The model derived also showed no reduction in airborne bacterial concentration from the installation of more efficient filters (99.997%) as recommended by some of the standards compared to less efficient filters (99.995% or 99.95%).

ACKNOWLEDGEMENTS

I should like to express my sincerest thanks to Mr Bill Whyte without whose supervision and guidance this thesis would not have been possible.

I also extend my thanks to Mrs Barbara MacLeod for typing the manuscript.

CONTENTS

<u>Chapter</u>	<u>Page</u>
List of Tables	i
List of Figures	iii
List of Plates	v
Nomenclature	vi
1. INTRODUCTION	1
1.1 Historical Background	1
1.2 Cleanroom Design	3
1.3 Environmental Standards	5
1.4 Review of the Theoretical Airborne Contaminant Concentration Models	7
1.5 Room Air Distribution Performance	14
1.5.1 Introduction	14
1.5.2 Air movement	15
1.5.3 Ventilation effectiveness	19
1.6 Dispersal of Contamination Within a Room	28
1.6.1 Introduction	28
1.6.2 Contaminant dispersion by people	28
1.6.3 Particulate generation from process machines	32
1.7 Review of the Surface-Deposition Studies	33
1.7.1 Introduction	33
1.7.2 Gravitational sedimentation	37
1.7.3 Inertial impaction	40
1.7.4 Brownian (molecular) diffusion	41
1.7.5 Turbulent (eddy) diffusion	44
1.7.6 Electrostatics	45
1.7.7 Thermophoresis	46
1.7.8 Deposition in a vessel	47
2. EXPERIMENTAL PROGRAMME	52
2.1 Cleanroom Air Distribution Performance	52
2.1.1 Introduction	52
2.1.2 Materials and methods	53
2.1.2.1 contaminant penetration into the air supply	58
2.1.2.2 air movement	59
2.1.2.3 ventilation effectiveness as assessed by decay rates	59
2.1.2.4 ventilation effectiveness as assessed by lateral air distribution	61
2.1.2.5 ventilation effectiveness as assessed by constant source dispersion	62
2.2 Dispersal of Airborne Particles and Bacteria by People	63
2.2.1 Introduction	63
2.2.2 Description of dispersal chamber	63
2.2.3 Experimental methods	65

<u>Chapter</u>	<u>Page</u>
2.3 Particle Emissions from Machines in Cleanrooms	67
2.3.1 Introduction	67
2.3.2 Materials and methods	67
2.3.2.1 Bausch & Stroebel vial-filling machine	67
2.3.2.2 Bosch-Strunck vial-filling machine	68
2.4 Outdoor Airborne Particulate and Bacterial Concentration	69
2.4.1 Introduction	69
2.4.2 Materials and methods	69
2.5 Surface-Deposition of Airborne Particles in a Chamber	70
2.5.1 Introduction	70
2.5.2 Description of chamber	70
2.5.3 Agitation of air and calculation of fan power transmitted to air in chamber	70
2.5.4 Particle production	73
2.5.5 Particle sizing	75
2.5.5.1 wet sizing	75
2.5.5.2 dry sizing	76
2.5.6 Sampling of airborne particles	77
2.5.7 Experimental method	77
2.6 Verification of the Airborne Concentration Model by Monitoring of Airborne Particles and Bacteria in Industrial Cleanrooms	79
2.6.1 Introduction	79
2.6.2 Materials and methods	79
3. COMPUTATIONAL MODELLING	82
3.1 Introduction	82
3.2 Derivation of the Models	83
3.2.1 Steady-state airborne contaminant concentration	83
3.2.2 Build-up of airborne contaminant concentration	86
3.2.3 Airborne contaminant losses due to surface- deposition	87
3.2.4 Decay of airborne contaminant concentration	100
3.2.5 Cumulative airborne contaminant size distribution	103
3.3 Development of Computer Software Package	106
4. RESULTS	115
4.1 Cleanroom Air Distribution Performance	115
4.1.1 Contaminant penetration into the air supply	115
4.1.2 Air movement	116
4.1.3 Ventilation effectiveness as assessed by decay rates	117
4.1.4 Ventilation effectiveness as assessed by lateral air distribution	118
4.1.5 Ventilation effectiveness as assessed by constant source dispersion	119
4.1.6 Multiple regression analysis of constant source dispersion results	121

<u>Chapter</u>	<u>Page</u>
4.2 Dispersal of Airborne Particles and Bacteria by People	124
4.3 Particle Emission from Machines in Cleanrooms	125
4.3.1 Baush & Stroebel vial-filling machine	125
4.3.2 Bosch-Strunck vial-filling machine	126
4.4 Outdoor Airborne Particulate and Bacterial Concentration	126
4.5 Surface-deposition of Airborne Particles in a Cleanrom	126
4.6 Verification of Airborne Concentration Model by Monitoring of Airborne Particles and Bacteria in Industrial Cleanrooms	129
 5. DISCUSSION AND CONCLUSION	 185
5.1 Cleanroom Air Distribution Performance	185
5.1.1 Contaminant penetration into the air supply	186
5.1.2 Air movement	187
5.1.3 Contaminant decay rates	189
5.1.4 Lateral air distribution	191
5.1.5 Constant contaminant dispersion	193
5.2 Contaminant Dispersion by People and Process Machines	196
5.3 Outdoor Airborne Contamination	198
5.4 Surface Deposition	199
5.5 Airborne Contaminant Concentration	204
5.5.1 Theoretical Model	204
5.5.2 Experimental validation of the model	207
References	209
Appendix A Decay Rates	220
Appendix B Experimental errors	242

LIST OF TABLES

<u>Table</u>		<u>Page</u>
1.1	Previous deposition studies in parallel flow.	34
1.2	Previous deposition studies in cross flow.	35
3.1	Log-normal distribution parameters for particles dispersed from people.	105
3.2	Log-normal distribution parameters for bacteria-carrying particles dispersed from people.	105
3.3	Log-normal distribution parameters for particles in outdoor air.	107
3.4	Log-normal distribution parameters for bacteria in outdoor air.	107
3.5	Log-normal distribution parameters for filter penetration.	108
4.1	Performance indicies as assessed by decay rates.	143
4.2	Performance indicies as assessed by lateral air distribution - Multislot diffusers.	145
4.3	Performance indicies as assessed by lateral air distribution - Adjustable vane grilles	146
4.4	Performance indicies as assessed by lateral air distribution - Dump air supply.	147
4.5	Performance indicies as assessed by lateral air distribution - Jet air supply.	148
4.6	Performance indicies as assessed by constant source dispersion - Multislot diffusers with smoke released at R_{p1} .	149
4.7	Performance indicies as assessed by constant source dispersion - Multislot diffusers with smoke released at R_{p2} .	150
4.8	Performance indicies as assessed by constant source dispersion - Adjustable vane grilles with smoke released at R_{p1} .	151
4.9	Performance indicies as assessed by constant source dispersion - Adjustable vane grilles with smoke released at R_{p2} .	152
4.10	Performance indicies as assessed by constant source dispersion - Dump air supply with smoke released at R_{p1} .	153
4.11	Performance indicies as assessed by constant source dispersion - Dump air supply with smoke released at R_{p2} .	154

<u>Table</u>	<u>Page</u>
4.12 Performance indicies as assessed by constant source dispersion - Jet air supply with smoke released at R_{p1} .	155
4.13 Performance indicies as assessed by constant source dispersion - Jet air supply with smoke released at R_{p2} .	156
4.14 Multiple regression analysis for various data and dependent variables.	157
4.15 Steady-state contaminant dispersion rates by females.	161
4.16 Steady-state contaminant dispersion rates by males.	163
4.17 Dispersal of airborne contaminants by people.	164
4.18 Comparison of male and female airborne dispersion rates.	165
4.19 Particle concentration when operator and Baush & Stroebel machine working.	169
4.20 Particle concentration when operator working in the room.	170
4.21 Average steady-state particles generated from Baush & Stroebel machine.	171
4.22 Average steady-state particles generated from Bosch-Strunk machine.	171
4.23 Mean outdoor airborne contaminant concentration.	172
4.24 Theoretical deposition velocities (cm/sec) for various aerodynamic particle diameters and equivalent ventilation rates.	178
4.25 Experimental deposition velocities (cm/sec) for various aerodynamic particle diameters and equivalent ventilation rates. Polarity air ioniser <u>in</u> use.	179
4.26 Experimental deposition velocities (cm/sec) for aerodynamic particle diameter of $0.8\mu\text{m}$ and various equivalent ventilation rates. Polarity air ioniser <u>not</u> in use.	180
4.27 Cleanroom conditions during environmental cleanliness tests.	181
4.28 Verification and classification of OCLI cleanroom.	182
4.29 Verification and classification of Organon cleanroom.	183
4.30 Model output for cleanrooms.	183
4.31 Sensitivity analysis of the airborne contaminant concentration model to input parameters.	184

LIST OF FIGURES

<u>Figure</u>		<u>Page</u>
1.1	Morrison's model of contaminant mass balance.	9
1.2	Kawamata's model of contaminant mass balance.	12
2.1	Plan of the diagnostic filling area at Organon Pharmaceutical Manufacturing Laboratory Ltd.	54
2.2	Sectional view (xx) of the diagnostic filling area at Organon.	55
2.3	Comparison of dump and jet air supply.	56
2.4	Diagram of dispersal chamber.	64
2.5	Diagram of spray for homogeneous particles.	74
3.1	Model of contaminant mass balance for a conventionally ventilated cleanroom.	85
3.2	Flow chart of the surface deposition model.	98
3.3	Flow chart of the airborne contamination model.	109
4.1	Isopleth diagram of the isothermal dump air supply with 20 AC/hr.	130
4.2	Isopleth diagram of the isothermal jet air supply with 4 AC/hr.	131
4.3	Isopleth diagram of the isothermal jet air supply with 15 AC/hr.	132
4.4	Isopleth diagram of the isothermal jet air supply with 22 AC/hr.	133
4.5	Isopleth diagram of the isothermal dump air supply with 4 AC/hr.	134
4.6	Air movement patterns in cleanroom along major and minor vertical sections of the room - Dump air supply with 20 AC/hr.	135
4.7	Air movement patterns in cleanroom along major and minor vertical sections of the room - Dump air supply with 3 AC/hr.	136
4.8	Air movement patterns in cleanroom along major and minor vertical sections of the room - Adjustable vane grilles with 15 AC/hr.	137
4.9	Air movement patterns in cleanroom along major and minor vertical sections of the room - Adjustable vane grilles with 3 AC/hr.	138

<u>Figure</u>		<u>Page</u>
4.10	Air movement patterns in cleanroom along major and minor vertical sections of the room - Multislot diffusers with 20 AC/hr.	139
4.11	Air movement patterns in cleanroom along major and minor vertical sections of the room - Multislot diffusers with 15 AC/hr.	140
4.12	Air movement patterns in cleanroom along major and minor vertical sections of the room - Jet air supply with 20 AC/hr.	141
4.13	Air movement patterns in cleanroom along major and minor vertical sections of the room - Jet air supply with 15 AC/hr.	142
4.14	Comparison of bacterial dispersion rates for indoor clothing.	166
4.15	Comparison of bacterial dispersion rates for cleanroom clothing.	166
4.16	Comparison of particle dispersion rates $\geq 0.5\mu\text{m}$ for indoor clothing.	167
4.17	Comparison of particle dispersion rates $\geq 0.5\mu\text{m}$ for cleanroom clothing.	167
4.18	Comparison of particle dispersion rates $\geq 5\mu\text{m}$ for indoor clothing.	168
4.19	Comparison of particle dispersion rates $\geq 5\mu\text{m}$ for cleanroom clothing.	168
4.20	Motor characteristics at various air pressure.	173
4.21	Fan power of motor in relation to air pressure.	174
4.22	Calibration of Rotameter size 10 with a stainless steel float.	175
4.23	Calibration of droplet size from atomizer.	176
4.24	Theoretical deposition velocity vs particle diameter.	177

LIST OF PLATES

<u>Plate</u>		<u>Page</u>
2.1	Experimental apparatus for studying particle deposition. Front elevation of the glove box.	71
2.2	Experimental apparatus for studying particle deposition. Side elevation of the glove box.	72

NOMENCLATURE

<p>A = Surface area</p> <p>A_e = Exposed surface area</p> <p>A_n = Avogadro's number</p> <p>A_t = Air terminal device</p> <p>A' = Constant</p> <p>a = Constant of integration</p> <p>B = Breadth</p> <p>B_m = Dynamic mobility</p> <p>C = Steady-state airborne contaminant concentration</p> <p>C_0 = Outdoor airborne contaminant concentration</p> <p>C_o = Output concentration</p> <p>C_A = Average airborne particulate concentration</p> <p>C_{Ai} = Sum of the individual averages of particle concentration</p> <p>C_i = Initial airborne contaminant concentration at time zero</p> <p>C_j = Sum of the individual sampled particle concentration</p> <p>$C^*(d_p)$ = Airborne contaminant concentration of size d_p and greater</p> <p>C_m = Measured steady-state airborne particulate concentration</p> <p>C_{max} = Maximum airborne contaminant concentration</p> <p>C_s = Airborne contaminant concentration of prefiltered air</p> <p>C_t = Transient-state airborne contaminant concentration</p> <p>$C(K_n)$ = Cunningham slip correction factor</p> <p>\bar{c} = Mean velocity of the gas molecules</p> <p>D = Brownian (molecular) diffusion coefficient</p> <p>D_1 = Debye function</p> <p>D_c = Diameter of round aerosol jet</p> <p>D_e = Turbulent eddy diffusivity</p> <p>D_{ep} = Effective particle diffusivity</p> <p>D_t = Diameter of the cylindrical stirred tank</p> <p>d_a = Aerodynamic particle diameter</p>	<p>UNITS</p> <p>A mixture of SI and imperial units are used in the cleanroom industry. Both types of unit are given in the text with original units from references followed by the equivalent in the other system.</p>
---	---

d_p	=	Particle diameter
d_p'	=	Droplet diameter
$\frac{dT}{dx}$	=	Temperature gradient
$\frac{du}{dx}$	=	Velocity gradient
e	=	Electron charge
F_d	=	Drag force
F_m	=	Filter efficiency of make-up air
F_p	=	Primary filter efficiency
F_r	=	Filter efficiency of recirculated air
F_s	=	Final(HEPA) filter efficiency
F_b	=	Filter efficiency of unidirectional flow cabinet
G	=	Rate of particle generation per unit volume of room
g	=	Acceleration due to gravity
H	=	Height
J	=	Particle flux
K	=	Boltzman's constant
K_e	=	Eddy diffusion coefficient
K_g	=	Gas thermal conductivity
K_n	=	Knudsen number
K_p	=	Particle thermal conductivity
k	=	Mixing factor
k'	=	Karman's constant
L	=	Length
LCL	=	95% Lower confidence limit
ϱ	=	Smallest dimension of the obstacle in the plane normal to the mean flow
ϱ_p	=	Circumference of the pulley
M	=	Mass of mixing air in the chamber
M_A	=	Mean of the averages of particle concentrations

M_g	=	Mass of gas molecules
m	=	Ratio of outdoor air volume to total supplied air volume
m_p	=	Mass of particle
N	=	Number of air changes per hour
$N(d_p)$	=	Number of particles of size d_p deposited
$N^*(d_p)$	=	Number of particles of size d_p and greater deposited
N_{eff}	=	Effective ventilation rate
N_g	=	Number of gas molecules per unit volume of gas
N_L	=	Number of sampling locations
N_S	=	Number of samples taken at each location
n	=	Number and sign of elementary charges used in Boltzman's charge distribution table
\dot{n}	=	Fall out rate (no. of particles $> 5\mu m$ per ft^2 per 24 hours)
P	=	Pressure
PI	=	Performance Index
P_0	=	Atmospheric pressure
P_c	=	Power consumption into the air in the chamber
P_{mr}	=	Mutual repulsion deposition efficiency in a cylinder
Q	=	Volumetric flow rate of air supplied into the room
Q_b	=	Volumetric flow rate of air supplied from the unidirectional flow cabinets
Q_e	=	Volumetric flow rate of air exiting from the room
Q_{e+l}	=	Volumetric flow rate through exhaust plus leakage
Q_0	=	Volumetric flow rate of outdoor air
Q_r	=	Volumetric flow rate of recirculated air
q	=	Charge carried by a particle
R	=	Gas constant
R_p	=	Release position of smoke
R_D	=	Rate of particle deposition per unit volume of room
R_d	=	Deposition velocity x surface area

R_e = Reynolds number
 R_s = Radius of spherical vessel
 R_t = Tube radius
 r = Ratio of recirculated air volume to total
supplied air volume
 r_p = Particle radius
 r_s = Spherical coordinate
 \hat{r} = Unit vector in the r direction

 S = Total contaminant dispersion rate
 S_A = Vessel surface area
 S_m = Particulate generation rate from machines and processes
 S_p = Contaminant dispersion rate from people
 S_w = Wilson's temperature used in Schlichting equation = 110.4K
 SD = Standard deviation
 SE = Standard error
 T = Absolute temperature
 TP = Torque power
 t = Time
 t_e = Exposure time
 t_{eff} = Effective residence time
 U = Average velocity of the air stream
 UCL = 95% upper confidence limit
 V = Room volume
 V_{ad} = Average deposition velocity
 V_{bd} = Diffusion velocity
 V_c = Velocity of a particle due to an image charge towards
a conducting surface
 V_d = Particle deposition velocity
 V_e = Magnitude of electrostatic drift velocity

$(V_d)_{\text{sides}}$	= Particle deposition velocity on the vertical sides
$(V_d)_{\text{base}}$	= Particle deposition velocity on the base
$(V_d)_{\text{top}}$	= Particle deposition velocity over the top
V_f	= Mean fluid velocity
V_g	= Mean velocity of gas
V_p	= Particle velocity
V_{p0}	= Initial or undisturbed velocity of air stream
V_s	= Terminal settling velocity
V_{slip}	= Slip velocity
V_t	= Thermophoretic velocity
W_d	= Dead weight of the pan
W_i	= Imposed weight on the pan
W_{KI}	= Weight percentage of the Potassium iodide
W_s	= Spring weight
X_s	= Distance of the particle from the surface
x	= Distance
$(\bar{x})^2$	= Mean square displacement of a particle
y	= Distance measured normal to a surface

Greek Letters

α	= Accommodation coefficient
β	= Surface loss rate coefficient
γ'	= Dimensionless number
δ	= Boundary layer thickness
δ_r	= Rebound correction factor
δd_p	= Intervals of width δd_p
ϵ_0	= Permittivity of free space
ϵ_c	= Elementary unit of charge

ϵ_d	=	Average turbulent energy dissipation rate
ϵ_r	=	Relative permittivity (or dielectric constant)
η	=	Efficiency of impaction
θ	=	Angle of inclination of a surface to the vertical
λ	=	Mean free path of the gas molecules
λ_d	=	Removal rate coefficient due to deposition
λ_t	=	Micro-scale of turbulence
λ_{tr}	=	Total removal coefficient
λ_v	=	Removal rate coefficient due to ventilation
μ	=	Geometric mean particle diameter
μ_g	=	Dynamic gas viscosity
μ_{gT}	=	Dynamic gas viscosity at absolute temperature T
ρ_{cp}	=	Density for the combined particle
ρ_{KI}	=	Density of the Potassium iodide
ρ_g	=	Gas density
ρ_p	=	Particle density
σ	=	Dimensionless coefficient
σ_g	=	Geometric standard deviation
τ	=	Aerodynamic relaxation time
τ_t	=	Theoretical residence time
τ'	=	Dimensionless residence time for slug flow in a circular tube
ν	=	Kinematic viscosity of fluid
ν	=	Root-mean-square fluctuating velocity of fluid in a direction normal to the wall
$\Phi(x)$	=	Probability density function
φ	=	Constant used in the Kinetic theory model
ψ	=	Stokes number
ω	=	Angular velocity of rotation

1. INTRODUCTION

1.1 Historical Background

Contamination control technology has developed in industry since the 1950's to provide a protected environment for research, development and manufacturing operations and has now achieved widespread application.

The type of cleanroom found in the early 1950's was basically a room constructed to prevent excessive air infiltration from adjacent contaminated areas and utilizing materials that could be readily cleaned and resisted abrasion and the shedding of contamination. Ventilation rates into these rooms were usually limited to less than twenty air changes per hour, the air being filtered and conditioned for personnel comfort but providing very slow removal of contamination from the room. In an attempt to compensate for this slow removal rate, strict personnel management procedures and manual cleaning were used to control contamination. However, applying the presently used cleanroom classification method (US Federal Standard 209D, 1988), Class 100,000 (the statistically allowable number of particles $\geq 0.5\mu\text{m}$ per ft^3 of sampled air is 100,000) was about the best level that could be achieved in these early cleanrooms. This was considered to be a very clean room which met most of the requirements of that time. Class 10,000 was achieved by reducing the level of operations and the number of personnel in the cleanroom for short periods of time but it could not be maintained on a continuous basis.

As miniaturization and sensitive solid-state devices evolved during the 1950's much cleaner rooms were needed. However, the design of early cleanrooms had two fundamental limitations which prevented significant improvements in airborne cleanliness. The major limitation was the use of conventional air-handling systems that could not handle the much needed increase of air volumes without causing severe air-turbulence problems. The other limitation was the cleanroom's inability to control air movement needed to create isolation zones for critical work, due to inherent air turbulence, mixing and entrainment of surrounding contaminated air caused by that design.

In 1960, the High Efficiency Particulate Air (HEPA) filter (efficiency $\geq 99.97\%$ against $0.3\mu\text{m}$ particles and larger) was commercially introduced. It had the ability to handle greater volumes of air than previous high efficiency filters and because of its relatively high pressure ^{drop} (176–196 Pa or 18–20 mm water gauge) it achieved an even distribution of air across its supply face; because of this a radically different design of unidirectional cleanroom ventilation was possible. This can be attributed to two independent lines of thought: Whitfield (1962) working at Sandia Corporation laboratories in USA and Professor Charnley (1964) in UK.

Sandia's responsibility was to study and apply contamination control methods to the USA atomic weapons programme and Professor Charnley was concerned with preventing surgical sepsis after total hip replacement operations. Whitfield was the first to recognize that if an entire wall or a ceiling of a room was fitted with HEPA filters and the wall or floor opposite was perforated to allow the air to exit undisturbed, the resulting straight-line air-movement flow through the room could virtually purge all the airborne contamination. Professor Charnley used diffuser bags instead of HEPA filters but achieved the same type of unidirectional flow. The increased filtered air volume of this design radically reduced the level of airborne contamination in the cleanroom and provided excellent isolation of one operation from another. Class 100 conditions were maintained with moderate personnel and cleanroom operations control. Some modern versions of this type of cleanroom are being operated at Class 10 and Class 1 levels. These levels are possible with improved close-woven non-linting cleanroom clothing fabrics, high efficiency particulate air filters and closely controlled cleanroom layout and operations.

By the early 1970's, the principle of the "unidirectional flow" system had been carried from the laboratory and was freely available in various manufacturing industries. Cleanroom technology has now developed into the much broader discipline of contamination control. Today its applications cover a wide spectrum in the different industries and specialities such as:

Pharmaceutical	Operating theatres
Chemical	Precision mechanics
Biotechnological	Instrumentation optics
Blood products	Vacuum and thin layer technology
Dairy products	Audio compact disc
Semiconductor	Aerospace
Photographic films	Automotive

1.2 Cleanroom Design

Cleanrooms are divided into two major types, these being based on the type of air distribution designed for the facility.

The first type of cleanroom, which was also the first to be used, was designed with turbulent-flow air conditions existing within the room. This is commonly referred to as a conventional cleanroom; it is still used and will continue to be used in the future. The air cleanliness in a conventionally-ventilated cleanroom is affected by the method of introduction of clean air as this transports airborne contaminants, set free by the process and the personnel, to the outlet. As airborne cleanliness is achieved by the mixing of clean supplied air with the circulating contaminated room air, one can call this a dilution system. Air flow of this type has the advantage that the room is ventilated with a relatively small air volume which gives it a good velocity, temperature and humidity distribution. On the other hand, this type of air distribution scatters airborne contamination over the entire room and contamination can make several passes over a work station before leaving the environment. Because of personnel comfort, one usually limits the ventilation rate to about 40 air changes per hour. The air cleanliness of such a room is limited to Class 10,000 to 100,000 (Federal Standard 209D). Upgrading these rooms can be achieved by adding unidirectional flow cabinets or portable unidirectional flow modules that provide Class 100 conditions or better where required.

The second type of cleanroom utilizes unidirectional air (in one direction)

from the area where the filtered air enters the room to a point past the work area. The clean supplied air displaces contaminated room air to the exhaust without mixing (or with very limited mixing). This has the advantage of minimizing the formation of eddy currents and preventing stagnant areas that can entrap contamination. Unidirectional flow cleanrooms have two major divisions - vertical and horizontal flow.

Vertical unidirectional cleanrooms consist of high efficiency filters covering as close to 100% of the ceiling above the critical area as possible. The air supply velocity is about 0.30 ± 0.05 m/s. Such an air speed is sufficient to overcome convection currents, produced by a heat source in the flow as well as the turbulence produced by an obstruction in the flow. In this type of cleanroom, air is normally delivered to the filters through ducts or through a plenum above the filter grid by fans that draw return air from a cavity beneath the floor. The under-floor space is used to run exhaust ducts and has the advantage of being used to distribute power, water and gas to any point in the cleanroom, thus keeping dust-collecting equipment safely out of the cleanroom space. One of the advantages of a vertical unidirectional-flow system is the freedom permitted in laying-out production lines. The product should be as safe, during transfer, as it is on the work surface itself.

In the horizontal unidirectional flow room, the high efficiency filter banks cover an entire wall and the opposite wall becomes the air return. Although the horizontal unidirectional flow starts with ultra-clean air in front of the filter bank, it picks up contamination as it passes close to contaminant-producing activities. To achieve the same level of airborne contamination as vertical unidirectional flow system, air velocities are somewhat higher for horizontal flow (0.45 ± 0.1 m/s), than for vertical unidirectional flow (0.30 ± 0.05 m/s). Because of the reduced number of filters in comparison with the amount of floor area and the exclusion of the raised floor, horizontal flow systems are much less costly than vertical flow systems.

1.3 Environmental Standards

The dominant method of measuring the effectiveness of a cleanroom is to measure the concentration of particles in the air. These measurements have usually been made with light-scattering optical or nuclei-condensation particle counters. Normally, a measurement is made of the total concentration of particles larger than some specific size; often the size is that of the lower detection limit of the instrument. Based on the particle concentrations measured in the air, a cleanroom is designated as falling into one of several air cleanliness classifications. The US Federal Standard 209D (1988) and BS 5295 (1989) specify six and ten classes of environmental cleanliness, respectively, according to various levels of particulate content in the room. The class number of both standards is taken from the upper limits of the concentration of particles in a given volume of air (1ft^3 in Federal Standard 209D and 1m^3 in BS 5295) of a size equal to or greater than $0.5\ \mu\text{m}$. The standards allow measurements of the particle concentration at certain other sizes. The concentrations of particles allowed for each class, at each particle size, are not meant to imply a particle size distribution in any specific environment.

These standards give little advice on how the required airborne cleanliness should be achieved. A most important aspect of designing a cleanroom is the ability to predict the probable airborne contaminant concentration, and this requirement is lacking in these standards. Cleanroom design is not, at present, based on scientific principles, but solely dependent on the designer's experience in air volumes, air movement and filter efficiency to arrive at the required level of cleanliness. Cleanrooms are frequently badly overdesigned and unnecessarily costly. Furthermore, these standards do not give any suggestion of the bacteriological requirements in cleanrooms and therefore they are mainly aimed at engineering (e.g. micro-electronics, aerospace, optical) rather than medical and pharmaceutical fields. A number of standards for microbiological control in cleanrooms do exist. Three of these are extensively used. These are:

1. Standards for Clean Rooms and Work Stations for the Microbially Controlled

Environment (National Aeronautics and Space Administration, NASA, 1967).

2. Guide to Good Pharmaceutical Manufacturing Practice (HMSO, 1983).
3. The Rules Governing Medicinal Products in the European Community (EEC, 1989).

The above documents suggest airborne microbial levels for various air cleanliness grades. They recommend steps which should be taken, as necessary and appropriate, by those interested in controlling microbial contamination (e.g. manufacturers of medicinal products), with the object of ensuring that their products are of the quality intended.

The NASA (1967) standard is now considered as obsolete. The maximum permitted number of viable organisms, given in both HMSO (1983) and EEC (1989) standards for any designated class, is based on the condition when the room is unmanned although the microbiological level of a cleanroom would be mainly required under operational conditions.

Although requirements for various grades of environmental cleanliness are laid down, these standards do not give any information as to how to obtain the intended level of airborne microbial cleanliness. In fact, the Guide to Good Pharmaceutical Manufacturing Practice (HMSO, 1983) is inaccurate in specifying various grades of microbially controlled environments in terms of air change rates. Airborne contaminant concentration is dependent on the total volumetric flow rate of supplied air into the room and not on the rate of air change; any specification should therefore be in this form. Furthermore, the Guide to Good Pharmaceutical Manufacturing Practice (HMSO, 1983) places undue emphasis upon the final filter efficiency. The document recommends that two different grades of airborne microbial cleanliness (1/B and 2) can be achieved by employing corresponding final filter efficiencies (99.995% and 99.95% as determined by BS3928, 1969) with a minimum ventilation rate of 20 air changes per hour. However, micro-organisms are normally associated with particles averaging 12-14 μm (Noble *et al.*, 1963), so nothing is to be gained by using more efficient filters (99.995%) as opposed to less efficient filters (99.95%).

From the preceding remarks it is thus more desirable to use an analytical and systematic method that will ensure the cleanroom is completed to the required classification within a small limit of acceptable error.

1.4 Review of the Theoretical Airborne Contaminant Concentration Models

The most widely used simple formulae for assessing the steady-state airborne contaminant concentration dates back to the work of Bourdillon *et al* (1948). They stated that, once time has passed from the initial condition of the room, equilibrium will be reached and the nominal airborne bacterial concentration (assuming perfect mixing and constant source of particles) can be calculated as:

$$C = S / Q \quad (\text{Eq. 1.1})$$

where

C = airborne contaminant concentration

S = contaminant dispersion rate

Q = volumetric flow rate of supplied air

However, their main interest was to control infections in hospitals and their main concern was bacteria-carrying particles which had an equivalent size of $12\mu\text{m}$. They therefore suggested that the steady-state airborne bacterial concentration was reduced because bacteria were deposited on the floor due to gravitational sedimentation. This was taken into account and equation (1.1) was modified to:

$$C = S / (Q + A \cdot V_s) \quad (\text{Eq. 1.2})$$

where

A = surface area of the floor

V_s = terminal settling velocity

The work of Austin (1970) suggested that the particle concentration of the supply air must also be known to estimate the airborne particulate concentration in the room. Thus he modified equation (1.1) to include final filter efficiency and derived the transient airborne particulate concentration as:

$$C_t = \frac{60 S}{F_s \cdot N \cdot V} \left[1 - \exp \left[- \frac{F_s \cdot N \cdot t}{60} \right] \right] \quad (\text{Eq. 1.3})$$

where

C_t = particulate concentration at time 't'

- N = number of air changes per hour
- V = volume of the room
- F_S = final filter efficiency
- S = total particles dispersed per minute

As the airborne particulate concentration of outdoor air is not included in Equation (1.3), the model derived by Austin (1970) has assumed a 100% recirculated air discharging into the room. Thus this model would only be suitable for rooms with unidirectional flow cabinet discharging 100% recirculated air into the room and not to the rooms with supplied air discharged from air terminal devices. However this is unrealistic since almost all cleanrooms are supplied with a small percentage of outdoor air to pressurize the room and also for fresh air requirements for occupants.

Using energy or mass balances mathematical expressions have been derived to predict the airborne particulate concentration (Woods and Crawford, 1978; Wadden and Scheff, 1983). These can be reflected in the work of Morrison (1973). He applied mass flow analysis to a conventionally-ventilated cleanroom (Figure 1.1) and derived a differential equation of the form:

$$\frac{V \cdot dC}{dt} = Q_0 \cdot C_0(1-F_m) + Q_r \cdot C(1-F_r) + G \cdot V - Q_r \cdot C - R_D \cdot V - Q_{e+l} \cdot C$$

(Eq. 1.4)

where

Q₀ = volumetric flow rate of outdoor air

Q_r = volumetric flow rate of recirculated air

Q_{e+l} = volumetric flow rate through exhaust plus leakage

C₀ = outdoor airborne particulate concentration

F_m = filter efficiency of make-up air

F_r = filter efficiency of recirculated air

G = rate of particle generation per unit volume
of room

R_D = rate of particle deposition per unit volume
of room

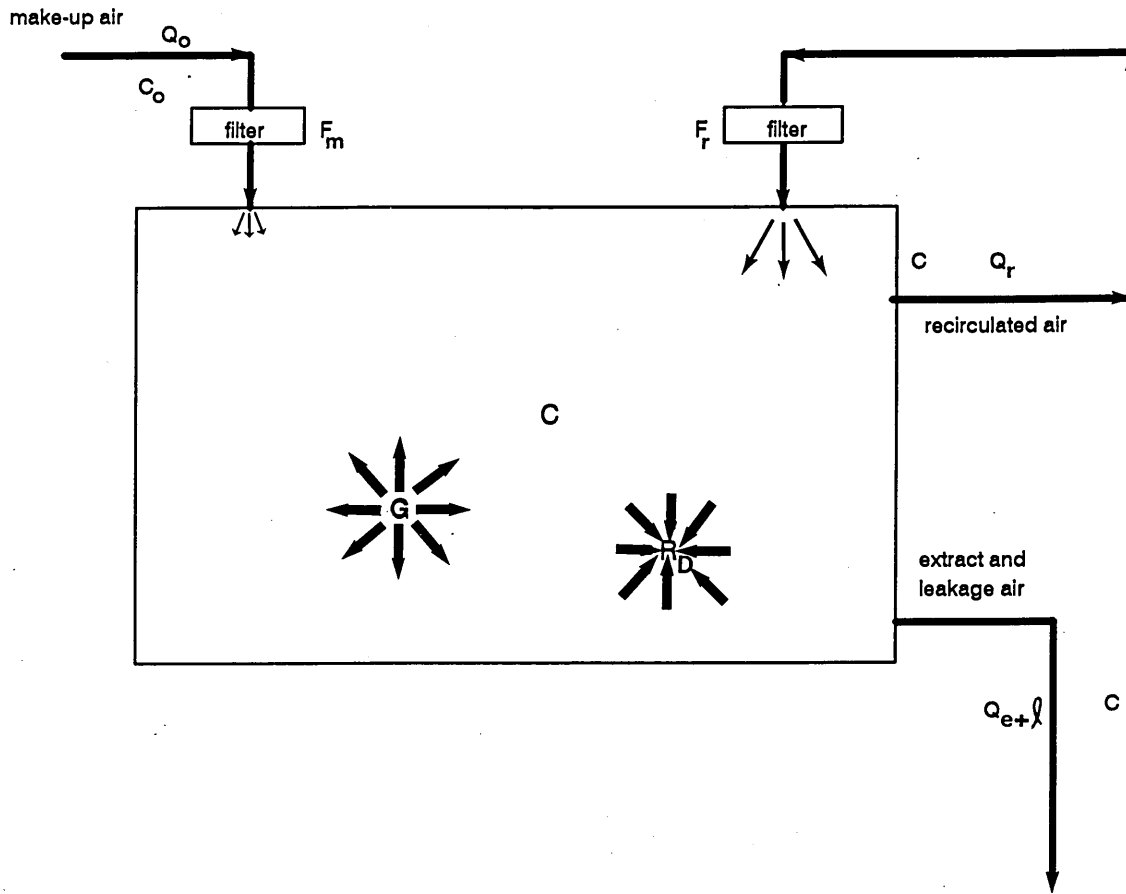


Fig. 1.1 Morrison's model of contaminant mass balance

C = Airborne particle concentration (particles/volume)

Q = Air supply flow rate (air volume/time)

G = Rate of particle generation per unit volume of room (particles/(time.volume))

R_D = Rate of particle deposition per unit volume of the room (particle/(time.volume))

F_m = Filter efficiency of make-up air

F_r = Filter efficiency of recirculated air

He then solved the differential equation (1.4) by assuming that both G and R_D are constant and the general solution of the differential equation was found to be:

$$C_t = K_1 \cdot C_0 (1 - \exp(-K_2 \cdot t)) + G/K_2 (1 - \exp(-K_2 \cdot t)) + C_i \cdot \exp(-K_2 \cdot t)$$

i.e.

$$K_1 = m(1 - F_m)/Y$$

$$m = Q_0/Q$$

$$Y = m + r \cdot F_r + R_d \cdot V/Q$$

$$r = Q_r/Q$$

$$R_D = R_d \cdot C$$

$$K_2 = Y \cdot Q/V$$

$$R_d = V_{ad} \cdot A_e/V$$

where

V_{ad} = average deposition velocity

A_e = exposed surface area

C_i = initial indoor airborne concentration at
time zero

m = ratio of outdoor air volume to supplied air
volume

r = ratio of recirculated air volume to supplied
air volume

He then described that the solution is the sum of the transient and steady-state terms. For the steady-state condition the general solution reduces to:

$$C = K_1 \cdot C_0 + \frac{G}{K_2} \quad (\text{Eq. 1.5})$$

There is a limitation, however, to these models in that the make-up air is not mixed with recirculated air (Figure 1.1) before it discharges into the room. Therefore the model derived has no generality in application.

The work of Kawamata (1982) suggests that to predict more precisely the airborne particulate concentration in a conventionally-ventilated cleanroom, it is necessary to consider the transition-state. He therefore derived a mathematical expression by considering the following assumptions:

(1) perfect mixing of incoming supplied air with contaminated room air

- (2) particles do not deposit
- (3) the rate of particle dispersion from sources in the room and from outdoors are constant
- (4) there is no air infiltration into the room

The mathematical expression was derived using Figure 1.2 as:

$$C_t = C_0 \exp\{-Nt[1-r(1-F_s)]\} + \frac{\{C_0 N(1-r)(1-F_s) + 60S/V\} \{1 - \exp\{-Nt[1-r(1-F_s)]\}\}}{N[1-r(1-F_s)]}$$

For steady-state condition, this reduces to:

$$C_{t \rightarrow \infty} = \frac{C_0 \cdot N(1-r)(1-F_s) + (60S/V)}{N[1-r(1-F_s)]} \quad (\text{Eq. 1.6})$$

The work of Liqun and Yongnian (1982) suggests that the airborne particulate concentrations in different parts of a conventionally-ventilated cleanroom are not equal and performance indices (correction factors as they refer to them) are needed to calculate the actual airborne particulate concentration. They introduce two performance indices (PI), one for the lower particulate concentration and the other for the upper limit of particulate concentration. They suggest that the PI's for each sampling point must be multiplied by the average airborne contaminant concentration to find the lower and upper limits of particle concentration in the room.

A more detailed mathematical model was proposed by Stowers (1984 and 1985) to predict the steady-state airborne particulate concentration in a vertical unidirectional cleanroom. Two models were developed for a vertical unidirectional flow cleanroom, one based on perfect mixing and the other on imperfect mixing. He reported that the two assumptions (perfect and imperfect mixing) represent extreme conditions and reality resides somewhere between these two extreme cases. Furthermore, he extended the two models by applying them at several discrete particle sizes by utilizing distribution curves to calculate specific and integrated size distribution curves for the particular situation.

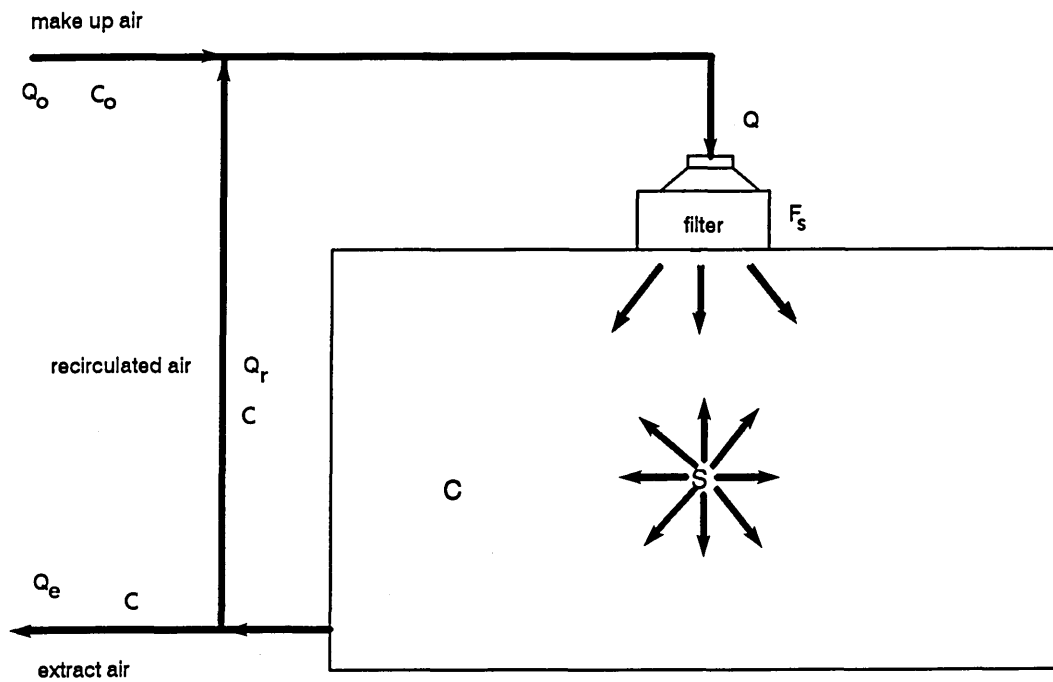


Fig. 1.2 Kawamata's model of contaminant mass balance

S = Particle dispersion rate (particles/time)

C = Airborne particle concentration (particles/volume)

Q = Volumetric flow rate (volume/time)

F_s = Final filter efficiency

Ensor *et al* (1987) proposed a mathematical model for calculating the concentration of particles leaving the HEPA filters (not in the whole cleanroom) in a vertical unidirectional cleanroom. They derived a model by using a simple balance of contaminant flow, assuming steady-state conditions and no leakage in the room. However the main objective of their investigation was to assess the at-rest conditions in vertically unidirectional flow cleanrooms and they stated that contaminants from sources within the room itself is another important area of consideration meriting future research.

Up to date all the theoretical models developed to predict the airborne contaminant concentration are only applicable for one discrete particle size. However this is unrealistic as an accumulative size distribution is required to meet the current cleanroom standards and the counts given by particle counters have not been considered. The models developed by Stowers (1985) to take into account several particle sizes was guided by empirical analysis. No theoretical model by which the values of the distribution could be readily deduced was suggested. His models were not tackled fundamentally and did not have generality in application. They were solved graphically for one particular case of a vertical unidirectional cleanroom.

The model proposed by Ensor *et al* (1987) was derived to investigate both the importance of filter penetration and outdoor airborne particulate concentration on the concentration of submicron particles leaving the HEPA filter during the "at-rest" condition in a vertical unidirectional cleanroom. No models were proposed to predict the overall airborne concentration in the room. They did however report that the filter penetration curve and the atmospheric size distribution can be approximated by a log-normal function.

The limitation of all the models discussed above is that they either ignored the removal of particles by deposition in the room or, when taken into account, they only considered deposition due to gravitational sedimentation for a spherical discrete particle size. In reality, particles are not spherical but irregular in shape. No consideration for this in calculating the terminal settling velocity has been

given. In calculating the terminal settling velocity to obtain deposition rates on the floor, they assumed an aerosol of one discrete size present in the cleanroom. However, a great range of particle sizes is normally encountered in cleanrooms and for accurate modelling the removal rates of all particle sizes must be taken into account.

The other limitation to these models is that only inanimate particles have been considered and bacteria excluded (except Bourdillon *et al*, 1948). Another drawback of these models is that they do not introduce terms for particulate generation from machines and processes carried out in the room as well as volumes of clean air entering the room from unidirectional flow work benches. As will be shown later, the foregoing parameters are important for assessing the airborne contaminant concentration in a cleanroom.

As the airborne cleanliness classifications given by the current standards are based on the maximum number of particles of size $0.1\mu\text{m}$, $0.3\mu\text{m}$ or $0.5\mu\text{m}$ and larger, it is therefore necessary to establish a method of predicting the integrated size distribution and not the concentration at a discrete size as given by all the previous models discussed.

1.5 Room Air Distribution Performance

1.5.1 Introduction

To derive a mathematical model which predicts the airborne contaminant concentration in a cleanroom, information concerning the air movement and mixing of supplied air with the room air is required. As these rooms have various air terminal devices (diffusers, grilles, jet) discharging high ventilation rates (usually 20 to 30 AC/hr), it is necessary to understand the parameters and mechanism responsible for air mixing as well as the relative merits of each ventilation system in mixing under these conditions.

This study begins with a review of research on air movement and enquires into the effectiveness of various ventilation systems in dilution. The review makes specific references to the parameters having greatest influence on mixing the

supplied air with the room air. It also considers different ways in which the investigation may be approached in order to achieve a better understanding of the roots of the problem.

1.5.2 Air movement

The air movement in a conventionally-ventilated cleanroom is usually very complex involving primary supplied air, secondary room air, convection currents and obstructions. These can create regions of entrainment, turbulent mixing and stagnant air within the room. A detailed measurement of air movement is difficult. A hand-held smoke puffer, smoke bombs, helium filled soap bubbles and thermal-based smoke generators have all proven to be satisfactory in visualising the air movement patterns.

When an air supply jet discharges into a conventionally-ventilated room, the boundary of the jet begins to spread due to the process of entrainment of room air by the supply air. This process induces mixing and hence air movement within the room. Koestel *et al* (1952), Farquharson (1952), Tuve (1953), Freaun and Billington (1955), Parkinston and Billington (1957) were among the early investigators to describe the behaviour of an air supply jet discharged into a large room at the same temperature (free isothermal jet). This occurs in four stages which are as follows:

- (1) The first stage, where the velocity of the jet remains constant along the centre line for up to and about four equivalent diameters from the plane of the outlet.
- (2) The second stage (transition zone) which is about 5-8 equivalent diameters from the plane of outlet, the centre-line velocity (V_x), is inversely proportional to $(x)^{\frac{1}{2}}$, where x is the distance from the plane of outlet.
- (3) The third stage, where turbulent flow has been fully established and the inertial forces dominate the viscous forces. This is the main zone of engineering interest which extends for the next 25 to 100 equivalent diameters of jet length, depending on the initial velocity and the outlet shape. In this stage, the centre-line velocity (V_x) is proportional to $1/x$.

(4) The final stage at the end of the turbulent zone, where the centre line velocity (V_x) decays rapidly to a value below 0.25 m/s and hence the jet becomes indistinguishable from its surroundings.

The performance characteristics of primary air supply discharged from an air terminal device have been described in terms of throw, drop and spread of the supplied air. These characteristics have been shown by Van Gunst *et al* (1967), Nevins (1976), the HEVAC Association (1981), Whittle (1986), Jackman (1986) to be affected by:

- (i) Type of air terminal devices
- (ii) Velocity of supplied air
- (iii) Differential temperature between the supply air and the room air
- (iv) Location of obstructions

The different types of air terminal devices can vary widely in the manner in which they diffuse or disperse the supply air into the room and induce or entrain room air into the primary supplied air. To achieve satisfactory air movement in an air conditioned space, the HEVAC Association (1981) and Whittle (1986) have investigated the performance of various air terminal devices.

Wall-mounted grilles discharged air in a three-dimensional stream which flowed normal in a direction perpendicular, or near perpendicular, to the face of the grille. The discharged air usually had an included angle of about 20° . A little distance from the grille the air velocity reduced in direct proportion to the distance from the grille.

The air from linear grilles, slot and linear diffusers discharged in a wide stream which was taken as two-dimensional. The supplied air mainly expanded across the thinner section, again at an included angle of about 20° . The primary air velocity reduction was in proportion to the square root of the distance from the device.

The air supplied into a room from circular or rectangular diffuser discharged in a thin stream. This allowed the supplied air velocity to reduce rapidly as the surrounding room air was entrained into the supplied air. The supplied air

velocity reduced in direct proportion to the distance from the diffuser.

The terminal air devices which have a high induction rate result in a rapid temperature equalisation and short throw. Ceiling diffusers with a radial pattern fall into this category, having a shorter throw and obtaining a more rapid temperature equalisation than, for example, a slot or linear diffuser.

The performance characteristics of an air supply jet are directly affected by the density differences between a jet and its surroundings due to the temperature difference between the supply air and the room air. This can cause a projected jet to deflect from its initial trajectory, either upwards if the supplied air is warmer than the room air and downwards if cooler. This would result in either an increase or decrease of the throw of the jet, depending on the direction of discharge of the jet and also on the temperature difference between the jet and the room air.

As part of an investigation to develop design information Jackman (1973) described air movement in rooms with circular and linear ceiling mounted diffusers. His test programme included three types of circular ceiling diffusers:

- (1) Plate diffuser
- (2) Plaque diffuser
- (3) Multi-cone diffuser and a linear two-slot diffuser equal in length to the width of the test room which was mounted flush with the ceiling in three alternative strategies:
 - (i) Diffuser centrally isolated, horizontal discharge in opposite directions.
 - (ii) Diffuser located 150 mm from external wall, single slot with horizontal discharge across ceiling.
 - (iii) Diffuser located 150 mm from external wall, two slots with horizontal discharge across ceiling.

He found that the patterns of air movement were similar for all the different types and arrangement of diffusers. With isothermal conditions and a uniformly distributed heat load, the air movement was basically symmetrical. However, assymmetrical patterns were generated when the window was either heated or

cooled.

The performance characteristics of the supplied air can also be influenced when the discharged air stream passes along and is close to a surface. This is because induction in the region close to the surface will be largely prevented (this is commonly referred to as the Coanda effect). Consequently, less of the supplied air original momentum is expended in accelerating entrained air and the throw of the supplied air is correspondingly increased.

The behaviour of an air stream upon encountering an obstruction has not been well investigated. In all design information for predicting the performance of jets it is assumed that the jet is flowing over a smooth surface. However, in practice, obstructions due to ceiling beams or light fittings may cause the jet to deflect from the ceiling and down into the occupied zone of the room. Holmes and Sachariewicz (1973) proposed a simple method to predict the effect of ceiling beams and light fittings on ventilating jets.

The velocity decay of the jet is also influenced by the obstructions within the space (e.g. people, furniture) which can deflect the air flow patterns. Jackman (1973) showed that the influence of furniture in a ventilated room can cause a reduction in the mean room air speed. The reduction becomes very noticeable by increasing the volume of supplied air and the space occupied by the furniture.

Whyte and Shaw (1974) reported the results of experiments carried out to investigate the effect of obstructions in a unidirectional flow operating room. They demonstrated that large turbulent eddies behind an object can be created by obstructions (such as operating lamps or persons) in the airflow. Therefore it can be concluded that in order to minimize the turbulence within a unidirectional cleanroom, it is important to consider the arrangement and shape of equipment as well as people within the working zone.

In attempting to explore the mixing process within a ventilated room, the HEVAC Association (1981) demonstrated that the exhaust grilles affect the air distribution only within their immediate vicinity and that the location of them had only slight influence on the air distribution patterns. As the supply air spreads

and streams as soon as it discharges into the room, due to its momentum being expended by entrainment and mixing of surrounding air, the extract fan can not short circuit the supplied air without appreciable mixing taking place. Even when the supply air inlet is located very close or directly opposite to an exhaust terminal only a small quantity of supply air would be short circuited. Air approaches an exhaust from so many directions so that significant velocities only occur very close to the exhaust.

As seen from this review very little investigation has been carried out to study the air flow behaviour in a conventionally-ventilated cleanroom. The type of air supply discharged into a conventionally-ventilated cleanroom can differ from the types (diffused air supply) already discussed. The air discharged into these rooms is normally directed flow, with high ventilation rates. This can affect the air supply characteristic (spread, drop and throw) and hence vary the amount of room air entrained by the supplied air. Also short circuiting is commonly assumed to be a major problem, especially when a jet air supply is used. As part of this research it is therefore necessary to investigate all these problems.

1.5.3 Ventilation effectiveness

In exploring airflow behaviour and the performance of various ventilating systems in diluting and removing contamination within a room many investigators have carried out experiments (Lidwell and Williams, 1960; Lidwell *et al*, 1967; Drivas *et al*, 1972; Foord and Lidwell, 1973, 1975; Viegersma, 1980; I'Anson *et al*, 1982; Prior *et al*, 1983; Irwin *et al*, 1984; Niemelä *et al*, 1984; Lagus and Persily, 1985). Depending on the information desired, there have been three methods of studying the efficiency of ventilation (Sandberg, 1981). These are as follows:

- (1) The decay method: This is the simplest and most widely used in ventilation studies. The room is filled with a contaminant (e.g. tracer gas or particles) and with the aid of fans, the air is mixed to an even initial airborne contaminant concentration. The fans are then turned off and the decay of the contaminant is continuously recorded at different points of interest within

the room.

- (2) The source method: A constant flow of contaminant is admitted to the supply air duct (or liberated within the room) and the growth and steady-state airborne concentration of the contaminant is recorded at different points of interest within the room.
- (3) The pulse method: A small quantity of contaminant is admitted to the supply air duct and the growth and decay of the concentration is continuously recorded at different points of interest within the room.

Lidwell and Lovelock (1946) were among the early investigators to carry out detailed study on air movement in operating rooms. They used nitrous oxide (N_2O) as a tracer gas to simulate the movement of airborne bacterial contamination. The gas was liberated in measured amounts and continuous samples were taken from different sampling positions within the room. They concluded that when the room air was well mixed (i.e. primary supply air mixed well with the room air), the tracer gas concentration decayed according to the expression:

$$C_t = C_i \cdot e^{-N \cdot t} \quad (\text{Eq. 1.7})$$

where C_t = contaminant concentration at time t
 C_i = initial concentration at time zero
 N = theoretical ventilation rate

They defined the theoretical ventilation rate (N) as:

$$N = \frac{Q}{V} \quad (\text{Eq. 1.8})$$

where Q = volumetric flow rate of supplied air
 V = volume of the room

The authors reasoned that if the mixing process within the room is not perfect, then the rates of decay in the localized areas of the room will be different. However they noted that it is usually possible to fit an exponential curve for different points in the room described as:

$$C_t = C_i \cdot e^{-N_{\text{eff}} \cdot t}$$

where N_{eff} = effective ventilation rate

The effective ventilation rate was determined from the slope of the decay curve during the exponential decrease of the gas concentration. They found that the effective ventilation rate (N_{eff}) could be either smaller or greater than the theoretical ventilation rate (N).

Lidwell and Williams (1960) liberated nitrous oxide (N_2O) at three different heights (5 ft, 3 ft and 1.5 ft above floor) in operating theatres to assess the performance of various ventilating systems. Their observations were confined to contamination reaching the centre of the operating table since the main purpose of their investigation was an attempt to ascertain which ventilating system or systems were most able to protect the wound from extraneous airborne contamination.

Two types of ventilation system were included in their test programme:

- (1) Piston-type downward displacement ventilation as advocated by Blowers *et al* (1960).
- (2) Turbulent mixing ventilation systems.

In order to evaluate the effectiveness of various ventilating systems in reducing airborne contamination of the wound to a minimum, they introduced a dimensionless quality referred to as "Performance Index" (PI). The index indicated the advantage or disadvantage that a particular ventilating system had in comparison to a hypothetical system with perfect mixing. The index was calculated as the ratio of the quantity of tracer gas recovered at the sampling point to that quantity that would have been recovered, with the same volume of ventilating air, assuming perfect mixing of supplied air with the room air. PI's greater than 1 indicate a higher airborne concentration than would be expected with perfect mixing and PI's less than 1 indicate lower concentration than expected. Their findings can be summarized into two parts:

- (1) With turbulent ventilation systems, adequate mixing was obtained at all heights where the contamination was liberated and volumes of ventilating air supply, except when the contamination was released 3 feet (0.9 m) above floor level and when the air velocity over the operating table was below 25 ft/min (0.13 m/s).

- (2) The small PI's obtained (0.08, 0.5, 0.7) when the contamination was liberated at a low level (1.5 ft or 0.46 m) for a downward displacement system suggests that the system is capable of extremely effective removal of contamination from the theatre.

Blowers *et al* (1960) have reported the results of an extensive series of measurements carried out in operating theatres. The purpose of their investigation was to determine the effectiveness of various ventilation systems in diluting and removing airborne bacterial contamination. The influence of the following parameters studied in their test programme were:

- (1) Ventilation rates
- (2) Type, number and position of air terminal devices
- (3) Temperature
- (4) Human activity
- (5) Number and location of exhaust grilles
- (6) Humidity

The conclusions gained from their investigation are as follows:

- (1) The efficiency of a ventilation system using a diffuser terminal improves as the volume of the supplied air increases until the supplied air volume reaches a critical value. After this any increase in the volume of the supplied air decreases the efficiency of the ventilation system.
- (2) The differential temperature between the supplied air and the room air had significant effects on the ventilation efficiency.
- (3) The activity of two people walking continuously in a room under test conditions had a negligible effect on ventilation efficiency.
- (4) Number, location and arrangement of exhaust grilles had very little influence on ventilation effectiveness.
- (5) The ventilation efficiency was not affected by changing the relative humidities ranging from 32% to 80%.

Kethley *et al* (1962) reported the results of experimental investigations conducted in a simulated operating room (16 x 12 x 10 ft high or 4.9 x 3.7 x

3.1 m high). The three types of air terminal devices included in their test programme were:

- (1) End-wall grille (air directed either straight out or down 45°)
- (2) Single central ceiling diffuser (air directed either in a flat, horizontal pattern, or down in a narrow vertical pattern)
- (3) Perforated ceiling panels (two rows of five panels spaced 3 ft apart, or three rows of five panels, spaced 1 ft apart; each panel measured 1 by 2 ft)

The volumes of air supplied into the room for the first two air terminal devices (Nos. 1 and 2) were 300 ft³/min (0.14 m³/s), 600 ft³/min (0.28 m³/s), 900 ft³/min (0.42 m³/s) and for the last one (No. 3) were 450 ft³/min (0.21 m³/s), 600 ft³/min (0.28 m³/s) and 750 ft³/min (0.35 m³/s). For all the tests, there were at least two exhaust grilles, positioned uniformly near the floor.

Ventilation effectiveness for each ventilation scheme was evaluated by means of a performance index (PI) at the vicinity of the operation site and overall for the room. A single circular diffuser adjusted for horizontal discharge tested for all different volumes of air resulted in overall room PI of 1.0. The same diffuser adjusted for vertical discharges for the same volume of air discharged into the room produced a PI of 0.9. For the end wall grilles the overall PI varied from 0.6 to 1.2 and for the perforated ceiling panels from 0.4 to 0.5. They concluded that: perfect mixing occurs in a room with circular diffusers; reasonable mixing with end wall grilles; and, not much mixing with perforated ceiling panels. However, it was noted that overall room PI's were biased due to the use of simple arithmetical averaging which gave significance to single point results far removed from the median. Thus unrealistic conclusions were reported for overall room mixing. It is thought that a more balanced mixing description would be gained by the method discussed later in this work.

Lidwell *et al* (1967) investigated the bacteriological contamination of the air in an operating room fitted with three alternative supply systems. These were:

- (1) Downward displacement 'Piston'
- (2) Moderate velocity turbulence

(3) Low velocity turbulence

The importance of their findings included:

- (1) When the tracer gas was liberated at a low level (1.5 ft or 0.46 m) above the floor, nearly half as much gas (Performance Index 0.4) was transferred just above the operating table for both downward displacement and moderate velocity systems.
- (2) When the tracer gas was liberated at 3 ft (0.91 m) above the floor, all of the three ventilating systems indicated perfect mixing over the table (Performance Index 1.0 to 1.1).
- (3) The high Performance Index (3.6) for the downward displacement system found over the operating table when the tracer gas was liberated at a high level (5.5 ft or 1.68 m) above the floor and the reduced value (0.6) at the 5.5 ft (1.68 m) level when the tracer was liberated at table level (3 ft or 0.91 m) was associated with some layering and restriction of mixing at levels higher than 3 ft (0.91 m) above the floor.
- (4) The volume of the air discharged into the room was the only sole determining factor to influence the level of airborne contamination in the room.
- (5) No significant differences were detected between three ventilating systems in controlling the level of airborne contamination. However, it should be noted that effective air-piston downward-displacement was not achieved due to the convection air currents generated by the temperature differential within the walls, and between the walls themselves and the room air.
- (6) The patterns of air movement within the room was easily influenced by thermal convection currents due to differences in wall temperature.

A number of studies (Constance, 1970; Drivas *et al*, 1972) have utilized the concept of mixing factors to evaluate the efficiency of ventilation systems in diluting and removing airborne contamination within buildings. They state that perfect mixing is not always attained and a mixing factor must be applied to assess the airborne contaminant concentration within the room. Therefore they

demonstrated that the exponential decay equation (1.7) should reduce to:

$$C_t = C_i \cdot e^{-k \cdot N \cdot t} \quad (\text{Eq. 1.9})$$

where $k =$ mixing factor

The idea is similar to that used by Lidwell and Lovelock (1946) in their use of effective ventilation rate (N_{eff}) as:

$$N_{\text{eff}} = k \cdot N$$

Constance (1970) discussed that if the mixing factor (k) is 1, then the airborne contamination within the room dilutes and removes by a system of perfect mixing action. Furthermore he described that in practice this type of system is unattainable and depends on:

- (1) Contaminant property (which he calls toxicity)
- (2) Uniformity of airborne contaminant distribution in the room space
- (3) Location of air supply systems and exhausts
- (4) Room geometry and population

He suggested that a mixing factor ranging from 1/3 to 1/10 should be employed in equation (1.9) to evaluate the actual airborne contaminant concentration.

The mixing factors used by Constance (1970) was defined by Drivas *et al* (1972) as:

$$k = \frac{\tau_t}{t_{\text{eff}}}$$

where $\tau_t =$ theoretical residence time

$t_{\text{eff}} =$ effective residence time

The theoretical well-mixed residence time (τ_t) was calculated as:

$$\tau_t = \frac{V}{Q}$$

The effective (or experimental) residence time (t_{eff}) was estimated by the negative reciprocal of the slope of decay line. Furthermore, they reported the results of mixing factors obtained using sulphur hexafluoride (SF_6) as a tracer to observe the decay rate of the contaminants. The mixing factor was found to be 0.9 with fans

and ranged from 0.3 to 0.7 without fans. They concluded that, the fans produced perfect air mixing in the room.

Various definitions for describing ventilation efficiency were discussed by Sandberg (1981). Using tracer gas (N_2O) techniques he examined three alternative definitions of ventilation efficiency based on:

- (1) The slope of decay curve during the exponential decrease of the tracer gas.
- (2) The ratio between airborne contaminant concentration.
- (3) The area under the decay curves.

His experimental programme was carried out in a room of size 3.6 x 4.2 x 2.7 m high, having an air supply system located centrally in the ceiling and the exhaust air terminal 0.2 m beneath the ceiling. However he stated that this system is classified as a short circuiting system, due to the location of the air supply and exhaust terminals. The rates of air supply studied corresponded to 1, 2 and 4 nominal air changes per hour and the supplied air temperature was varied to provide 0.2, 4 and 8K above the occupied zone (the zone up to 1.8 m above the floor) mean temperature.

Their findings can be summarized as follows:

- (1) Good air mixing was established with all the three ventilation rates for isothermal conditions.
- (2) Generally, as the ventilation rate was increased, the ventilation efficiency improved and thus provided better mixing (except at a high differential temperature 8K between the supplied air and the room air).
- (3) Due to the random fluctuations and the measuring errors during the transient phase of the experiment the slope of the decay curve should not be used to estimate the efficiency of ventilation. However as the area under the curve evens out such fluctuations in the data it can be used to give a better prediction of the ventilation efficiency.

As part of an investigation to evaluate the relative merits of different ventilation arrangements, Potter (1988) reported the results of the ventilation effectiveness of three different mechanical ventilation systems tested under various

rates of air supply (1, 2 and 7 AC/hr). These were:

- (1) Natural inlet and mechanical extract
- (2) Wall-mounted high-level supply grille with low-level extract
- (3) Floor-mounted supply grilles (twist) with high-level extract

Important findings of his study included:

- (1) The presence of a simulated occupant in a room can have a marked effect on the air movement due to thermal and respiratory emission.
- (2) All ventilation arrangements tested produced a good mixing of supplied air with the room air. The maximum difference in ventilation effectiveness index between the three ventilation arrangement for a given air change rate was approximately 28%, with floor-mounted supply grilles producing almost perfect air mixing (ventilation effectiveness index of 0.97 for 1 AC/hr).
- (3) The effect of reducing the ventilation rate improved the ventilation effectiveness and thus provided better mixing of supplied air with the room air.

From the review of the research literature reported here it is concluded that parameters having the greatest influence on air mixing are:

- (1) Air supply flow rate into the room
- (2) Type of air terminal devices
- (3) Differential temperature between the supplied air and the room air
- (4) Location of obstructions and occupants
- (5) Geometry of the room

However, the review highlights the lack of information regarding the effectiveness of typical air terminal devices used with high ventilation rates found in conventionally-ventilated cleanrooms. As discussed previously, high ventilation rates and directed flow can affect the air distribution performance in the room. It is therefore necessary to extend the investigation of these variables and carry out experiments to assess any deviation from theoretical phenomena of perfect mixing.

1.6 Dispersal of Contamination Within a Room

1.6.1 Introduction

The air supplied into a cleanroom is filtered through high efficiency filters and therefore contains few particles. Also the extract air volume is less than the supplied air volume to maintain a higher pressure (positive) than the adjacent areas so that particle-laden outside air will not leak into the room. Airborne particles in a cleanroom can therefore only arise from people and process machines within the room. To calculate the airborne contaminant concentration in cleanrooms, data on the dispersal of airborne contaminants by people and process machines are therefore required.

1.6.2 Contaminant dispersion by people

Jansen *et al* (1974) have demonstrated that people shed one outermost layer of skin and a complete layer is replaced, on average, in less than twenty-four hours. MacIntosh *et al* (1978) showed that a complete layer of skin corresponds to about 2×10^9 cells and the mean projected dimensions of these are about $33 \times 44 \mu\text{m}$. These divide into skin fragments with the median about $20 \mu\text{m}$ with 7-10% less than $10 \mu\text{m}$. Many of these cells can carry bacteria. Whyte *et al* (1976) have demonstrated that people continuously disperse large quantities of particles and bacteria-carrying particles. These particles become airborne and will deposit into surgical wounds or containers of aseptically produced pharmaceutical products.

Duguid and Wallace (1948) were among the early investigators to study the effectiveness of fabrics in preventing airborne bacterial dispersion from the skin of the operating team during surgery. They demonstrated the ineffectiveness of ordinary cotton surgical gowns, and showed that by replacing these with a more impermeable fabric, the dispersal rate would reduce to 10% or even less. The problem with the surgical gowns commonly used in the operating room, is that they are made of relatively loosely-woven cotton fabrics. Lidwell and MacIntosh (1978) and Whyte and Bailey (1985) have shown that the pore diameter of cotton fabrics is usually greater than $80 \mu\text{m}$. Ordinary cotton fabrics do little in filtering the dispersal of airborne bacteria-carrying particles. Bethune *et al* (1965) and

Doig (1972) have demonstrated that indoor personal clothing is just as effective in preventing airborne bacteria dispersion as ordinary cotton fabrics. Whyte *et al* (1976) have found that surgical cotton gowns only prevent one third of the bacteria dispersed from people. May and Pomeroy (1973) and Hill *et al* (1974) have shown that bacteria-carrying particles are mainly dispersed from the lower part of the body (under the waist). Therefore it can be concluded that the ineffectiveness of the gowns is not only caused by the bacteria-carrying particles passing through the weave but also issuing from under the gown. Blowers and McCluskey (1965) have demonstrated the use of tighter woven fabric made into trousers such as Ventile (pore diameter $20\mu\text{m}$) to reduce the airborne bacterial dispersion. Clearly a tightly woven fabric would reduce airborne bacterial dispersion, but at the same time it will have a lower air permeability and hence less air exchange. As a result people wearing this type of fabric feel very hot and uncomfortable.

Charnley (1969), using Ventile cloth designed a total-body exhaust system to minimize the bacterial dispersion and at the same time keep the wearer cool and refreshed. Whyte *et al* (1976, 1978, 1983) and Lidwell *et al* (1983) have demonstrated that with the total body exhaust system, bacteria can issue from under the gown so its full effectiveness can only be achieved in a unidirectional Ultra-Clean Air (UCA) System. An extensive study carried out by Lidwell *et al* (1982, 1983) showed that Ultra-Clean Air (UCA) Systems used with conventionally designed operating room clothing, can approximately halve the rate of joint sepsis, as compared with conventionally-ventilated operating rooms. Furthermore, they showed that if total-body exhaust gowns are used in UCA Systems, the rate of joint sepsis would reduce to one quarter. Unfortunately, many surgeons find the total-body exhaust system uncomfortable, claustrophobic, and the exhaust hose restricting. However there are various synthetic clothing materials used in pharmaceutical and micro-electronic cleanrooms which are very effective in preventing airborne bacterial dispersion and yet reasonably comfortable to wear. A disadvantage of these fabrics is their high-surface electrical resistance which can

develop significant electrostatic charges. Therefore because of anti-static regulations to prevent explosions they cannot be used in the operating room.

Whyte *et al* (1978, 1983) have shown that a disposable non-woven fabric known as Fabric 450 can overcome the above difficulties. This cloth is as efficient as the closely-woven Ventile material in preventing airborne bacterial dispersion. Their tests showed that the air permeability of Ventile cloth is only 0.39 ml/cm²/sec compared with 15.1 ml/cm²/sec for cotton cloth and 32.7 ml/cm²/sec for the disposable Fabric 450. Their study concluded that due to higher air exchange being an important factor in comfort, disposable Fabric 450 is more convenient and more comfortable than the total-body exhaust systems and may be as comfortable as cotton clothing.

Lidwell and MacIntosh (1978) reported the results of experiments carried out to assess the effectiveness of fabrics in preventing airborne dispersion. The fabrics tested were made up into trousers which were worn by volunteers during exercise in a dispersal chamber. The results of their findings fall into four groups:

- (1) Utopia plus, Balloon cotton and the Feather proofed cotton all with high pore size showed around 50% penetration.
- (2) The closely-woven cotton i.e. Pima and Ventile, together with the Fabric 450 non-woven fabric showed around 10% penetration.
- (3) Tyvek, an impermeable synthetic material showed a penetration of about 3%.
- (4) The two woven, wholly synthetic fabrics, Nylon taffeta (extremely open weave) and ceramic terylene (closely woven fabric) showed a penetration as low as 1%. The nylon material was thought to be effective because it had a high surface electrical resistance and developed significant electrostatic charge which would attract the bacterial particles and prevent dispersion.

Fujii *et al* (1982) have obtained information of the size distribution of particles dispersed from a volunteer wearing various garments (underwear, new cotton, washed cotton, four kinds of non-woven clothes, polyester 'A' and polyester 'B') and performing various activities (walking, standing/sitting, physical exercises). They stated that the greatest particle dispersion rate was achieved

when the person was wearing cotton fabrics. They showed that wearing polyester 'B' was 10 times more effective in reducing airborne contamination than washed cotton. They also showed that the dispersion rate was directly related to the level of activity. The lowest dispersion was achieved when the person was walking and the highest when performing physical exercises.

Fujii and Minamino (1982) have reported the results of particles released by people in a cleanroom wearing two different types of garment design, viz. coverall and gown. The gown was worn over the trousers. The size and distribution curves plotted for dispersion rates of particles from each type of garment had a very consistent shape, although the total dispersion rate varied. The dispersion rate for the coverall-type garment was on average 1.75×10^5 per minute for particles $\geq 0.3 \mu\text{m}$. The dispersion rate for a gown design varied from 1.31×10^5 per minute for particles $\geq 0.3 \mu\text{m}$ for 100% polyester fabric to 1.02×10^7 per minute for particles $\geq 0.3 \mu\text{m}$ for a cellulose-fibres fabric.

Whyte *et al* (1983) have shown that some non-woven fabrics can be about 10 times more effective in preventing airborne bacterial dispersion than ordinary cotton. Furthermore they demonstrated that the efficiency of a garment in preventing airborne bacterial dispersion is not only determined by the filtering efficiency of the fabric but also the amount of bacterial particles pumped out through the neck, trousers, etc. Therefore they concluded that the greatest efficiency can be obtained from garments which fully envelop and enclose the wearer.

Whyte and Bailey (1985) have reported the results of investigations carried out to assess the effectiveness of fabrics in preventing microbial dispersion in terms of pore size, air permeability and particle removal. From eight fabrics studied (Ventile, Celon, Ceramic polyester, Nomex, Herringbone polyester, Gortex, Tyvek and Selguard) they found that Ceramic polyester, when made into a conventionally designed garment (i.e. coverall tucked into knee-length boots and a separate hood tucked into the neck of the coverall), gave the lowest microbial dispersion. They reasoned that although the equivalent pore diameter (about $22 \mu\text{m}$) and particulate

removal efficiency (50% of the 0.5 μm and 95% of the 5.0 μm) of this fabric is not particularly good, the fabric was effective because the median of the skin fragments dispersed from people is about 20 μm . They also found that Ceramic polyester was about ten times more effective in preventing microbial dispersion than Celon (equivalent pore diameter of 102 μm) and Nomex (equivalent pore diameter of 103 μm). They also demonstrated that a Gortex fabric having a pore size of about 0.2 μm with a low air permeability of 0.06 ml/cm²/sec suffered from the problem of "pumping". The effectiveness of the fabric can only be realised if it is made into a suit with effective seals at the neck, trousers and waist. This type of fabric performed 1000 times better than ordinary cotton clothing. They therefore concluded that the overall design of the fabric is a very important criteria for contamination control.

The contaminant (particles and bacteria-carrying particles) dispersion rates of people, particularly on the basis of a male/female comparison has not been widely investigated. Thus to gain realistic data for utilization in the airborne contaminant concentration model, it is essential to gather data on a large sample of male and female volunteers.

1.6.3 Particulate generation from process machines

Low airborne particulate levels have become a necessity in micro-electronics wafer fabrication cleanrooms to help prevent yield loss. This has resulted in the introduction of automation and robots. Therefore, there is a need to measure the effectiveness of machines and robots in dispersing particles.

Ro and Unno (1986) have demonstrated experimentally the particles generated by two robots; assembly SSR-H and wafer-mover robot ALPHA II. They found that the SSR-H robot generated 3.1×10^5 particles ($> 0.11 \mu\text{m}$) per minute. The lubricating oil used for the drive motor was responsible for originating the particles. The ALPHA II robot generated 350 ($> 0.13 \mu\text{m}$) particles per minute. Therefore it can be concluded that robots disperse far fewer particles than that of humans wearing good cleanroom clothing (1×10^6 particles $\geq 0.5 \mu\text{m}$ per minute) and robots should be used in silicon wafer handling areas. However, it is

important to note that the use of robots will not eliminate the formation of eddy currents that can entrap contamination within unidirectional cleanrooms as vortices can still develop around the robot arms and cause particle deposition.

Rogers and Bailey (1987) reported the results of particulate generation rates from 2 small DC brush-type gearmotors. The results are not given in terms of the particle size, but it is assumed that it is for 0.1 μm particles. The first gearmotor started generating 22,000 particles/minute and decreased over time to a total of 7400 particles/minute. The second gearmotor started generating a total of 200 particles/minute and increased to 120,000 particles/minute over a period of five hours.

This review clearly shows that there is little published information on particle emission from machines. It is therefore necessary to gather data from the other machines used in cleanrooms.

1.7 Review of the Surface-Deposition Studies

1.7.1 Introduction

The airborne contaminant concentration in a cleanroom may be reduced by deposition of particles on to surfaces. Deposition of aerosol particles has been studied in great detail in parallel flow (i.e. in pipes, human lungs, wind tunnel) and in cross flow about collectors (filter fibres, cylinders, ribbons, spheres, plates) as shown in Tables 1.1 and 1.2, but no work has been devoted to the in-depth study of surface deposition within chambers and rooms. However, as part of this research it was necessary to assess the significance of each deposition mechanism involved. Towards this end the information on deposition in chambers and rooms is reviewed and the following facts revealed.

In general, the deposition on surfaces in a room or chamber depends on the airborne particle concentration, particle size and density, room or chamber size and shape, air mixing characteristics and mixing intensity. To assess the surface deposition rates, these inter-dependences must be evaluated.

TABLE 1.1 PREVIOUS DEPOSITION STUDIES IN PARALLEL FLOW

PIPES	HUMAN LUNGS	WIND TUNNEL
<p>Gormley & Kennedy (1949) Alexander and Colder (1951) Thomas (1958) Davies (1966) Beal (1968) Sehmel (1968, 1970) Montgomery & Corn (1970) Ilori (1971) Liu & Agarmal (1974) Liu & Ilori (1976) Brockman (1981) Pui <i>et al</i> (1987)</p>	<p>Wilson (1947) Weibel (1963) Beeckmans (1965) Davies (1972, 1975) Fry and Black (1973) Takahashi and Ito (1976) Itoh <i>et al</i> (1985)</p>	<p>Gregory & Stedman (1953) Rosinski (1957) Davies (1960) Langer (1965) Chamberlain (1967) Rosinski & Langer (1967) Sehmel (1973) Wedding <i>et al</i> (1975) Fairchild & Eillery (1982) McCready (1984)</p>

TABLE 1.2 PREVIOUS DEPOSITION STUDIES IN CROSS FLOW

Filter fibres	Cylinder	Sphere	Disks	Plates
Wong <i>et al</i> (1956) Kuwabara (1959) Stern <i>et al</i> (1960) Natanson & Ushakov (1961) Kirsch & Fuchs (1967) Wilson & Cavanagh (1967, 1971) Lee & Liu (1982)	Albrecht (1931) Davies (1950, 1952) Ranz & Wong (1952) Fuchs (1964) Friedlander (1977) Callily <i>et al</i> (1986)	Fuchs (1964) Davies (1966) Hidy & Brock (1970) Friedlander (1977) May & Clifford (1967) Starr (1967)	May & Clifford (1967) Liu & Ahn (1986) Chirifu <i>et al</i> (1987) Ensor <i>et al</i> (1987) Cooper <i>et al</i> (1988) Peters <i>et al</i> (1988)	Davies & Aylward (1951) Ranz & Wong (1952) Stern <i>et al</i> (1960) Wells & Chamberlain (1967) Dabros & Van de Ven (1983) Hidy (1984)

Particles may be deposited on surfaces by the following mechanisms:

- (1) gravitational sedimentation
- (2) inertial impaction
- (3) molecular (Brownian) diffusion
- (4) turbulent (eddy) diffusion
- (5) electrostatics
- (6) thermophoresis

A brief resume of each of these mechanisms is as follows:

- (1) gravitational sedimentation: airborne particles falling under the influence of gravitational forces rapidly reach their terminal settling velocity due to drag forces. Larger particles fall more rapidly than the smaller ones and this deposition is effective for particles with an equivalent diameter greater than about 1 μm . Deposition also increases with the density of the particles.
- (2) inertial impaction: large particles carried along on an air stream and which have too great an inertial force are not able to follow the air stream when it turns round an obstruction. Provided the air stream velocity is high enough, the particles will have sufficient momentum to continue along their original path and coast through the boundary layer to the surface. Small particles may fail to reach the surface due to fluid drag and insufficient momentum. The inertial force increases with increasing particle diameter, density and air velocity.
- (3) molecular (Brownian) diffusion: air molecules bombarding very small airborne particles possess sufficient energy to cause random displacement of the particle and as a result particles deposit onto the surface they may come into contact with. This type of deposition is only dominant for relatively small airborne particles (i.e. those less than about 0.5 μm), because the Brownian diffusion coefficient decreases rapidly with increasing particle size. The deposition does not depend on the density of the particles.
- (4) turbulent (eddy) diffusion: when a turbulent air stream carrying suspended particles flows along a surface, particles are unable to follow the eddy motion

because of the fluctuating velocity component normal to the surface which is caused by the incurion of turbulent eddies are projected towards the surface through the boundary layer and hence are deposited.

- (5) electrostatics: when two surfaces are rubbed together and/or separated from each other electrostatic forces may occur. Most airborne particles are to some extent electrically charged as a result of collision of ions created by natural radioactivity and cosmic rays. These particles may be transported to an electrostatic field provided by a charged surface. Charged particles will be repulsed by a similarly charged surface but attracted by an oppositely charged surface and encouraged to deposit.
- (6) thermophoresis: if a temperature gradient is established between a surface and that of the surrounding air and when the latter is at a higher temperature, deposition of airborne particles occurs due to thermophoresis. This is because the gaseous molecules furthest away from the surface possess a higher energy than those near the surface and this energy imparts, in turn, a higher average velocity of gas molecules on the "warm" side of the particles such that transport of particles in the air stream is towards the "cold" surface.

1.7.2 Gravitational sedimentation

The process of gravitational sedimentation of a cloud of monodispersed particles has been investigated in great detail (Burgers, 1942; Slack, 1963; Adachi *et al*, 1978). The motion of small, spherical particles in a fluid is governed by particle inertia, gravity, buoyancy and drag forces from the relative motion of particle and fluid (Fuchs, 1964; Davies, 1966; Clift *et al*, 1978; Maxey and Riley, 1983).

Stokes (1850) having solved the equation of motion for a rigid spherical particle falling through a continuous viscous stagnant fluid at relatively constant velocity and neglecting inertial effects arising from the fluid being displaced by the particle, obtained the expression:

$$F_d = - 6 \pi \mu_g \cdot r_p \cdot V_s$$

where

F_d = drag force

μ_g = dynamic gas viscosity

r_p = particle radius

V_s = terminal settling velocity

The -ve sign indicates the opposite direction of terminal settling velocity to the drag force. The above equation is based on two assumptions. The first is that the inertial forces are negligible compared to viscous forces i.e.

$$Re = (r_p \cdot V_p / \mu_g) < 0.1$$

where

Re = Reynolds number

V_p = particle velocity

The second is that a no-slip boundary condition exists at the surface of the spherical particle. Stokes law was modified to include slip correction factor by Cunningham (1910) as:

$$F_d = - 6 \pi \mu_g \cdot r_p \cdot V_s / C(K_n)$$

i.e.

$$C(K_n) = 1 + A' \cdot K_n$$

$$K_n = \lambda / r_p$$

where

$C(K_n)$ = Cunningham slip correction factor

K_n = Knudsen number

λ = mean free path of the gas molecules

A' = constant

The empirical factor $C(K_n)$ proposed by Cunningham, was later evaluated by Davies (1945) as:

$$C(K_n) = 1 + K_n [1.257 + 0.4 \exp(-1.1/K_n)]$$

Millikan's data were re-evaluated by Rabee (1976) using a nonlinear least squares function fitting which lead to a better approximation:

$$C(K_n) = 1 + K_n [1.155 + 0.471 \exp(-0.596/K_n)]$$

Provided the particles are sufficiently small, the fluid force on a particle is simply a modified Stokes drag force which balances the gravitational forces as:

$$\frac{4}{3}\pi r_p^3(\rho_p - \rho_g)g = 6\pi\mu_g r_p \cdot V_s / C(K_n)$$

where ρ_p = particle density
 ρ_g = gas density
 g = acceleration due to gravity

Since $\rho_p \gg \rho_g$ then the terminal settling velocity on a horizontal surface is:

$$V_s = \frac{g \cdot C(K_n) \cdot \rho_p \cdot d_p^2}{18 \mu_g}$$

where d_p = particle diameter

Fuchs (1964) characterized the terminal settling velocity as:

$$V_s = g \cdot \tau$$

where τ = aerodynamic relaxation time

The deposition velocity due to gravitational sedimentation is proportional to the cross sectional area of the particle, and the ratio of its density to the gas viscosity. For surfaces having an angle of inclination (θ) to the vertical, the gravitational deposition velocity would change proportionally to $\cos(\theta)$.

To assess the airborne cleanliness in both a conventionally and unidirectionally ventilated cleanrooms, most investigators (Kethley *et al*, 1962; Hamberg, 1982; Stowers, 1984, 1985) have assumed that gravitational sedimentation is the only deposition mechanism to be considered.

Hamberg (1982), using fall-out rate data collected in cleanrooms, derived an empirical relationship to predict the number of particles settling due to gravity as:

$$\dot{n} = 2.851(10^3)(C)^{0.773}$$

where

\dot{n} = fall out rate (no. of particles $> 5 \mu\text{m}$ settled/ $\text{ft}^2/24$ hrs)

C = airborne concentration (no. of particles $> 5 \mu\text{m}/\text{ft}^3$ of air)

1.7.3 Inertial impaction

It has been demonstrated (Cooper, 1986; Liu and Ahn, 1986) that impaction is an important deposition mechanism under some circumstances (e.g. from a high velocity shaped jet), but is probably not an effective deposition mechanism to be considered in a cleanroom. Impaction is governed by the Stokes parameter (ψ) as:

$$\psi = U \cdot \tau / \ell$$

where ℓ = smallest dimension of the obstacle in the plane normal to the mean flow

U = average velocity of the air stream

τ = aerodynamic relaxation time

The study of particle impaction from variously shaped high velocity jets onto plates has attracted many investigators, because of its application in sampling instruments (eg. Cascade impactors). The first important investigation was by Albrecht (1931). Using potential flow equations of motion of the particles, he derived an expression for the flow field in a two-dimensional jet of ideal fluid impinging on a body collector. Because of the complexity of the equations, the trajectories were calculated by a step-by-step method. This general approach has been standard in all such calculations.

Later, Davies and Aylward (1951) developed a model for the flow field in a two-dimensional jet impinging on a flat plate. They used a simple approximation model for the flow field in the region immediately upstream of the surface and numerically calculated the trajectories of the particle. They then proposed a method for calculating the theoretical collection efficiency on the plate by introducing dimensionless parameters. This was defined as the ratio of the numbers of particles striking the surface, to the number of particles which would strike the surface if the particle trajectories were all in straight lines parallel to the direction of the undisturbed fluid flow. They plotted the efficiency of

collection against Stokes number for various air stream velocity and particle sizes. The theoretical data obtained showed that the efficiency increases rapidly as the distance between orifice and plate is reduced.

Ranz and Wong (1952) carried out experiments to obtain data which they compared with the mathematical model they derived. Their experiments entailed generating particles in the range of 0.34 to 1.38 μm . They studied both circular and rectangular jets at velocities ranging from 10 to 180 m/s; particles were very small compared with the collector dimension, so that the interception effect was negligible.

In general, the above workers have found that the theory derived overestimates the experimental deposition rates. This is to be expected due to the considerable simplification in the theoretical derivation and the accuracy of the model being dependent on the production of homogenous particles and accurate sizing of these particles. Deviation between theory and experiment can be further explained by the shattering of particles on impact with the plate and the failure of impacted particles to adhere.

1.7.4 Brownian (molecular) diffusion

It is well known from studies of aerosol collection by fibre media that Brownian diffusion can play a significant role in collecting particles under certain conditions. This mechanism is a major factor in the removal of small particles (usually $< 0.5 \mu\text{m}$) by high efficiency particulate air (HEPA) filters.

When the particle is very small compared to the mean free path of the gas molecules, the drag force (F_d) can be written as:

$$F_d = \frac{4}{3} \pi r_p^3 \cdot \delta_r (N_g \cdot M_g \cdot V_g) V_p$$

where

r_p = particle radius

δ_r = rebound correction factor

N_g = number of gas molecules per unit volume of gas

M_g = mass of gas molecules

V_g = mean velocity of gas

V_p = particle velocity

Because the small particles are moving randomly by the bombardment of gas molecules, the average motion has to be treated statistically. This method is known as "random walk". Einstein (1905) described the statistical motion in terms of the mean square displacement of a small particle in a time t as:

$$(\bar{x})^2 = (2 R \cdot T \cdot t) / (3 \pi \mu_g \cdot A_n \cdot d_p)$$

where

$(\bar{x})^2$ = mean square displacement

R = gas constant

t = time

A_n = Avogadro's number

μ_g = dynamic gas viscosity

T = absolute temperature

d_p = particle diameter

He then showed that:

$$(\bar{x})^2 = 2 D \cdot t$$

where D = Brownian diffusion coefficient

Furthermore he explained that the Brownian diffusion coefficient (D) can be written as:

$$D = K \cdot T \cdot B_m \quad (\text{Eq. 1.10})$$

where K = Boltzman's constant = 1.38×10^{-16} (dyne cm/K or erg/K)

B_m = dynamic mobility

As in the case of terminal settling velocity, it is necessary to apply Cunningham slip correction factor when dealing with small particles. This modifies the dynamic mobility (B_m) to:

$$B_m = C(K_n) / (3 \pi \mu_g \cdot d_p) \quad (\text{Eq. 1.11})$$

where $C(K_n)$ = Cunningham slip correction factor

The linear relationship between the flux and the concentration gradient for diffusion of particles in a stationary fluid is known as Fick's first law of diffusion.

In one-dimensional (x-direction) concentration gradient it reduces to:

$$J_x = - D \cdot \frac{\partial C}{\partial x}$$

where J_x = particle flux in x-direction

$\partial C / \partial x$ = concentration gradient in x-direction

When the fluid has the same properties in all directions, similar equations can be written in any direction as:

$$J_y = - D \cdot \frac{\partial C}{\partial y}$$

$$J_z = - D \cdot \frac{\partial C}{\partial z}$$

By considering an elemental volume of fluid in space and calculating the net rate of transport through the element, Fick derived the second law of diffusion in 3 dimensional concentration gradient as:

$$\frac{\partial C}{\partial t} = D \left[\frac{\partial^2 C}{\partial x^2} + \frac{\partial^2 C}{\partial y^2} + \frac{\partial^2 C}{\partial z^2} \right] = D \cdot \nabla^2 C \quad (\text{Eq. 1.12})$$

where $\partial C / \partial t$ = rate of change of concentration

Particle deposition due to Brownian diffusion on simple geometric body collectors can be predicted once a boundary layer calculation has been made. Hidy (1984) proposed a model for the diffusion velocity (V_{bd}) for a flat plate at some distance away from the leading edge in the direction of the mean flow (assumed laminar flow) as:

$$V_{bd} = 0.34 D (V_f \cdot \rho_g / \mu_g \cdot x)^{1/2} (\mu_g / \rho_g \cdot D)^{1/3}$$

where V_f = mean flow velocity

x = distance from the leading edge

ρ_g = gas density

Mathematical expressions have been derived (Stowers, 1984) for deposition due to Brownian diffusion between parallel plates by introducing a dimensionless number (γ') as:

$$\gamma' = (D \cdot L) / (V_f \cdot H^2)$$

where L = length of channel in the direction of flow

H = height of channel

It has been shown that Brownian diffusion is effective for γ' greater than 0.02. However, a useful conclusion from this study can be gained by using the analogy between the deposition in parallel plates and the unidirectional flow cleanrooms, assuming that the plates are the walls of a unidirectional cleanroom and air is flowing through it with an average velocity V_f . To predict the deposition rate of particles accumulated on the tube walls, an empirical relationship relating ratio of input (C) to output concentration (C_o) has been derived as follows:

$$C / C_o = 0.915 \exp(-1.88t) + 0.059 \exp(-22.3t) + 0.026 \exp(-151.8t)$$

To predict the deposition rates on surfaces, investigators have used the heat and mass transfer analogy. This is basically an extension of Reynolds analogy between momentum and heat transfer and depends on the similarity between transport mechanism for momentum, heat and matter. Liu and Ahn (1986) calculated the rate of particle diffusion (Brownian) and sedimentation on the semiconductor wafer surface in a unidirectional cleanroom using the correlation similarity between the mechanisms of particulate mass transfer and that of convective heat transfer.

1.7.5 Turbulent (eddy) diffusion

Theories of turbulent deposition in pipe flow have progressed much further than those for surface deposition in a turbulent-flow room or chamber.

A general approach to calculate the deposition velocity due to turbulent (eddy) diffusion has been to combine the turbulent (eddy) diffusion with Brownian diffusion giving the total diffusion model as:

$$J = - (D + D_e) \partial C / \partial x \quad (\text{Eq. 1.13})$$

where D_e = turbulent eddy diffusivity

The difficulty in evaluating equation (1.13) is in the determination of the turbulent diffusivity of particles. The basic assumption that the diffusivities of the particles

and of the fluid are identical has been extensively used. Once particle diffusivities are equated to fluid diffusivity, expressions for the latter must be found before the equation (1.13) can be integrated.

A model for assessing the effective particle diffusivity in the boundary layer of a turbulent fluid has been evaluated as:

$$D_{ep} = D_e + \nu^2 \cdot \tau$$

where D_{ep} = effective particle diffusivity

ν = root-mean-square (rms) fluctuating velocity of the fluid in a direction normal to the wall

τ = aerodynamic relaxation time

1.7.6 Electrostatics

Most airborne particles come into charge equilibrium with ions created by natural radioactivity and cosmic rays (Liu and Pui, 1987). Particles generated by atomization, powder dispersion or removal from a solid surface are usually charged. On the other hand, particles formed by vapour condensation are either neutral or carry only a low level charge.

Several investigators have studied the relationship between the charge carried and the size of the particle. Arendt and Kallman (1926) found that the charge carried by small fog particles in regions of high ion density can be approximately proportional to the particle radius. Kunkel (1950) carried out experiments which determined that the charge on dust particles is proportional to less than the square of the particle radius. Daniel and Brackett (1951) reported the proportionality between the average charge and the square of the particle radius.

It has been demonstrated (Willeke, 1980) that there are two forces responsible for depositing charged particles onto surfaces: one due to the image charge on the surface and one due to the mutual repulsion between like charges.

The velocity of a particle (V_c) due to an image charge towards a conducting surface is given by:

$$V_c = \frac{B_m \cdot q^2}{16 \pi \epsilon_0 \cdot x_s^2}$$

where q = charge carried by the particle
 ϵ_0 = permittivity of free space
 x_s = distance of the particle from the surface
 B_m = dynamic mobility of the particle

The time for the particle to reach the surface is given by:

$$t = \frac{16 \pi \epsilon_0 \cdot x_s^3}{3 B_m \cdot q^2}$$

The other charge deposition mechanism is due to mutual repulsion of the like charges causing a unipolar aerosol cloud to expand into the walls of the container. Wilson (1947), Fuchs (1964) and Faith *et al* (1967) have obtained an expression for the mutual repulsion deposition efficiency (P_{mr}) in a cylinder as:

$$P_{mr} = \frac{4 \pi C \cdot R_t^3 \cdot \tau'}{1 + 4 \pi C \cdot R_t^3 \cdot \tau'}$$

where τ' = dimensionless residence time
 R_t = tube radius
 C = number concentration of particles

The dimensionless residence time (τ') was derived by Yu (1977) for slug flow in a circular tube of length (L) as:

$$\tau' = \frac{B_m \cdot q^2 \cdot L}{4 \pi \epsilon_0 \cdot R_t^3 \cdot V_f}$$

1.7.7 Thermophoresis

The phenomena and theory of thermophoresis have been discussed by Epstein (1924). Later Waldmann and Schmitt (1966) modified the theory for the free-molecular regime. For particles much smaller than the mean free path of the gas molecules (λ), the motion of particles in a temperature gradient is easy to understand and the thermophoretic velocity (V_t) has been derived from the kinetic theory of gases by Waldmann and Schmitt (1966) as:

$$V_t = - \frac{3 \nu}{4(1 + \pi \alpha/8)T} \cdot \frac{dT}{dx} \quad (\text{for } d_p \ll \lambda) \quad (\text{Eq. 1.14})$$

where ν = kinematic viscosity of fluid
 α = accommodation coefficient (usually about 0.9)

$$\begin{aligned}
T &= \text{absolute temperature} \\
d_p &= \text{particle diameter} \\
\frac{dT}{dx} &= \text{temperature gradient}
\end{aligned}$$

The negative sign indicates that the motion is in the direction of decreasing temperature. As can be seen from equation (1.14), the thermophoretic velocity for $d_p \ll \lambda$ is not dependent on particle size.

It has been reported (Friedlander, 1977) that it is more difficult to explain the motion of particles larger than the mean free path of gas molecules. The explanation given by Kennerad (1938) is based on the tangential slip velocity that develops at the surface of a particle in a temperature gradient. This creep velocity is directed towards the high temperature side, propelling the particle in the direction of lower temperature. Epstein (1924) derived an equation for the thermophoretic velocity (V_t) by solving the equation of fluid motion with a slip boundary condition as:

$$V_t = - \frac{2 K_g \cdot \sigma}{2 K_g + K_p} \left[\frac{K_g}{P} \right] \frac{dT}{dx} \quad (\text{for } d_p \gg \lambda) \quad (\text{Eq. 1.15})$$

where

- K_g = gas thermal conductivity
- K_p = particle thermal conductivity
- σ = dimensionless coefficient
- P = gas pressure

The slip velocity (V_{slip}) has been defined as:

$$V_{\text{slip}} = \sigma \cdot \frac{K_g}{P} \cdot \frac{dT}{dx}$$

The value of σ used in the theory is usually 0.2. The thermophoretic velocity again does not depend on particle size. When the ratio of particle-to-gas thermal conductivities is not too high (less than about 10, as for oil droplets), the equation (1.15) is in good agreement with experimental data. However, for particles of higher thermal conductivity, such as sodium chloride with a $k_p/k_g \approx 100$, the equation (1.15) underestimates the thermophoretic velocity (V_t).

1.7.8 Deposition in a vessel

In attempting to gain a better understanding of the different surface deposition

mechanisms described previously and to estimate their significance in a room, it is advisable to turn to mathematical models developed for stirred tank reactors. A conventionally-ventilated cleanroom can be considered analogous to a stirred tank reactor with steady-state continuous flow, feed and product stream.

Wall loss rates are generally expressed by the wall loss coefficient β , defined as:

$$\partial C / \partial t = - \beta \cdot C$$

where $C(d,t)$ = particle size distribution function in the vessel

This equation is valid provided the aerosol in the vessel is well mixed. However there will be a small boundary layer near the walls whose volume will not be mixed. Its total volume is negligible compared to that of the vessel and should have little effect on the above equation.

Investigators (Fuchs, 1964; Stein *et al*, 1972) have suggested the loss rate coefficient (β) as:

$$\beta = \frac{V_s}{H} + \frac{S_A \cdot D}{V \cdot \delta} \quad (\text{Eq. 1.16})$$

where V_s = terminal settling velocity

H = height of the vessel

S_A = vessel surface area

D = Brownian diffusion coefficient

V = vessel volume

δ = diffusion boundary layer thickness

As demonstrated by Crump and Seinfeld (1981) the difficulty in evaluating the wall loss rate coefficient (β) is the determination of diffusion boundary layer thickness (δ); this is an abstraction and can not be measured. The diffusion boundary layer thickness (δ) depends generally on particle size, vessel shapes and intensity of mixing.

Experiments have been carried out by many investigators to investigate the validity of the equation (1.16). Van de vate (1972) using polystyrene latex sphere with diameters ranging from 0.09 to 1.3 μm obtained satisfactory results by using $\delta = 0.85$ mm in equation (1.16). However in his calculation he assumed the

density of polystyrene latex particles to be 950 kg/ m^3 , instead of the 1050 kg/ m^3 used in most aerosol publications.

Harrison (1979) also carried out experiments with polystyrene latex spherical particles and proposed an empirical relationship as:

$$\delta = 3.7 d_p^{-1.7} \quad (\text{Eq. 1.17})$$

where d_p = particle diameter

However the accuracy of equation (1.17) is doubtful, as with increasing particle diameter, one would expect the wall loss rate due to Brownian diffusion to decrease. The reason for this is not clear but one possibility is that deposition due to electrostatic charge could have affected his experimental results.

Crump and Seinfeld (1981) removed the inconsistency of hypothetical diffusion boundary layer thickness (δ) and proposed a theoretical model for the wall loss coefficient (β) in a vessel of arbitrary shape. Their model included deposition due to sedimentation, Brownian diffusion and turbulent diffusion and for a spherical vessel yielded to:

$$\beta = \frac{6(K_e \cdot D)^{1/2}}{\pi R_s} \cdot D_1 \left[\frac{\pi V_s}{2(K_e \cdot D)^{1/2}} \right] + \frac{V_s}{4 R_s / 3}$$

where K_e = eddy diffusion coefficient

R_s = radius of spherical vessel

D_1 is the Debye function given by:

$$D_1(x) = \frac{1}{x} \int_0^x \frac{t}{e^t - 1} dt$$

Crump and Seinfeld's (1981) theoretical model reduced to the formulae of Corner and Pendlebury (1951) for a cubical vessel as:

$$\beta = \frac{1}{L} \left[\frac{8(K_e \cdot D)^{1/2}}{\pi} + V_s \cdot \coth \left[\frac{V_s \pi}{4(K_e \cdot D)^{1/2}} \right] \right]$$

where L = length of the cubical vessel

and Takahashi and Kasahara (1968) for a cylindrical vessel as:

$$\beta = \frac{8(K_e \cdot D)^{1/2}}{\pi D_t} + \frac{V_s}{H} \cdot \coth \left[\frac{V_s \pi}{4(K_e \cdot D)^{1/2}} \right]$$

where D_t = diameter of the cylindrical stirred tank

The theory of Corner and Pendlebury (1951) was compared with the experiment carried out by Langstroth and Gillespie (1947) to observe the change in concentration with particle size of an ammonium chloride smoke in a chamber of approximately 1 m³ cube, for various intensities of mixing. The theoretical model agreed well with the experimental results obtained.

Okuyama *et al* (1977, 1984) also found good agreement between the theoretical deposition model proposed by Takahashi and Kasahara (1968) for wall deposition experiments in a cylindrical stirred, acrylic tank of surface area 1234.3 cm² and volume 2606 cm³.

Crump *et al* (1983) compared their theory derived (Crump and Seinfeld, 1981) with experiments in a spherical continuous-stirred tank reactors of approximately 118 litre capacity. The observed wall loss deposition rates were in good agreement with their theoretical model.

However, the theory of Crump and Seinfeld (1981) did not explain the deposition of charged particles investigated by McMurray and Rader (1985) in a Teflon smog chamber. In particular, measured wall deposition rates for particles in the range 0.1 to 1.0 μm exceeded prediction of the Crump and Seinfeld (1981) theory. They reported that one possible reason for this discrepancy was that electrostatic deposition were not included in the Crump-Seinfeld theory. They further demonstrated that Teflon tends to acquire electrostatic charge which may lead to a local electric field near the surface. Such fields will influence the deposition of charged particles. However, it has been reported (John, 1980) that if the wall material is a dielectric rather than a conductor, the image charge (-q) is replaced by:

$$\left[\frac{(\epsilon_r - 1)}{(\epsilon_r + 1)} \right] \left(\frac{1}{R_s - r_s} \right)^2$$

where ϵ_r relative permittivity (dielectric constant)

When image forces are dominant using electrostatic theory (Jackson, 1962), McMurray and Rader (1985) derived a vector equation to predict the electrostatic drift velocity of charged particles in Teflon film bags. Their equation was derived by balancing electrostatic and aerodynamic drag forces on the particle such that:

$$\vec{V}_e = \left[\frac{C(K_n) \cdot n^2 \cdot e^2}{48 \pi^2 \epsilon_0 \cdot \mu_g \cdot d_p} \right] \left[\frac{\epsilon_r - 1}{\epsilon_r + 1} \right] \left[\frac{1}{R_s - r_s} \right]^2 \hat{r}$$

where

\vec{V}_e = electrostatic drift velocity vector

$C(K_n)$ = Cunningham slip correction factor

n = number and sign of elementary charges on a particle ($n > 0$ for positively charged particles and $n < 0$ for negatively charged particles)

e = electron charge = 1.602×10^{-19} Coulombs

ϵ_0 = permittivity of free space = 8.854×10^{-12} Farad/m

μ_g = dynamic gas viscosity

ϵ_r = dielectric constant for Teflon = 2.01

r_s = spherical coordinate

\hat{r} = unit vector in the r direction

As demonstrated the airborne contaminant concentration may be reduced by deposition of the airborne particles. Thus to develop a mathematical model which can predict the airborne contaminant concentration, it was necessary to investigate theoretically and experimentally all the possible surface deposition mechanisms involved.

2. EXPERIMENTAL PROGRAMME

The objective of this project was to develop a practical model which could predict the cumulative airborne contaminant concentration within conventionally ventilated cleanrooms. Towards this end several experiments were carried out. These were concerned with:

- (1) Cleanroom air distribution performance.
- (2) Dispersal of airborne particles and bacteria by people.
- (3) Particle emissions from machines in cleanrooms.
- (4) Outdoor airborne particulate and bacterial concentration.
- (5) Surface-deposition of airborne particles in a chamber.
- (6) Verification of the airborne concentration model by monitoring of airborne particles and bacteria in industrial cleanrooms.

2.1 Cleanroom Air Distribution Performance

2.1.1 Introduction

The primary objective of this investigation was to assess the validity of the assumption of perfect mixing used in the mathematical models derived (Chapter Three). The secondary object was to gather information on the air movement in conventionally-ventilated cleanrooms and establish the relative merits of various air terminal devices.

Parameters which were established, from a review of the literature, as having the greatest influence on air mixing, assuming constant geometry of the room and the obstructions within it, were:

- (i) Type of air terminal device.
- (ii) Air supply flow rate into the room.
- (iii) Differential temperature between the supplied air and the room air.
- (iv) Location of the contaminant source.

These parameters were therefore investigated as factors contributing to the degree of mixing of supplied air with room air.

2.1.2 Materials and methods

Experiments were carried out in a conventionally-ventilated cleanroom 7m x 4.61m x 2.76m (height) in size, this being the diagnostic filling area at Organon Pharmaceutical Manufacturing Laboratory Ltd. at Newhouse near Glasgow. Three air supply terminals discharging air directly from HEPA filters were located along one side of the ceiling (Figure 2.1). The exhaust air was extracted at low level through three grilles on the opposite wall (Figure 2.2). A stainless steel table was placed in the cleanroom to simulate the presence of an obstruction caused by a filling machine (Figures 2.1 & 2.2).

The four types of air terminal devices studied were:

- (1) *Multislot Diffusers*. These were concentric square diffusers (35cm x 35cm) with three slots uniformly distributed along four sides. The air supply discharged in thin streams in multiple layers in four directions.
- (2) *Adjustable Vane Grilles*. These were rectangular (50cm x 48cm) with 25 adjustable blades, one behind the other, which could be adjusted to discharge the supply air in an upward or downward direction. The blades were adjusted at an angle of 70° to the horizontal, so that the air supply would be directed towards the working table.
- (3) *Dump*. These were a non diffuser type the air being discharged directly from the HEPA filter (40cm x 40cm) into the room, as shown in Figure 2.3. No additional frames were added.
- (4) *Jet*. These were the same as the *dump air terminal device* but with additional frames built round the HEPA filter to minimize the air entrainment into the air just under the filter (Figure 2.3). It was expected that they would perform identically to the air terminal devices normally found in cleanrooms.

The ventilation rate was varied to correspond to a nominal 20, 15 and 3 air changes per hour. The air supply flow rates were measured using an Abbirko rotating-vane anemometer and a Balometer (an air-quantity measuring box of exit area 462 cm²). For each ventilation scheme the volume of supply and exhaust air were adjusted to the prescribed value and the differential pressure between the

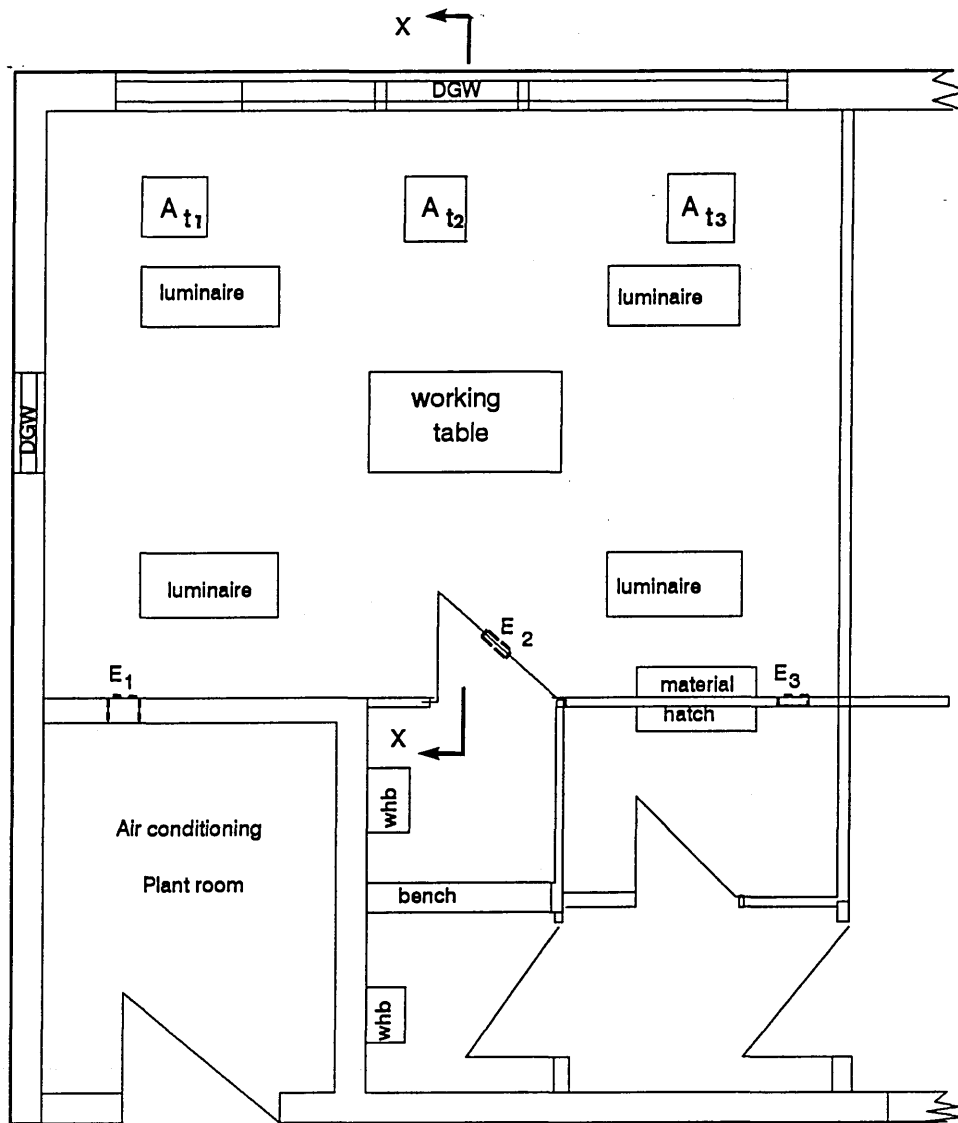


Fig. 2.1 Plan of the diagnostic filling area at Organon.

Legend:

A_t = Air terminal device

E = Exhaust grille

whb = Wash hand basin

DGW = Double glazing window

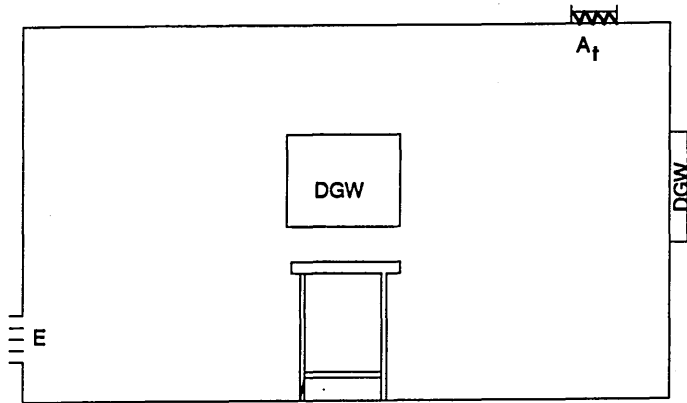


Fig 2.2 Sectional view (XX) of the diagnostic filling area at Organon

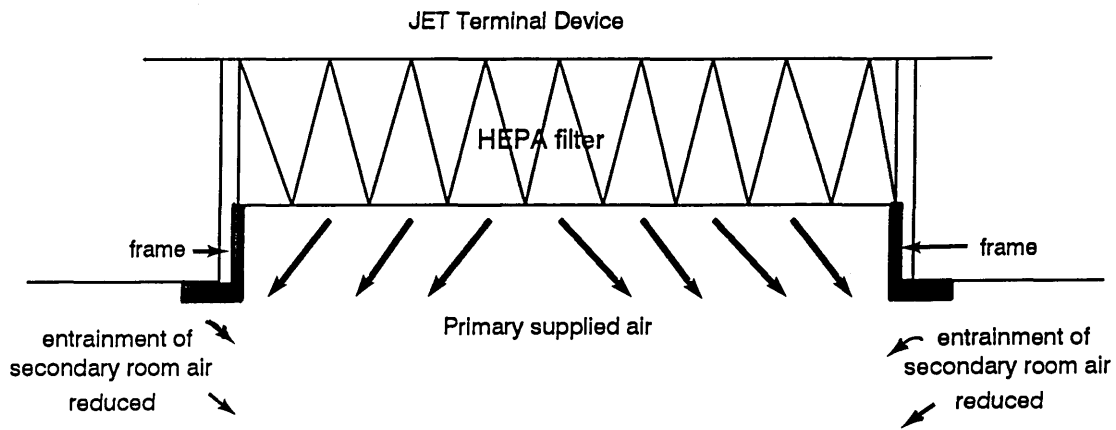
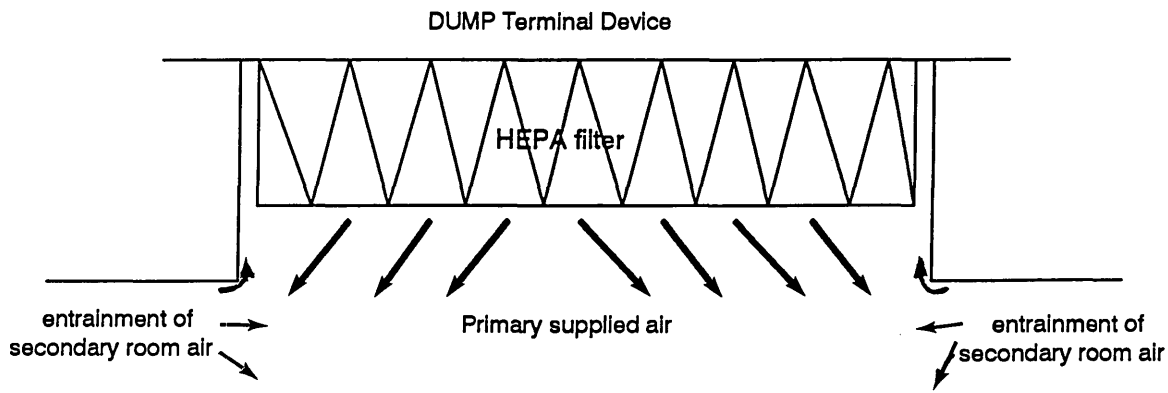


Fig. 2.3 Comparison of DUMP and JET air supply

room and its surroundings checked using inclined manometers to ensure that the room was positively pressurised with respect to its adjacent areas. The room was allowed to equilibrate under the specific ventilation rate and differential temperature conditions. The room, when supplied with 20 and 15 nominal air changes per hour, was in positive pressure with the three exhausts extracting air. When the ventilation rate was reduced to 3 air changes per hour, it was found that the room was no longer in positive pressure, the air supplied to the room being less than the volume extracted. The two exhaust (E_1 and E_3) louvres were closed to obtain the minimum air intake and a positive pressure in the room was re-established.

The supply air temperature was varied to obtain differential temperatures between it and the room air temperatures of 0K, +2K (supply air colder) and -2K (supply air hotter). The temperature differential was limited to -2K (supply air hotter); because the high heat gains in cleanrooms makes the requirement for a hot air supply unlikely.

Temperature measurements were made using a Comark instrument with copper-constantan thermocouples. One sensor was placed just below the face of the HEPA filter to measure the air supply temperature and another in the exhaust to measure an overall average ambient temperature. The supplied air temperature was adjusted by thermostat setting in the air conditioning plant. However maintenance of a steady-state temperature differential was not possible with the automatic controls and it was necessary to adjust the air conditioning plant manually, as required, when a deviation was found. Because the thermal load has a strong influence on the air movement in the room, continuous monitoring of thermal condition and manual adjustment throughout the experiment was maintained.

A di-octyl phthalate (DOP) cold particle generator was used to generate particles. The dispersion rate was adjusted, so that the particles were not emitted with high velocity. This ensured that the smoke generated did not have appreciable momentum relative to room air as to affect the air movement and

mixing process in the room. The points in the room where the particles were dispersed are discussed below.

To allow for experimental variation, each individual test was carried out three times at random intervals. All tests were conducted with one person in the room, lights on and the working table in position.

To maximize the insight that could be gained from the experiments, the sampling (particle concentration and velocity) locations were chosen to include representative regions of the room air. Hence, samples were taken from points in the region of entrainment, region of turbulent mixing, region of stagnant or still air and from the exhaust air to provide an overall picture of the air movement in the room.

The experimental work was carried out in five parts.

2.1.2.1 contaminant penetration into the air supply

Tests were carried out to investigate the amount of air entrained from the room into the clean zone of the air supplied by terminal devices. This was done by continuously releasing smoke at four points around the middle air terminal device (A_{t2}) and measuring the concentration of smoke that penetrated into the clean zone of supplied air.

The investigation started with *dump* air supply. It was observed that the inner edge of the HEPA filter drew in the smoke from the room and caused a flow of smoke inwards and upwards towards the negative pressure area under the filter (Figure 2.3). The smoke then entrained and rapidly mixed with the supplied air. The situation was rectified by introducing rectangular metal frames round the HEPA filter so the air discharged unidirectionally and minimized the air entrainment (Figure 2.3). The area under two types of air supply (*dump and jet*) was studied. Particle counts were taken at the air supply face to give a background reading. Relative to this background value, particle counts were taken at sampling points under the air terminal device, and the zones of equal particulate concentration (Isopleths) determined. These were defined as varying percentages of particle penetration into the zones.

2.1.2.2 air movement

Tests were carried out to make a detailed assessment of the room air movement. Two perpendicular sampling grids along major and minor axes of the room were assembled. The air movement at each sample point on the grids was characterized by direction and speed. A hand-held smoke-puffer along with a hot wire anemometer (Airflow Development Ltd - Model TA400) were used to visualize the mean direction and measure the mean air stream velocity at each sampling point. It was necessary to measure air stream velocity over 30 seconds to obtain a reliable mean value, since the air movement was turbulent, having a large amplitude and a low-frequency dominant fluctuation.

The hot wire anemometer was calibrated at Glasgow University using a low speed wind tunnel and a joss stick. Smoke was generated by burning a joss stick placed at one end (close to the fan) of the wind tunnel. The smoke was observed and the time taken to travel two metres to the remote end of the tunnel was recorded. The velocity calculated was then compared to the readings on the hot wire anemometer placed at the remote end of the tunnel. The whole procedure was repeated for different fan speeds. The hot wire anemometer was shown to be greater than 95% accurate over the range 0.17 to 0.59 m/s.

Air movement patterns along major and minor vertical sections of the room for all the air terminal devices (*multislot, adjustable vane, dump and jet*), ventilation rates (20, 15 and 3 AC/hr) and differential temperatures (0K, +2K supply air colder and -2K supply air hotter) were obtained. In the first 14 experiments a large number of points were measured in the room. It was considered that such detail was not necessary and fewer points were measured after experiment 14.

2.1.2.3 ventilation effectiveness as assessed by decay rates

Smoke was released into the room in a 10 seconds burst. The smoke was generated by the DOP generator pressurized at 4.6 kN/m^2 (kPa) by a pump. The smoke was mixed for about 2 minutes by a small fan to an even airborne concentration and the decay of the smoke particles was then continuously recorded

at three different sampling points. The sampling point locations, which were 1m from the floor, were:

- Position No. 1 Directly below the central air terminal device A_{t2} .
- Position No. 2 Middle of the room on top of the working table.
- Position No. 3 Near the middle exhaust E_2 .

A sampling probe from the Royco airborne particle counter (sampling rate of 0.1 ft³/min) was placed at each sampling point in turn. Every minute, the automatic particle-counter simultaneously recorded concentrations of airborne particles greater than or equal to 0.5 μ m and 5.0 μ m.

Each test was continued until the airborne concentration decayed by about 99% of its initial value.

To assess the effectiveness of various ventilation schemes a dimensionless quality, referred to as performance index (PI), was used. This expressed the ability of the supplied air to dilute the contaminants generated in the room. The performance index (PI) at each sampling location, for each ventilation scheme, was calculated from:

$$PI = N / N_{eff}$$

where N = theoretical ventilation rate (air changes/hour)

N_{eff} = effective ventilation rate (air changes/hour)

The theoretical (nominal) ventilation rate (N), based on perfect mixing, was evaluated from the equation:

$$N = Q / V \qquad \qquad \qquad (Eq. 2.1)$$

where Q = total volumetric flow rate into the room (m³/hr)

V = room volume (m³)

The effective ventilation rates (N_{eff}) at the three sample locations were estimated graphically by plotting the natural logarithm of the smoke concentration (C) remaining at a given time, against the time (t), fitting the best straight line through the linear portion of the curve and evaluating the decay slope from the relation:

$$N_{\text{eff}} = (1 / t) \ln (C_i / C_t)$$

where

C_i = measured concentration at time zero (particles/ft³)

C_t = measured concentration at time 't' (particles/ft³)

t = time taken from ' C_i ' to ' C_t ' (hr)

2.1.2.4 ventilation effectiveness as assessed by lateral air distribution

To represent contamination released in the peripheral area of the room, smoke was released continuously through a plastic tube placed on the centre of the end air terminal device (A_{t3}). To establish the effectiveness of ventilation in mixing the air across the length of the room a sampling probe of the Royco airborne particle counter was placed in the three exhausts (E_1 , E_2 , E_3) to measure the particle concentration. Each ventilation scheme was compared by calculating the PI for each exhaust from:

$$PI = C_m / C$$

where C_m = measured steady-state concentration (particles/ft³)

C = theoretical steady-state concentration, assuming perfect mixing (particles/ft³)

The theoretical airborne particulate concentration (C), neglecting the surface losses caused by deposition and assuming perfect mixing, can be evaluated from:

$$C = S / Q$$

where S = release rate of particles (particles/min)

Q = total flow rate of supplied air (m³/min)

The release rate (S), neglecting leakage from the room, was estimated from:

$$S = (C \cdot Q)_{E_1} + (C \cdot Q)_{E_2} + (C \cdot Q)_{E_3}$$

$$\therefore PI = \frac{C_m \cdot Q}{(C \cdot Q)_{E_1} + (C \cdot Q)_{E_2} + (C \cdot Q)_{E_3}}$$

The subscripts 1, 2 and 3 denote the corresponding exhaust numbers (E_1 , E_2

and E_3) with its air volume outlet and particulate concentration.

To measure the quantity of air flowing out through exhausts, an Abbirko rotating-vane anemometer was used to measure the average velocity at the exhaust grille and this was multiplied by the net area of the grille. The total amount of air was the sum of the volumes flowing out of all the three exhausts. To determine the average velocity, the grille face was divided into five equal spaces, along the centre line of the length of the grille. The velocity was measured at the approximate centre of each of these and the average velocity calculated. The inside dimensions (length and width) of the grille were measured to obtain the area of the air exhaust. A correction of 15% of the face area was allowed for the space occupied by the vanes in the grille. The quantity of air was then determined.

2.1.2.5 ventilation effectiveness as assessed by constant source dispersion

DOP smoke was continuously released to simulate contamination dispersed by an operator's working activities. The release positions were alternated from between the area below the central air terminal device and the table (R_{p1}) to between the central exhaust and the table (R_{p2}). When release was from R_{p1} , air samples were taken from all three exhausts (E_1, E_2, E_3), the working table (position No 2) and near the central exhaust (position No 3). When it was from R_{p2} air samples were taken from all three exhausts (E_1, E_2, E_3), the working table (position No 2) and beneath the central air terminal device (position No 1).

Tests were carried out for all combinations of air terminal devices (*multislot, adjustable vane, dump* and *jet*), differential temperatures (0K, +2K supply air colder, -2K supply air hotter) and nominal ventilation rates (20, 15 and 3 AC/hr).

The effectiveness of various air supply in diluting contaminants generated in the room was compared by means of the performance index defined as:

$$PI = \frac{C_m \cdot Q}{(C \cdot Q)_{E_1} + (C \cdot Q)_{E_2} + (C \cdot Q)_{E_3}}$$

To study the importance of parameters affecting the mixing of supply air with room air it was necessary to use a statistical method as there is no true classical

relationship among the studied variables. This statistical method, namely multiple regression analysis, has to rely on empirical evidence to develop relationships among all the studied variables. The analysis quantified how the mixing of supplied air with the room air, as expressed as a PI, is related to a set of explanatory variables. A statistical software package (Minitab) was used to construct empirical relationships from the test results as follows:

$$PI = A + K_1 \cdot N + K_2 \cdot \Delta T + K_3 \cdot A_t + K_4 \cdot R_p$$

where

A = constant

N = ventilation rate (air changes/hr)

ΔT = differential temperature (K)

A_t = air terminal device

R_p = release position of smoke

The quantities K_1 , K_2 , K_3 and K_4 are called partial regression coefficients and each measures the variation in the mixing (performance index) due directly to the variation in the respective variables.

The statistical significance of each variable was assessed by using t-ratio analysis where the results were converted into the probability significance level.

2.2 Dispersal of Airborne Particles and Bacteria by People

2.2.1 Introduction

This part of the programme was designed to obtain data on dispersal of airborne contamination by people which could be utilized in the mathematical models derived (Chapter Three). To determine the amount of airborne contaminant dispersion, people were studied in a dispersal chamber.

2.2.2 Description of dispersal chamber

The dispersal chamber used is shown in Figure 2.4. It was 0.68 m x 0.52 m x 2 m high (volume of 25 ft³ or 0.71 m³), being metal framed with perspex fixed all round it. On one side of the chamber was a door. Air was drawn from the exterior by a variable speed centrifugal fan (A) on top of the chamber, and discharged unidirectionally into the chamber through a HEPA filter (B) at a

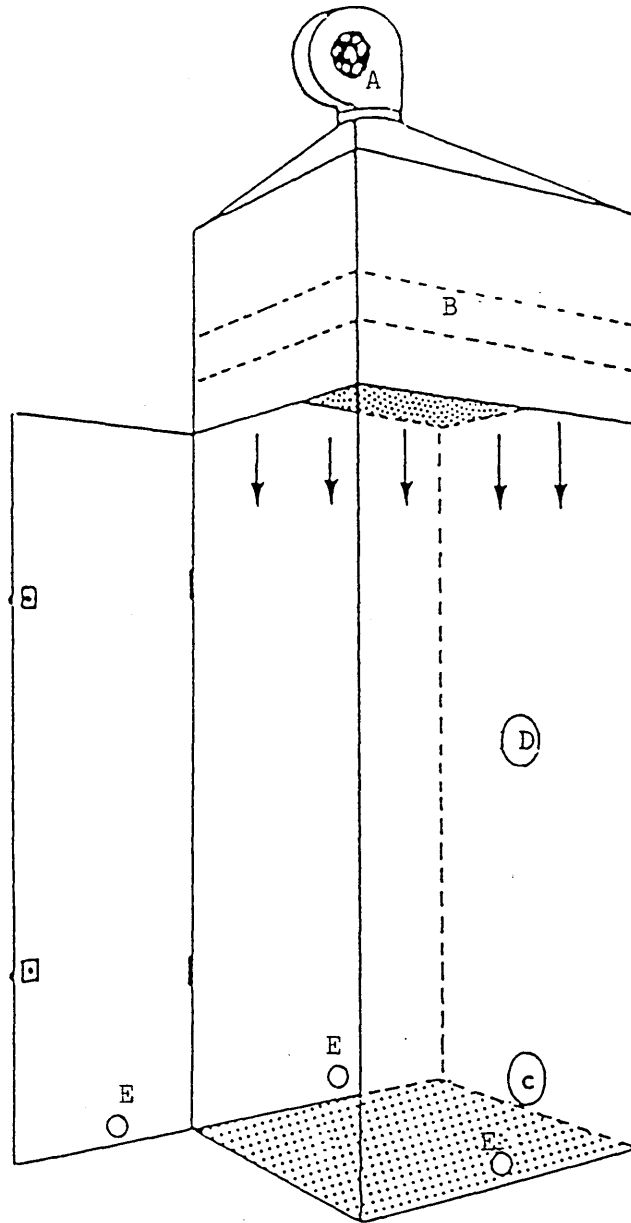


Fig. 2.4 Diagram of dispersal chamber.
 (A)centrifugal fan;(B)HEPA filter;
 (C) particle sampling port;(D)bacteria
 sampling port;(E)exhaust ports.

normal flow rate of 720 l/min (25.4 ft³/min). Air was extracted at a rate of 0.1 ft³/min (2.83 x 10⁻³ m³/min) by a sampling probe of the Royco airborne particle counter through sampling port (C). Air was also extracted by a bacterial sampler (Cassella slit sampler) at a rate of 700 l/min (24.7 ft³/min) through sampling port (D). The air supply was sufficient to replace the total sampled air volume of 700 l/min (24.7 ft³/min) and to maintain a slight positive pressure inside the chamber, even when the subject was exercising (this was checked by an Abbirko rotating-vane anemometer at exhaust ports E).

2.2.3 Experimental methods

Observations were made on 55 subjects (25 male, 30 female). These were volunteers from personnel working at Organon Pharmaceutical Manufacturing Laboratory Ltd. and the Mechanical Engineering Research Annexe, Glasgow University. Each subject was tested whilst wearing two types of clothing:

- (1) Personal indoor clothing. This consisted of trousers (both male and female) and shirts or blouse with or without jerseys and with clean plastic overshoes over their shoes.
- (2) A ceramic polyester coverall worn on top of personal indoor clothing as was the usual working practice at Organon Laboratories. This was a hot calandered polyester produced in the UK by Carrington Performance Fabrics Ltd. The coverall was tucked into knee-length boots and a separate hood, covering a mouth mask, was tucked into the neck of the coverall leaving only the eyes bare.

The test procedure was as follows:

- (1) The chamber was flushed with clean air at 720 l/min until the airborne particle count was practically zero.
- (2) The subject wearing the required clothing entered the chamber.
- (3) The air supply was increased to its maximum with the subject at rest until the airborne particle count shown on the Royco was reduced to practically zero and became steady.
- (4) The air supply was then reduced to normal (720 l/min).

- (5) The subject started marching to the beat of a metronome (1 beat/sec), for 2 minutes in the case of personal indoor clothing and 6 minutes in the case of ceramic polyester coverall.
- (6) After the first minute of the exercise, the bacterial sampler was switched on for the durations specified below:
- (i) 30 secs for male wearing personal indoor clothing
 - (ii) 1 min for female wearing personal indoor clothing
 - (iii) 5 mins for all wearing polyester ceramic coverall
- (7) Bacterial air samples were taken by the slit sampler onto bacterial plates containing Tryptone soya agar (Oxoid Ltd). This contained 37.5% Tryptone, 12.5% soya peptone, 12.5% sodium chloride and 12.5% agar w/w. The plates were then incubated for 24 hrs at 37°C before counting the bacterial colonies which had grown. To minimize errors, plates were tested for sterility before use.
- (8) The automatic Royco airborne particle counter was set to record simultaneously concentrations of particles greater than or equal to 0.5 μm and 5.0 μm, at one minute intervals during the period of exercise.
- (9) The subject left the chamber and the air supplied was increased to a maximum to flush the chamber; the chamber, the step into the chamber and the floor of the experimental room was disinfected with 70% Isopropanol in water.

The airborne contaminant (bacteria and particles) dispersion rates from each subject was calculated as follows:

$$S = C_{\max} \cdot Q \quad (\text{Eq. 2.2})$$

where S = airborne contaminant dispersion rate (bacteria or particles/min)

C_{\max} = airborne contaminant concentration (bacteria or particles/m³)

Q = volumetric flow rate of air supplied into the chamber (m³/min)

As the total volume of air supplied into the chamber was 0.72 m³/min then the

equation (2.2) simplifies to:

$$S = 0.72 C_{\max}$$

2.3 Particle Emissions from Machines in Cleanrooms

2.3.1 Introduction

At the present time, there is little published information on particle emission from machines. To gather realistic data for utilization in the airborne contaminant concentration model (Chapter 3) experiments were carried out to measure the particle emission from a Bausch & Stroebel as well as a Bosch-Strunck vial-filling machine.

2.3.2 Materials and methods

2.3.2.1 Bausch & Stroebel vial-filling machine

The experiment was conducted in the conventionally-ventilated cleanroom at Organon Laboratories which has been described previously (size 7m x 4.61m x 2.76m height). The three air terminal units had adjustable vane grilles (size 50cm x 48cm with 25 individual blades). These were located along one side of the ceiling. Exhaust air was normally extracted at low level through three grilles on the opposite wall (Figures 2.1 and 2.2). However, two of these exhausts were blocked so that the particles generated in the room would pass through only one exhaust. A sampling probe of a Rion light-scattering airborne particle counter was placed in the exhaust to measure the number of particles and their size distribution.

Two tests were performed. In the first test, an operator wearing cleanroom clothes (ceramic polyester coverall, mask, full hood, gloves and knee length boots) entered the room, switched on the vial-filling machine, attended to the machine as it filled ampules at 1200/hr. In the second test, the operator simulated her normal working activities but with the machine switched off.

Every minute, the automatic particle counter simultaneously measured and recorded concentrations of airborne particles greater and equal to five different diameters (0.3 μ m, 0.5 μ m, 1 μ m, 2 μ m and 5 μ m). The flow rate of the air sample withdrawn from the exhaust by the particle counter was 1 ft³/min. The

experiments were continued for 16 minutes in the first experiment and 13 minutes in the second.

The air supply flow rates were measured using an Abbirko rotating-vane anemometer and the Balometer (air-quantity measuring box of exit area 462 cm²).

It was found experimentally that the airborne particle concentration obtained for both tests were a percentage of the theoretical steady-state concentration which had not been reached. However the dispersion rate in the room was calculated from the decay equation:

$$C_t = \frac{S}{Q} (1 - e^{-N \cdot t}) + C_i \cdot e^{-N \cdot t} \quad (\text{Eq. 2.3})$$

where

C_t = concentration at time 't' (particles/m³)

C_i = initial concentration at time t=0 (particles/m³)

S = dispersion rate (particles/min)

N = air change rate (AC/hr)

Q = volumetric flow rate into the room (m³/min)

t = time (hrs)

The air supply velocities from the three adjustable vane grilles using the Balometer (exit area 462 cm²) were 3.15, 3.03 and 3.04 m/s. This resulted in a volumetric flow rate of 1534 m³/hr giving nominal ventilation rate of 17.22 air changes per hour.

The average particles generated with the operator working and machine running was calculated as well as the average particles generated with the operator only working in the room. The results were subtracted to give the particles generated from the machine.

2.3.2.2 Bosch-Strunck vial-filling machine

The experiment was carried out at a pharmaceutical manufacturing company (Sandoz) in France. These were kindly carried out by Mr Gonzales. Open ampules were washed in a washing machine, sterilized in a tunnel and entered into a plastic film isolation system. There they were filled with either 1 ml or 2 ml

of fluid by a Bosch-Strunck AVR E. 06 filling machine allowing 80,000 ampules to be filled a day. Particle concentration measurements were carried out 20 cm above the filling point for two different particle diameters ($\geq 0.5\mu\text{m}$ and $\geq 5.0\mu\text{m}$).

The steady-state particle generation rate was calculated from the following:

$$S = C_{\text{max}} \cdot Q$$

where

S = steady-state particle generation-rate (particles/min)

C_{max} = steady-state airborne-particulate concentration
(particles/ft³)

Q = total volumetric flow rate of supplied air (ft³/min)

As the total volumetric flow rate of supplied air into the isolation system was 294 ft³/min (0.14 m³/s), the equation reduces to:

$$S = 294 C_{\text{max}}$$

The steady-state average particulate concentration with the machine running was calculated as well as the average background particulate concentration. The results were subtracted to give the particulate generation rate from the machine.

2.4 Outdoor Airborne Particulate and Bacterial Concentration

2.4.1 Introduction

Experiments to measure the airborne bacteria and particles present in the outdoor atmosphere were carried out in different climatic conditions (wind, sun and rain) at different locations (urban and rural) to gain realistic data for incorporation in the mathematical models.

2.4.2 Materials and methods

The Royco airborne particle counter was used to measure the concentration of particles ($\geq 0.5\mu\text{m}$ and $\geq 5.0\mu\text{m}$) in the outdoor air. Twenty readings were taken for each condition and averaged.

Bacterial air samples were taken by a Casella slit sampler, drawing air at 700 l/min, onto Tryptone Soya agar (Oxoid Ltd) plates. The duration of air samples

was 5 mins and three samples were taken for each condition.

2.5 Surface-Deposition of Airborne Particles in a Chamber

2.5.1 Introduction

To gain a better understanding of the different surface-deposition mechanisms and to estimate their significance, experiments were designed and carried out as detailed below. The ultimate objective was to exclude mechanisms of negligible significance from inclusion in any proposed mathematical models suitable for adaption as a software package.

2.5.2 Description of chamber

The chamber used to study particle deposition was a 1.53 x 0.84 x 0.94 m glove box, comprising of mild steel frame with perspex glazing. One side was removable to allow access. The experimental apparatus is shown in Plates 2.1 and 2.2.

2.5.3 Agitation of air and calculation of fan power transmitted to air in chamber

A double-bladed stirrer was used to produce agitation and mixing of air in the chamber. Two stirrers were used, having blade dimensions of 170 x 64 mm and 50 x 62 mm, respectively, both types having a blade pitch angle of 5°. The stirrer was supported on a vertical axle passing down through the centre top of the chamber and driven by an air motor system external to the chamber. The speed of rotation was determined with the aid of a Tachometer revolution counter and the amount of energy dissipated into the chamber by each of the stirrers was determined by using a pulley brake system.

Calibration of the stirrers was achieved by measuring the speed of rotation at set air pressures (motive force) with varying imposed weights (braking power) and converting the data obtained to torque power by use of equation (2.4). This was done (i) when the shaft only was revolving and (ii) the revolving shaft with each type of stirrer.

$$TP = 10^{-6} g \cdot \ell_p (\omega/60) (W_s - W_d - W_i) \quad (\text{Eq. 2.4})$$

where TP = torque power (watts)

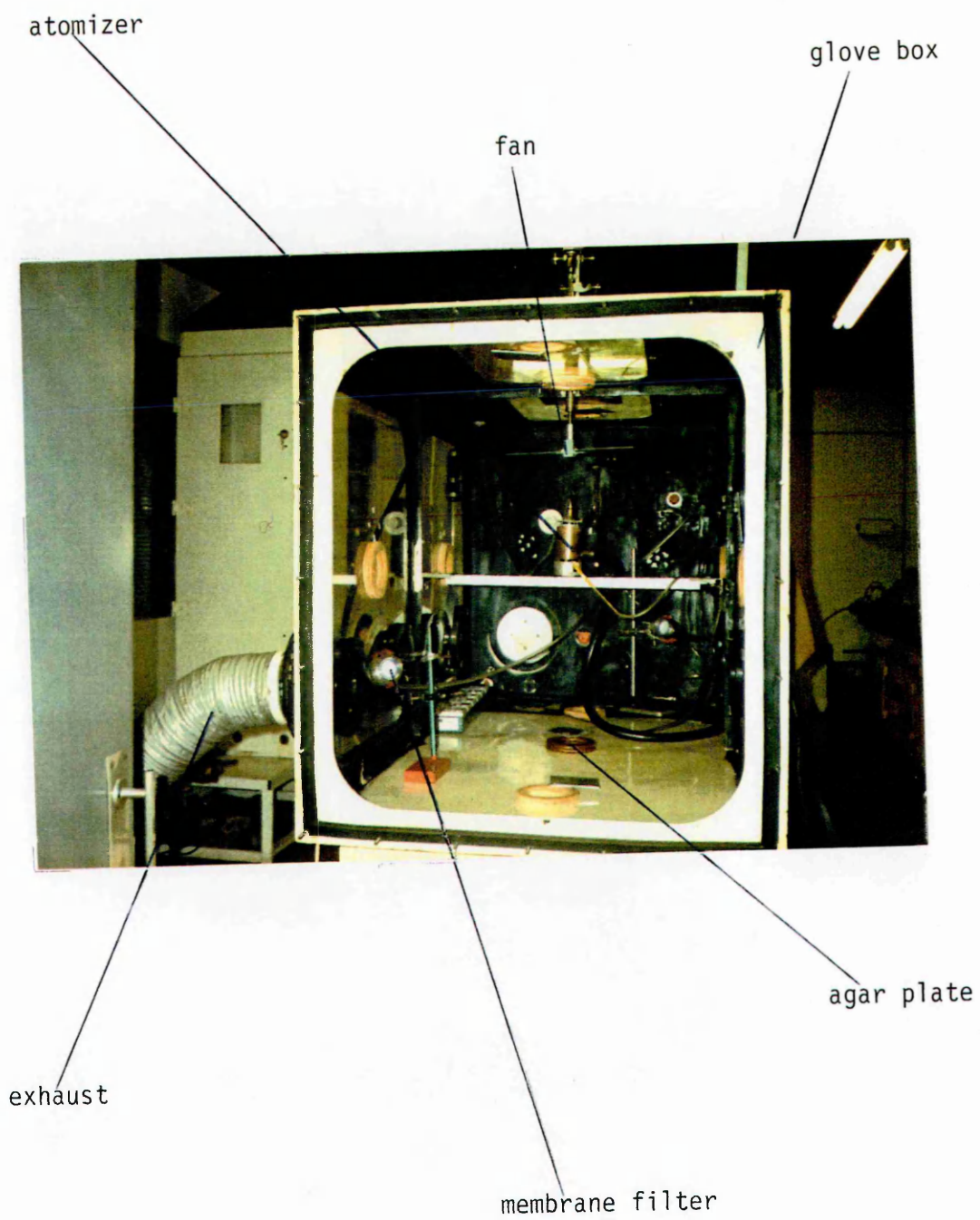


Plate 2.1 Experimental apparatus for studying particle deposition.
Front elevation of the glove box.

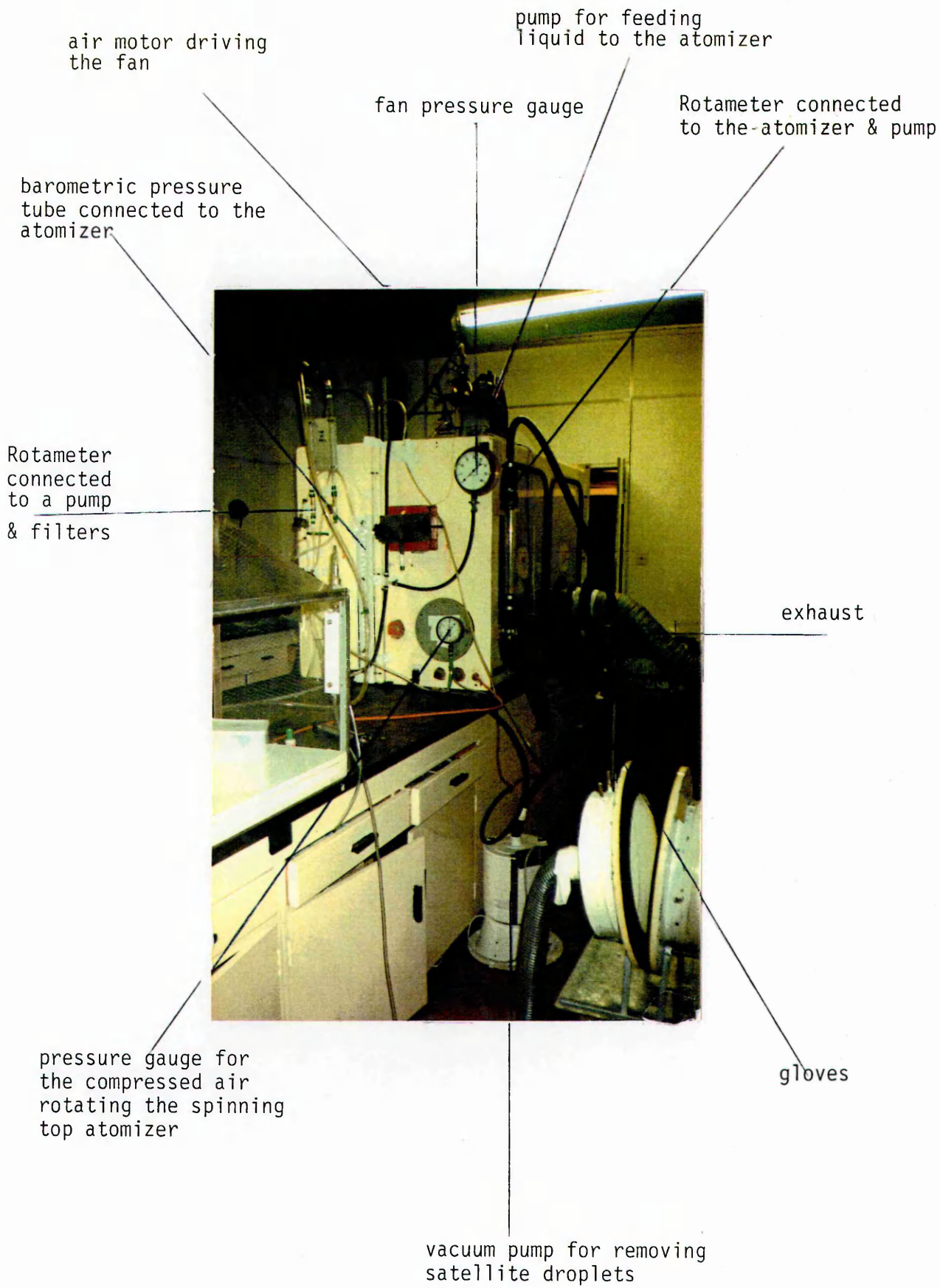


Plate 2.2 Experimental apparatus for studying particle deposition. Side elevation of the glove box.

- W_s = spring weight (gms)
- W_d = dead weight of the pan (usually 50 gms)
- W_i = imposed weight on the pan (gms)
- g = acceleration due to gravity (9.81 m/s^2)
- ℓ_p = circumference of the pulley (144 mm)
- ω = angular velocity of rotation (rev/min)

Fan power was derived for each type of stirrer. This being the difference between torque power of the shaft with stirrer less the torque power of the shaft only. From this data, graphs of fan power versus speed, speed versus pressure and fan power versus pressure were drawn.

To calculate the equivalent air change rates produced in the chamber, each of the blades and air driven motor was placed at one end of a duct and the effective air speed at the other end was measured by either an Abbirko rotating-vane anemometer for speeds in excess of 0.25 m/s or a DISA low velocity anemometer for speeds below 0.3 m/s. The revolutions per minute of the blades in the duct was established which corresponded to equivalent of 20 and 200 air changes per hour in the chamber; the former being the air change rate often found in conventionally-ventilated cleanrooms and the latter approaching that used in unidirectional cleanrooms.

2.5.4 Particle production

Droplets were produced by an air-driven spinning-top, originally designed by Walton and Prewett (1949) and later modified by May (1966). This spinning-top atomizer was built in the Engineering Workshop of Glasgow University to the design shown in Figure 2.5. The major part of the instrument is a cone-like top that is rotated by jets of compressed air. The pressure of the jet was measured by a barometric pressure tube and ranged between 20 and 60 cm Hg. Operational stability was provided by an oil-damped flexible-metal bellows as a stator-mounting and a minimum of sprung weight. In order for the system to have a correct viscous damping fluid of 500-1000 cp, as suggested by May (1966), a 15% w/w solution of polystyrene moulding chips in dibutylphthalate was used.

A fine continuous jet of a solution containing 80% ethanol (Aq), spores of

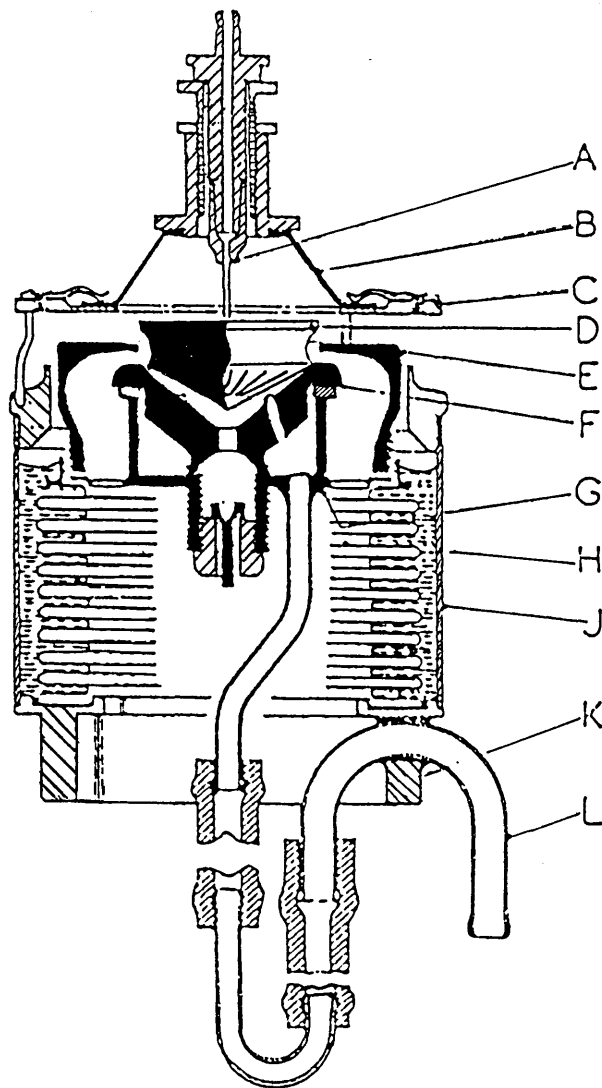


Fig. 2.5 Diagram of spray for homogeneous particles

- Legend: (A) tube (B) cap piece (C) hypodermic needle
 (D) spinning top (E) light alloy dome
 (F) stator (G) compressed air supply housing
 (H) bronze bellows (J) outer cylindrical wall
 (K) base ring (L) external compressed air pipe

Bacillus subtilis var. *globigii*, commonly known as *Bacillus globigii* and a varied concentration of Potassium iodide (KI) was introduced through the tube (A) on the lower end of which was a hypodermic needle (C) which fed to the centre of the upper surface of the spinning disk and sprayed it off the edge as droplets. The clearance between the tip of the needle and the flat upper surface of the rotor was adjusted and precisely centred over the rotor for correct spraying. The number of particles atomized was controlled by adjusting the feed rate and spray time. The feed rate was also optimized to avoid flooding the disk, thus minimizing the effect of coagulation and over-rapid surface deposition.

Originally, for particles other than 0.8 μm , the particles produced were heterogeneous in size and shape. This was due to the secondary production of satellite droplets approximately one fourth of the main droplet size. Removal of these satellite droplets was satisfactorily achieved throughout the main experiments by applying a suction pump to the body of the generator, thus giving homogeneity.

2.5.5 Particle sizing

2.5.5.1 wet sizing

A complete size calibration of the wet airborne droplets projected from the rim of the spinning disk was made. This was done by the method suggested by May (1966) and entailed preparing a magnesium oxide layer by moving burning magnesium ribbon to and fro under a glass slide. The oxide which adhered to the glass was smooth, soft and gave a layer of adequate thickness for droplet penetration. The microscopic slide was exposed to the spray, so that sample droplets struck the oxide layer and penetrated the surface. This left a well-defined circular impression which was viewed with strong transmitted light under the microscope. The impressions then appeared as bright white spots on a darker background. Traverses were made across the slide with the microscope, sizing each drop crossing a line on the eyepiece scale. A graticule May (1966) which was calibrated by a stage micrometer was used to measure the particle size.

The wet particle size of particles generated by the atomizer run at pressures between 4 and 72 cm Hg with spraying solution of 80% v/v aqueous ethanol was

established. The particle size obtained by viewing the Magnesium oxide filter was multiplied by 0.86 as suggested by May (1966) to find the true wet drop size. This gave a size range of between 25 μm and 150 μm . A detailed calibration curve of true wet-drop size versus pressure of air was plotted.

2.5.5.2 dry sizing

The final airborne particles were of spores combined with Potassium iodide (KI). They were produced by evaporation, leaving dry solid spore/KI conglomerate particles. This diameter was calculated from the formula:

$$d_p = d_p' \left[\frac{W_{KI}}{100\rho} \right]^{\frac{1}{3}}$$

where d_p = dry particle diameter (μm)

d_p' = droplet diameter (μm)

W_{KI} = percentage concentration by weight of the Potassium iodide solution (%)

ρ = density of the Potassium iodide (3.13 g/cm^3)

Different sizes of particles were sprayed by varying the pressure of the compressed air and the concentration of the potassium iodide solution fed to the spinning disk. The KI concentrations used were 0.1% and 7.2% (maximum possible) by weight.

An alternative and probably more exact estimate of the dry particle size was obtained by spraying droplets in the chamber for a longer time than normal and drawing air through two 47 mm diameter cellulose-nitrate membrane filters (Millipore Ltd) of 0.45 μm pore size. A quadrant of the filter was cut, placed on a microscope slide, immersion oil applied, and then covered with a plastic slide cover. The filter was then examined microscopically under oil magnification (x1000).

The volume of the potassium iodide was calculated as the volume of the sphere of the combined particle minus the volume of the spores. The volume of spores was taken as the volume of sphere with radius taken as 0.4 μm . The average combined particle density was then determined as:

$$\rho_{cp} = \frac{(\rho \cdot V)_{KI} + (\rho \cdot V)_{spores}}{(V)_{cp}}$$

where ρ = density (g/cm³)
 V = volume of the sphere (μm^3)

The subscript 'cp' denotes the variable for the combined particle.

Since the particles were not spherical but were irregular in shape the concept of an aerodynamic particle diameter was adopted. The aerodynamic particle diameter (d_a) of arbitrary shape and density whose terminal settling velocity would be equivalent to that of a sphere of unit density was calculated as:

$$d_a = d_p \left[\rho_{cp} \right]^{\frac{1}{2}}$$

2.5.6 Sampling of airborne particles

Two 47 mm diameter cellulose-nitrate membrane filters (Millipore Ltd) of 0.45 μm pore size in plastic membrane holders were placed in the chamber to determine the airborne particulate concentration. Two Rotameters of metric size 10, fitted with a solid stainless steel float (metric type s), were used to measure the volumetric flow rate of air drawn through the filters by a vacuum pump. The flow calibration for the Rotameters was calculated using the calibration data described in the Rotameter Manufacturing Co. Ltd. The charts and families of curves presented by the company in leaflet (RP300) express the relationship between the variables involved. Using the known meter and air flow constants, the parameters of the characteristic curve were evaluated and from these the flow calibration was established. A detailed calibration curve of the volumetric flow rate versus scale reading for different suction pressures was plotted.

2.5.7 Experimental method

Before each run, the interior surface of the glove box was disinfected and cleaned with a 70% Isopropanol alcohol (Aq) solution. An antistatic solution (containing 75% De-ionized water, 20% Quaternary Ammonium Ethosulphate and 5% Buthanol) was then applied to the interior surfaces of the glove box to minimize any losses of particles drawn to the surfaces by electrostatic effects. The

interior surface resistivity was significantly reduced by this method. When measured by a megohmmeter, using the method suggested in BS 5958 (1980), a significant reduction of resistance was registered: 7×10^7 ohms compared to 5×10^{14} ohms when no antistatic solution was used. A negative polarity air ioniser (Statimate E type) was activated 30 minutes prior to each experiment in the hope of minimizing the electrostatic effects of the particles by saturating the air with ions. As the ioniser had a fan which mixed the air in the chamber it was switched off prior to collection of particles during the still condition experiments but was allowed to run where stirred condition was involved.

Ten of 9 cm Petri dishes containing Tryptone soya agar (Oxoid Ltd) were attached to the inside of the chamber, four on the sides, three on the base and three on the top of the chamber. Due to surface roughness which can be an important factor for turbulent (eddy) deposition mechanism, the petri dishes were filled to the lip with Tryptone soya agar. Initially the experiments involved removing and replacing the lids of agar plates, using gloved hands. It was suspected that hand movement caused undue disturbance of the air flow inside the chamber. Externally controlled rods were therefore designed to open and close each agar plate.

The pressure of the compressed air supply to the atomizer was adjusted to obtain the required particle size. Thus droplets projected from the rim of the spinning disk were introduced into the chamber and mechanically stirred gently for a short period (usually 1 minute) to obtain a uniform airborne concentration. The speed of the stirrer was then raised or lowered to the desired level to simulate equivalent ventilation rates of 0, 20 and 200 air changes per hour. The agar plates were then exposed for 30 minutes, during which airborne particles containing bacterial spores were deposited upon their surfaces. The aerial concentration of the spore-bearing particles was determined by drawing a sample of air through a membrane filter by a vacuum pump. To avoid excessive deposition on the filters, the air was drawn for a limited time. To observe the particle concentration decay, sampling was done 1 minute after the experiment started and 1 minute

before the experiment ended. Two different sampling locations were used to ensure that the aerosol was uniformly distributed through the chamber. The filters were removed from the holders and placed on the surface of agar plates which were then placed in an incubator. Following 24 hrs incubation, the bacterial colonies were counted.

Because thermophoretic effects could be a contributory factor on deposition, the temperature of the air in the chamber and of the nutrient agar was monitored during the experiment.

Each test described was carried out three times at random intervals, when the appropriate test conditions prevailed. When the bacterial spores were deposited too rapidly, or a deposition rate was inconveniently slow, the test was repeated with a different concentration of *Bacillus globigii* spores and potassium iodide.

2.6 Verification of the Airborne Concentration Model by Monitoring of Airborne Particles and Bacteria in Industrial Cleanrooms

2.6.1 Introduction

To assess the validity of the airborne contaminant concentration model derived (Chapter Three), experiments were carried out to measure the number of particles and, where appropriate bacteria, in the air of cleanrooms and compare them to those obtained by calculation.

2.6.2 Materials and methods

The experiments were carried out in conventionally-ventilated cleanrooms at Optical Coatings Ltd. in Fife and at Organon Pharmaceutical Manufacturing Laboratory Ltd at Newhouse near Glasgow.

The method used in measuring particle concentration was that described in Federal Standard 209D (1988). The minimum number of sampling locations should be equal to the floor area (ft²) divided by the square root of the airborne particulate cleanliness class designation and in no case should be less than 2 sample locations. The number of sampling locations were uniformly spaced throughout the cleanroom. At each sampling location a Royco airborne particle

counter was used to measure each individual sample particle concentration greater and equal to $0.5\mu\text{m}$. According to the Federal Standard 209D (1988) the minimum volume per sample for air cleanliness class of 10,000 measuring particle size of $0.5\mu\text{m}$ is 0.1 ft^3 . The sampling time (1 min) was calculated by dividing the sample volume by the sample flow rate.

The average particle concentration (C_A) at a location was defined as:

$$C_A = (C_1 + C_2 + \dots + C_N) / N_S$$

where C_j = sum of the individual sample particle counts

N_S = number of samples taken at each location

The mean of the averages (M_A) was calculated as:

$$M_A = (C_{A1} + C_{A2} + \dots + C_{AL}) / N_L$$

where C_{Ai} = sum of the individual averages

N_L = number of sampling locations

The standard deviation (SD) of averages was calculated as:

$$SD = \left[\frac{(C_{A1} - M_A)^2 + (C_{A2} - M_A)^2 + \dots + (C_{AL} - M_A)^2}{N_L - 1} \right]^{\frac{1}{2}}$$

The Standard Error (SE) of the mean of the averages (M_A) was determined as:

$$SE = SD / (N_L)^{\frac{1}{2}}$$

The 95% upper (UCL) and lower (LCL) confidence limit of the mean of the averages was determined as:

$$UCL = M_A + (95\% \text{ CL Factor} \times SE)$$

$$LCL = M_A - (95\% \text{ CL Factor} \times SE)$$

where the 95% CL factors for 3 and 4 locations are 2.9 and 2.4 respectively.

Additionally, airborne bacterial samples were carried out at Organon Laboratory by means of a high volume slit sampler (Casella Ltd) extracting 700 litres of air per minute, onto Tryptone Soya agar (Oxoid Ltd) plates. Three sampling locations uniformly spaced throughout the room were chosen. The

duration of air samples was 15 minutes and two samples were taken from each location. To minimize variation in bacterial counting that can be caused by insufficient incubation time, the plates were left in the incubator at 37°C for 48 hours. To minimize errors, plates were tested for sterility before use.

3. COMPUTATIONAL MODELLING

3.1 Introduction

The ever-growing demands to minimize the airborne contaminant concentration and resultant deposition on critical surfaces in cleanrooms has led to a realization that there is insufficient data, analyses and theory relating to the ventilation performance of the room. Probably the most important facet of designing a cleanroom is the determination of the probable airborne contaminant concentration. Present cleanroom design practices are based on guesswork and rely on the designer's experience in air volumes, air movement, and filter efficiency to predict the likely airborne contaminant concentration. These design techniques are inadequate. These are also costly as the rooms built can often have a great deal of overdesign.

To comply with the current standards (US Fed. Std. 209D, 1988 or BS 5295, 1989) measurement of the airborne contaminant concentration is required. This can only be done after the room is ready for commissioning and failure to reach the desired standard for classification can result in modification and alterations to the facility. As this may happen more than once before the designated class is reached, the procedure can be lengthy and costly. It is thus more desirable to have a predictive and systematic method that will ensure the cleanroom is completed to the required classification within a small limit of acceptable error.

At the present time, there is no analytical method to assess cumulative airborne contaminant concentration in a cleanroom. In this present work such a method has been introduced by a simulation developed from algorithms used in previous models. This provides an efficient method of design analysis for examining different cleanroom configurations quickly and easily. It has been coded into an user-friendly computer software package, allowing engineers to make pre-build changes and modifications in their design, with an immediate assessment of their effects. The developed program enables an assessment of the likely airborne contaminant concentration inside a conventionally-ventilated cleanroom with size distribution, contaminant deposition rates (onto surfaces and/or into containers)

and contaminant decay rates. This can be carried out for both bacterial and inanimate particles.

3.2 Derivation of the Models

The models developed in the present work are for the calculation of:

- (1) Steady-state airborne contaminant concentration
- (2) Build up of airborne contaminant concentration
- (3) Airborne contaminant losses due to surface-deposition
- (4) Decay of airborne contaminant concentration
- (5) Cumulative airborne contaminant size distribution

These are described in detail in the following subsections.

3.2.1 Steady-state airborne contaminant concentration

An explicit and practically-useful expression for assessing the airborne contaminant concentration can be derived by considering the sources and sinks of contaminants (particles or bacteria). The potential sources are the outdoor air and indoor generators such as people and machinery. The sinks are removal processes such as ventilation and deposition on surfaces.

The model which will be presented is based on two assumptions. The first is that a steady-state representation of all the variables formulating the model is adequate for design purposes. That is, it is assumed that all parameters can be represented by constant values or by values which represent time-weighted-average conditions. This presumes that all contamination entering and dispersing within a room will continue for a sufficient length of time and that all concentrations will approach and stabilize at constant values. The second assumption is that perfect mixing of incoming air and air within the room will occur. As a result the airborne contamination will have a uniform concentration throughout the room.

The above assumptions seem reasonable for a conventionally-ventilated cleanroom as the entrainment of room air by the supplied air is likely to spread the supplied air and dilute the contaminants generated in the room. Also higher than normal room air quantities would enable steady-state conditions to be reached

quite quickly.

To illustrate the concept upon which the model is based, consider the conventionally-ventilated cleanroom shown in Figure 3.1. The outdoor air with a flow rate of Q_o and a contaminant concentration of C_o is passed through a prefilter of efficiency F_p . The prefiltered outdoor air mixes with the recirculated air with a flow rate of Q_r and a contaminant concentration of C . This mixed air is considered to have a flow rate of Q with a contaminant concentration of C_s . This now passes through a secondary filter of efficiency F_s . The filtered air enters the room and mixes with the contaminants dispersed from people (S_p) and generated by machines and processes (S_m). The volume of air supplied from unidirectional flow cabinet is Q_b and its filter efficiency F_b . Two different volumetric flow rates Q_r and Q_e exit from the room.

For the room shown (Figure 3.1) there are two mixing areas to be considered. The first mixing area is where the recirculated air (Q_r, C) mixes with the prefiltered outdoor air [$Q_o, C_o(1-F_p)$]. Whenever two air streams are joined in the system, it is assumed that perfect mixing takes place within the turbulent flow patterns of the ducts. Applying a mass balance gives the following equation:

$$Q_o \cdot C_o(1 - F_p) + Q_r \cdot C = Q \cdot C_s \quad (\text{Eq. 3.1})$$

The second mixing area is within the room itself where the supplied air mixes with the contaminant dispersed from people (S_p) and particulate generated from machines and processes (S_m). For a steady-state condition, the sum rate of contaminant entering and generated within the room must balance the sum rate exiting, captured and deposited within the room. Hence applying a mass balance, gives the following equation:

$$C_s \cdot Q(1-F_s) + S_p + S_m + C \cdot Q_b(1-F_b) = C \cdot Q_r + C \cdot Q_e + R_d \cdot C + C \cdot Q_b \quad (\text{Eq. 3.2})$$

where R_d = deposition velocity x available surface area

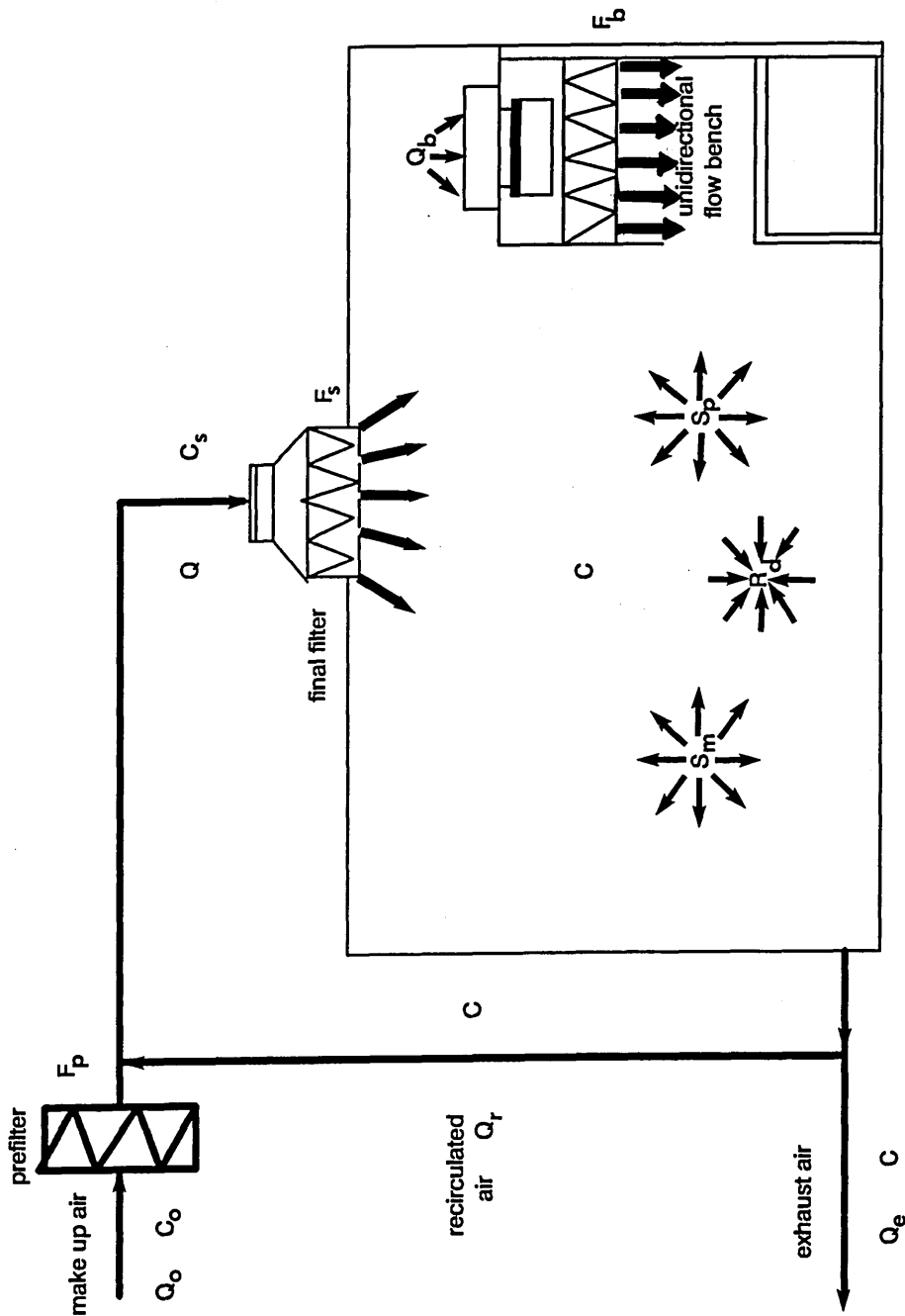


Fig. 3.1 Model of contaminant mass balance for a conventionally-ventilated cleanroom

- C = Airborne contaminant concentration (particles/volume)
- S_m = Particulate generation rate from machines and processes (particles/time)
- S_p = Contaminant dispersion rate from people (particles/time)
- R_d = Deposition velocity x surface area (length.area/time)
- Q = Volumetric flow rate (volume/time)

F = Filter efficiency

It is assumed that all ductwork is airtight.

Now by continuity it is noted that:

$$Q = Q_0 + Q_r$$

$$Q = Q_r + Q_e$$

hence:

$$Q_e = Q_0$$

By evaluating the expression $C_s \cdot Q$ from equation (3.2) and substituting in equation (3.1) and then algebraically solving for C gives:

$$C = \frac{Q_0 \cdot C_0 (1 - F_s)(1 - F_p) + S_p + S_m}{Q_0 + Q_b \cdot F_b + Q_r \cdot F_s + R_d} \quad (\text{Eq. 3.3})$$

3.2.2 Build up of airborne contaminant concentration

A differential equation resulting from all the sources and sinks of contaminants (Figure 3.1) as a function of time can be written as:

$$V \cdot \frac{dC}{dt} = S_m + S_p + C_s \cdot Q(1 - F_s) + C \cdot Q_b(1 - F_b) - C(Q_r + Q_e) - R_d \cdot C - C \cdot Q_b$$

where V = volume of the room

The airborne contaminant dispersion rate is a function of activity and may vary with time. However assuming it is a constant and rearranging, substituting and separating the variables, the differential equation leads to:

$$\int \frac{dC}{C - (X/Y)} = - \frac{Y}{V} \cdot Q \int dt$$

where $X = \left[\frac{(S_m + S_p)}{Q} + C_0 \cdot m(1 - F_p)(1 - F_s) \right]$

$$Y = \left[r(F_s - 1) + 1 + \frac{Q_b}{Q} \cdot F_b + \frac{R_d}{Q} \right]$$

$$m = Q_0 / Q$$

$$r = Q_r / Q$$

$$m + r = 1$$

Integrating both sides of the equation gives:

$$\ln \left[C - \frac{X}{Y} \right] = - \frac{Y}{V} \cdot Q \cdot t + a$$

where $a = \text{constant of integration}$

Now we have at $t = 0$, $C = C_i$

and at $t = t$, $C = C_t$

$$\therefore a = \ln \left[C_i - \frac{X}{Y} \right]$$

$$\ln \left[\frac{\left[C_t - \frac{X}{Y} \right]}{\left[C_i - \frac{X}{Y} \right]} \right] = - \frac{Y}{V} \cdot Q \cdot t$$

$$\therefore C_t = \frac{X}{Y} \left[1 - \exp \left[-Y \cdot \frac{Q}{V} \cdot t \right] \right] + C_i \cdot \exp \left[-Y \cdot \frac{Q}{V} \cdot t \right]$$

3.2.3 Airborne contaminant losses due to surface-deposition

Airborne particles in a cleanroom may be deposited on surfaces by various deposition mechanisms described previously (section 1.7). To assess the significance of each deposition mechanism a computational model was developed to calculate the deposition of aerosol particles in the chamber described in experimental programme (section 2.5).

In the derivation of the models it has been assumed that the airborne particles are perfectly mixed in a turbulent core of the chamber or room and only in small turbulent boundary layer a concentration gradient occurs. This gradient may give rise to deposition by inertial impaction, turbulent (eddy) diffusion and Brownian (molecular) diffusion. Superimposed upon these is the process of gravitational settling, whereby particles fall to the floor, with a terminal settling velocity, V_s . The airborne concentration of submicron particles may be further reduced by the electrical charge carried by the particles, electrical fields existing near the surface, and by thermophoretic effects.

Let us first consider the deposition due to gravitational sedimentation, Brownian (molecular) diffusion and turbulent (eddy) diffusion. In the case of stirred aerosol, the rate of diffusion of particles to the surface is more than the unstirred case due to turbulent mixing and the reduced thickness of the boundary layer

through which particles must diffuse. The increase in the rate of diffusion in the boundary layer can be accounted for by including turbulent eddy diffusivity (D_e) in the Fick's first law of diffusion applied to stationary fluid. The rate of transport of particles across a surface at a point (flux J_y) from the high to the low concentration is proportional to the local concentration gradient ($\partial C/\partial y$) such that:

$$J_y = - (D + D_e) \frac{\partial C}{\partial y} \quad (\text{Eq. 3.4})$$

where D = Brownian (molecular) diffusion coefficient

y = distance measured normal to the surface

The rate of change of concentration ($\partial C/\partial t$) within the boundary layer thickness can be modelled by using Fick's second law of diffusion. This entails considering an elemental volume of fluid ($\delta x \cdot \delta y \cdot \delta z$) fixed in space. The rate of transport across the surface into the elemental volume is:

$$\left[J_y - \frac{\partial J_y}{\partial y} \cdot \frac{\delta y}{2} \right] \delta x \cdot \delta z$$

The rate at which particles leave the elemental volume is:

$$\left[J_y + \frac{\partial J_y}{\partial y} \cdot \frac{\delta y}{2} \right] \delta x \cdot \delta z$$

The net rate of transport is:

$$- \delta x \cdot \delta y \cdot \delta z \cdot \frac{\partial J_y}{\partial y}$$

Using Fick's second law of diffusion the rate of change of particle concentration in the elemental volume ($\delta x \cdot \delta y \cdot \delta z$) equals the net rate of particle transport such that:

$$\frac{\partial C}{\partial t} = - \frac{\partial J_y}{\partial y} \quad (\text{Eq. 3.5})$$

Over the vertical side of the chamber or room, the particle flux to the surface is by eddy and Brownian diffusion. The rate of change of concentration

$(\partial C/\partial t)$ within the boundary layer thickness can be modelled by substituting equation (3.4) into equation (3.5), thus:

$$\frac{\partial C}{\partial t} = \frac{\partial}{\partial y} \left[\frac{\partial C}{\partial y} (D_e + D) \right] \quad (\text{Eq. 3.6})$$

Now the turbulent eddy diffusivity (D_e) decreases rapidly as the surface is approached and is proportional to the square of the distance from the wall (Prandlt mixing length theory) and can be written as:

$$D_e = K_e \cdot y^2$$

where K_e = eddy diffusion coefficient

Substituting D_e in equation (3.6) we get:

$$\frac{\partial C}{\partial t} = \frac{\partial}{\partial y} \left[(K_e \cdot y^2 + D) \frac{\partial C}{\partial y} \right] \quad (\text{Eq. 3.7})$$

At the base of the chamber or floor of the room, the deposition rate is enhanced by gravitational sedimentation and this can be taken into account by adding the effect of gravitational sedimentation (terminal settling velocity, V_s) in the boundary layer thickness as:

$$\frac{\partial C}{\partial t} = \frac{\partial}{\partial y} \left[(K_e \cdot y^2 + D) \frac{\partial C}{\partial y} \right] + V_s \cdot \frac{\partial C}{\partial y} \quad (\text{Eq. 3.8})$$

At the top of the chamber or ceiling of the room, the deposition rate is reduced due to the effect of gravitational sedimentation downwards. This can be taken into account by subtracting the effect of gravitational sedimentation in the boundary layer thickness as:

$$\frac{\partial C}{\partial t} = \frac{\partial}{\partial y} \left[(K_e \cdot y^2 + D) \frac{\partial C}{\partial y} \right] - V_s \cdot \frac{\partial C}{\partial y} \quad (\text{Eq. 3.9})$$

Equation (3.7) can be solved by separating the variables and assuming a solution of the form:

$$C = f_1(y) \cdot g_1(t) \quad (\text{Eq. 3.10})$$

Hence we obtain:

$$\frac{1}{g_1} \frac{dg_1}{dt} = -\beta$$

$$\therefore \frac{d}{f_1 \cdot dy} \left[(K_e \cdot y^2 + D) \frac{df_1}{dy} \right] = -\beta \quad (\text{Eq. 3.11})$$

where $\beta = \text{constant}$

The constant (β) is the surface loss rate coefficient determined by the boundary conditions at the wall given by:

$$C = 0 \quad \text{when } y = 0$$

$$C = C \quad \text{when } y = \delta$$

From equation (3.10) it follows that:

$$(\partial C / \partial t) = -\beta \cdot C$$

In a similar fashion, we can write dC / dt as:

$$(dC / dt) = -\beta \cdot C$$

By setting $y = [(D / K_e)^{\frac{1}{2}} \cdot z]$ and substituting into equation (3.11)

we get:

$$(z^2 + 1) \frac{d^2 f_1}{dz^2} + 2z \frac{df_1}{dz} + \frac{\beta}{K_e} \cdot f_1 = 0$$

Now the last term ($\beta \cdot f_1 / K_e$) will be very small compared to the other terms, so we may ignore it.

We have at $y = 0$, $f_1 = 0$, so to fix the scale of f_1 we make $f_1 = 1$ at $y = \delta$

$$\therefore f_1 = \frac{\tan^{-1}[y(K_e / D)^{\frac{1}{2}}]}{\tan^{-1}[\delta(K_e / D)^{\frac{1}{2}}]}$$

Now $(\delta^2 \cdot K_e / D) \gg 1$, therefore it follows that $[\delta(K_e / D)^{\frac{1}{2}}] \gg 1$

$$\therefore f_1 = \frac{\tan^{-1}[y(K_e / D)^{\frac{1}{2}}]}{\pi / 2}$$

The deposition velocity on vertical sides of a chamber (or walls of a room) is thus given by:

$$(V_d)_{\text{side}} = D \cdot \frac{df_1}{dy} \Big|_{y=0} = D \cdot \frac{d}{dy} \left[\frac{\tan^{-1} [y(K_e / D)^{\frac{1}{2}}]}{\pi / 2} \right]_{y=0}$$

$$\therefore (V_d)_{\text{side}} = \frac{2}{\pi} (K_e \cdot D)^{\frac{1}{2}} \quad (\text{Eq. 3.12})$$

Using a similar technique to solve equations (3.8) and (3.9) for the deposition velocity over the top and base of the chamber we assume a solution of the form:

$$C = f_2(y) \cdot g_2(t)$$

and obtain the deposition velocity over the top interior surface of a chamber (or ceiling of a room) as:

$$(V_d)_{\text{top}} = (K_e \cdot y^2 + D) df_2 / dy - V_s \cdot f_2$$

now $f_2(y) = 1$ at $y = \delta$

and $f_2(y) = 0$ at $y = 0$

we get:

$$\frac{1}{V_s} \cdot \ln \left[1 + \frac{V_s}{(V_d)_{\text{top}}} \right] = \frac{1}{(D \cdot K_e)^{\frac{1}{2}}} \cdot \frac{\pi}{2}$$

$$1 + \frac{V_s}{(V_d)_{\text{top}}} = \exp \left[\frac{\pi V_s}{2 (D \cdot K_e)^{\frac{1}{2}}} \right]$$

$$\therefore (V_d)_{\text{top}} = \frac{V_s}{\exp \left[\frac{\pi V_s}{2 (D \cdot K_e)^{\frac{1}{2}}} \right] - 1} \quad (\text{Eq. 3.13})$$

Similarly setting $C = f_3(y) \cdot g_3(t)$ we obtain for the deposition velocity on the base of a chamber (or floor of a room) as:

$$(V_d)_{\text{base}} = (K_e \cdot y^2 + D) df_3 / dy + V_s \cdot f_3$$

using $f_3(y) = 1$ at $y = \delta$
 and $f_3(y) = 0$ at $y = 0$

we get:

$$\frac{1}{V_s} \cdot \ln \left[1 - \frac{V_s}{(V_d)_{\text{base}}} \right] = \frac{1}{(D \cdot K_e)^{\frac{1}{2}}} \cdot \frac{\pi}{2}$$

solving for $(V_d)_{\text{base}}$ we get:

$$(V_d)_{\text{base}} = - \frac{V_s}{\exp \left[- \frac{\pi V_s}{2 (K_e \cdot D)^{\frac{1}{2}}} \right] - 1} \quad (\text{Eq. 3.14})$$

Thus equations 3.12, 3.13 and 3.14 give deposition velocities on various surfaces of room (or chamber). To solve these equations several unknown quantities in these equations must be determined. These are:

(1) The terminal settling velocity (V_s). As discussed and shown in the literature review (section 1.7.2) the terminal settling velocity (V_s) on a horizontal surface is given by Stokes law with the slip correction factor as:

$$V_s = \frac{\rho_p \cdot d_p^2 \cdot g \cdot C(K_n)}{18 \mu_g} \quad (\text{Eq. 3.15})$$

where ρ_p = particle density
 d_p = particle diameter
 g = acceleration due to gravity
 $C(K_n)$ = Cunningham slip correction factor
 μ_g = dynamic gas viscosity

Stokes law was derived for a rigid spherical particle, moving through a continuous viscous stagnant fluid at relatively constant velocity. In general, particles are not spherical but irregular in shape. To compensate for this discrepancy an aerodynamic particle diameter (d_a) which is the diameter of a sphere of unit density whose terminal settling velocity is equal to that of the irregular particle has been defined as:

$$d_a = \left[\frac{18 V_s \cdot \mu_g}{g \cdot C(K_n)} \right]^{\frac{1}{2}}$$

$$\therefore d_a = d_p(\rho_p)^{\frac{1}{2}}$$

- (2) To evaluate the terminal settling velocity V_s (Eq. 3.15), the dynamic gas (air) viscosity (μ_{gT}) at any absolute temperature (T) in the chamber (or room) can be calculated from:

$$\mu_{gT} = \mu_{g20} (T / T_{20})^{1.5} \left[\frac{T_{20} + S_w}{T + S_w} \right]$$

where μ_{gT} = dynamic gas (air) viscosity at absolute temperature T

Wilson (1972) recommended that the best value to date for the dynamic air viscosity is:

$$\mu_{g20} = 1.819 \times 10^{-4} \text{ g / (cm sec) and } S_w = 110.4 \text{ K}$$

$$\therefore \mu_{gT} = 1.819 \times 10^{-4} (T / 293.15)^{1.5} [403.55 / (T + 110.4)]$$

- (3) The Cunningham slip correction factor $C(K_n)$ used in equation (3.15) has been defined as:

$$C(K_n) = 1 + K_n [1.155 + 0.471 \exp(-0.596/K_n)]$$

where K_n = Knudsen number

The Knudsen number (K_n) is given by:

$$K_n = \lambda / r_p$$

where λ = mean free path of the gas (air) molecules

r_p = particle radius

The mean free path of the gas molecules (λ) can be determined from a Kinetic theory model as:

$$\lambda = \mu_g / (\varphi \cdot \rho_g \cdot \bar{c})$$

where ρ_g = gas (air) density

\bar{c} = mean velocity of the gas molecules

φ = constant

The value of λ used in most aerosol work is $0.0662 \mu\text{m}$ for $\varphi = 0.449$, absolute temperature (T) of 296K and atmospheric pressure (P_0) of 760 mm Hg. However, to correct the mean free path at any absolute temperature (T)

and pressure (P), the equation derived by Willeke (1976) was used, i.e.

$$\lambda = \lambda_0 (T / T_0) (P_0 / P) \left[\frac{1 + (S_w / T_0)}{1 + (S_w / T)} \right]$$

The subscript '0' refers to the value of λ used for the appropriate pressure and temperature.

(4) The coefficient of Brownian diffusion (D) was calculated as:

$$D = K \cdot T \cdot \frac{C(K_n)}{6 \pi \cdot \mu_g \cdot r_p}$$

where K = Boltzman's constant

T = absolute temperature

Finally (5) The eddy diffusion coefficient (K_e) characterizing the intensity of mixing was evaluated from:

$$K_e = K' \cdot du / dx$$

where K' = Kármán turbulence constant

du / dx = velocity gradient of the mean motion within the boundary layer (assuming a linear distribution)

The velocity gradient (du/dx) is given by Saffman and Turner (1956) as:

$$du / dx = [2 \epsilon_d / (15 \nu)]^{\frac{1}{2}}$$

where ϵ_d = average turbulent energy dissipation rate

ν = kinematic viscosity of air

The above equation is basically the Prandlt mixing length formulae, where

$$(\epsilon_d / \nu)^{\frac{1}{2}} \propto (du / dx)$$

and
$$K_e \propto (\epsilon_d / \nu)^{\frac{1}{2}}$$

Assuming a complete turbulent dissipation into the air, the energy dissipation rate (ϵ_d) is:

$$\epsilon_d = P_c / M$$

where

P_c = power consumption into the air (in the chamber or room)

M = mass of mixing air (in the chamber or room)

According to the theory of isotropic turbulence proposed by Kolmogoroff, the micro-scale of turbulence (λ_t) can be calculated as:

$$\lambda_t = (v^3 / \epsilon_d)^{\frac{1}{4}}$$

Let us now consider the importance of deposition of particles due to inertial impaction. The surface deposition due to particle's inertia in a chamber (or room) can be calculated by modelling the particle trajectories over a flat plate and then solving the trajectories by a step-by-step integration of vector equations. The equation of motion for a particle moving in a flow field such that the force of gravity and electrostatic attraction can be neglected is:

$$m_p \cdot \frac{dV_p}{dt} = - F_d \quad (\text{Eq. 3.16})$$

where m_p = mass of particle
 V_p = particle velocity
 t = time
 F_d = drag force

The drag force (F_d) opposing the relative movement of the particle through the fluid is given by:

$$F_d = \frac{6 \pi \mu_g \cdot r_p (V_p - V_f)}{C(K_n)} \quad (\text{Eq. 3.17})$$

where V_f = fluid velocity

To utilize equations 3.16 and 3.17 in the present study it was necessary to transform these into tangential (x) and normal (y) components as:

$$m_p \left[\frac{dV_p}{dt} \right]_x = - 6\pi \mu_g \cdot r_p (V_p - V_f)_x / C(K_n)$$

$$m_p \left[\frac{dv_p}{dt} \right]_y = -6\pi \mu_g \cdot r_p (v_p - v_f)_y / C(K_n)$$

Thus:

$$\left[\frac{dv_p}{dt} \right]_x = \frac{1}{\tau} (v_f - v_p)_x$$

$$\left[\frac{dv_p}{dt} \right]_y = \frac{1}{\tau} (v_f - v_p)_y$$

Where τ is the aerodynamic relaxation time given by:

$$\tau = \frac{\rho_p \cdot d_p^2 \cdot C(K_n)}{18\mu_g}$$

To solve this set of equations, it is necessary to resort to an approximation method outlined by Fuchs (1964). The time is divided into equal intervals and the trajectory of the particle into corresponding segments. Then the flow field equations are approximated by a numerical integration. Ranz and Wong (1952) investigated and extended analytical solutions for impaction efficiency for various geometry of aerosol jet and body collectors. Their flow field for round aerosol jet (of diameter D_c) on flat plate of infinite extent has been reduced to:

$$\left. \begin{array}{l} v_x = -2x \\ v_y = y \end{array} \right\} \text{for region} \left\{ \begin{array}{l} -\frac{1}{2} < x < 0 \\ -1 < y < 1 \end{array} \right.$$

$$\left. \begin{array}{l} v_x = 0 \end{array} \right\} \text{for region} \left\{ \begin{array}{l} -\frac{1}{2} < x < 0 \\ y > 1 \text{ and } y < -1 \end{array} \right.$$

These flow fields give the efficiency of impaction (η) as:

$$\eta = \left[\frac{S_2 - S_1}{S_2 \cdot \exp(S_1 \cdot \tau_1) - S_1 \cdot \exp(S_2 \cdot \tau_1)} \right]^2$$

$$\text{i.e. } S_1 = -\left[\frac{1}{4\psi}\right] + \left[\left[\frac{1}{4\psi}\right]^2 + \left[\frac{1}{2\psi}\right]\right]^{\frac{1}{2}}$$

$$S_2 = -\left[\frac{1}{4\psi}\right] - \left[\left[\frac{1}{4\psi}\right]^2 + \left[\frac{1}{2\psi}\right]\right]^{\frac{1}{2}}$$

$$\tau_1 = \left[\frac{1}{q_1}\right] \tan^{-1} \left[\frac{(1-4\psi)8\psi \cdot q_1}{(8\psi - 1) + (4\psi \cdot q_1)^2} \right]$$

$$q_1 = \left[\left[\frac{1}{\psi}\right] - \left[\frac{1}{4\psi}\right]^2 \right]^{\frac{1}{2}}$$

The Stokes number (ψ) is given as:

$$\psi = \frac{V_{p0} \cdot d_p^2 \cdot C(K_n)}{18\mu_g \cdot D_c}$$

where V_{p0} = initial or undisturbed velocity of air stream

To calculate the minimum particle size below which impaction due to particle's inertia cannot occur it is necessary to calculate the critical Stokes number (ψ). Impaction due to particle's inertia cannot occur until the critical Stokes number is reached. By solving the above equations it is verified that the critical Stokes number for complete impaction is 1/4. Solving these equations for the worst possible case during the surface-deposition experiment (section 2.5), the Stokes number is less than the critical Stokes number and that complete impaction due to particle's inertia occurs for particles larger than 36 μm . Therefore inertial impaction is not an effective deposition mechanism to be considered.

The deposition model (gravitational sedimentation, Brownian diffusion and eddy diffusion) derived was developed to run on a mainframe computer, and was coded in Fortran 77 as shown in the flow chart (Figure 3.2). The program was run to compute the theoretical deposition velocities for various aerodynamic particle diameters and equivalent ventilation rates for the experiment described (section 2.5).

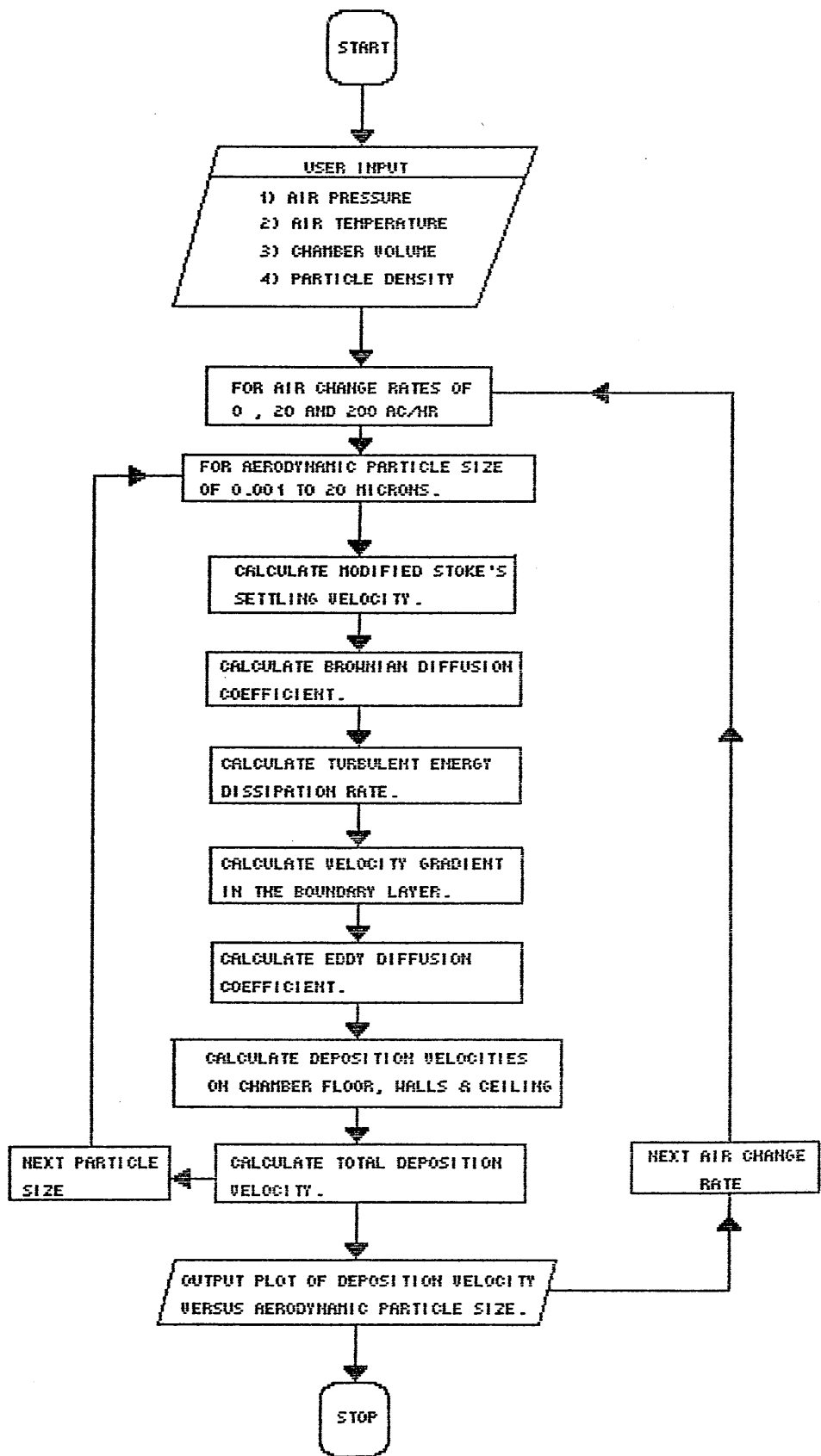


Fig. 3.2 Flow chart of the surface deposition model

Now from Equations 3.12, 3.13 and 3.14 we had:

$$(V_d)_{\text{side}} = \frac{2}{\pi} (K_e \cdot D)^{\frac{1}{2}}$$

$$(V_d)_{\text{top}} = \frac{V_s}{\exp \left[\frac{\pi V_s}{2(K_e \cdot D)^{\frac{1}{2}}} \right] - 1}$$

$$(V_d)_{\text{base}} = - \frac{V_s}{\exp \left[- \frac{\pi V_s}{2(K_e \cdot D)^{\frac{1}{2}}} \right] - 1}$$

The chance of a particle deposited on a surface is proportional to the airborne contaminant concentration (C) in the room, the deposition velocities (V_d) and the available surface areas (A) to deposit in the room. Thus the total sum of each deposition velocity multiplied by its appropriate surface area is defined as:

$$R_d = (V_d \cdot A)_{\text{top}} + (V_d \cdot A)_{\text{base}} + (V_d \cdot A)_{\text{sides}}$$

$$\text{Let } x = \frac{\pi V_s}{4(K_e \cdot D)^{\frac{1}{2}}}$$

Then

$$\begin{aligned} (V_d \cdot A)_{\text{top}} + (V_d \cdot A)_{\text{base}} &= V_s \cdot L \cdot B \left[\frac{1}{e^{2x} - 1} - \frac{1}{e^{-2x} - 1} \right] \\ &= V_s \cdot L \cdot B \left[- \frac{(e^{2x} - e^{-2x})}{2 - (e^{2x} + e^{-2x})} \right] \\ &= V_s \cdot L \cdot B \left[- \frac{\sinh(2x)}{1 - \cosh(2x)} \right] \\ &= V_s \cdot L \cdot B \left[- \frac{2 \sinh(x) \cosh(x)}{1 - \cosh^2(x) - \sinh^2(x)} \right] \\ &= V_s \cdot L \cdot B \left[- \frac{2 \sinh(x) \cosh(x)}{-2 \sinh^2(x)} \right] \\ &= V_s \cdot L \cdot B \cdot \coth(x) \end{aligned}$$

where

L = length
B = breadth
H = height

This leads to:

$$R_d = \frac{4H(B + L)(K_e \cdot D)^{\frac{1}{2}}}{\pi} + B \cdot L \cdot V_s \cdot \coth \left[\frac{\pi V_s}{4(K_e \cdot D)^{\frac{1}{2}}} \right] \quad (\text{Eq. 3.18})$$

The number of particles deposited (onto surfaces or into containers) was obtained from:

$$N(d_p) = V_d(d_p) \cdot C(d_p) \cdot A_e \cdot t_e$$

where $N(d_p)$ = number of particles of size d_p deposited

$V_d(d_p)$ = deposition velocity of particles of size d_p

$C(d_p)$ = airborne contaminant concentration of size d_p

A_e = exposed surface area

t_e = exposure time

However, the above equation is only valid for one particle size (d_p). To assess the cumulative surface particle size distribution, the above equation has to be integrated with respect to the particle diameter as follows:

$$N^*(d_p) = A_e \cdot t_e \int_{d_p}^{\infty} V_d(d_p) \cdot C(d_p) \, dd_p \quad (\text{Eq. 3.19})$$

where $N^*(d_p)$ = number of particles of size d_p and greater deposited

3.2.4 Decay of airborne contaminant concentration

Although not a functional requirement of the operating standards applying to any particular cleanroom, knowledge of the decay rate of airborne contaminant concentration can be a useful tool in assessing the ventilation performance in such a room. Particularly where the contamination within a room requires to be quickly reduced (e.g. air locks). However no work has been carried out to establish an accurate model including various surface deposition mechanisms. As part of this study it was therefore necessary to derive a mathematical model.

There are three components of decay rate.

- (i) Ventilation
- (ii) Deposition

(iii) Biological death

Within a cleanroom, with a naturally-occurring airborne bacterial-particles, the death rate of organisms is generally small in comparison to the removal process by ventilation and deposition on surfaces and therefore it can be neglected (Chamberlain, 1967).

When an initial airborne contaminant concentration (C_i) within a cleanroom of volume (V) is left to die away, the subsequent change in airborne concentration (δC) during time (δt) is given by:

$$\frac{\delta C}{\delta t} = - \lambda_{tr} \cdot C \quad (\text{Eq. 3.20})$$

i.e. $\lambda_{tr} = \lambda_v + \lambda_d$

where λ_{tr} = total removal coefficient

λ_v = removal rate coefficient due to ventilation

λ_d = removal rate coefficient due to deposition

Now substituting λ_{tr} in equation (3.20) and integrating with respect to time (t) we get:

$$\int \frac{dC}{C} = - \int (\lambda_v + \lambda_d) dt$$

hence: $\ln C = -t(\lambda_v + \lambda_d) + a$

where a = constant of integration

At $t = 0$, $C = C_i$, $\therefore a = \ln C_i$

$$\ln \left[\frac{C}{C_i} \right] = -t(\lambda_v + \lambda_d)$$

$\therefore C = C_i \cdot \exp [-t(\lambda_v + \lambda_d)]$

To determine λ_d , we need the total deposition velocities on all surfaces of the chamber (or room). From the foregoing analysis (Equations 3.12, 3.13 and 3.14) we had:

$$(V_d)_{side} = \frac{2}{\pi} (K_e \cdot D)^{\frac{1}{2}}$$

$$(V_d)_{\text{top}} = \frac{V_s}{\exp \left[\frac{\pi V_s}{2(K_e \cdot D)^{\frac{1}{2}}} \right] - 1}$$

$$(V_d)_{\text{base}} = - \frac{V_s}{\exp \left[- \frac{\pi V_s}{2(K_e \cdot D)^{\frac{1}{2}}} \right] - 1}$$

Now, multiplying each deposition velocity by its appropriate surface area in the chamber (or room) and adding all these and dividing by the volume of the chamber (or room) gives the total removal rate coefficient due to deposition as:

$$\begin{aligned} \lambda_d &= \frac{2}{\pi}(K_e \cdot D)^{\frac{1}{2}} \cdot \frac{2(L+B)H}{L \cdot B \cdot H} + \frac{L \cdot B}{L \cdot B \cdot H} \left[\frac{V_s}{\exp \left[\frac{\pi V_s}{2(K_e \cdot D)^{\frac{1}{2}}} \right] - 1} \right] \\ &\quad + \frac{L \cdot B}{L \cdot B \cdot H} \left[\frac{-V_s}{\exp \left[- \frac{\pi V_s}{2(K_e \cdot D)^{\frac{1}{2}}} \right] - 1} \right] \\ \lambda_d &= \frac{4(L+B)(K_e \cdot D)^{\frac{1}{2}}}{\pi(L \cdot B)} + \frac{V_s}{H \left\{ \exp \left[\frac{\pi V_s}{2(K_e \cdot D)^{\frac{1}{2}}} \right] - 1 \right\}} - \frac{V_s}{H \left\{ \exp \left[- \frac{\pi V_s}{2(K_e \cdot D)^{\frac{1}{2}}} \right] - 1 \right\}} \\ \therefore \lambda_d &= \frac{4(L+B)(K_e \cdot D)^{\frac{1}{2}}}{\pi(L \cdot B)} + \frac{V_s}{H} \cdot \coth \left\{ \frac{\pi V_s}{4(K_e \cdot D)^{\frac{1}{2}}} \right\} \end{aligned}$$

Now recalling that the removal rate coefficient due to ventilation is basically the air change rate in the room, i.e. $\lambda_v = Q / V$

$$\therefore \lambda_{\text{tr}} = \frac{Q}{V} + \frac{4(L+B)(K_e \cdot D)^{\frac{1}{2}}}{\pi(L \cdot B)} + \frac{V_s}{H} \cdot \coth \left\{ \frac{\pi V_s}{4(K_e \cdot D)^{\frac{1}{2}}} \right\}$$

We had $C = C_i \cdot \exp[-(\lambda_v + \lambda_d)t]$

Therefore the decay rate of the airborne contaminant concentration can be evaluated from:

$$C = C_i \cdot \exp -t \left[\frac{Q}{V} + \frac{4(L+B)(K_e \cdot D)^{\frac{1}{2}}}{\pi(L \cdot B)} + \frac{V_s}{H} \cdot \coth \left\{ \frac{\pi V_s}{4(D \cdot K_e)^{\frac{1}{2}}} \right\} \right] \quad (\text{Eq. 3.21})$$

3.2.5 Cumulative airborne contaminant size distribution

The steady-state airborne contaminant concentration model derived (section 3.2.1, Eq. 3.3) is only valid for one discrete particle, or bacterial-carrying particle, size. To comply with the current standards (Fed. Std. 209D, 1988 and BS 5295, 1989) the airborne contaminant concentration for a greater than and equal to a particular particle size (usually $0.1\mu\text{m}$, $0.3\mu\text{m}$, $0.5\mu\text{m}$) is required. As discussed in the literature review (section 1.4) so far, all the theoretical models developed to predict the airborne contaminant concentration are only applicable to one discrete particle size. This is unrealistic as there is a range of particle sizes normally encountered in cleanrooms and for accurate modelling the contribution of all particle sizes must be taken into account.

The cumulative airborne contaminant size distribution (larger than particle diameter d_p) is defined as:

$$C^*(d_p) = \int_{d_p}^{\infty} C(d_p) dd_p$$

where $C^*(d_p)$ = airborne contaminant concentration of size d_p and greater

$C(d_p)$ = airborne contaminant concentration of size d_p

To predict the cumulative airborne contaminant concentration required in standards, such as Fed. Std. 209D (1988) and BS 5295 (1989), the size distribution of a number of individual factors have to be determined. These are as follows:

- (1) Particles dispersed from people
- (2) Bacteria-carrying particles dispersed from people
- (3) Particles in outdoor air
- (4) Bacteria-carrying particles in outdoor air
- (5) Prefilter penetration
- (6) Final filter penetration

All the above distributions reported in previous literature (cited later) conform well to a log-normal function. The equation for a log-normal distribution is given by the following equation:

$$f(x) = \frac{1}{(2\pi)^{\frac{1}{2}} d_p \ln \sigma_g} \cdot \exp \left[-\frac{\ln^2 (d_p/\mu)}{2 \ln^2 \sigma_g} \right] \quad (\text{Eq. 3.22})$$

where μ = geometric mean particle diameter

σ_g = geometric standard deviation

The distribution parameters μ and σ_g for each distribution were determined by plotting the cumulative size distribution against the particle size, on probability-log paper. The geometric mean particle diameter is the point which half of the results lie below and half above it and the geometric standard deviation is the slope of the distribution curve. In some cases, where the raw data were available, the distribution parameters were evaluated using the Minitab Statistical Package.

Fujii and Minamino (1982) have reported the numbers of particles released by people in a cleanroom. Their measurement was carried out for two types of garments by determining the particle counts from 0.3 to 10 μm into 15 steps. Polyester coverall and cotton gowns were used in their study. The size distribution curves plotted had a very consistent shape although the total dispersion rate varied. The average data for the polyester coverall was used to represent particle dispersion rate from people wearing good cleanroom clothing. The data from the cotton gown was used for people wearing poor clothing such as only smocks, surgical gowns and laboratory coats. Table 3.1 summarizes the log-normal distribution parameters (geometric mean particle diameter and geometric standard deviation) compiled from their data and the experimental results obtained by the author, for female and male particulate dispersion.

The bacterial dispersion rate (% cumulative counts) from a volunteer wearing personal indoor clothing and underwear plus Ceramic terylene in a dispersion chamber has been determined by Whyte (1986). Table 3.2 summarizes the

TABLE 3.1 LOG-NORMAL DISTRIBUTION PARAMETERS FOR PARTICLES
DISPERSED FROM PEOPLE

Type of Clothing	Disperser	μ (μm)	σ_g	Mean (Part $\geq .3\mu\text{m}/\text{min}$)
Good	Male	0.805	2.084	2.2×10^6
	Female	0.805	2.084	8×10^5
Poor	Male	1.097	1.770	3.5×10^6
	Female	1.097	1.770	2.5×10^6

TABLE 3.2 LOG-NORMAL DISTRIBUTION PARAMETERS FOR BACTERIA-
CARRYING PARTICLES DISPERSED FROM PEOPLE

Type of Clothing	Female			Male		
	μ (μm)	σ_g	Mean (Bact/min)	μ (μm)	σ_g	Mean (Bact/min)
Good	12	2.25	57	12	2.25	85
Poor	12	2.25	363	12	2.25	1600

distribution parameters recalculated from his bacterial size distribution together with the results of the dispersion chamber test carried out by the author.

The concentration of particles in outdoor air has been reported by Willeke and Whitby (1975). From their extensive measurements over a wide range of urban and rural locations it can be concluded that the outdoor size distributions curve has a very consistent shape, although the total concentration varied from 4000 to 200,000 particles/cm³. Table 3.3 summarizes the distribution parameters calculated from their data.

Outdoor bacterial size distribution has been reported by Whyte (1968) to conform very well to a log-normal function. Table 3.4 summarizes the distribution parameters calculated from his results together with the results achieved by the author.

The filter penetration curve has been reported by Bergman *et al* (1983) and Liu *et al* (1985). Table 3.5 summarizes the distribution parameters for HEPA, ULPA and prefilter penetration compiled from their experiments. The distribution parameters calculated for HEPA and ULPA filters was for a face velocity of 2.5 cm/sec.

3.3 Development of Computer Software Package

The mathematical models presented have been coded into a user-friendly software package as shown in the flow chart (Figure 3.3).

The objectives in the development of the package were to:

- be efficient in terms of time.
- standardize formats of output, as required by the current standards.
- include all possible sources of contamination.
- include the principle method of deposition.
- be derived fundamentally.
- have generality in application.
- minimize the amount of data required.
- be flexible in order to allow for the future extensions.

TABLE 3.3 LOG-NORMAL DISTRIBUTION PARAMETERS FOR PARTICLES IN OUTDOOR AIR

Location	μ (μm)	σ_g	Total (Part/ m^3)
Rural	0.05	2.24	4×10^9
Urban	0.05	2.24	2×10^{11}

TABLE 3.4 LOG-NORMAL DISTRIBUTION PARAMETERS FOR BACTERIA IN OUTDOOR AIR

Location	μ (μm)	σ_g	Mean (Bact/ ft^3)
Rural	16.0	5.3	0.53
Urban	16.0	5.3	0.64

TABLE 3.5 LOG-NORMAL DISTRIBUTION PARAMETERS FOR FILTER PENETRATION

Type	μ (μm)	σ_g	Penetration at peak fraction
HEPA	0.15	1.50	9.4×10^{-5}
ULPA	0.15	1.60	2.6×10^{-6}
Pre-filter	0.13	1.49	14.4×10^{-2}

HEPA Filter = High Efficiency Particulate Air Filter

ULPA Filter = Ultra Low Penetration Air Filter

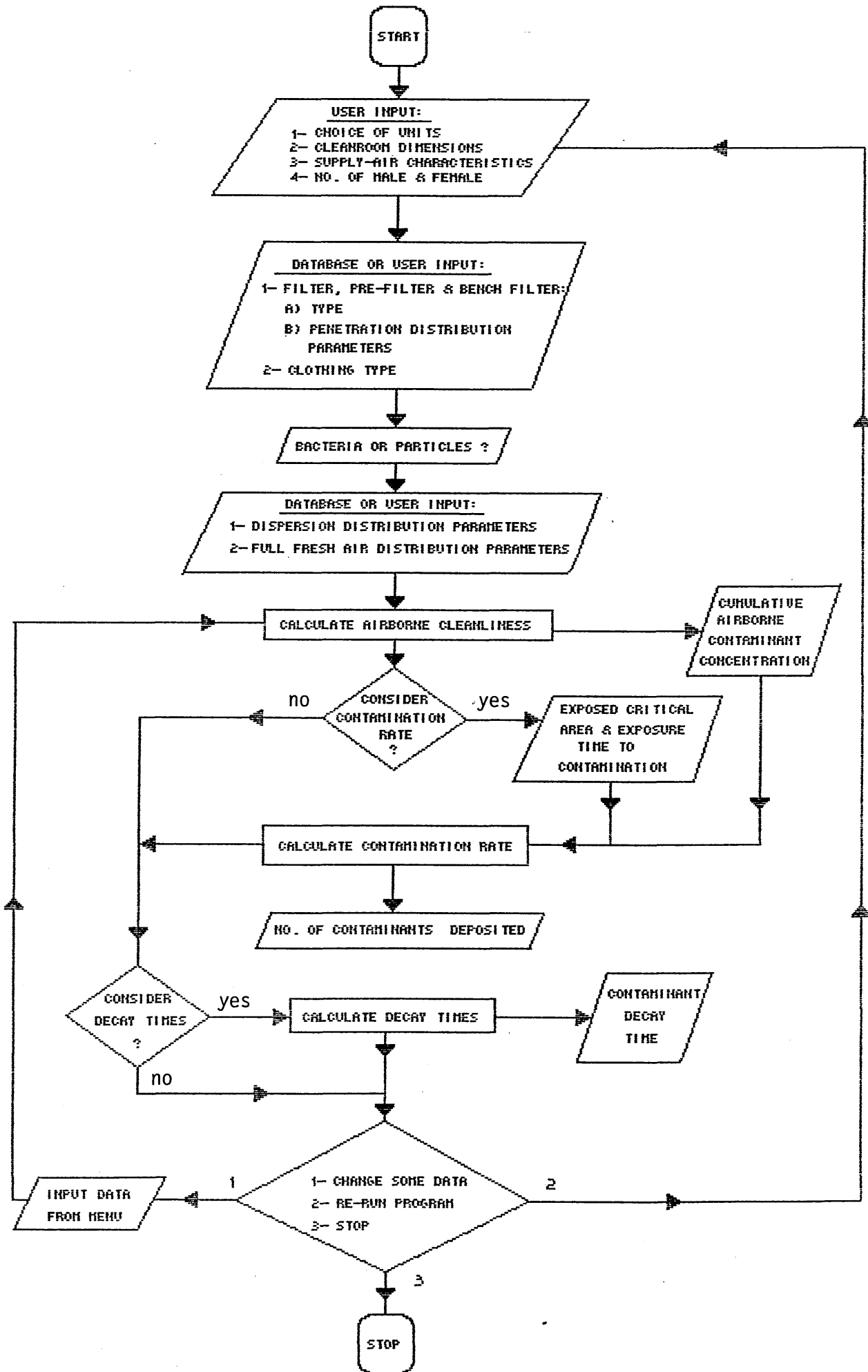


Fig. 3.3 Flow chart of the airborne contamination model

run on an IBM or IBM-compatible personal computer.

To increase the efficiency with which data from monitoring and modelling studies could be analysed, Random Access files and data base files were set up in the program.

The data required to run the program is as follow:

1. Dimensions of the room (length, width, height).
2. Total volume of air supplied to the room through air terminal devices and unidirectional flow cabinets.
3. Number of people working in the room (male and female).
4. Percentage of recirculated air into the room.
5. Distribution parameters for the following variables:
 - (i) Particles dispersed from people (male and female)
 - (ii) Bacteria-carrying particles dispersed from people (male and female)
 - (iii) Particles in outdoor air
 - (iv) Bacteria in outdoor air
 - (v) Prefilter penetration
 - (vi) Secondary filter penetration
 - (vii) Particles generated from the machines

The output results contained:

- (a) cumulative airborne contaminant concentration
- (b) contaminant deposition rates (onto surfaces and/or into containers)
- (c) airborne contaminant decay rates

The deposition of airborne particles in the previously described chamber (section 2.5) was investigated theoretically and experimentally. Agreement between predicted and measured surface deposition rates was satisfactory. The conclusion drawn was that gravitational sedimentation is the predominant loss mechanism. However, electrostatic effects must also be considered when generating highly charged particles but in most cleanrooms the particles will not be as highly charged, so electrostatic effects can be ignored. Therefore gravitational sedimentation was the only effective deposition mechanism taken into account in

the computer program. In calculating the terminal settling velocity to obtain deposition rates on the floor, the programme evaluates the deposition of all the particle sizes (particle size distribution) existing in the room.

As the airborne cleanliness classification laid down by the current standards are based on the maximum allowable number of particles ($0.1\mu\text{m}$, $0.3\mu\text{m}$ or $0.5\mu\text{m}$ and larger), it was therefore necessary to calculate the cumulative airborne particle concentration. The distribution parameters for all the input variables discussed previously (section 3.2.5) were used to compute the cumulative airborne contaminant concentration in the room. These distributions were used to derive the relationship between particle diameter and the percentage of particles above a given size. The probability $[\Phi(x)]$ that a random variable, normally distributed with zero mean and unit variance will be less than x was calculated as follows:

$$\Phi(x) = \frac{1}{(2\pi)^{\frac{1}{2}}} \int_{-\infty}^x \exp(-0.5t^2) dt \quad (\text{Eq. 3.23})$$

As all the distributions conformed well to a log-normal function, x (the upper limit of integration in equation 3.23) was calculated as:

$$x = \frac{\ln(d_p/\mu)}{\ln \sigma_g}$$

where d_p = particle diameter
 μ = geometric mean particle diameter
 σ_g = geometric standard deviation

The equation used to predict the cumulative airborne contaminant concentration was as follows:

$$C^*(d_p) = \int_{d_p}^{\infty} C(d_p) dd_p$$

where $C(d_p)$ = airborne contaminant concentration of size d_p
 $C^*(d_p)$ = airborne contaminant concentration of size d_p and greater

The airborne contaminant concentration of size d_p was derived before (Section 3.2.1, Eq. 3.3) as:

$$C = \frac{Q_0 \cdot C_0 (1 - F_s)(1 - F_p) + S_p + S_m}{Q_0 + Q_b \cdot F_b + Q_r \cdot F_s + R_d}$$

As discussed previously the maximum number of particles equal to and greater than a particular size ($0.1\mu\text{m}$, $0.3\mu\text{m}$ or $0.5\mu\text{m}$) is required by the standards. The equation for airborne contaminant concentration at one discrete particle size (Eq. 3.3) is integrated to obtain the concentration which exceeds a given size. This integrated function corresponds to the way the standards have been defined. When the prediction was carried out for contaminants to be inanimate particles, the lower limits of integration for cumulative airborne concentration were $0.1\mu\text{m}$, $0.3\mu\text{m}$ or $0.5\mu\text{m}$. However, as almost all bacteria-carrying particles are larger than $1\mu\text{m}$ (Whyte, 1968), this was taken as the size for its lower limit of integration. The upper limit for both contaminants (particles and bacteria) was taken as $50\mu\text{m}$. In the case of bacteria-carrying particles the median size dispersed from people is about $20\mu\text{m}$ with 7-10% less than $10\mu\text{m}$ (MacIntosh, 1978). This size range (up to $50\mu\text{m}$) was used since the validity of the Stokes law above that size becomes questionable as particles above that size appear to be accelerating so fast that Stokes law can no longer predict their motion. Also the percentage of airborne particles above that size is very small probably because few are generated and those that do will deposit rapidly.

To perform the numerical integration (integrated size distribution) the procedure adopted in the computer program was as follows:

- (1) The range of particle diameters was divided into approximately equal logarithmic intervals of width δp .
- (2) The mean diameter of each interval was used to calculate the filter's penetration using the equation (3.22).
- (3) The removal of airborne particles by gravitational sedimentation was calculated ($R_d = V_s \cdot A$) for the mean diameter of each interval.

- (4) The probability density function $\Phi(x)$ in equation (3.23) was used to determine what percentage of the particles, by count, for each distribution in equation (3.3) were greater than and equal to d_p and greater than and equal to $d_p + \delta d_p$.
- (5) The percentage of particles greater than and equal to d_p was subtracted from the percentage greater than and equal to $d_p + \delta d_p$ to give the percentage of particles in that interval.
- (6) The steady-state airborne contaminant concentration (C) was then calculated using equation (3.3) for the mean diameter of the interval.
- (7) Results were then summed to give the cumulative airborne contaminant concentration (i.e. concentration exceeding a given size).

The equation used to calculate the gravitational deposition of airborne contamination onto surfaces or into containers was as follows:

$$N^*(d_p) = A_e \cdot t_e \int_{d_p}^{\infty} V_s(d_p) \cdot C(d_p) dd_p$$

The procedure adopted in the computer programme was identical up to step (6) as given above. However further steps were required to complete the numerical integration and these were:

- (7) The modified Stokes settling velocity (V_s) was calculated for the mean diameter of the interval.
- (8) The results in step (6) was multiplied by the result in step (7) to give the particle flux for the interval.
- (9) The whole procedure (1 to 8) was repeated till the upper limit of the particle size was reached.
- (10) The particle flux in each interval was then added to give the total flux within the required size range.
- (11) The result was then multiplied by the exposed surface area for a given exposure time to give the gravitational deposition of airborne contamination onto surfaces or into containers.

As verified by experiments, it is known that gravitational sedimentation is the

only loss mechanism to be considered. Therefore the decay rate equation (Eq. 3.21) derived has been simplified to take into account only the effect of gravitational sedimentation. This reduced to:

$$C_t = C_i \cdot \exp \left[-t \left[\frac{Q}{V} + \frac{V_s}{H} \right] \right]$$

The time taken for the airborne contaminant concentration to reach to any level of its initial value was calculated as:

$$t = \frac{1}{\left[\frac{Q}{V} + \frac{V_s}{H} \right]} \cdot \ln \left[\frac{C_i}{C_t} \right]$$

For 99% of its initial value this reduced to:

$$t = \frac{10.05 \times 10^{-3}}{\left[\frac{Q}{V} + \frac{V_s}{H} \right]}$$

4. RESULTS

The results are described under six headings:

- (1) Cleanroom air distribution performance.
- (2) Dispersal of airborne particles and bacteria by people.
- (3) Particle emissions from machines in cleanrooms.
- (4) Outdoor airborne particulate and bacterial concentration.
- (5) Surface-deposition of airborne particles in a chamber.
- (6) Verification of the airborne concentration model by monitoring of airborne particles and bacteria in industrial cleanrooms.

4.1 Cleanroom Air Distribution Performance

To assess the validity of the assumption of perfect mixing used in the mathematical models (Chapter 3) and explore the air movement in a conventionally-ventilated cleanroom, experiments were carried out at Organon Pharmaceutical Manufacturing Laboratory Ltd. The influence of various parameters on air mixing were studied. Assuming constant geometry of the room and the obstructions within it, the parameters which were established from a review of the literature as having the greatest influence were:

- (1) Type of air terminal device.
- (2) Air supply flow-rate into the room.
- (3) Differential temperature between the supplied air and the room air.
- (4) Location of the contaminant source.

The results are described in the following six sections.

4.1.1 Contaminant penetration into the air supply

Tests were carried out to study the entrainment process of supplied air with the room air for the dump and jet air terminal devices. These two air terminal devices were studied because the device known as the dump should have discharged the supplied air like a jet. However it became evident that the dump air supply drew in smoke from the room air causing a flow of smoke towards a negative pressure area under and at the periphery of the HEPA filter. This smoke was

then rapidly entrained into the clean supplied air. This situation was rectified by introducing rectangular metal plates around the HEPA filter to minimize the entrainment and ensure that the air discharged like a jet (Figure 2.3). This modified air terminal device is known as a jet device.

Figures 4.1 to 4.5 demonstrate the various amount of air entrained from the room into the uncontaminated supply air for the two types of air terminal devices (dump and jet). The isopleth diagrams (Figures 4.1 to 4.5) clearly show how the jet, as compared to the dump air supply, reduces the amount of surrounding room air which penetrates into the uncontaminated supply air. The diagrams also show that the air supply from the dump air terminal device spreads as soon as it discharges into the room, the room air being rapidly induced into the air supply.

4.1.2 Air movement

The air movement pattern obtained in the conventionally-ventilated cleanroom from various air terminal devices (multislot, adjustable vane, dump and jet), ventilation rates (3 AC/hr, 15 AC/hr and 20 AC/hr) and differential temperatures between the supplied air and the room air (0K, +2K, supply air colder and -2K, supply air hotter) are summarized in Figures 4.6 to 4.13. To evaluate the effectiveness of air mixing a detailed assessment of the room air movement was carried out along major and minor vertical axes of the room. Measurements of air movement samples were taken at places chosen to include representative regions of the room air, i.e. region of entrainment, region of turbulent mixing and region of stagnant air. This exercise produced an overall picture of the air movement typical of that which would be established in conventionally-ventilated cleanrooms. As observed from values given at the air velocity arrows, actual measurements are given, but the diagrammatic representation of these values, which could be shown by the length of the arrows, is not to scale. This was not possible because of the great range and number of values to be indicated and, in some cases, it would have been impossible to visually represent the stagnant areas in the room. In the first 14 experiments (each experiment contained measurements along both axes) a

large number of points were measured in the room. As the experiments continued it could be seen that the air pattern could be adequately represented by fewer readings. The experiments were therefore continued in this way.

It is clear from the diagrams (Figures 4.6 to 4.11) that for three of the air terminal devices (multislot, adjustable vane and dump), at the given ventilation rates (3 AC/hr, 15 AC/hr and 20 AC/hr) and temperature differentials, (0K, +2K, supply air colder and -2K, supply air hotter) there were no significant differences in the pattern of air movement. These air terminal devices provided very high induction which resulted in a rapid velocity decay. On the other hand, the jet device discharged the air vertically downward with more throw and less entrainment (Figures 4.12 and 4.13). As a result of this there was more clean air available under the jet.

4.1.3 Ventilation effectiveness as assessed by decay rates

In exploring the effectiveness of air flow behaviour in diluting and removing contamination within the room, the decay of the contaminant for the various ventilating schemes was continuously recorded at three sampling locations (Appendix A). The sampling locations which were 1m from the floor were:

- Position No. 1. Directly below the central air terminal device
- Position No. 2. Middle of the room on top of the working table
- Position No. 3. Near the middle exhaust

The effectiveness and performance of various ventilation schemes in diluting and removing contamination was calculated by means of a performance index. The performance index was calculated as the ratio of theoretical (nominal) ventilation rate to the effective ventilation rate. Theoretical ventilation rates based on perfect mixing were calculated as the ratio of air supply flow rate into the room to the volume of the room. Effective ventilation rates were estimated graphically by the slope of each decay lines (Appendix A). Table 4.1 shows the calculated performance indices at each sampling location (Position No's 1, 2 and 3), for each ventilation scheme. The differential temperature between the supply air and the ambient room air was calculated by averaging all the one minute

interval results obtained during the experiment. The differential temperature when positive indicates colder supply air and when negative indicates hotter supply air.

For perfect mixing of clean supplied air with the contaminated room air, the performance index would be 1. When the performance index is below 1 this indicates that the ventilation system is more effective in removing contamination. When the performance index is greater than 1 this indicates that the clean supplied air does not appear to mix effectively with the contaminated room air.

The performance indices obtained (Table 4.1) for three of the air terminal devices (multislot, adjustable vane and dump) for various ventilation rates and differential temperatures at various sampling positions (Position No's 1, 2 and 3) were close to 1. These show good mixing of the clean supply air with the contaminated room air. For these type of air terminal devices under all air change conditions, the maximum deviations in performance indices from 1 (perfect mixing) was small being from -27% to +25%.

Table 4.1 shows that the lowest and highest performance indices were obtained from the jet air terminal device at different sampling locations. The lowest performance index was 0.56 for the jet at Position No. 1 (directly below the air terminal device). The maximum performance index of 1.52 was again obtained for the jet supply, although this was at Position No. 3 (near the middle exhaust). These rather large discrepancies between theoretical and effective local ventilation rates at the various sampling positions are due to the inadequate air mixing achieved by the jet air terminal device.

4.1.4 Ventilation effectiveness as assessed by lateral air distribution

Tables 4.2 to 4.5 summarize the results of further tests carried out to study the effectiveness of mixing of various ventilating schemes. The results assess how rapidly the smoke particles diffused and mixed throughout the room when released at one end of the room. To measure the lateral air distribution, air samples were continuously recorded from the three exhausts (E_1 , E_2 and E_3). The effectiveness of various ventilating schemes in mixing the air across the length of the room was compared by means of a performance index. The performance index for each

ventilating scheme was calculated as the ratio of the measured airborne particulate concentration to the expected airborne particulate concentration at any particular sampling point on the assumption of perfect mixing.

The test results (Tables 4.2 to 4.5) clearly show that out of the four air terminal devices (multislot, adjustable vane, dump and jet) tested, the multislot diffusers and jet produced the best and worst air mixing in the room, respectively. Multislot diffusers produced (Table 4.2) near perfect mixing across the length of the room for all ventilation rates (3 AC/hr, 15 AC/hr and 20 AC/hr).

The adjustable vane grilles produced near perfect mixing (Table 4.3) at the vicinity of exhausts E_1 and E_3 , but the clean supplied air tended to be more directed towards the central exhaust E_2 .

The results for dump air terminal device (Table 4.4) show near perfect mixing for ventilation rates of 3 and 15 air changes per hour. However when the ventilation rate was increased to 20 air changes per hour, more throw and less spread of the supplied air occurred. As a result the efficiency of mixing within the room was reduced.

The results of tests for the jet air terminal device (Table 4.5) show that efficient mixing was obtained at 3 air changes per hour. However the efficiency of mixing reduced when ventilation rates were increased to 15 and 20 air changes per hour. It should be noted that when the jet terminal was tested only the central terminal was discharging a localized piston-type air supply. The other two terminals had not been modified and were still acting as dump air terminal devices. This increased the entrainment and diffusion across the length of the room.

4.1.5 Ventilation effectiveness as assessed by constant source dispersion

To detect, describe and confirm any deviation from the theoretical phenomena of perfect mixing, further observations were made on the effectiveness of various ventilating systems in diluting and removing contamination within the room. The results of measurements for its four air terminal devices, differential temperatures, ventilation rates and contaminant release locations are summarized in Tables 4.6 to

4.13. For this set of results, two different release positions were considered. The release positions, which were both 1m from the floor, were alternated from between the central air terminal device and the table (Release Point R_{p1}) to between the central exhaust and the table (Release Point R_{p2}). As seen from Tables 4.6 to 4.13 when the release was at R_{p1} , air samples were taken from all three exhausts (E_1 , E_2 and E_3) at the top of the working table (Position No. 2) and near the middle exhaust (Position No. 3). When smoke was released at R_{p2} , air samples were taken from all three exhausts (E_1 , E_2 and E_3), at the top of the working table (Position No. 2) and from beneath the central air terminal device (Position No.1). The sampling Positions (No's. 1, 2 and 3) were all 1m from the floor.

The results of tests (Tables 4.6 to 4.11) show that three of the air terminal devices (multislot, adjustable vane and dump) produced good mixing of supplied air with the room air at ventilation rates of 3 and 15 air changes per hour for all the differential temperatures and both release positions. However when the multislot diffuser was tested at 20 air changes per hour, there appeared to be some restriction in the mixing of supplied air with room air, the throw of the supplied air being increased and hence there was more clean air available under the terminal. In this situation, when smoke was released at R_{p1} , the airborne particle concentration at the centre of the room (Position No. 2) was much higher than the rest of the room. It was also noted that the airborne concentration under the terminal and thus the air quality under the terminal was better than that predicted by assuming perfect mixing.

When the jet air terminal device was tested, reasonable mixing was only obtained at 15 air changes per hour when smoke was released between the terminal device and the table. When smoke was released between the table and the middle exhaust, there appeared to be very limited mixing for all the ventilation rates (3, 15 and 20 AC/hr) and differential temperatures studied.

It is clear from the results (Tables 4.6 to 4.13) that when jet terminal device was in use much lower PI was obtained under the jet (Position No. 1) than when

any other air terminal devices were used. This much reduced PI value obtained under the jet (Position No 1) shows the quality of air under the jet (Position No 1) is better than when any other air terminal devices were used. The reduction of average PI's with increasing volume of jet supplied air indicates that, due to more throw of the supplied air and less entrainment, the quality of air only under the jet improves.

4.1.6 Multiple regression analysis of constant source dispersion results

A multiple regression analysis was carried out on the results obtained and described in the previous section (4.1.5). This analysis derives equations which relate a dependent variable to various independent variables. The dependent variable to be predicted in these equations was the performance index at the three different sampling positions, i.e.

- (1) Directly below the central air terminal device (Position No. 1)
- (2) Middle of the room on top of the working table (Position No. 2)
- (3) Near the middle exhaust (Position No. 3)

The independent variables or predictors studied were:

- (i) Ventilation rate into the room
- (ii) Type of air terminal device (jet or multislots)
- (iii) Smoke dispersion point (R_{p1} or R_{p2})
- (iv) Temperature difference between supply and room air

The type of equation obtained from the analysis was in the form:

$$PI = \text{Constant} + k_1(\text{AC/hr}) + k_2(\Delta T) + k_3 \begin{bmatrix} \text{Type of device} \\ \text{Jet} = 0 \\ \text{Multislots} = 1 \end{bmatrix} + k_4 \begin{bmatrix} \text{Release point} \\ R_{p1} = 0, R_{p2} = 1 \end{bmatrix}$$

where the value of the ventilation rate and temperature difference is that established during the experiment and the type of device and release point either 0 or 1, as shown in the equation.

Table 4.14 gives the values of the various coefficients (constant and k_1 to k_4) derived from each analysis of the data. Only regression coefficients which are

statistically significant are included in the equations. The level of significance as percentage probability is given in Table 4.14. Normally the coefficient was regarded as significant if the probability was less than 5%. However, it is possible that at probability levels between 5% and 10% the variables were statistically significant. These were therefore included in the equations but, when that occurred, their probability level was shown in brackets in the equation.

The final forms of the equations can be used to predict PI's for different conditions. By inputting the ventilation rate, temperature difference, type of device (0 for a jet and 1 for a multislot) and release point (0 for R_{p1} and 1 for R_{p2}) into the relevant equation, the PI can be calculated. The equation also enables the numerical importance of the independent variables to be calculated.

The results were analyzed in four groups. These groups were:

- A. all results
 - B. results when smoke was released at R_{p1}
 - C. results when smoke was released at R_{p2}
 - D. results separated into those obtained from either multislot or jet
- A. The first set of data tested included all the test results. The regression equations predicting the performance indices for each sampling point are as follows:

$$(PI)_1 = 0.736 - 0.032N + 0.370A_t$$

$$(PI)_2 = 0.693 + 0.016N + 0.050\Delta T + 0.720A_t + 0.953R_p$$

$$(PI)_3 = 0.897 + 0.531R_p$$

where N = ventilation rate (AC/hr)

ΔT = differential temperature (K)

A_t = air terminal device

R_p = release position of smoke

It can be seen that the most significant factors which influenced the mixing of the supplied air with the room air under the air supply terminal (Position No. 1) were the air change rates and the type of air terminal device, while the temperature differential and the location of smoke released had no

statistically significant effect. It should be noted that an increase in ventilation rate decreased the amount of mixing. All factors had a significant effect on mixing in the centre of the room (Position No. 2). For all the cases except one ($R_p = 0$ and $A_t = 0$), the effect of decreasing the ventilation rate improved the mixing. Near the middle exhaust (Position No. 3) it was only where the smoke was released had any significant effect. When smoke dispersion point was at R_{p1} , the smoke mixed better, relatively, than when released at R_{p2} .

- B. When the data was analysed from the results obtained when smoke was released only between the middle air terminal device and the working table (release position R_{p1}), the two regression equations for each sampling position yielded the following:

$$(PI)_2 = 0.556 (P < 10\%) + 0.055N + 1.121A_t$$

$$(PI)_3 = 0.819 + 0.600A_t$$

These equations reflect the fact that the mixing process in the centre of the room (Position No. 2) and near the middle exhaust (Position No. 3) are mainly affected by the type of air terminal device. Higher ventilation rates influence the mixing in the centre of the room (Position No. 2) but not near the middle exhaust (Position No. 3). The effect of increasing the ventilation rate reduced the amount of mixing by multislotted diffusers, although in the case of jet device, the mixing reduces after the ventilation rate has reached 8 air changes per hour.

- C. When only the data which was derived from the tests where the smoke was released between the middle exhaust and the working table (R_{p2}) was analysed the following regression equations were obtained:

$$(PI)_1 = 0.738 - 0.034N + 0.352A_t$$

$$(PI)_2 = 0.721 - 0.020N + 0.438A_t$$

The results show that both the jet air terminal device and an increase in the air change rates both decrease the amount of air mixing. However the mixing in the centre of the room by multislotted diffusers only reduced when the

ventilation rate increases from 8 air changes per hour. Temperature difference had no effect.

- D. When the data was divided and analyzed according to the type of air terminal devices (multislot and jet) the following regression equations for the three positions were obtained:

Jet

$$(PI)_1 = 0.714 - 0.032N + 0.038\Delta T \quad (P < 8.5\%)$$

$$(PI)_2 = 1.221 + 0.151\Delta t \quad (P < 8\%) - 0.873R_p$$

$$(PI)_3 = 0.988 + 0.195\Delta T$$

Multislot

$$(PI)_1 = 1.110 - 0.036N$$

$$(PI)_2 = 2.010 - 1.422R_p$$

$$(PI)_3 = 1.654$$

The above regression models suggest that the principal factors contributing to air mixing under the terminal (Position No. 1) for both air terminal devices (multislot and jet) was the air change rates, although the temperature difference may have had some effect on the air issuing from the jet device. Again the results show that increasing the ventilation rate reduces the amount of mixing. Significant factors which influence the mixing in the centre of the room could be demonstrated in the case of the jet device where the release position and possibly the temperature difference were significant and in the case of the multislot terminal device where only the release position was significant. Near the middle exhaust (Position No. 3) the air mixed by the multislot diffuser was not affected by any variable and in the case of the jet device, only the temperature difference.

4.2 Dispersal of Airborne Particles and Bacteria by People

Data on the dispersal of airborne contaminants by male and female volunteers was gathered for utilization in the airborne contaminant concentration model.

Tables 4.15 to 4.18 show the amount of airborne contaminant dispersed from personnel who worked at Organon Laboratories and the Mechanical Engineering Research Annexe. Tables 4.15 and 4.16 show the mean steady-state dispersion rate measured from 30 female and 25 male volunteers. A comparison of male and female dispersion rates is shown in Tables 4.17 and 4.18. The number dispersed by individuals appeared to be log-normally distributed as shown in frequency distribution diagrams (Figures 4.14 to 4.19). These results show great variability in dispersal from different subjects, especially so in the case of male subjects. Furthermore, the results show that males disperse more contamination than females. This is particularly in the case of bacterial dispersion where males dispersed about 5 times more bacteria than females when wearing indoor clothes. However it is interesting to note that when cleanroom clothing was worn this difference in bacterial dispersion between males and females was reduced to about 1.5 times.

4.3 Particle Emissions from Machines in Cleanrooms

To gather realistic data for utilization in the airborne contaminant concentration model, experiments were carried out to measure the particle emission from two vial-filling machines.

4.3.1 Baush & Stroebel vial-filling machine

Tables 4.19 and 4.20 show the change in the particle concentration of airborne particles greater and equal to five different particle diameters ($0.3\mu\text{m}$, $0.5\mu\text{m}$, $1\mu\text{m}$, $2\mu\text{m}$ and $5\mu\text{m}$) with respect to time when sampling $1\text{ ft}^3/\text{min}$ of air. Table 4.19 corresponds to the results when the operator and the machine were working and Table 4.20 corresponds to the operator working and the machine off. From both tables (4.19 and 4.20) it is clear that due to a high initial burst of particles dispersed into the room, the airborne particulate concentration increased and reached a peak, after which time the concentration gradually decreased. It was also evident from the experimental data obtained for both tests (Tables 4.19 and 4.20) that the results did not have sufficient time to drop to a plateau but

were a percentage of the average steady-state concentrations. The average steady-state particles generated in both tests was therefore obtained by using the decay equation (Eq. 2.3). The results from both tests were then subtracted to give the particles generating from the machine (Table 4.21). The results show that the vial-filling machine generated about 2×10^6 particles/min of particles $\geq 0.5\mu\text{m}$.

4.3.2 Bosch-Strunck vial-filling machine

Table 4.22 shows the average steady-state particles generated from the Bosch-Strunck vial-filling machine. The results show that the particles generated from the machine ($2.7 \times 10^4 \geq 0.5\mu\text{m}$) are about 100 times less than the Baush & Stroebel vial-filling machine.

4.4 Outdoor Airborne Particulate and Bacterial Concentration

Table 4.23 shows the mean airborne contamination present in the outdoor air at different locations (urban and rural) and climatic conditions (wind, sun and rain). It would appear from the results (Table 4.23) that the weather and location influenced the airborne contaminant concentration. The mean airborne bacteria concentrations for rural and urban locations were averaged for the three climatic conditions and found to be $0.53/\text{ft}^3$ ($18.7/\text{m}^3$) and $0.64/\text{ft}^3$ ($22.6/\text{m}^3$) respectively. Furthermore, as expected, it can be seen that the airborne particle concentration is more in urban locations than the rural locations. Minimum airborne bacterial concentration ($0.45/\text{ft}^3$ or $16/\text{m}^3$) and minimum particulate concentrations ($1.6 \times 10^5/\text{ft}^3$ or $5.8 \times 10^6/\text{m}^3$ for particles $\geq 0.5\mu\text{m}$ and $600/\text{ft}^3$ or $2.1 \times 10^4/\text{m}^3$ for particles $\geq 5\mu\text{m}$) were obtained on a windy day and on a rainy day respectively.

4.5 Surface-Deposition of Airborne Particles in a Chamber

To gain an understanding of various surface deposition mechanisms and to estimate their significance, the surface deposition of airborne particles in the previously described chamber (section 2.5) was investigated theoretically and experimentally. The ultimate objective was to exclude mechanisms of negligible

significance from inclusion in the airborne contaminant concentration model described (Chapter 3) although the results also gave an insight into the theoretical and actual deposition rates of the various mechanisms of particle deposition.

To calculate the variation of surface-deposition with equivalent ventilation rate, the average turbulent energy dissipation rate into the air by the stirrer was required. This was related to the power put into the air by the stirrer. Given in Figure 4.20 is the graph of motor shaft power against angular speed for various operating air pressures. The fan power was calculated as the difference between torque power of the shaft with blades, less the torque power of the shaft only. From this the relationship between fan power and air pressure for the two stirrers was established (Figure 4.21).

To predict the deposition flux, the airborne particulate concentration had to be evaluated. Samples of air were taken, the volume of sample being determined by a Rotameter flowmeter. The Rotameter was calibrated by drawing air through the filter by the vacuum pump and determining its scale reading at different suction pressures (Figure 4.22).

Shown in Figure 4.23 is the size calibration of the wet airborne droplets projected from the rim of the air-driven spinning-top atomizer used to produce droplets during the experiments. Figure 4.23 shows the calibration curve of the true wet drop size between 25 μm and 150 μm generated by the atomizer running at pressures between 4 and 72 cm Hg when spraying solution of 80% v/v aqueous ethanol. This calibration curve was used to estimate the dry particle size and also to compare it with the dry size observed when using the microscope.

Table 4.24 shows the theoretical deposition velocities calculated for various aerodynamic particle diameters (0.8 μm , 6.3 μm and 11.2 μm) and equivalent ventilation rates in the chamber (0 AC/hr, 20 AC/hr and 200 AC/hr). These deposition velocities have been computed from the deposition model taking into account the surface loss rate due to gravitational sedimentation, Brownian (molecular) diffusion and turbulent (eddy) diffusion for uncharged particles. These theoretical results (Table 4.24) suggested that there would be no difference between

deposition under both still and stirred air for aerodynamic particle diameters of $6.3\mu\text{m}$ and $11.2\mu\text{m}$. Furthermore they suggest that practically all particles of these sizes ($6.3\mu\text{m}$ and $11.2\mu\text{m}$) would deposit on the floor of the chamber. Figure 4.24 shows the graph of theoretical deposition velocity against particle diameter for various equivalent ventilation rates (0 AC/hr, 20 AC/hr and 200 AC/hr). One feature of these theoretical deposition curves (Figure 4.24) was that all the three curves (0AC/hr, 20 AC/hr and 200 AC/hr) gave a size of particle with a minimum deposition, deposition increasing below and above this size. The values of particle size which gave minimum deposition is shown (Figure 4.24) to vary between $0.3\mu\text{m}$ and $0.8\mu\text{m}$, depending on the stirrer speed. Furthermore the deposition curves (Figure 4.24) clearly show that there is likely to be no difference in deposition under both still air and stirred air conditions for particles greater than about $1.5\mu\text{m}$. However, deposition is likely to increase for particles below $0.5\mu\text{m}$ as the equivalent ventilation rate is increased. The deposition values (Table 4.24) show that at any fixed flow condition (still or stirred) gravitational sedimentation is the predominant loss mechanism.

Table 4.25 shows the deposition velocities calculated from the number of bacterial-carrying particles found to deposit in the chamber. This was for various aerodynamic particle diameters ($0.8\mu\text{m}$, $6.3\mu\text{m}$ and $11.2\mu\text{m}$) and equivalent ventilation rates (0AC/hr, 20 AC/hr and 200 AC/hr). It is clear from these results that particles of aerodynamic diameters $6.3\mu\text{m}$ and $11.2\mu\text{m}$ all deposit on the floor of the chamber, under both still and stirred air conditions and are therefore in good agreement with theory. However, the theoretical results obtained (Table 4.24 and Figure 4.24) appear to underestimate the experimental results for particles of aerodynamic diameter of $0.8\mu\text{m}$. The probable reason for this was that particles were formed by spraying solutions and used within a short time; they would therefore carry a very high charge which enhanced surface deposition. In the hope of minimizing the electrostatic effects of the particles and establishing whether electrostatic effect was the likely reason an air ioniser was used to saturate the air with ions. The results obtained (Table 4.25) when the air ioniser

was used compared to that when no air ioniser was used (Table 4.26) show there was about a 50% reduction in surface deposition. This deposition rate is still 3 times greater than that predicted.

4.6 Verification of Airborne Concentration Model by Monitoring of Airborne Particles and Bacteria in Industrial Cleanrooms

Table 4.27 shows the conditions of the cleanrooms used to assess the validity of the airborne contaminant concentration model derived in Chapter 3. The results are from conventionally-ventilated cleanrooms at Optical Coating Ltd. (OCLI) in Fife and at Organon Ltd, a pharmaceutical manufacturing laboratory at Newhouse near Glasgow. Tables 4.28 and 4.29 show the contaminant concentration in the air of cleanrooms. The method used in determining particle concentration was that described in Federal Standard 209D (1988). Both cleanrooms conformed to Class 10,000 of Federal Standard 209D. Airborne bacterial sampling was additionally carried out at Organon Pharmaceutical Laboratory, as shown in Table 4.29. Validation of the model was accomplished (Table 4.30) by running the computer program developed on the IBM PC with the input of experimental data as shown in Table 4.27. On the basis of inputting mean airborne contaminant dispersal obtained from people, the predicted airborne contaminant concentration was between the lower 95% confidence limit and the mean of the averages measured in the rooms.

Inputting arbitrary variables with deviance of $\pm 50\%$ in the computer model allowed the determination of the significant impact that each variable has on the overall result. This sensitivity analysis of the airborne contaminant concentration model to input variables is summarized in Table 4.31. The effect of changing all the input variables on the airborne contaminant concentration indicated that the airborne contaminant concentration is strongly influenced by the contaminant dispersion rate and the volumetric flow rate of supplied air into the room. Furthermore, it demonstrates that little is to be gained by the use of highly efficient final filters as opposed to filters 50% less efficient.

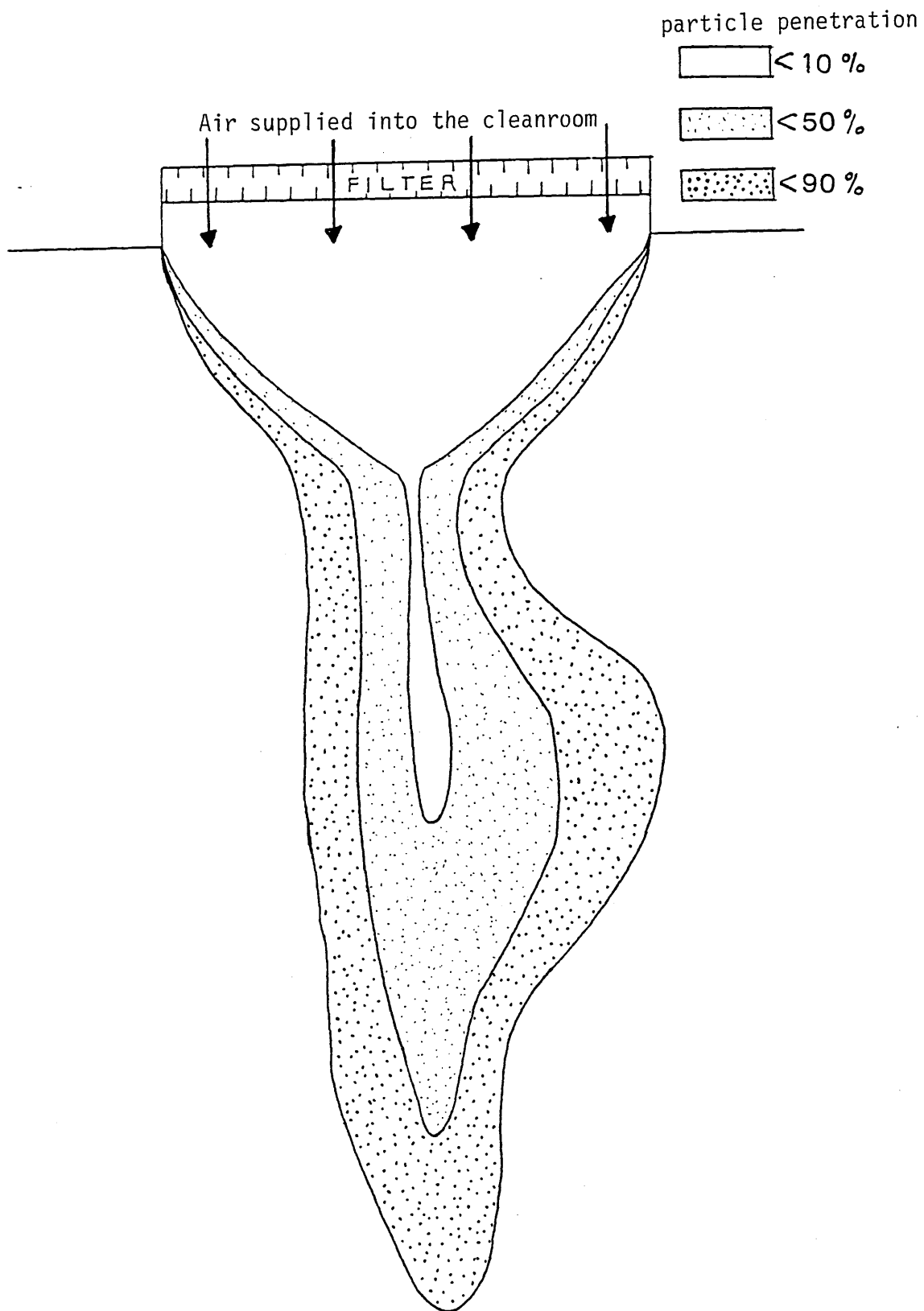


Fig. 4.1 Isopleth diagram of the isothermal dump air supply with 20 AC/hr

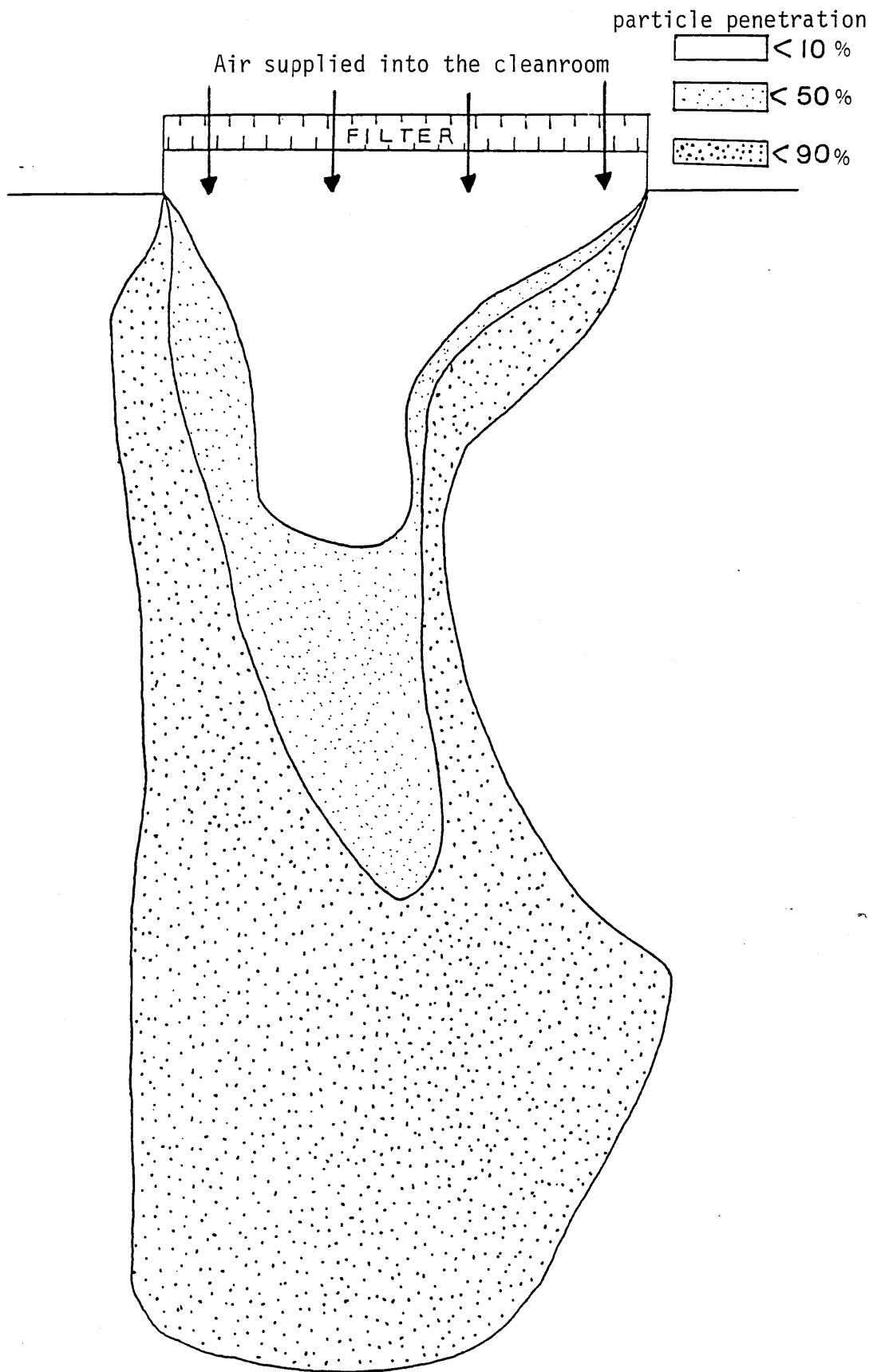


Fig. 4.2 Isopleth diagram of the isothermal jet air supply with 4 AC/hr

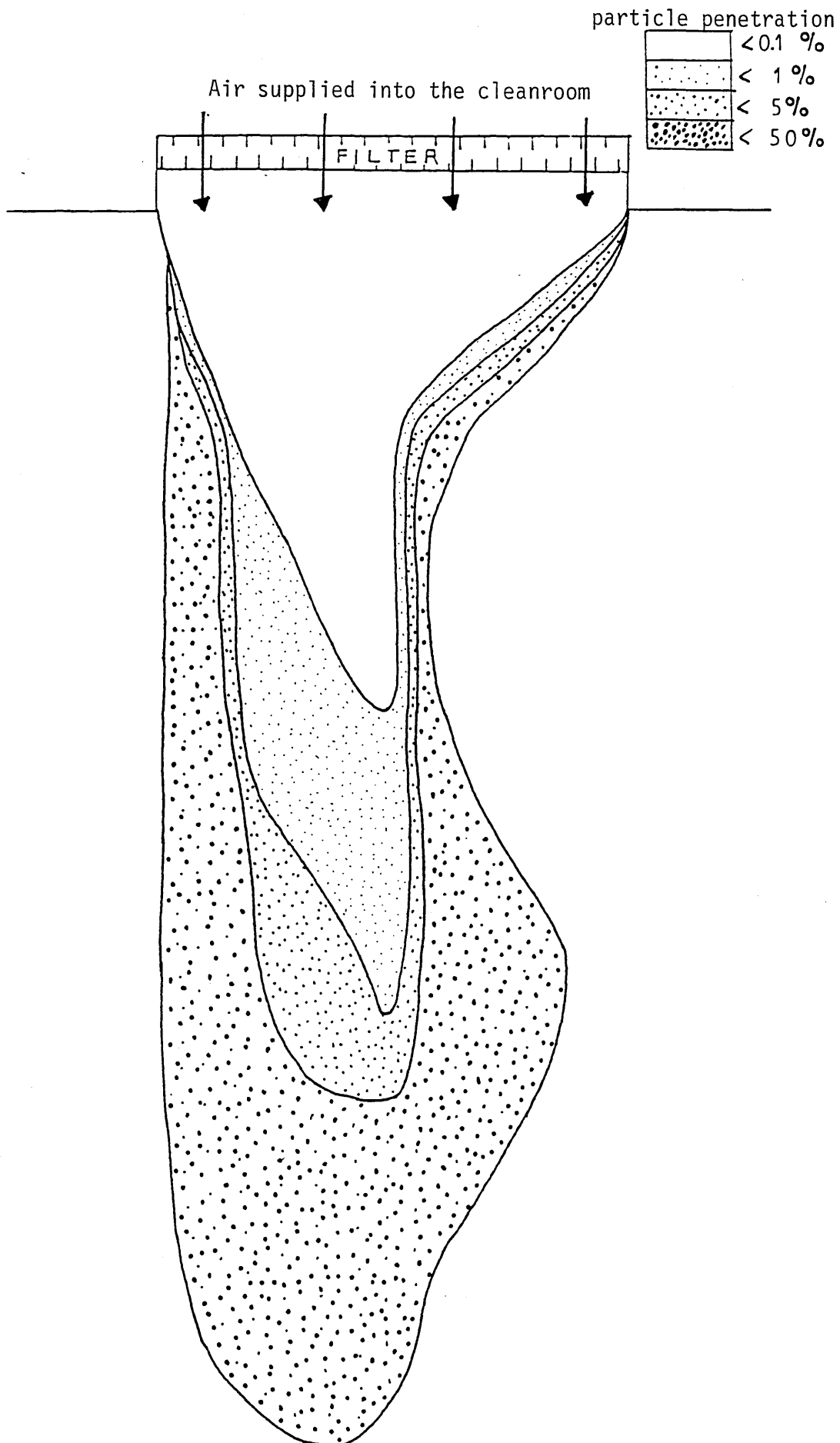


Fig. 4.3 Isopleth diagram of the isothermal jet air supply with 15 AC/hr

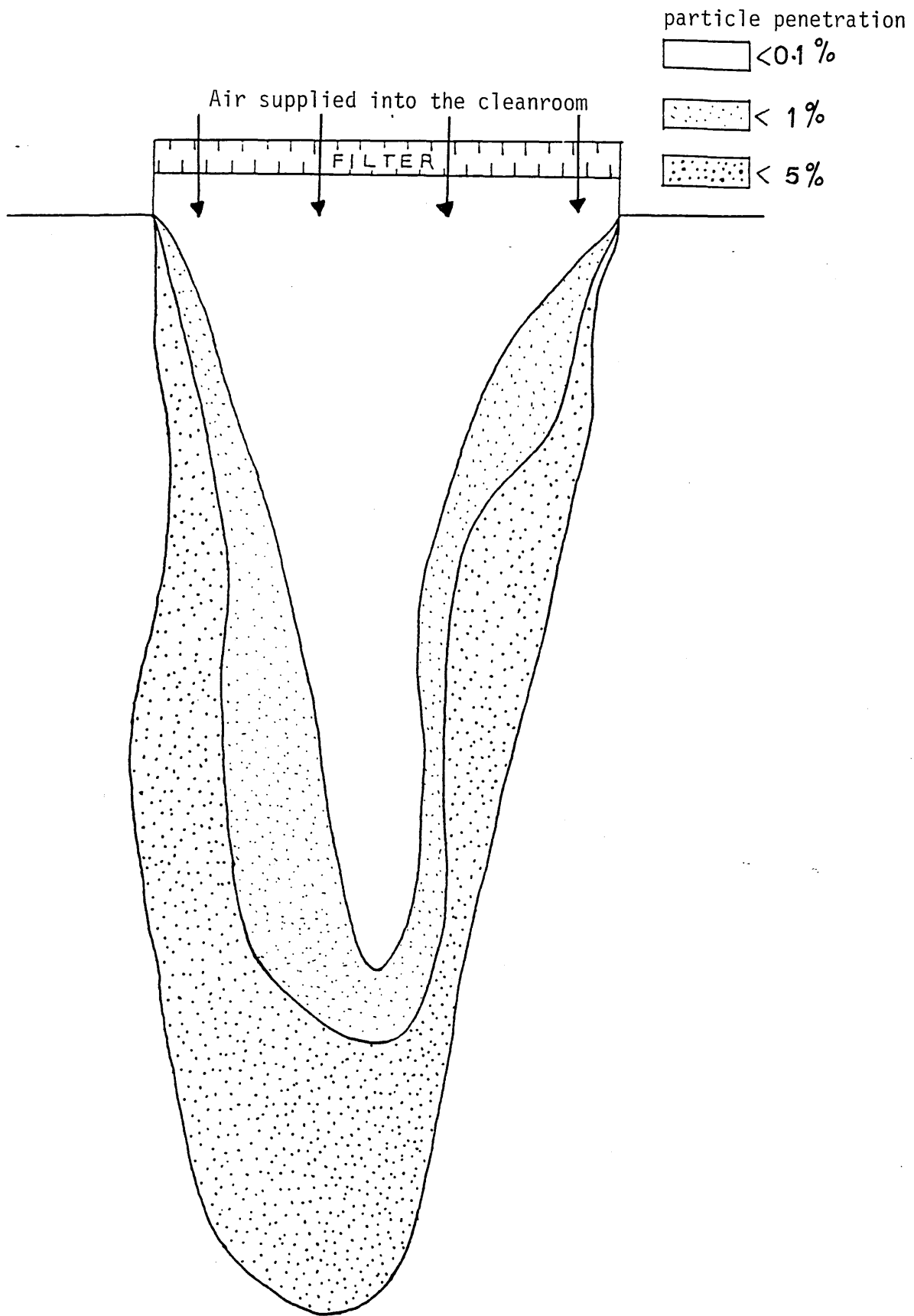


Fig. 4.4 Isopleth diagram of the isothermal jet air supply with 22 AC/hr

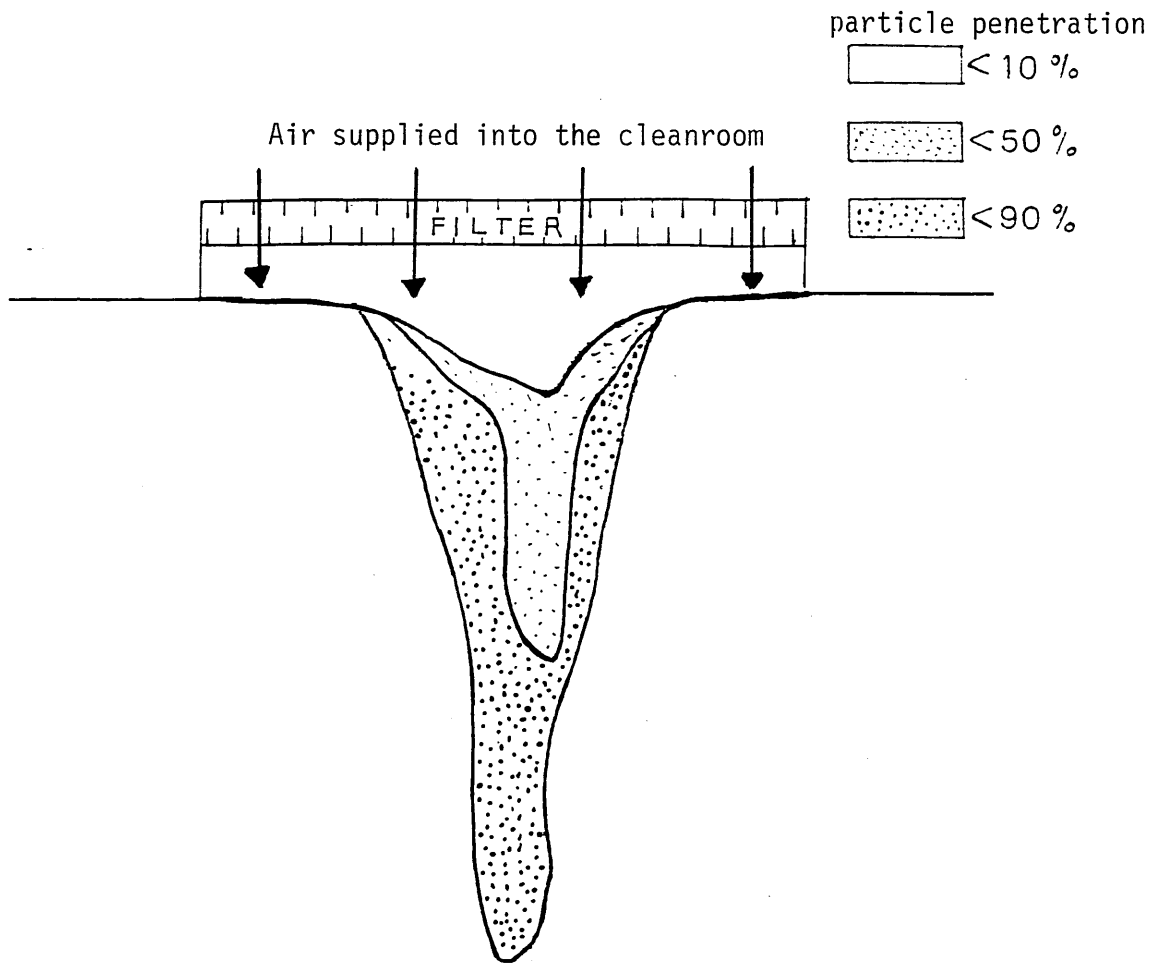
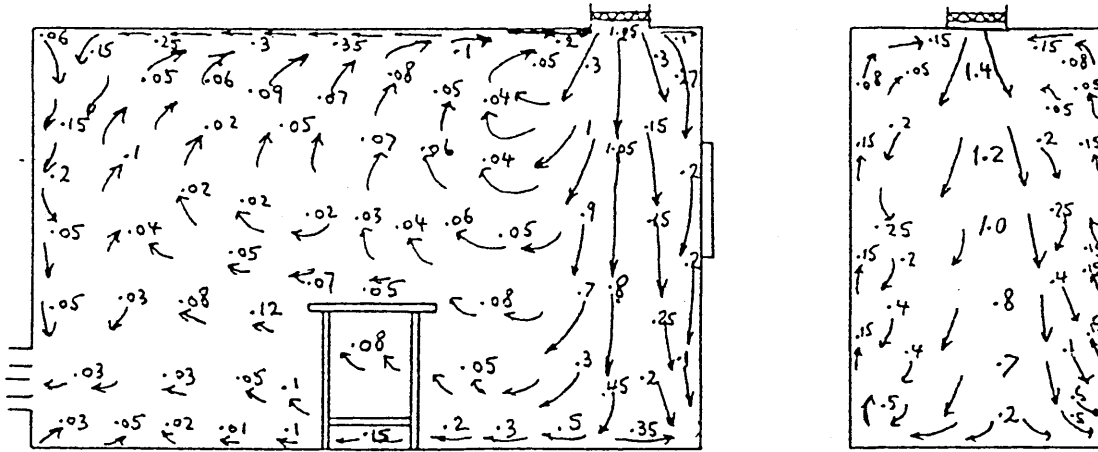
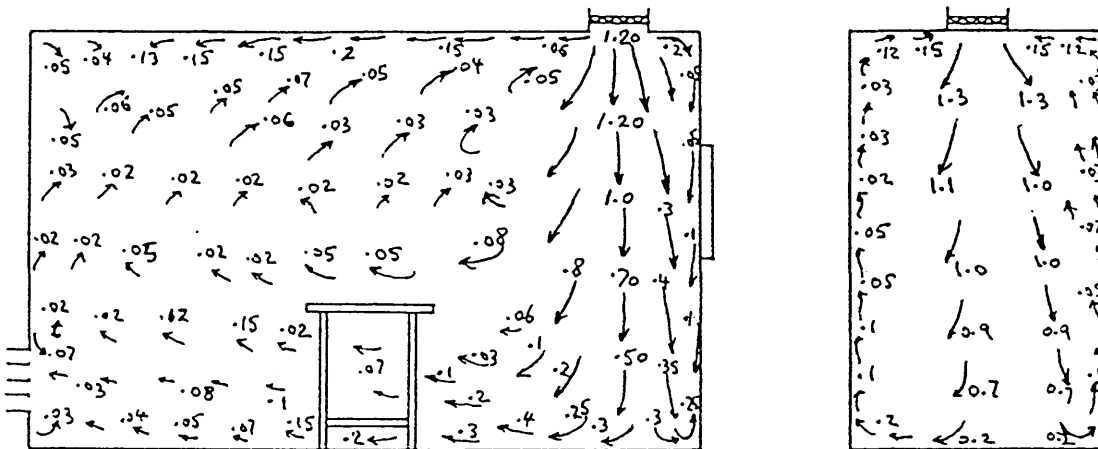


Fig. 4.5 Isopleth diagram of the isothermal dump air supply with 4 AC/hr

Nominal $\Delta T = +2K$



Nominal $\Delta T = 0 K$



Nominal $\Delta T = -2K$

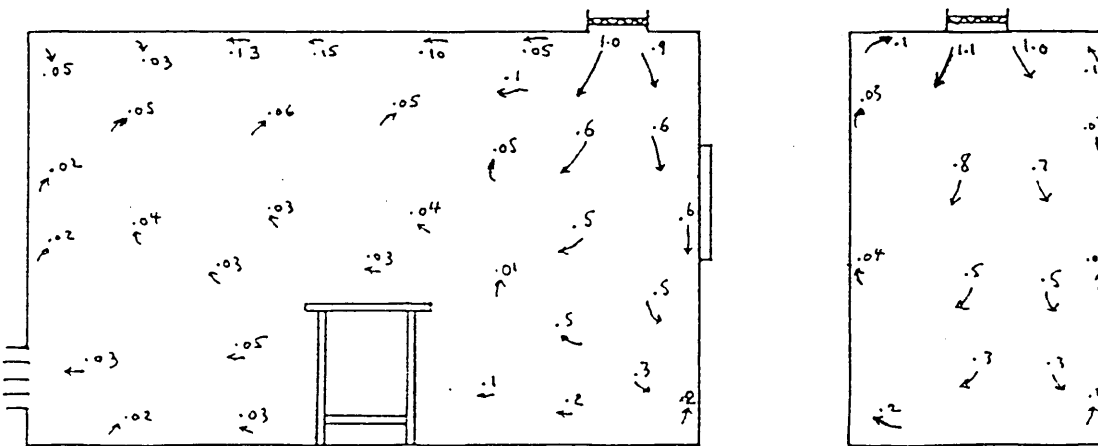
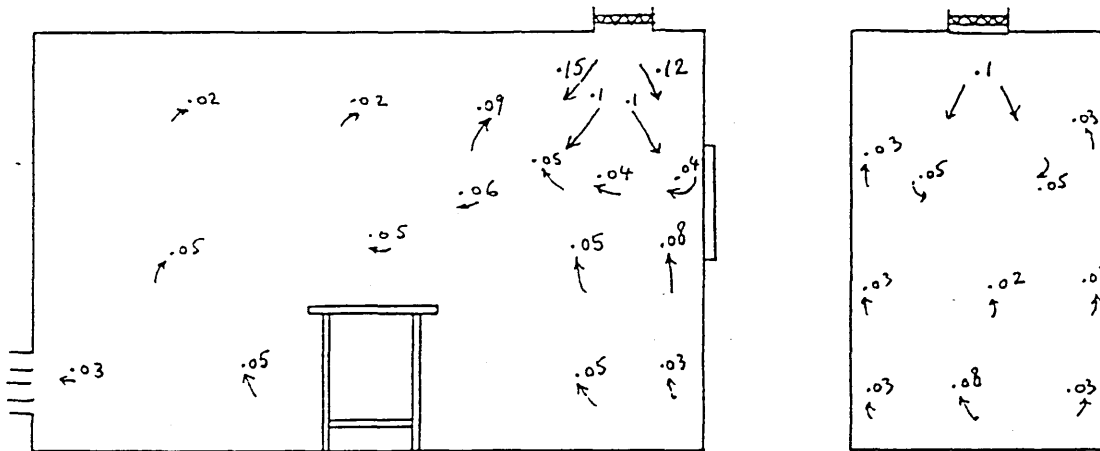
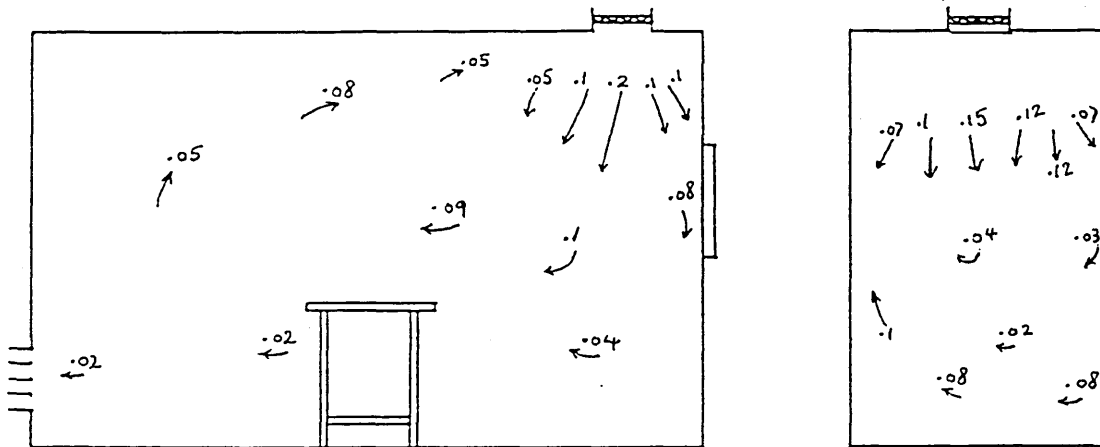


Fig. 4.6 Air movement patterns in cleanroom along major and minor vertical sections of the room - Dump air supply with 20 AC/hr

Nominal $\Delta T = +2K$



Nominal $\Delta T = 0K$



Nominal $\Delta T = -2K$

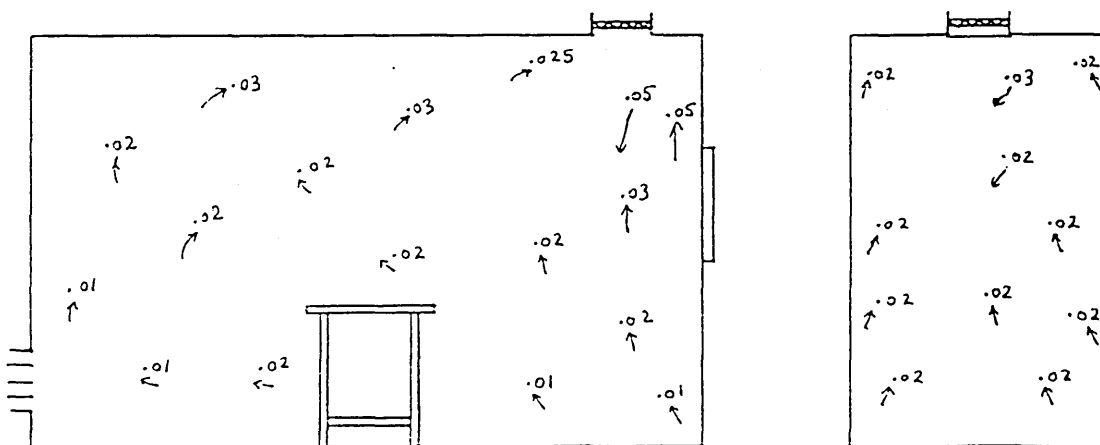
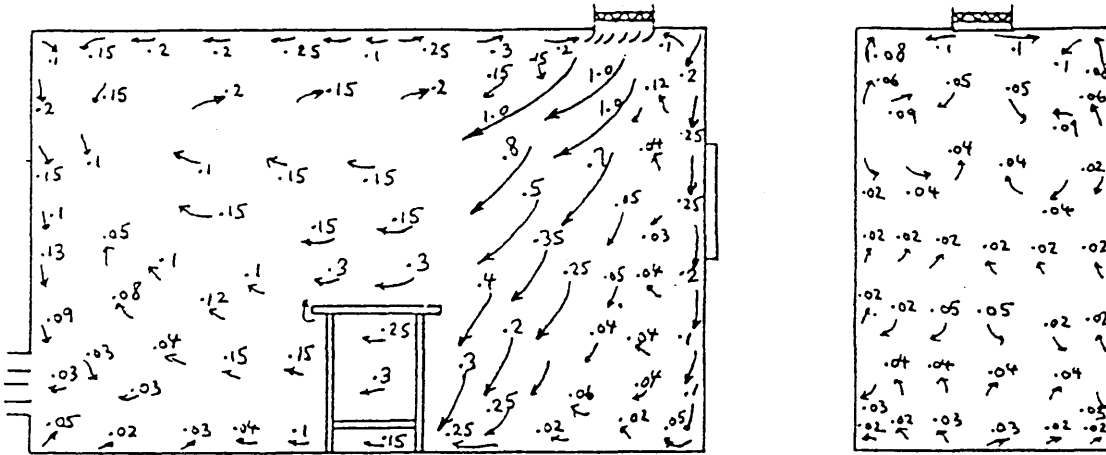
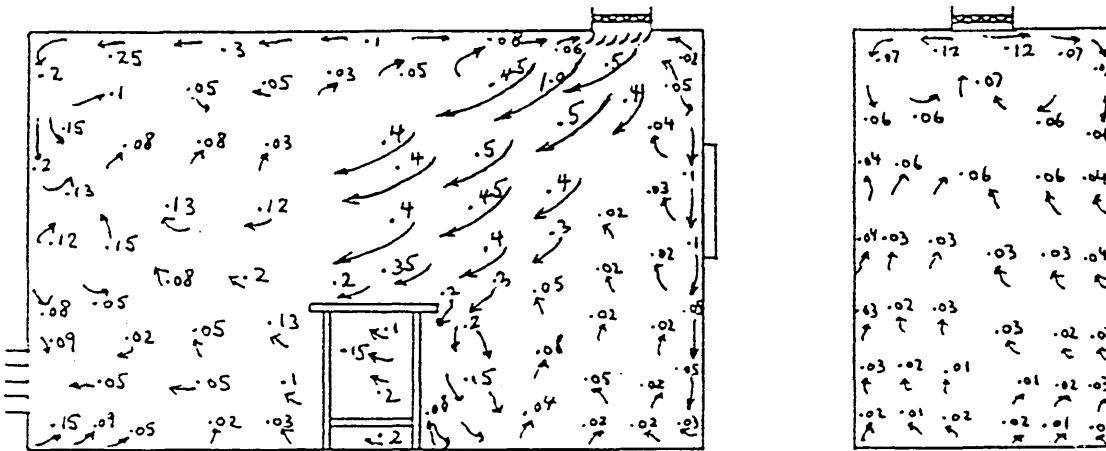


Fig. 4.7 Air movement patterns in cleanroom along major and minor vertical sections of the room - Dump air supply with 3 AC/hr

Nominal $\Delta T = +2 K$



Nominal $\Delta T = 0 K$



Nominal $\Delta T = -2 K$

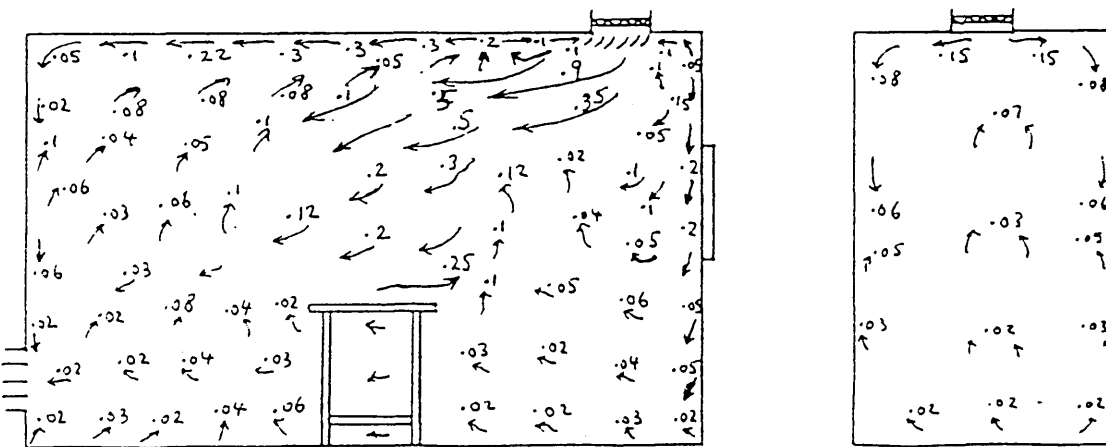
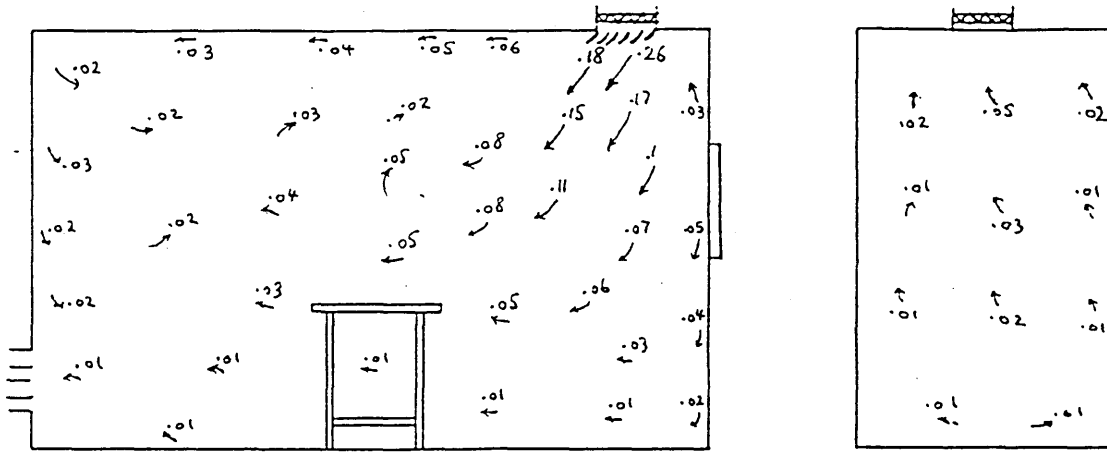
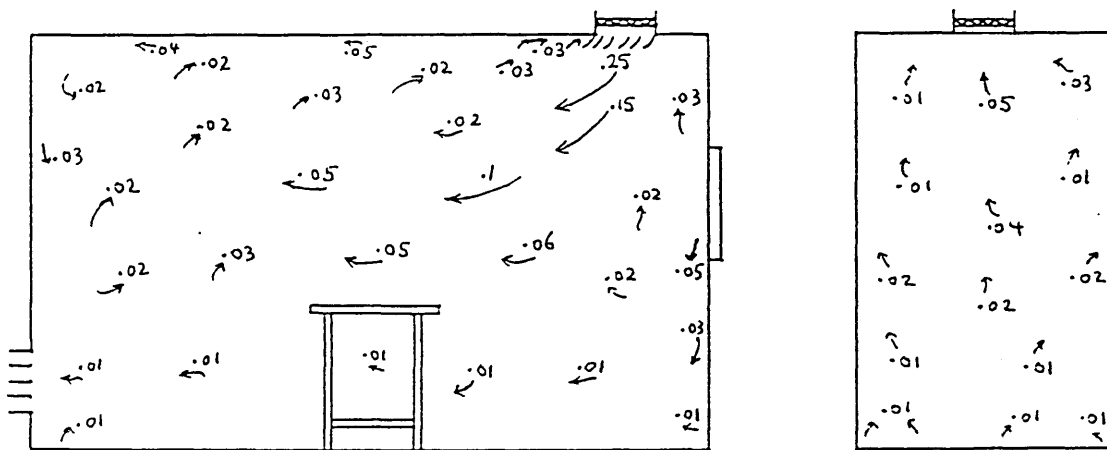


Fig. 4.8 Air movement patterns in cleanroom along major and minor vertical sections of the room - Adjustable vane grilles with 15 AC/hr

Nominal $\Delta T = +2K$



Nominal $\Delta T = 0K$



Nominal $\Delta T = -2K$

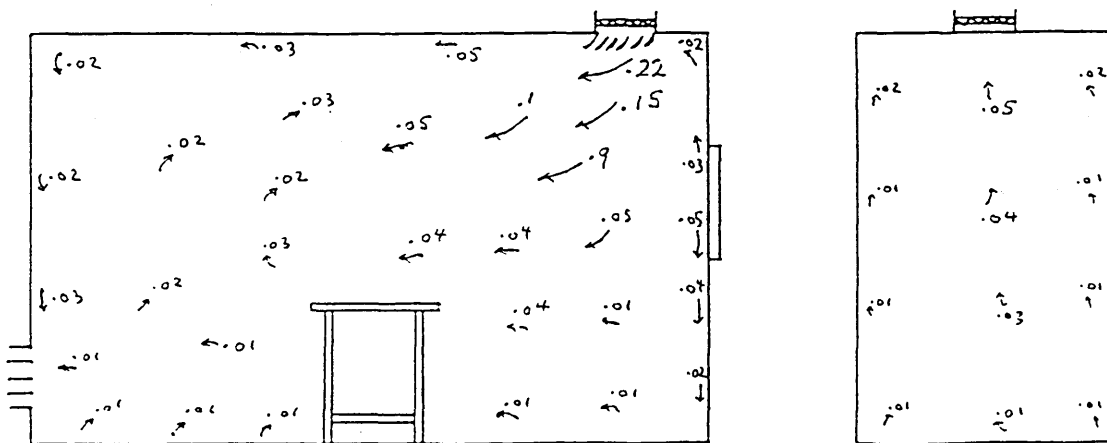
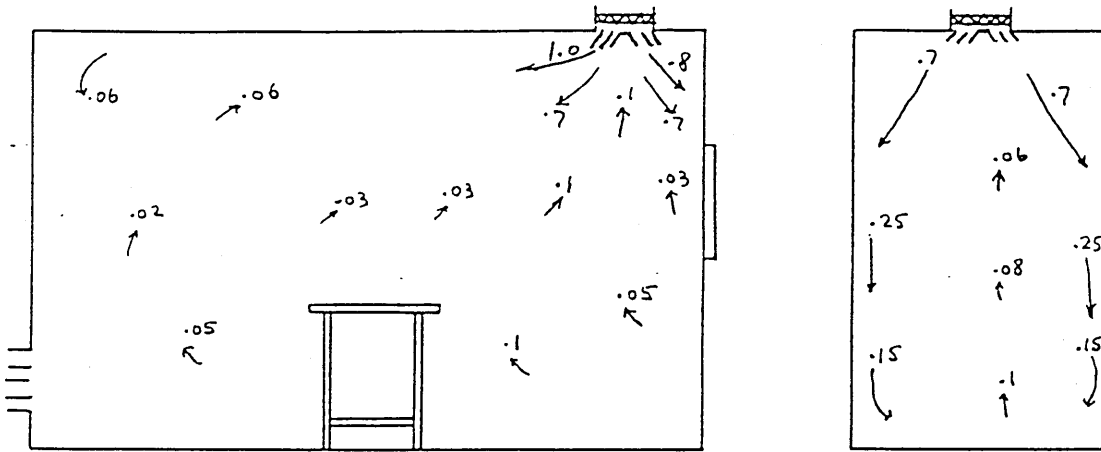
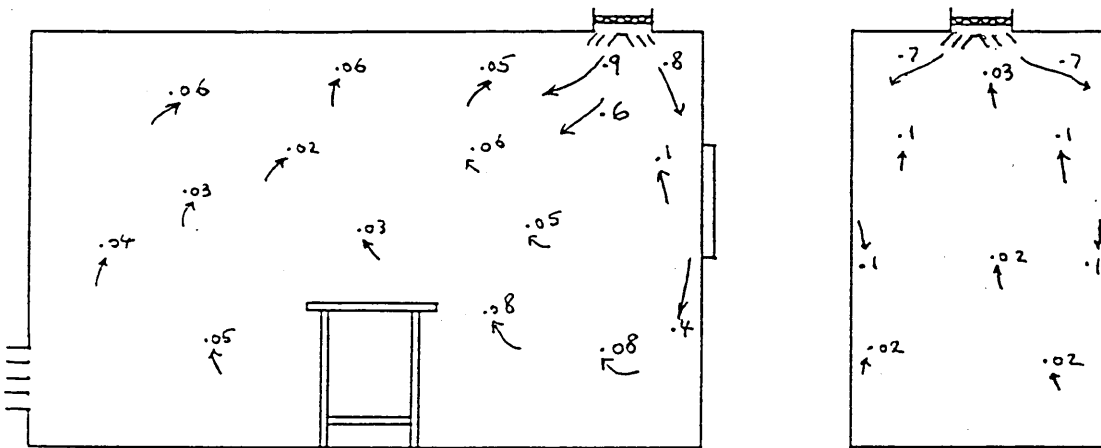


Fig. 4.9 Air movement patterns in cleanroom along major and minor vertical sections of the room - Adjustable vane grilles with 3 AC/hr

Nominal $\Delta T = +2K$



Nominal $\Delta T = 0K$



Nominal $\Delta T = -2K$

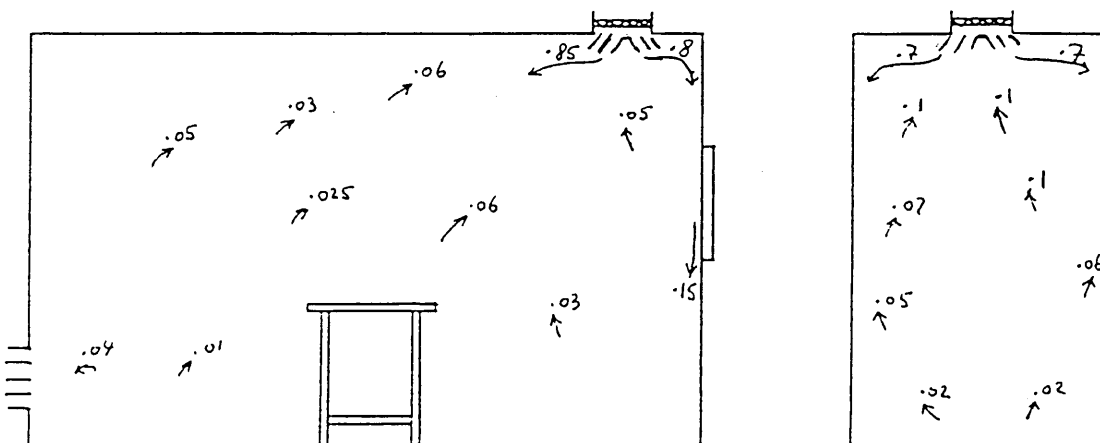
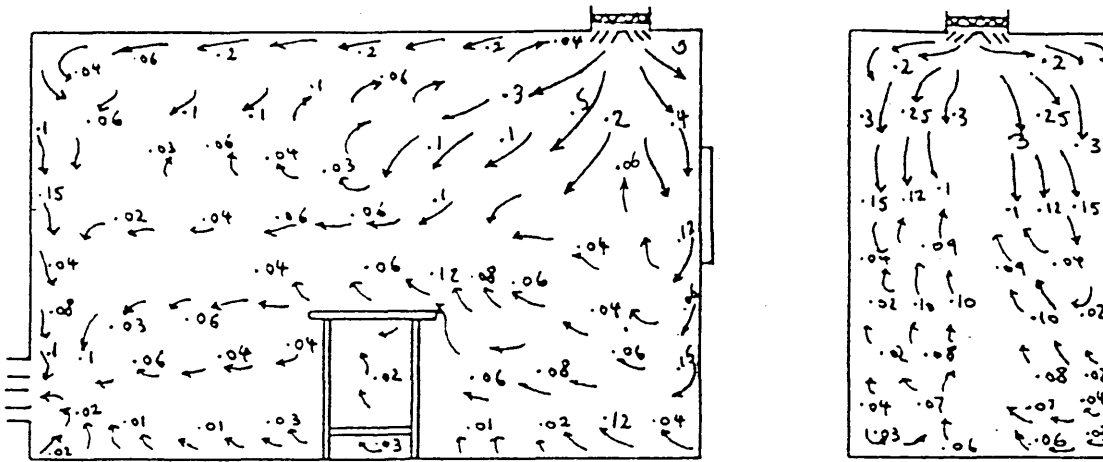
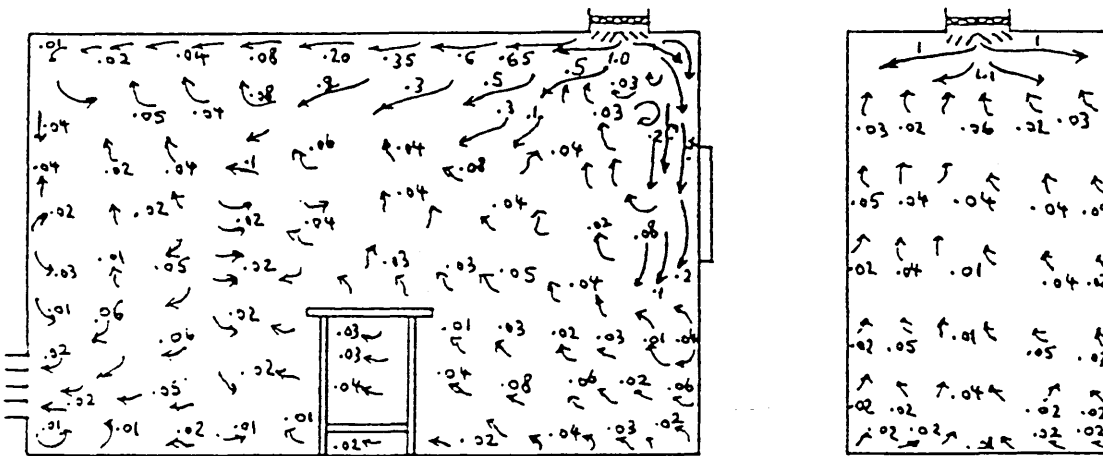


Fig. 4.10 Air movement patterns in cleanroom along major and minor vertical sections of the room - Multislot diffusers with 20 AC/hr

Nominal $\Delta T = +2K$



Nominal $\Delta T = 0K$



Nominal $\Delta T = -2K$

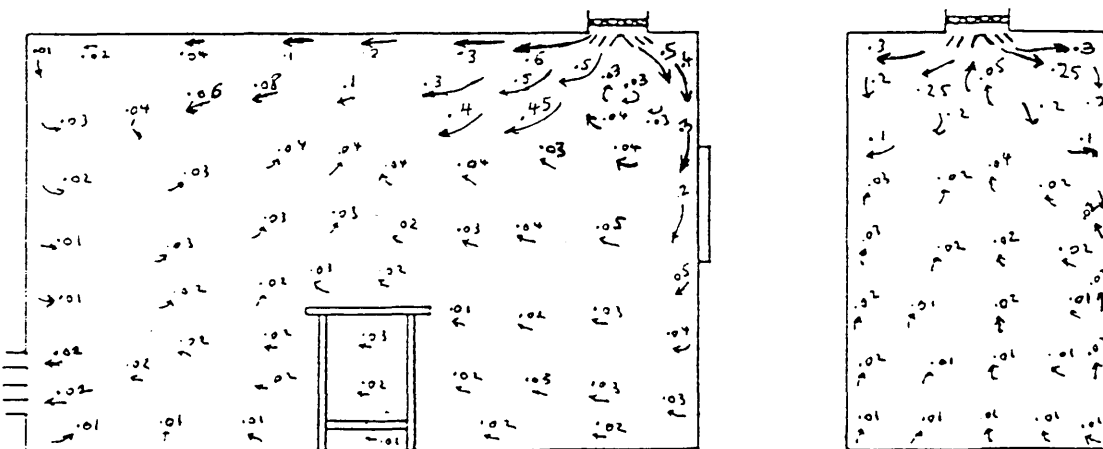
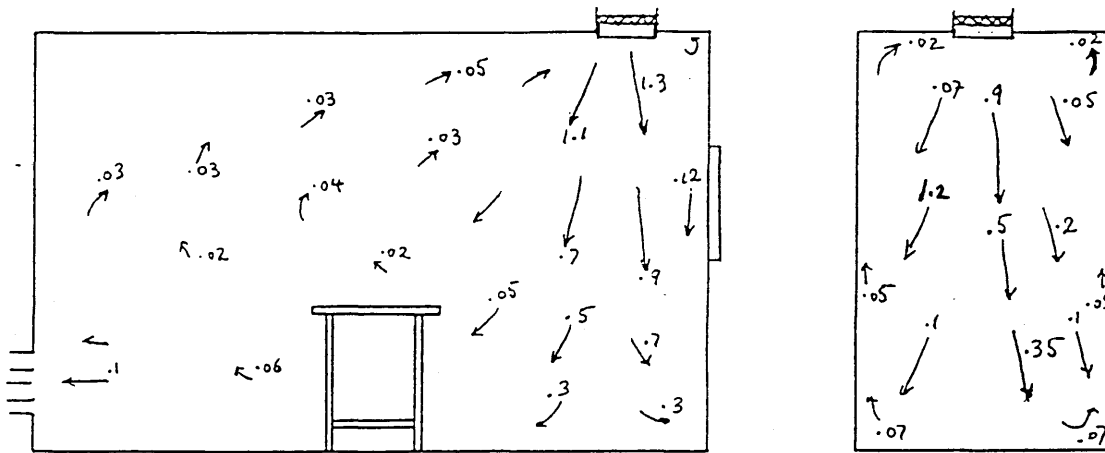
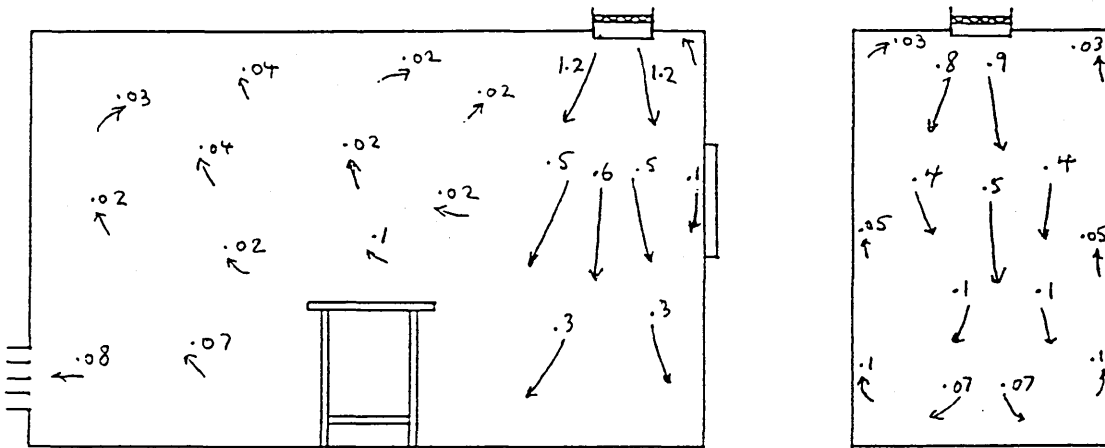


Fig. 4.11 Air movement patterns in cleanroom along major and minor vertical sections of the room - Multislot diffusers with 15 AC/hr

Nominal $\Delta T = +2K$



Nominal $\Delta T = 0K$



Nominal $\Delta T = -2K$

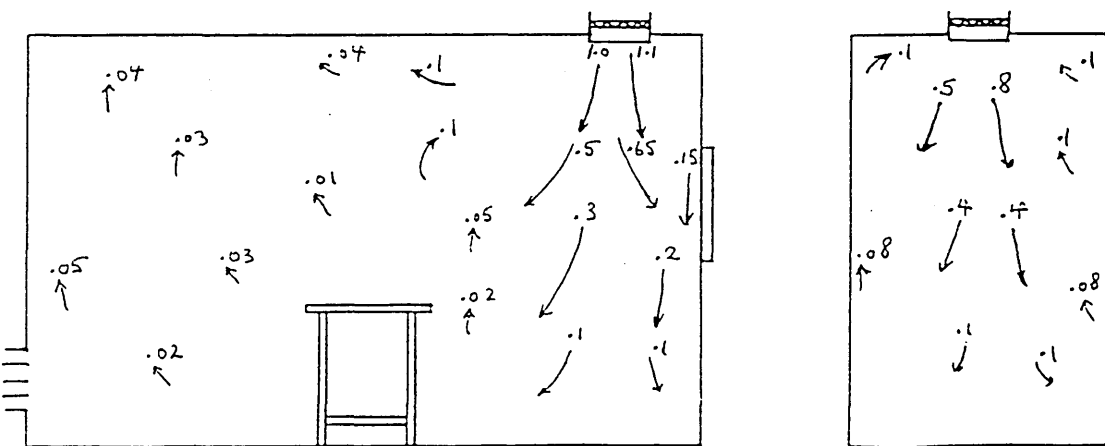
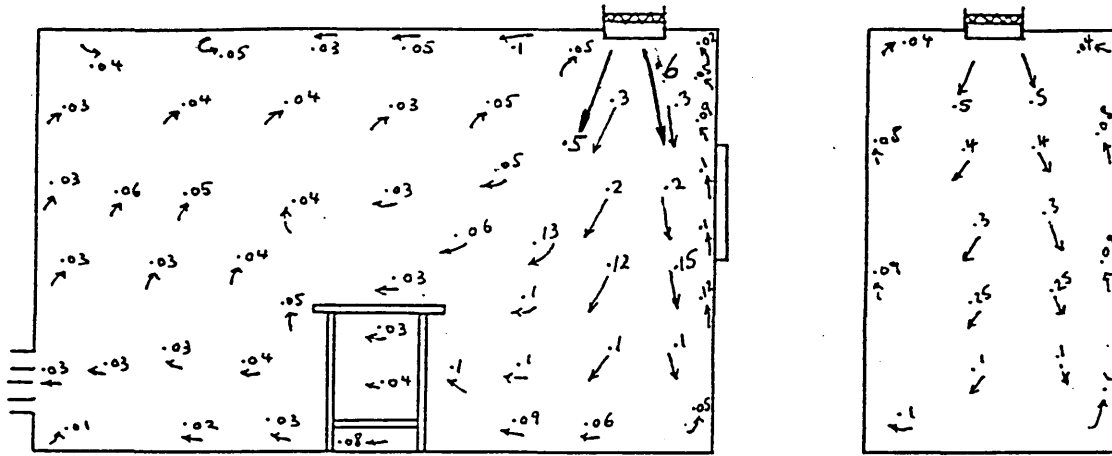
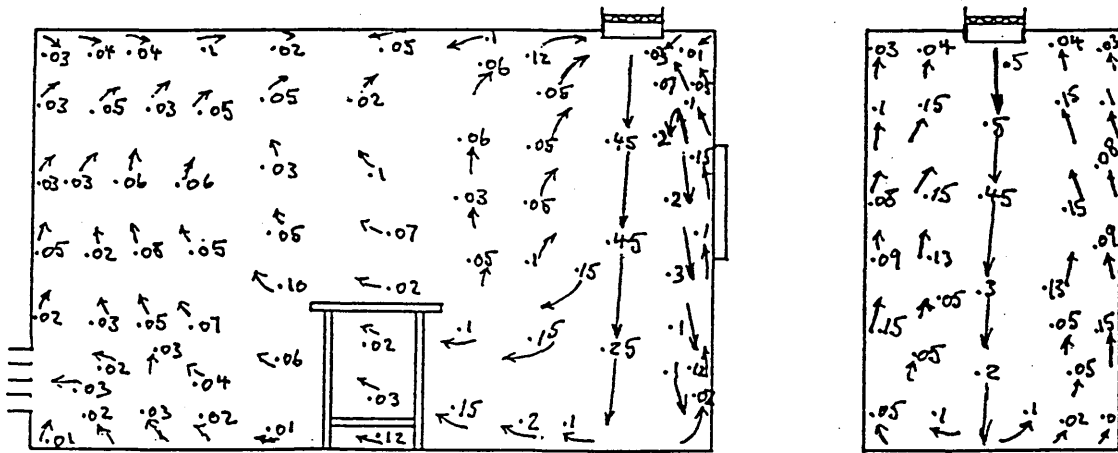


Fig. 4.12 Air movement patterns in cleanroom along major and minor vertical sections of the room - Jet air supply with 20 AC/hr

Nominal $\Delta T = +2K$



Nominal $\Delta T = 0K$



Nominal $\Delta T = -2K$

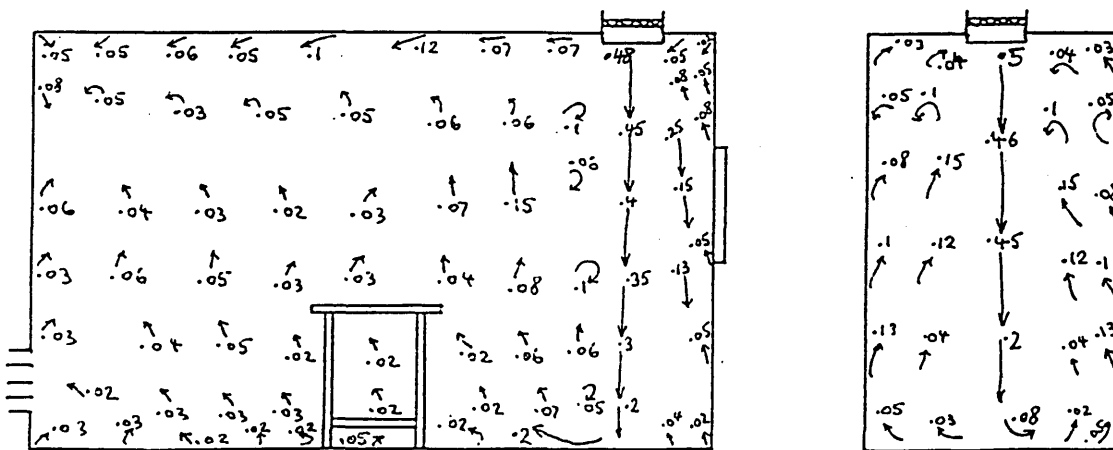


Fig. 4.13 Air movement patterns in cleanroom along major and minor vertical sections of the room - Jet air supply with 15 AC/hr

TABLE 4.1 PERFORMANCE INDICIES AS ASSESSED BY DECAY RATES

Air Terminal Device	Nominal ΔT (K)	Mean Effective Ventilation Rate (AC/hr)	Theoretical Ventilation Rate (AC/hr)	Performance index		
				Position No. 1	Position No. 2	Position No. 3
Multislot	-1.90	3.14	2.62	0.82	0.88	0.81
Multislot	0	14.50	13.81	0.92	0.96	0.98
Multislot	+2.12	13.03	13.81	1.08	1.03	1.07
Dump	-0.10	3.40	3.59	1.10	1.04	1.03
Dump	-0.40	4.08	3.59	0.91	0.97	0.78
Dump	+0.15	21.00	16.80	0.80	0.80	0.80
Dump	+0.11	14.70	13.81	0.97	0.92	0.93
Dump	+0.04	17.41	13.81	0.73	0.81	0.85
Dump	-2.28	11.33	13.81	1.16	1.25	1.25
Dump	-2.23	13.75	13.81	1.00	1.07	0.95
Adjustable	+0.13	3.14	3.30	1.05	1.01	1.10
Adjustable	+0.08	3.41	3.30	1.06	0.96	0.90
Adjustable	0	14.04	13.81	0.99	0.98	0.98
Adjustable	+1.79	14.16	13.81	0.94	0.96	1.03

TABLE 4.1 continued

PERFORMANCE INDICIES AS ASSESSED BY DECAY RATES

Air Terminal Device	Nominal ΔT (K)	Mean Effective Ventilation Rate (AC/hr)	Theoretical Ventilation Rate (AC/hr)	Performance index		
				Position No. 1	Position No. 2	Position No. 3
Jet	+0.15	15.34	14.70	0.70	1.06	1.32
Jet	+0.13	16.56	14.70	0.64	0.93	1.35
Jet	+0.17	16.51	14.70	0.63	0.89	1.52
Jet	-0.06	16.37	14.70	0.56	1.15	1.46
Dump	+1.96	13.56	13.81	1.04	1.10	0.93
Dump	+2.00	13.49	13.81	0.98	1.00	1.10
Dump	+2.10	14.64	13.81	0.97	1.06	0.83

ΔT +ve = Supplied air colder than the ambient room air

ΔT -ve = Supplied air hotter than the ambient room air

TABLE 4.2 PERFORMANCE INDICIES AS ASSESSED BY LATERAL

AIR DISTRIBUTION - MULTISLOT DIFFUSERS

Air Change Rate (AC/hr)	Nominal ΔT (K)	Average Steady-State Particulate Counts $\geq 0.5 \mu\text{m}/\text{ft}^3$			Performance Index		
		Exhaust E_1	Exhaust E_2	Exhaust E_3	Exhaust E_1	Exhaust E_2	Exhaust E_3
3	-1.05	463070	NA	437676	1.03	NA	0.97
3	-0.16	547242	NA	518076	1.03	NA	0.98
15	0	497395	504524	374201	1.11	1.13	0.84
15	0	501782	475077	522813	0.99	0.93	1.03
15	+0.05	415574	475070	495435	0.92	1.05	1.09
20	-0.04	78253	72304	62480	1.12	1.03	0.89
20	-0.10	85466	82972	69044	1.11	1.08	0.90

NA = Not Applicable

TABLE 4.3 PERFORMANCE INDICIES AS ASSESSED BY LATERAL
AIR DISTRIBUTION - ADJUSTABLE VANE GRILLES

Air Change Rate (AC/hr)	Nominal ΔT (K)	Average Steady-State Particulate Counts $\geq 0.5\mu\text{m}/\text{ft}^3$			Performance Index		
		Exhaust E_1	Exhaust E_2	Exhaust E_3	Exhaust E_1	Exhaust E_2	Exhaust E_3
15	+0.16	509554	368478	442982	1.08	0.78	0.94
15	+0.19	643149	427002	605985	1.05	0.70	0.99
15	+0.18	637274	410726	611741	1.05	0.67	1.00

TABLE 4.4 PERFORMANCE INDICIES AS ASSESSED BY LATERAL
AIR DISTRIBUTION - DUMP AIR SUPPLY

Air Change Rate (AC/hr)	Nominal ΔT (K)	Average Steady-State Particulate Counts $\geq 0.5\mu\text{m}/\text{ft}^3$			Performance Index		
		Exhaust E ₁	Exhaust E ₂	Exhaust E ₃	Exhaust E ₁	Exhaust E ₂	Exhaust E ₃
3	+0.17	515662	NA	564479	0.95	NA	1.04
3	+0.95	455846	NA	490122	0.96	NA	1.03
15	+0.15	484852	497860	460760	1.02	1.05	0.97
15	0	581772	373434	440704	1.15	0.74	0.87
15	0	498112	423394	458671	1.05	0.89	0.96
20	-0.01	65770	81867	150918	0.60	0.75	1.38
20	0	74586	91238	159978	0.63	0.77	1.35

NA = Not Applicable

TABLE 4.5 PERFORMANCE INDICIES AS ASSESSED BY LATERAL

AIR DISTRIBUTION - JET AIR SUPPLY

Air Change Rate (AC/hr)	Nominal ΔT (K)	Average Steady-State Particulate Counts $\geq 0.5\mu\text{m}/\text{ft}^3$			Performance Index		
		Exhaust E_1	Exhaust E_2	Exhaust E_3	Exhaust E_1	Exhaust E_2	Exhaust E_3
3	-0.13	558080	NA	486415	1.07	NA	0.93
3	-0.03	533060	NA	447080	1.09	NA	0.91
15	-0.13	83425	78883	124667	0.83	0.79	1.24
15	-0.02	88834	89466	162916	0.74	0.75	1.36
20	0	75028	58568	143657	0.72	0.56	1.38
20	0	70830	54348	148584	0.70	0.54	1.47

NA = Not Applicable

TABLE 4.6 PERFORMANCE INDICIES AS ASSESSED BY CONSTANT SOURCE DISPERSION - MULTISLOT DIFFUSERS WITH SMOKE RELEASED AT R_{p1}^*

Air Change Rate (AC/hr)	Nominal ΔT (K)	Average Steady-State Particulate Counts $> 0.5 \mu\text{m}/\text{ft}^3$						Performance Index	
		Position No 2	Position No 3	Exhaust E_1	Exhaust E_2	Exhaust E_3	Position No 2	Position No 3	
3	-0.05	537868	382868	455690	NA	462176	1.172	0.834	
3	0	629808	490910	570665	NA	528803	1.146	0.893	
3	+1.94	540011	594343	629014	NA	651272	0.844	0.928	
3	+1.92	612410	497600	312718	NA	301906	1.993	1.619	
3	+2.00	403660	160623	173210	NA	171168	2.344	0.933	
3	-1.31	1207698	1159346	301106	NA	401147	3.439	3.301	
3	-0.97	1213823	1259040	438490	NA	527618	2.513	2.606	
15	+1.91	473973	389209	417616	493930	384070	1.342	1.102	
15	+2.00	515891	638775	463665	579161	602728	0.760	0.941	
15	+0.14	407230	444324	390697	469891	460206	1.010	1.102	
15	0	1112343	635123	610668	730231	676681	0.951	0.543	
20	+0.09	312152	62873	66057	64907	130737	3.312	0.667	
20	+0.10	285333	78708	78943	81687	171172	2.389	0.659	
20	+1.90	330740	198043	101277	140573	65995	3.738	2.238	
20	+1.78	521678	271142	145016	136347	66268	4.742	2.465	
20	+1.62	127903	84003	53803	72377	73973	1.963	1.289	
20	-2.21	435918	83074	51136	204397	148553	4.192	0.799	
20	-1.83	508734	88283	70326	141953	186832	4.036	0.700	

* R_{p1} = Between the middle air terminal device and the working table

NA = Not Applicable

TABLE 4.7 PERFORMANCE INDICIES AS ASSESSED BY CONSTANT SOURCE DISPERSION - MULTISLOT DIFFUSERS WITH SMOKE RELEASED AT R_{p2} *

Air Change Rate (AC/hr)	Nominal ΔT (K)	Average Steady-State Particulate Counts $\geq 0.5 \mu\text{m}/\text{ft}^3$						Performance Index	
		Position No 1	Position No 2	Exhaust E_1	Exhaust E_2	Exhaust E_3	Position No 1	Position No 2	
3	+0.79	171435	194564	152362	NA	325777	0.717	0.813	
3	-0.01	427783	390224	455783	NA	463300	0.931	0.849	
3	+2.00	337887	386650	325373	NA	308573	1.066	1.220	
3	+2.14	294365	388822	356880	NA	331774	0.855	1.129	
3	-1.11	723878	826073	643767	NA	705860	1.073	1.224	
3	-1.86	707248	814825	720529	NA	78233	0.943	1.086	
15	0	499405	433099	329447	634513	396335	1.113	0.960	
15	0	477521	524316	563469	644779	587512	0.801	0.881	
15	+2.00	552569	459532	568058	538935	500540	1.032	0.861	
15	+2.00	474314	611698	398354	412134	605958	1.012	1.303	
20	+0.05	23688	23088	43210	72186	165896	0.240	0.234	
20	+0.13	18338	17790	36423	30534	149553	0.215	0.208	
20	+1.98	24328	184030	95018	241125	162365	0.181	1.371	
20	+2.13	25073	257568	115298	190958	135713	0.194	1.992	
20	-1.99	47354	55215	64456	115320	399498	0.221	0.258	
20	-1.84	38919	48081	63083	165958	253883	0.254	0.314	
20	-1.84	5223	14237	11643	13930	19200	0.335	0.914	

* R_{p2} = Between the middle exhaust and the working table

NA = Not Applicable

TABLE 4.8 PERFORMANCE INDICIES AS ASSESSED BY CONSTANT SOURCE DISPERSION -
ADJUSTABLE VANE GRILLES WITH SMOKE RELEASED AT R_{p1} *

Air Change Rate (AC/hr)	Nominal ΔT (K)	Average Steady-State Particulate Counts $\geq 0.5 \mu\text{m}/\text{ft}^3$				Performance Index		
		Position No 3	Position No 2	Exhaust E_1	Exhaust E_2	Exhaust E_3	Position No 3	Position No 2
15	+1.95	617375	600137	453371	717640	448704	1.14	1.11
15	+1.98	637830	487486	555240	432635	453772	1.31	1.01
15	0	447821	520313	472249	465642	570550	0.90	1.04
15	+0.06	632070	520537	532226	563053	328843	1.34	1.10

* R_{p1} = Between the middle air terminal device and the working table

TABLE 4.9 PERFORMANCE INDICIES AS ASSESSED BY CONSTANT SOURCE DISPERSION -
ADJUSTABLE VANE GRILLES WITH SMOKE RELEASED AT R_{p2}*

Air Change Rate (AC/hr)	Nominal ΔT (K)	Average Steady-State Particulate Counts $\geq 0.5 \mu\text{m}/\text{ft}^3$						Performance Index	
		Position No 1	Position No 2	Exhaust E ₁	Exhaust E ₂	Exhaust E ₃	Position No 1	Position No 2	
15	0	396182	395422	567051	537420	481359	0.75	0.75	
15	0	627373	382194	376847	445290	545375	1.38	0.84	
15	+1.90	446443	647267	529615	441866	451544	0.91	1.32	
15	+2.00	505723	534456	461279	562597	393371	1.07	1.13	

* R_{p2} = Between the middle exhaust and the working table

TABLE 4.10 PERFORMANCE INDICIES AS ASSESSED BY CONSTANT SOURCE
DISPERSION - DUMP AIR SUPPLY WITH SMOKE RELEASED AT Rp1 *

Air Change Rate (AC/hr)	Nominal ΔT (K)	Average Steady-State Particulate Counts $\geq 0.5 \mu\text{m}/\text{ft}^3$						Performance Index	
		Position No 3	Position No 2	Exhaust E ₁	Exhaust E ₂	Exhaust E ₃	Position No 3	Position No 2	
15	+0.02	525536	539127	520882	512242	482121	1.04	1.07	
15	+0.01	456406	464022	541044	438922	452798	0.95	0.97	
15	+2.00	459888	409610	578526	536722	659481	0.78	0.69	
15	+1.88	399833	643440	580095	382268	334693	0.93	1.49	

* Rp1 = Between the middle air terminal device and the working table

TABLE 4.11 PERFORMANCE INDICIES AS ASSESSED BY CONSTANT SOURCE
DISPERSION - DUMP AIR SUPPLY WITH SMOKE RELEASED AT R_{p2} *

Air Change Rate (AC/hr)	Nominal ΔT (K)	Average Steady-State Particulate Counts $\geq 0.5 \mu\text{m}/\text{ft}^3$						Performance Index	
		Position No 1	Position No 2	Exhaust E_1	Exhaust E_2	Exhaust E_3	Position No 1	Position No 2	
15	+1.88	514609	471019	445888	572554	502628	1.02	0.93	
15	+1.97	395781	643004	387455	515818	409952	0.91	1.47	
15	+0.01	572553	454225	546330	502558	614230	1.03	0.82	
15	+0.09	416510	355007	432119	574143	476607	0.85	0.72	

* R_{p2} = Between the middle exhaust and the working table

JET AIR SUPPLY WITH SMOKE RELEASED AT R_{p1} *

Air Change Rate (AC/hr)	Nominal ΔT (K)	Average Steady-State Particulate Counts $\geq 0.5 \mu\text{m}/\text{ft}^3$						Performance Index	
		Position No 2	Position No 3	Exhaust E_1	Exhaust E_2	Exhaust E_3	Position No 2	Position No 3	
3	+0.71	475828	333618	406867	NA	462189	2.476	1.736	
3	-0.71	397610	696330	562406	NA	363182	0.860	1.505	
3	-0.94	293493	223200	278743	NA	334040	0.961	0.731	
3	-1.16	174490	324083	414525	NA	485028	0.388	0.721	
3	-1.04	314213	255180	364010	NA	421200	0.800	0.650	
3	-1.16	242627	209373	445870	NA	517093	0.505	0.436	
3	-1.18	190902	188988	412272	NA	462617	0.437	0.433	
15	-0.26	145744	112088	78760	116013	144694	1.350	1.038	
15	-0.18	188698	132068	86493	124273	173148	1.517	1.062	
15	-1.19	144553	129303	140048	130075	127577	1.076	0.962	
15	-1.28	143866	136238	125578	119706	114942	1.190	1.127	
20	0	123237	105542	82416	118540	124188	0.982	0.841	
20	+0.11	185508	156708	68108	181635	150575	1.660	1.402	
20	-0.03	123237	112552	82416	118540	124188	1.188	1.085	
20	+1.57	247997	122254	46643	120863	123180	2.915	1.437	
20	+2.00	188508	146053	87837	150110	120747	1.772	1.373	
20	-1.69	178858	134580	143377	129794	117771	1.363	1.025	
20	-1.14	145379	165787	136370	169716	163021	0.968	1.104	
20	-0.15	165725	141874	76071	149522	167616	1.981	1.696	

NA = Not Applicable * R_{p1} = Between the middle terminal and the working table

TABLE 4.13 PERFORMANCE INDICIES AS ASSESSED BY CONSTANT SOURCE DISPERSION -
JET AIR SUPPLY WITH SMOKE RELEASED AT R_{p2} *

Air Change Rate (AC/hr)	Nominal ΔT (K)	Average Steady-State Particulate Counts $\geq 0.5 \mu\text{m}/\text{ft}^3$				Performance Index		
		Position No 1	Position No 2	Exhaust E_1	Exhaust E_2	Exhaust E_3	Position No 1	Position No 2
3	+0.78	250813	251033	370828	NA	384152	0.664	0.665
3	+0.73	312560	304917	375547	NA	361617	0.848	0.825
3	-1.96	275362	414871	556287	NA	459969	0.542	0.817
3	-0.79	229402	161513	508360	NA	437608	0.485	0.342
15	-0.16	7800	24253	54170	246906	319268	0.045	0.140
15	-0.48	7435	18905	74863	183773	315836	0.041	0.105
15	-2.14	17665	50430	63360	72817	451670	0.078	0.223
15	-2.01	21860	26647	20286	167955	247055	0.180	0.219
15	-2.59	20120	171890	63348	117532	172620	0.194	1.656
20	+0.20	9938	40347	84513	159591	363471	0.047	0.190
20	0.08	14256	30657	58706	54971	214230	0.116	0.249
20	+1.72	11048	12745	13678	157418	213874	0.100	0.115
20	+1.95	16485	10695	27690	433470	185264	0.205	0.133
20	-2.26	12542	39135	59390	528787	231723	0.076	0.237
20	-1.91	15937	54715	94666	160459	277926	0.089	0.305
20	-1.47	5028	18798	30222	160657	172778	0.046	0.170

* R_{p2} = Between the middle exhaust and the working table

NA = Not Applicable

TABLE 4.14 (Part 1)

MULTIPLE REGRESSION ANALYSIS FOR VARIOUS DATA AND DEPENDENT VARIABLES

Data Analysed	Dependent Variable	No of Cases Used	Correlation Coefficient and Level of Significance									
			Constant		Air Change Rates		Diff. Temp.		Air Terminal Device		Position of Smoke Released	
			Coeff.	Sig. level (%)	Coeff.	Sig. level (%)	Coeff.	Sig. level (%)	Coeff.	Sig. level (%)	Coeff.	Sig. level (%)
All	PI at No1	33	0.7356	<0.1	-0.0319	<0.1	0.0322	NS	0.3703	<0.1	0.0611	NS
All	PI at No2	70	0.6926	<0.1	0.0156	<0.1	0.0496	<0.1	0.7200	<0.1	0.9533	<0.1
All	PI at No3	37	0.8970	<0.1	-0.0059	NS	-0.0605	NS	0.3736	NS	0.5312	<0.1
R _{p1}	PI at No2	37	0.5560	<10	0.0549	<1	-0.0880	NS	1.1208	<0.2	NA	NA
R _{p1}	PI at No3	37	0.8192	<2	0.01605	NS	-0.1385	NS	0.6000	<5	NA	NA
R _{p2}	PI at No1	33	0.7377	<0.1	-0.0342	<0.1	0.0331	NS	0.3518	<0.1	NA	NA

NS = Not Significant

NA = Not Applicable

R_{p1} = Smoke released between the middle air terminal device and the working table.R_{p2} = Smoke released between the middle exhaust and the working table.

TABLE 4.14 continued (Part 2)

MULTIPLE REGRESSION ANALYSIS FOR VARIOUS DATA AND DEPENDENT VARIABLES

Data Analysed	Dependent Variable	No of Cases Used	Correlation Coefficient and Level of Significance									
			Constant		Air Change Rates		Diff. Temp.		Air Terminal Device		Position of Smoke Released	
			Coeff.	Sig. level (%)	Coeff.	Sig. level (%)	Coeff.	Sig. level (%)	Coeff.	Sig. level (%)	Coeff.	Sig. level (%)
R _{p2}	PI at No2	33	0.7210	<0.1	-0.0204	<5	0.0620	NS	0.4375	<0.8	NA	NA
Jet	PI at No1	16	0.7144	<0.1	-0.0324	<0.1	0.0378	<8.5	NA	NA	NA	NA
Jet	PI at No2	35	1.2211	<0.1	0.00915	NS	0.1514	<8	NA	NA	-0.8729	<0.1
Jet	PI at No3	19	0.9875	<0.1	0.01207	NS	0.1946	<3	NA	NA	NA	NA
Multi-slot	PI at No1	17	1.1096	<0.1	-0.03572	<0.1	0.0292	NS	NA	NA	NA	NA
Multi-slot	PI at No2	35	2.0095	<0.1	0.02665	NS	-0.0595	NS	NA	NA	-1.4216	<0.1

NS = Not Significant

NA = Not Applicable

R_{p1} = Smoke released between the middle air terminal device and the working table.R_{p2} = Smoke released between the middle exhaust and the working table.

MULTIPLE REGRESSION ANALYSIS FOR VARIOUS DATA AND DEPENDENT VARIABLES

Data Analysed	Dependent Variable	No of Cases Used	Correlation Coefficient and Level of Significance											
			Constant		Air Change Rates		Diff. Temp.		Air Terminal Device		Position of Smoke Released			
			Coeff.	Sig. level (%)	Coeff.	Sig. level (%)	Coeff.	Sig. level (%)	Coeff.	Sig. level (%)	Coeff.	Sig. level (%)		
Multi-slot	PI at No3	18	1.6538	<0.3	0.00377	NS	-0.3055	NS	NA	NA	NA	NA	NA	NA
Jet (Rp ₁)	PI at No2	19	1.1841	<0.1	0.02037	NS	0.4494	<0.1	NA	NA	NA	NA	NA	NA
Jet (Rp ₁)	PI at No3	19	0.9875	<0.1	0.01207	NS	0.19461	<3	NA	NA	NA	NA	NA	NA
Jet (Rp ₂)	PI at No1	16	0.71444	<0.1	-0.03243	<0.1	0.03784	<9	NA	NA	NA	NA	NA	NA
Jet (Rp ₂)	PI at No2	16	0.7430	<0.8	-0.02650	<9	-0.06238	NS	NA	NA	NA	NA	NA	NA

NS = Not Significant

NA = Not Applicable

Rp₁ = Smoke released between the middle air terminal device and the working table.Rp₂ = Smoke released between the middle exhaust and the working table.

TABLE 4.14 continued (Part 4)
 MULTIPLE REGRESSION ANALYSIS FOR VARIOUS DATA AND DEPENDENT VARIABLES

Data Analysed	Dependent Variable	No of Cases Used	Correlation Coefficient and Level of Significance											
			Constant		Air Change Rates		Diff. Temp.		Air Terminal Device		Position of Smoke Released			
			Coeff.	Sig. level (%)	Coeff.	Sig. level (%)	Coeff.	Sig. level (%)	Coeff.	Sig. level (%)	Coeff.	Sig. level (%)		
Multi-slot (Rp1)	PI at No2	18	1.6625	<0.8	0.06518	<9	-0.3108	NS	NA	NA	NA	NA	NA	NA
Multi-slot (Rp1)	PI at No3	18	1.6538	<0.7	0.00377	NS	-0.3055	NS	NA	NA	NA	NA	NA	NA
Multi-slot (Rp2)	PI at No1	17	1.1096	<0.1	-0.035721	<0.1	0.02919	NS	NA	NA	NA	NA	NA	NA
Multi-slot (Rp2)	PI at No2	17	1.0510	<0.1	-0.01386	NS	0.14989	<4	NA	NA	NA	NA	NA	NA

NS = Not Significant

NA = Not Applicable

Rp1 = Smoke released between the middle air terminal device and the working table.

Rp2 = Smoke released between the middle exhaust and the working table.

TABLE 4.15 STEADY-STATE CONTAMINANT DISPERSION RATES BY FEMALES

Code Letter	Bacterial Count/min		Average Particulate Count/min			
	Indoor Clothing	Clean Room Clothing	Indoor Clothing		Cleanroom Clothing	
			$\geq 0.5 \mu\text{m}$	$\geq 5.0 \mu\text{m}$	$\geq 0.5 \mu\text{m}$	$\geq 5.0 \mu\text{m}$
NB	2548	83	6586889	2108058	802103	23352
BB	242	37	362977	39344	365515	20306
MC	38	55	161182	3808	1102891	95440
*CB	349	25	383283	60919	94932	5077
MC	165	12	162451	10153	101532	10153
KC	256	41	859215	44420	252561	5077
CD	62	109	399782	8884	923434	47720
*AM	282	28	1311032	380745	339117	42136
IG	372	150	308404	45689	182250	23352
AG	127	198	356631	167528	832055	113716
KH	118	99	977246	178950	367038	42643
EH	96	23	145952	22845	127677	7615
EK	310	70	823678	131992	952370	57873
AM	173	65	1176502	149760	336325	35029
CM	194	230	728492	87571	539643	25383
GM	61	24	783066	196718	205095	13199
CM	141	93	1656241	224640	158136	139098
JM	209	43	425165	21576	135038	13707
*MG	343	13	142145	8884	546750	8630
KR	340	8	1704468	217025	97471	5077
ET	38	3	261445	6980	79703	0
MT	1185	81	11794210	703109	503599	60919
MC	208	32	5072793	347747	1641011	26652

* skirt on (other subjects had trousers on)

TABLE 4.15 CONTINUED

STEADY-STATE CONTAMINANT DISPERSION RATES BY FEMALES

Code Letter	Bacterial Count/min		Average Particulate Count/min			
	Indoor Clothing	Clean Room Clothing	Indoor Clothing		Cleanroom Clothing	
			$\geq 0.5 \mu\text{m}$	$\geq 5.0 \mu\text{m}$	$\geq 0.5 \mu\text{m}$	$\geq 5.0 \mu\text{m}$
KQ	1076	48	501314	101532	250023	12692
GM	36	28	270329	0	313480	20306
EM	466	26	8997004	1088931	415647	44420
*JC	924	54	812256	289366	195449	27921
*MW	402	18	526063	567310	506391	47593
SG	81	5	3667844	461971	489892	15230
AB	42	4	151029	30460	97471	1015

* skirt on (other subjects had trousers on)

TABLE 4.16 STEADY-STATE CONTAMINANT DISPERSION RATES BY MALES

Code	Bacterial Count/min		Average Particulate Count/min			
	Indoor Clothing	Clean Room Clothing	Indoor Clothing		Cleanroom Clothing	
			$\geq 0.5 \mu\text{m}$	$\geq 5.0 \mu\text{m}$	$\geq 0.5 \mu\text{m}$	$\geq 5.0 \mu\text{m}$
DA	429	60	2146133	195449	272613	14722
JR	551	132	187834	6346	227812	15230
WA	53	16	385187	17134	296093	5775
IM	1624	35	6376210	427704	1163811	11422
RC	1690	15	948055	196718	369957	5711
RM	216	9	625691	67265	282386	6980
CS	678	34	3108148	91379	222101	5077
JM	1624	50	3302328	756413	784335	46324
RJ	782	19	2002718	313480	968362	20941
FS	5320	83	7718970	904904	4973989	97217
NG	91	7	519082	103722	489892	6980
TV	3858	39	1420179	243677	130469	3046
WH	3912	329	1103923	431131	7483327	262686
JD	1080	112	1677033	205300	2167281	61343
PM	716	44	500389	143463	333428	23746
AB	2232	98	799683	180566	2011450	64806
RG	3904	105	14486547	1680249	2765868	57880
TS	2416	59	364347	150884	393781	67774
BH	574	188	3912335	415548	365089	84099
BM	42	38	325760	14841	1005725	42544
MH	694	125	873146	133569	2050037	71732
AA	2880	59	4830746	1375266	773711	71732
RY	2240	204	3701593	1334453	461060	47491
RK	420	65	249824	42050	1340142	16078
AK	1980	192	4224738	1111838	11669973	71237

TABLE 4.17 DISPERSAL OF AIRBORNE CONTAMINANTS BY PEOPLE
(Average Count per minute)

NATURE OF CONTAMINATION		MALE		FEMALE	
		Indoor Clothing	Clean Room Clothing	Indoor Clothing	Clean Room Clothing
Bacteria	Maximum	5320	329	2548	230
	Minimum	42	7	36	3
	Mean	1600	85	363	57
	Median	1080	59	209	39
	Standard Deviation	1446	77	505	56
	Standard Error	289	15	92	10
Particle $\geq 0.5\mu\text{m}$	Maximum	14486547	11669973	11794210	1641011
	Minimum	187834	130469	142145	79703
	Mean	2631624	1716108	1716970	431820
	Median	1420179	773711	627278	337721
	Standard Deviation	3202101	2673265	2808471	364942
	Standard Error	640420	96588	512754	78013
Particle $\geq 5.0\mu\text{m}$	Maximum	1680249	262686	2108058	139098
	Minimum	6346	3046	0	0
	Mean	422814	47303	256897	33044
	Median	196718	42544	116762	23352
	Standard Deviation	482939	53662	427292	33294
	Standard Error	534653	10732	66629	6079

TABLE 4.18 COMPARISON OF MALE AND FEMALE AIRBORNE DISPERSION RATES

Nature of Contamination	Ratio of male/female median dispersion rate	
	Indoor Clothing	Cleanroom Clothing
Bacteria	5.2	1.5
Particles $\geq 0.5\mu\text{m}$	2.3	2.3
Particles $\geq 5\mu\text{m}$	1.7	1.8

FIG. 4.14. COMPARISON OF BACTERIAL DISPERSION RATES FOR INDOOR CLOTHING
PERCENTAGE OF OCCURANCE

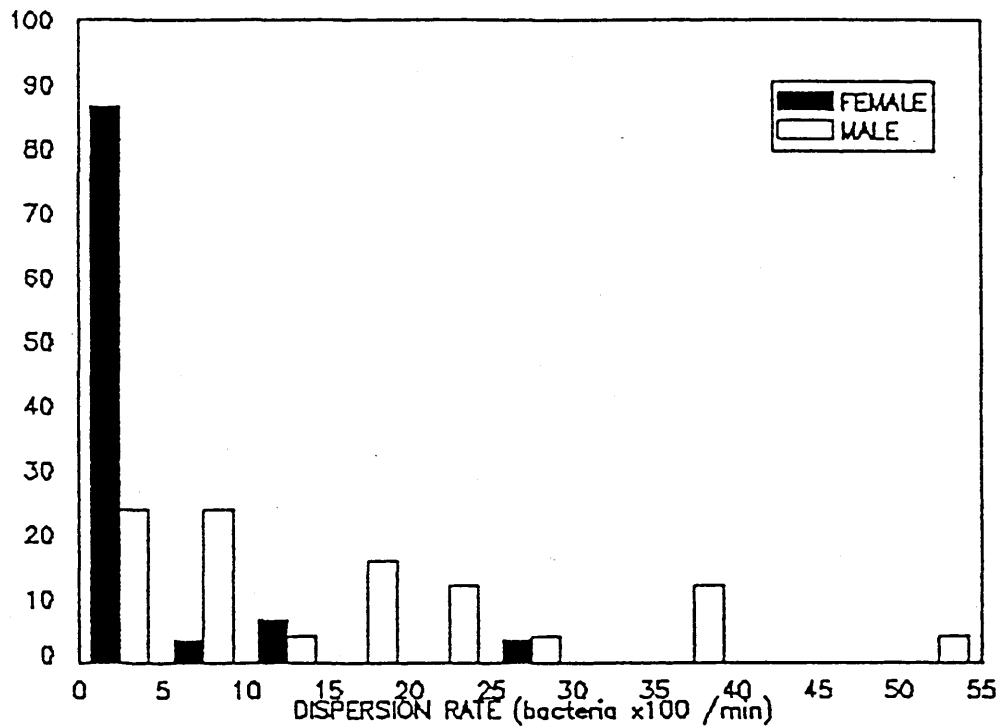


FIG. 4.15. COMPARISON OF BACTERIAL DISPERSION RATES FOR CLEANROOM CLOTHING
PERCENTAGE OF OCCURANCE

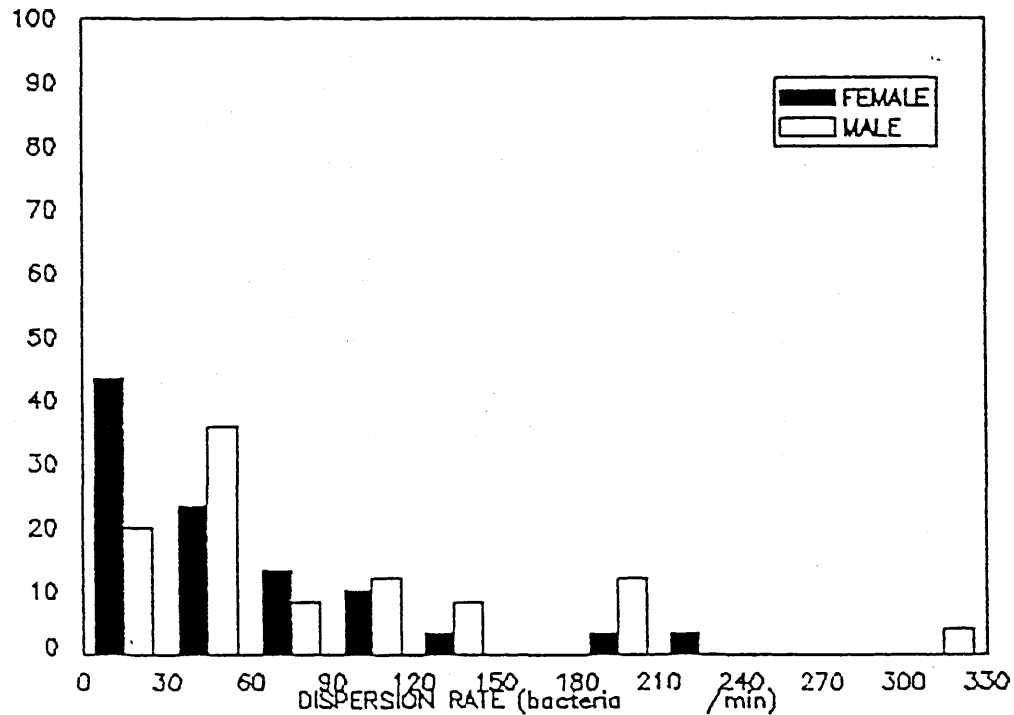


FIG. 4.16. COMPARISON OF PARTICULATE
DISPERSION RATES FOR INDOOR CLOTHING

PERCENTAGE OF OCCURANCE

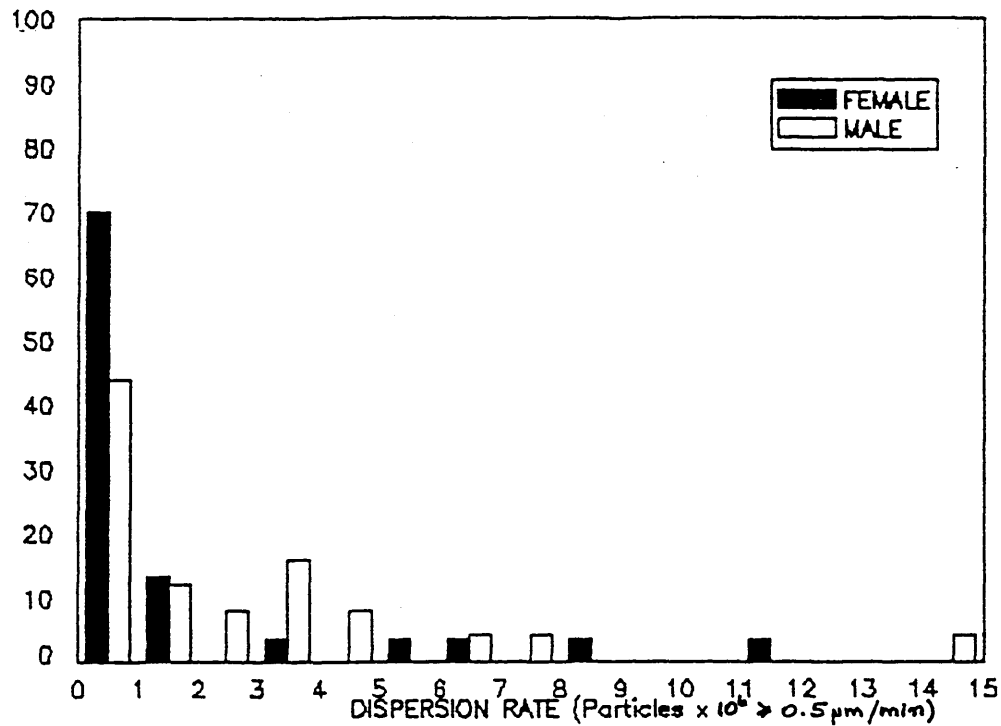


FIG. 4.17. COMPARISON OF PARTICULATE
DISPERSION RATES FOR CLEANROOM CLOTHING

PERCENTAGE OF OCCURANCE

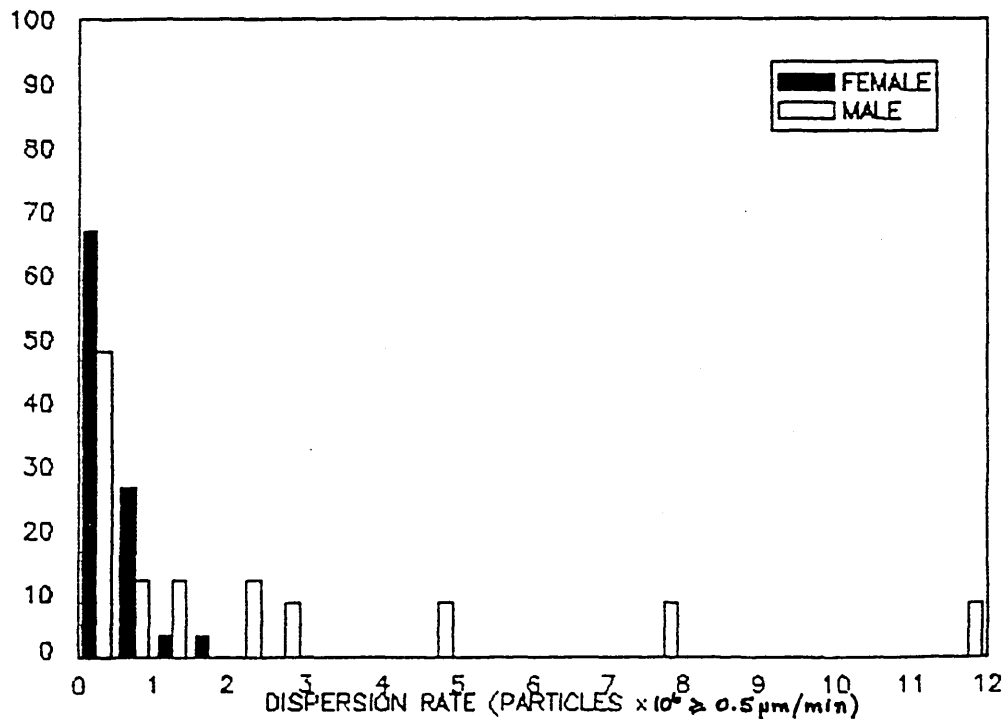


FIG. 4.18. COMPARISON OF PARTICULATE DISPERSION RATES FOR INDOOR CLOTHING

PERCENTAGE OF OCCURANCE

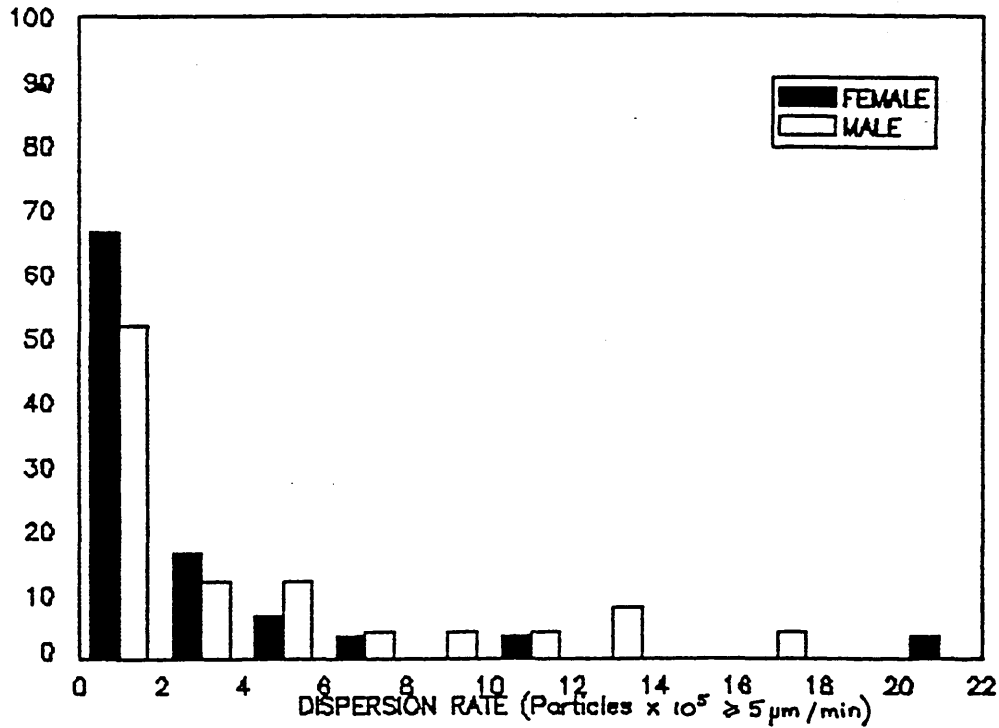


FIG. 4.19. COMPARISON OF PARTICULATE DISPERSION RATES FOR CLEANROOM CLOTHING

PERCENTAGE OF OCCURANCE

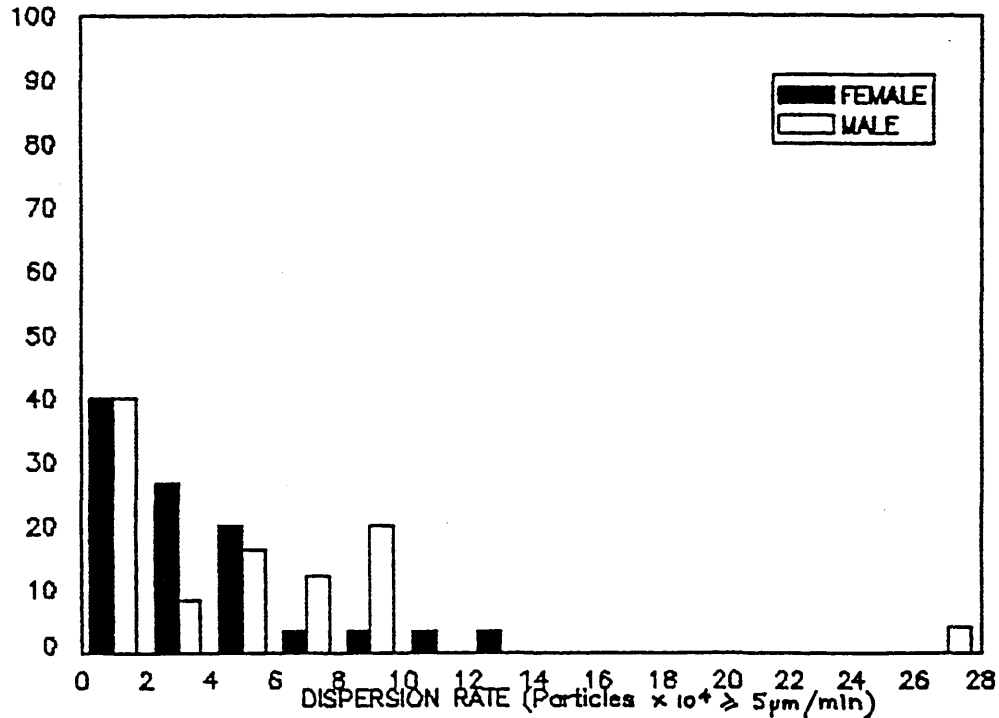


TABLE 4.19 PARTICLE CONCENTRATION WHEN OPERATOR
AND BAUSH & STROEBEL MACHINE WORKING
- counts taken at minute intervals

	Particle Size (μm)				
	≥ 0.3	≥ 0.5	≥ 1	≥ 2	≥ 5
Particle Concentration (particles/ft ³)	3604	700	109	41	21
	12822	1714	176	47	16
	42946	4877	442	122	26
	57838	7630	878	180	31
	59672	8168	901	215	23
	46432	6856	1000	202	23
	34616	5322	918	184	24
	27292	4559	914	212	42
	21625	3880	793	189	22
	18055	3256	670	134	21
	15625	2900	670	142	29
	15064	2777	673	164	33
	15841	2938	698	172	39
	15579	3113	645	131	16
	14276	2891	639	120	16
	14162	2872	642	134	22

TABLE 4.20 PARTICLE CONCENTRATION WHEN
 OPERATOR WORKING IN THE ROOM
 - counts taken at minute intervals

	Particle Size (μm)				
	≥ 0.3	≥ 0.5	≥ 1	≥ 2	≥ 5
Particle Concentration (particles/ft ³)	58088	2817	430	95	16
	62384	2822	587	192	52
	49228	2045	443	123	32
	37704	1569	329	86	12
	26179	1067	222	50	6
	18449	882	140	27	5
	14386	780	208	71	19
	10364	589	124	33	6
	7885	615	201	72	25
	6511	517	139	40	8
	5747	483	125	39	13
	5529	650	166	50	13
	411	512	109	26	9

TABLE 4.21 AVERAGE STEADY-STATE PARTICLES GENERATED FROM BAUSH & STROEBEL MACHINE

Particle Size (μm)	≥ 0.3	≥ 0.5	≥ 1	≥ 2	≥ 5
Dispersion Rate (Particles/min)	9308385	2061310	464788	41515	5415

TABLE 4.22 AVERAGE STEADY-STATE PARTICLES GENERATED FROM BOSCH-STRUNK MACHINE

Particle Size (μm)	≥ 0.5	≥ 5
Dispersion Rate (Particles/min)	26460	2940

TABLE 4.23 MEAN OUTDOOR AIRBORNE CONTAMINANT CONCENTRATION
(Numbers per ft³)

NATURE OF CONTAMINATION	CLIMATIC CONDITIONS	LOCATION	
		Urban	Rural
Bacteria	Wind	0.6	0.45
	Sun	0.73	0.65
	Rain	0.6	0.49
Particle ≥0.5μm	Wind	273100	254000
	Sun	313000	292000
	Rain	224321	163120
Particle ≥ 5μm	Wind	1830	1510
	Sun	1020	830
	Rain	841	600

Fig. 4.20 Motor characteristics at various air pressures

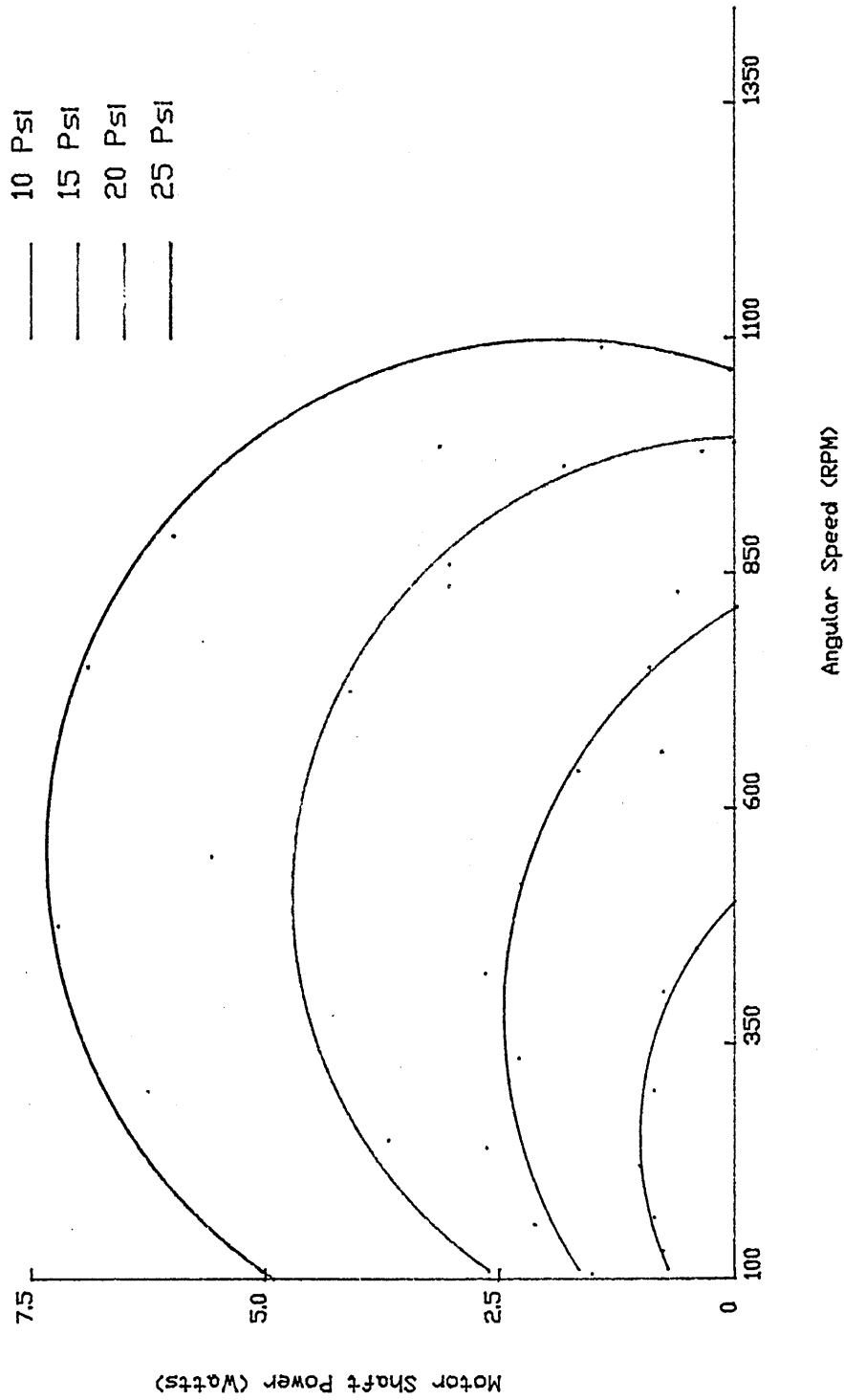


Fig. 4.21 Fan power of motor in relation to air pressure

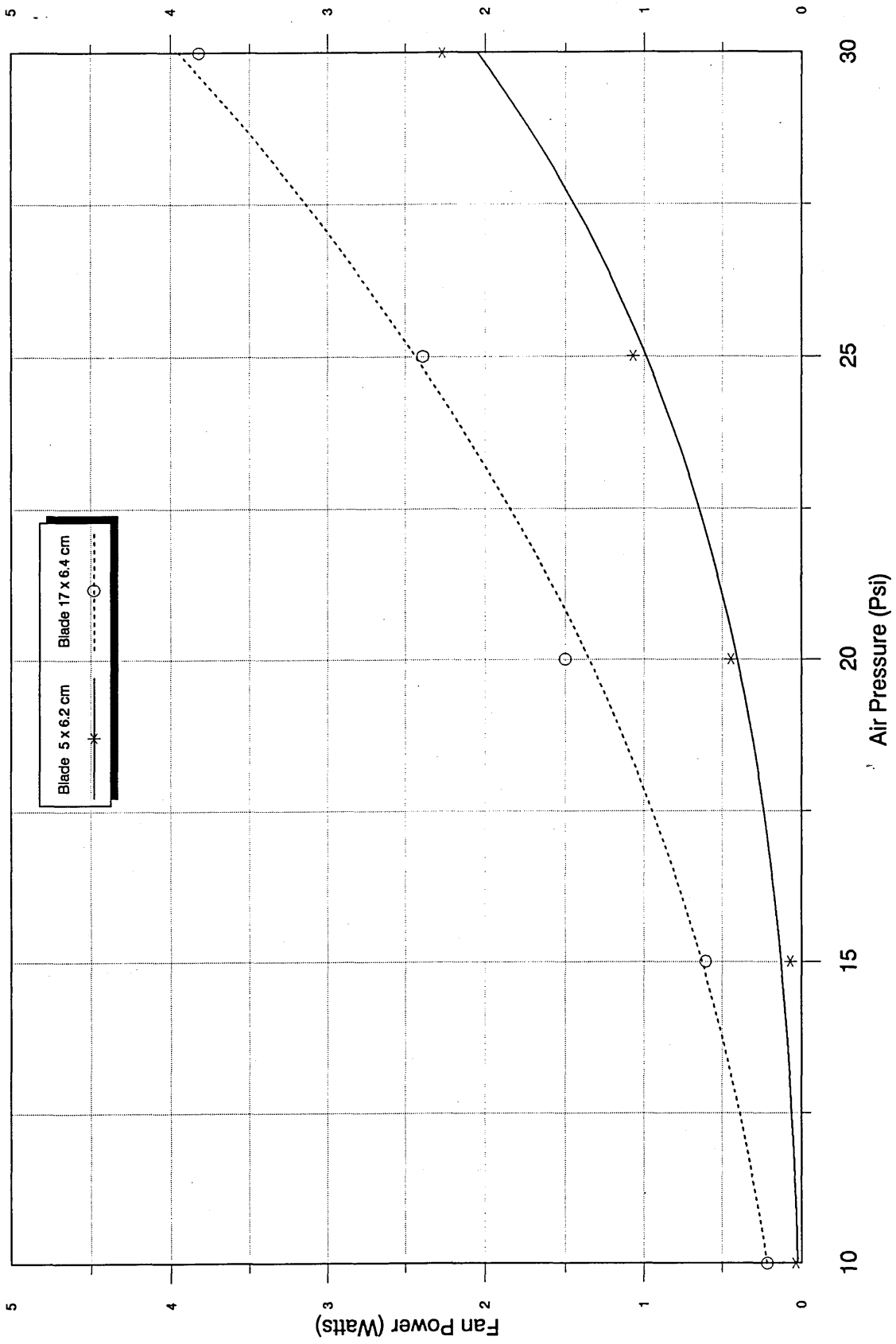


Fig. 4.22 Calibration of Rotameter size 10 with a stainless steel float

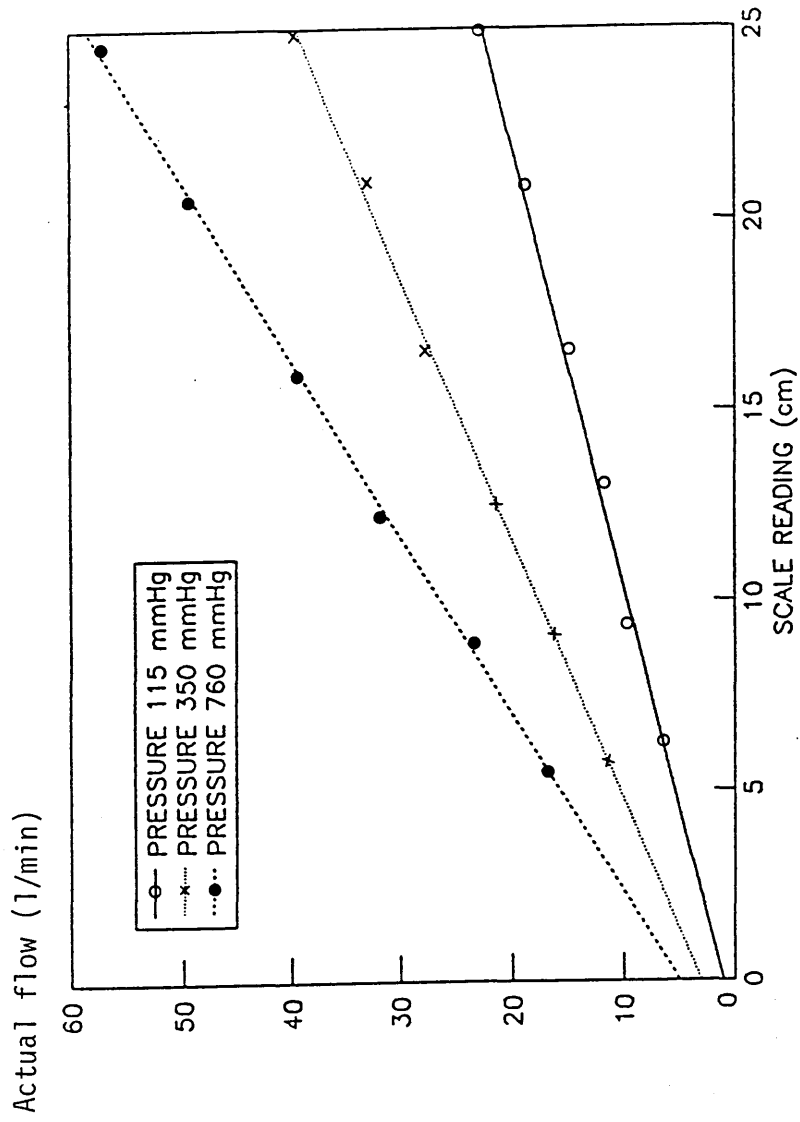


Fig. 4.23 Calibration of droplet size from atomizer

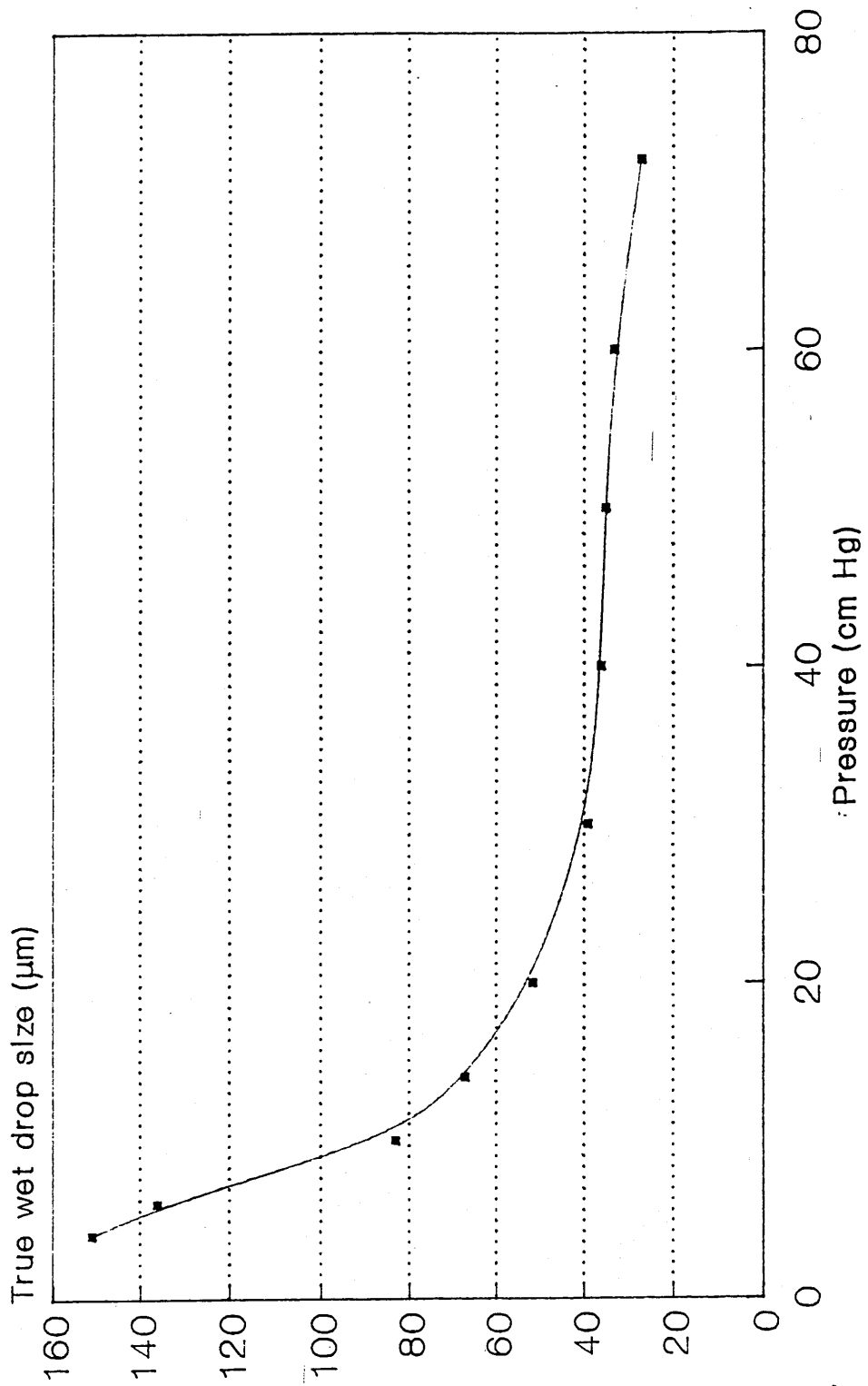


Fig. 4.24 Theoretical deposition velocity vs particle diameter

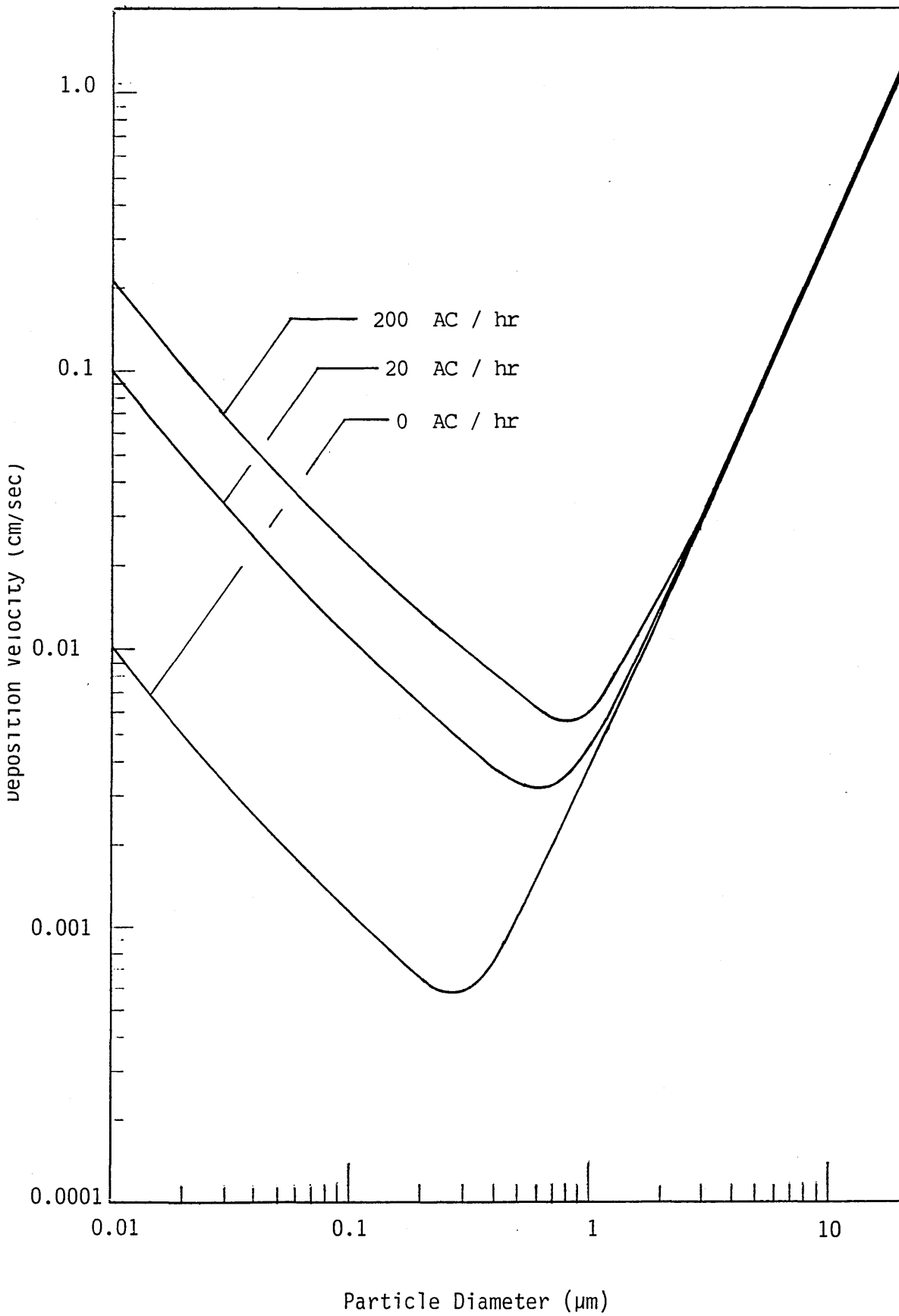


TABLE 4.24 THEORETICAL DEPOSITION VELOCITIES (CM/SEC) FOR VARIOUS AERODYNAMIC PARTICLE DIAMETERS AND EQUIVALENT VENTILATION RATES

Air Change Rate (AC/hr)	Aerodynamic Particle Diameter (μm)											
	0.8			6.3			11.2					
	Top	Side	Base	Top	Side	Base	Top	Side	Base			
0	0	0	0.002	0	0	0.123	0	0	0	0	0.383	
20	0	0.001	0.003	0	0	0.123	0	0	0	0	0.383	
200	0.001	0.002	0.003	0	0.001	0.123	0	0	0	0	0.383	

0 represents less than 10^{-3} cm/sec

TABLE 4.25 EXPERIMENTAL DEPOSITION VELOCITIES (CM/SEC) FOR VARIOUS AERODYNAMIC PARTICLE DIAMETERS AND EQUIVALENT VENTILATION RATES. POLARITY AIR IONISER IN USE

Air Change Rate (AC/hr)	Aerodynamic Particle Diameter (μm)												
	0.80			6.3			11.2						
	Top	Side	Base	Top	Side	Base	Top	Side	Base	Top	Side	Base	
0	0	0	0.006	0	0	0.113	0	0.001	0	0	0.263	0.388	0.296
Average	0	0	0.005	0	0	0.117	0	0	0	0	0.316		
20	0.003	0.018	0.018	0	0.001	0.107	0	0	0	0	0.365	0.331	0.294
Average	0.001	0.007	0.013	0	0	0.127	0	0	0	0	0.330		
200	0.002	0.007	0.023	0	0.003	0.102	0	0	0	0	0.354	0.362	0.302
Average	0.001	0.002	0.011	0	0.001	0.128	0	0	0	0	0.302		
Average	0.001	0.002	0.009	0	0	0.115	0	0	0	0	0.302		
Average	0.001	0.004	0.014	0	0.001	0.115	0	0	0	0	0.339		

0 represents less than 10^{-3} cm/sec

TABLE 4.26 EXPERIMENTAL DEPOSITION VELOCITIES (CM/SEC)
 FOR AERODYNAMIC PARTICLE DIAMETER OF $0.8\mu\text{m}$ AND
 VARIOUS EQUIVALENT VENTILATION RATES. POLARITY AIR
 IONISER NOT IN USE

Air Change Rate (AC/hr)	Top	Side	Base
0	0.001	0.005	0.011
	0.002	0.007	0.013
	0	0.001	0.080
Average	0.001	0.004	0.035
20	0.003	0.017	0.017
	0.006	0.006	0.020
	0.005	0.010	0.025
Average	0.005	0.011	0.021
200	0.004	0.009	0.024
	0.002	0.011	0.023
	0.001	0.006	0.018
Average	0.002	0.009	0.022

TABLE 4.27 CLEANROOM CONDITIONS DURING ENVIRONMENTAL CLEANLINESS TESTS

VARIABLES		OCLI	ORGANON
Room Dimension	Floor Area (m ²)	48.32	113.90
	Height (m)	3.00	2.73
Volume of Supplied Air into the Room (m ³ /s)		1.00	2.89
Volume of Air from Unidirectional Flow Cabinet (m ³ /s)		2.87	2.94
% Recirculated Air		88	85
Number of Females		3	5
Number of Males		2	2
Type of cleanroom clothing		white laboratory coats	Ceramic Terrylene coverall

TABLE 4.28 VERIFICATION AND CLASSIFICATION OF OCLI CLEANROOM

Location	Particle Counts $\geq 0.5 \mu\text{m}$ (particles/ft ³)				Average Counts (Particles /ft ³)
	1	2	3	4	
A	1780	2290	1620	1260	1738
B	4230	2410	870	1080	2148
C	6700	3920	5270	3000	4723
D	2370	2010	2030	1780	2048

Mean of averages of the particles $\geq 0.5\mu\text{m} = 2664$ particles/ft³

Standard deviation of the averages = 1384

Standard error of mean of the averages = 692

Upper 95% confidence limit = 4325 particles/ft³

Lower 95% confidence limit = 1003 particles/ft³

Airborne Particulate cleanliness Class = 10,000 of Fed. Std. 209D

TABLE 4.29 VERIFICATION AND CLASSIFICATION OF ORGANON CLEANROOM

Location	Particle Counts $\geq 0.5\mu\text{m}$ (particles/ft ³)				Average Particle Counts/ft ³	Bacterial Counts /m ³
	1	2	3	4		
A	880	880	1080	730	893	3.57
B	1920	1230	1320	1270	1435	2.71
C	790	720	560	820	723	3.86

Average bacteria concentration = 3.38 bacteria/m³

Mean of averages of the particles $\geq 0.5\mu\text{m}$ = 1017 particles/ft³

Standard deviation of averages = 372

Standard error of mean of the averages = 215

Upper 95% confidence limit = 1641 particles/ft³

Lower 95% confidence limit = 394 particles/ft³

Airborne particulate cleanliness class = 10,000 of Fed. Std. 209D

TABLE 4.30 MODEL OUTPUT FOR CLEANROOMS

Cleanroom	Cumulative airborne contaminant concentration	
	Particles $\geq 0.5\mu\text{m}/\text{ft}^3$	Bacteria/m ³
OCLI	1620	NA
Organon	678	1.1

NA = NOT Applicable

TABLE 4.31 SENSITIVITY ANALYSIS OF THE AIRBORNE CONTAMINANT CONCENTRATION MODEL TO INPUT PARAMETERS (4 people considered)

Variables	± 50% Variable Change	Cumulative Airborne Contaminant Concentration		% Change in Contaminant Concentration	
		Bacteria/m ³	Particles ≥0.5μm/m ³	Bacteria	Particles ≥0.5μm
Bacterial Dispersion Rate (bact/min)	300 200 100	4.27 2.85 1.42	NA	+50 0 -50	NA
Particle Dispersion Rate (p/min)	3.3 x 10 ⁶ 2.2 x 10 ⁶ 1.1 x 10 ⁶	NA	40891 27260 13630	NA	+50 0 -50
Total Vol. of Supplied Air (m ³ /sec)	6 4 2	1.97 2.85 5.22	17550 27260 54179	-31 0 +83	-36 0 +99
Area (m ²)	105 70 35	2.72 2.85 3.02	27174 27260 27351	-4.6 0 +6	-0.32 0 +0.33
Height (m)	6 4 2	2.85 2.85 2.85	27260 27260 27260	0 0 0	0 0 0
Filter Penetration	0.000141 0.000094 0.000047	2.85 2.85 2.85	27260 27260 27260	0 0 0	0 0 0
Pre-filter Penetration	0.21611 0.14407 0.07204	2.85 2.85 2.85	27260 27260 27260	0 0 0	0 0 0
% Recirculated Air	90 60 30	2.85 2.85 2.85	27260 27260 27260	0 0 0	0 0 0
Bacteria Outdoor Concentr'n (bact/m ³)	33.9 22.6 11.3	2.85 2.85 2.85	NA	0 0 0	NA
Particle Outdoor Concentr'n (p/m ³)	1.5 x 10 ¹¹ 1.0 x 10 ¹¹ 0.5 x 10 ¹¹	NA	27260 27260 27260	NA	0 0 0

5. DISCUSSION AND CONCLUSION

Development of a mathematical model to predict the airborne contaminant concentration within conventionally-ventilated cleanrooms was the prime objective of this investigation. This model required data on the dispersal of airborne contaminants by male and female volunteers, process equipment as well as the outdoor airborne contaminant concentration. The assumption of complete air mixing was used in the derivation of this model but that assumption required evaluation and thus a substantial part of the research program was devoted to that problem. The airborne contaminant concentration may be reduced by deposition of the airborne particles. Thus all possible surface deposition mechanisms were studied and the model developed which was verified experimentally. The important deposition mechanisms were then included in the airborne contaminant concentration model. Finally, the validity of the airborne contaminant concentration model was examined by comparing the predicted contaminant concentration with that found in real situations in industrial cleanrooms.

The complete study is discussed under five headings. These are as follows:

1. Cleanroom air distribution performance
2. Contaminant dispersion by people and process machines
3. Outdoor airborne contamination
4. Surface deposition
5. Airborne contaminant concentration.

5.1 Cleanroom Air Distribution Performance

To investigate the validity of the perfect-mixing assumption used in the mathematical models derived in Chapter Three as well as to gain an insight into the air movement in conventionally-ventilated cleanrooms, experiments described in Chapter Two (section 2.1) were conducted at Organon Pharmaceutical Manufacturing Laboratory Ltd.

The ventilation effectiveness of various ventilation schemes, as assessed by their ability to dilute and remove airborne contamination, was investigated in terms

of the following:

1. Contaminant penetration into the air supply
2. Air movement within the room
3. Contaminant decay rates
4. Lateral air distribution
5. Constant contaminant dispersion

The research was extended to include the effects of the following factors in the above study:

- (i) Type of air terminal devices
- (ii) Effective ventilation rates
- (iii) Location of contaminant source
- (iv) Differential temperature between the supplied air and the room air

The combined study of all the above provided an understanding of air movement in conventionally-ventilated cleanrooms and the mixing of clean supplied air with contaminated room air.

5.1.1 Contaminant penetration into the air supply

Tests were carried out to investigate the amount of air entrained from the room into the clean zone of the supplied air. This was done by releasing smoke around the outside of the dump and jet air terminal devices and measuring the airborne concentration of smoke particles that penetrated into the clean zone. It should be noted that the dump air terminal device was not a diffuser but the original device fitted in the room which discharged air from the HEPA filter in a generally downward direction into the room (Figure 2.3). The jet air terminal device was the same as the dump device but had a frame built round the HEPA filter to minimize the air entrainment into the air supply (Figure 2.3).

Comparison of the results between the dump and jet air terminal devices show significant differences (Figures 4.1 to 4.5). The jet effectively established a localized piston-type downward-displacement air supply. However, without the frames (dump) the adjacent room air was drawn up immediately towards the negative pressure area underneath the perimeter of the filter (Figure 2.3). The

ineffectiveness of the dump air terminal device in preventing air entraining from the surrounding room air into the clean supplied air is clear from the Isopleth diagrams (Figures 4.1 and 4.2). The smoke particles were kept out very effectively under the jet air terminal device (Figures 4.3, 4.4 and 4.5).

The results of tests on the dump air terminal device show that due to the penetration of room air into the supplied air, the outer boundary of the supplied air began to spread as soon as it was discharged into the room. The entrainment started with the edge of the supplied air and found its way through the clean zone providing rapid mixing of the uncontaminated clean supplied air with the contaminated room air. It was also observed with the dump terminal that the supplied air velocity decayed faster than when the jet terminal device was used. This is presumably caused by the surrounding room air being entrained into the supplied air causing frictional forces and hence a momentum transfer between the supplied air and the surrounding room air. Thus the dump terminal provided very high induction which resulted in a short throw, rapid velocity and temperature decay.

In the case of jet air terminal device there was less spread and hence more throw of the clean supplied air than the dump terminal. Thus, due to less entrainment, contamination under the jet was effectively reduced. For a given air change rate the volume of the uncontaminated air under the jet terminal was much more than when a dump terminal was used.

Lastly it can be said that the unsymmetrical isopleth patterns obtained for all the tests was due to the non-uniformity of the air velocity leaving the filter.

5.1.2 Air movement

Visualisation of air movement patterns (Figures 4.6 to 4.13), along with the detailed measurements of air speeds and temperature differentials, was carried out to establish the air movement patterns produced by the multislot, adjustable vane, dump and jet terminal devices.

All the air terminal devices were tested. With the exception of the jet, it was found that, for a given air change rate and a temperature differential, the

patterns of air movement were similar. It is clear from the results that, except for the jet device, the air terminal devices produced good mixing of uncontaminated supplied air with room air as well as good mixing of air within the room. This was not planned in the case of the dump terminal and highlights the difficulties that can be experienced if a good design of jet air terminal device is not installed. Good mixing throughout the room was induced by three air terminal devices (multislot, adjustable vane and dump) due to the rapid spread of the supplied air into the room and this was enhanced by entrainment.

For these three air terminal devices the ability of the supplied air to dilute the contamination generated in the room appeared to generally increase from 5 to 15 air changes per hour but as the ventilation rate was increased from 15 to 20 air changes per hour it decreased. This was thought to be a consequence of the increased throw of the supplied air.

It was also observed with these three air terminal devices (multislot, adjustable vane and dump), that a small portion of the supplied air, with a much lower velocity than the discharge velocity, tended to move rapidly below and along the ceiling surface (Figures 4.6, 4.8 and 4.10). However, this did not result in poor air distribution within the room since that supplied air, on reaching the walls, was deflected downwards and then circulated through the main body of the room causing efficient mixing.

Inspection of the results (Figures 4.6 to 4.11) showed that no significant differences could be detected between the multislot, adjustable vane and dump air terminal devices although the multislot diffusers produced the best air mixing. In this case it was found that room air was drawn upwards into the centre core immediately beneath the diffuser. The air discharged from the multislot diffusers in thin multilayer streams in four directions, swirling motions being imparted to the flow and thus the room air beneath the diffuser was entrained very fast into the supplied air, resulting in very good mixing.

The type of air movement pattern discussed above for the three types of air terminal device (multislot, adjustable vane and dump) was not observed with the

jet air terminal device. The jet terminal device discharged air vertically downward to the floor before circulating through the room (Figures 4.12 and 4.13). The degree of entrainment, and hence spread and mixing, was limited as the jet effectively established a localized piston-type air supply. This entrainment was limited with air changes of between 3 and 15 but further reduced by increasing the ventilation rate from 15 to 20 air changes per hour.

5.1.3 Contaminant decay rates

The effectiveness of ventilation in diluting and removing contamination in the cleanroom was obtained by measurement of the decay rates. The decay rate of airborne contaminant concentration at different points in the room was used to determine the performance index. Inspection of the performance indices at various sampling positions for diverse test conditions gave an insight into the nature of air mixing.

In interpreting the performance indices given in Table 4.1 it should be remembered that a value of unity corresponds to complete air mixing. The lower the value is from 1 the more effective the ventilation system. The higher the value from 1 the less effective the ventilation system.

From the 21 cases studied, the minimum performance index obtained was 0.56. This was from a jet air terminal device at Position No. 1 (directly below the air terminal device) with a mean effective ventilation rate of 16.37 air changes per hour. The degree of entrainment and mixing under the jet terminal (Position No. 1) was generally found to be less than the other sampling points (Position No. 2 and 3) and hence there was more clean air in that position; this was also reflected in the air movement patterns discussed previously.

The maximum performance index of 1.52 was also obtained by the jet air terminal device, although this was near the middle exhaust (Position No. 3). This is caused by the enhanced ventilation under the terminal ensuring that there is less clean air available to dilute the contamination elsewhere in the room, i.e. near the middle exhaust.

The performance indices found for all the other air terminal devices

(multislot, adjustable vane and dump) at various sampling positions (No. 1, 2, 3) were close to unity (Table 4.1), indicating good mixing of the clean supplied air with the contaminated room air. For all air change rates, differential temperatures and sampling positions considered, maximum deviations in performance indices from unity was small being from -27% to +25%. The maximum deviation in each performance indices (not averaged) between these three air terminal devices for all the air change rates and differential temperatures studied were 37% (under the terminal) and 36% (middle of the room).

The information discussed previously show that all the three air terminal devices (multislot, adjustable vane and dump) discharge a supply air that rapidly entrains room air and provides a very good air distribution pattern, and hence good mixing, in the room. There would therefore appear to be no evidence to suggest that any one of these three air terminal devices is significantly better than the others in diluting and removing contamination within the room and all effectively mix the room air.

Similar conclusions were drawn by Lidwell *et al* (1960) with turbulent ventilation systems in operating theatres. They obtained adequate mixing at all different heights of contaminant release and supply air volumes, except when contamination was released at a low level (3 ft or 0.91 m) and the air velocity over the operating table was very small (below 25 ft/min or 0.13 m/s).

The effect of supplying air hotter than the room air on the performance index can be seen with two types of air terminal devices (multislot and dump). With a multislot air terminal device the performance index increased for all the sampling positions as the supplied air temperature increased, whereas for the dump air terminal device the performance index increased at some positions and decreased at others. The higher and lower than ideal performance index, obtained at different locations for this strategy, shows that less mixing is accomplished by increasing the temperature of the supplied air, presumably because the supplied air is less dense, rises and does not mix quickly with the room air.

The effect of supplying the room with colder air than the room air brought

the performance index closer to 1 and thus the clean supplied air appeared to efficiently mix with the contaminated room air. This appeared to be caused by the supplied air spreading rapidly into the room due to increased density of supplied air.

These findings are in good agreement with the results of the work carried out by Sandberg (1981). He showed that by increasing the supplied air temperature relative to the mean room air temperature, an increase in the heavy layering effect of the tracer gas he used could be observed. It appears that as the supplied air temperature increases with respect to the room air, the supplied air tends to rise until it attaches itself close to the ceiling. Thus the buoyancy forces limits the supplied air mixing with the room air and hence the efficiency of mixing reduces.

5.1.4 Lateral air distribution

To add to the information obtained previously, further experiments were carried out to study the effectiveness of mixing of various ventilation schemes. This study was concerned with how rapidly smoke particles diffused and mixed throughout the room when released at one end of the room.

The results (Tables 4.11 to 4.14) show that out of the four air terminal devices tested the *multislot diffuser* produced the best air mixing under all test conditions (i.e. various ventilation rates and differential temperatures). The multislot diffuser produced almost perfect mixing across the whole length of the room under all the nominal ventilation rates of 3, 15 and 20 air changes per hour. For all the ventilation rates and differential temperatures studied the maximum deviation using the multislot diffuser in performance index from unity was +13% to -16%. With this type of air terminal device (multislot) the smoke particles diffused rapidly and it was observed that it imparted a swirl action to the supplied air to provide rapid mixing of supplied air with the surrounding room air.

The results of tests obtained from the *adjustable vane grilles* showed perfect mixing in the vicinity of the two end exhausts (E_1 and E_3) although relatively less mixing was obtained in the vicinity of central exhaust (E_2). The airborne particle

concentration observed at the two end exhausts (E_1 and E_3) were higher than the central exhaust (E_2) (a PI of 1 from E_1 and E_3 as compared to 0.72 from E_2). It appears that the clean supplied air was spread more efficiently towards central exhaust E_2 than the two end exhausts (E_1 and E_3).

The *dump air terminal device* produced good mixing of supplied air with the surrounding room air for ventilation rates of 3 and 15 air changes per hour. However, when the ventilation rate was increased to 20 air changes per hour the spread of the clean supplied air was stronger towards the exhaust's grilles E_1 and E_2 (PI's = 0.6 and 0.63 for E_1 and 0.75 and 0.77 for E_2) than towards exhaust's grille E_3 (PI's = 1.35 and 1.38). These unsymmetrical airborne particulate concentration contours were due to the increased throw of the supplied air which prevented perfect mixing. Furthermore, the increased air volume at one end of the room provided less clean air to dilute contaminants at the other end.

The results of tests for the *jet air terminal device* indicate that reasonable mixing was obtained at 3 air changes per hour. This is due to the fact that although the central terminal device was discharging a localized unidirectional jet the other two terminals had not been modified to jet terminals and were still acting as dump terminal devices and hence affecting the air movement across other planes. However, when the ventilation rate was increased to 15 and 20 air changes per hour there was more restriction of lateral air mixing. This, as explained before, is due to the increased throw of the supplied air coupled with the unidirectional air flow pattern discharged into the room. With the central air terminal, which was the only one modified to a jet device, the air was discharged vertically downward with more throw and less entrainment than the other two terminals. Therefore the airborne particle concentration was only effectively removed under the central air terminal device. The effect of increasing the ventilation rate from 3 to 15 then to 20 air changes per hour decreased the performance indices at the vicinity of exhaust's grilles E_1 and E_2 , but increased at the vicinity of exhaust's grille E_3 . The minimum performance indices were obtained in the vicinity of central exhaust's grille E_2 .

5.1.5 Constant contaminant dispersion

To detect, describe and confirm any deviation from the theoretical phenomena of perfect mixing, further observations were made on the effectiveness of the various ventilation schemes. The performance of the different air terminal devices were compared by means of the performance index (PI).

Comparison of the results from each series of tests (Tables 4.6 to 4.13) show that complete air mixing was established with three air terminal devices (multislot, adjustable vane and dump) at 15 air changes per hour for the two different locations of smoke released. Smoke was released either between the middle air terminal device and the working table (R_{p1}) or between the working table and the middle exhaust (R_{p2}). The maximum deviation of average PI from perfect mixing ($PI=1$) was -8% to $+17\%$. The maximum deviation in average PI between the three air terminal devices was 27% . As these deviations are small, there appear to be no significant differences between each of the three terminal devices in diluting and removing the contamination.

Good mixing was also obtained when the multislot diffuser was tested with 3 air changes per hour, although the efficiency in mixing reduced when smoke was released between the central terminal and the working table (Tables 4.6 and 4.7). As the ventilation rate is increased to 20 air changes per hour, the effectiveness of the system in mixing the supplied air with the room air reduces significantly (Tables 4.6 and 4.7). This is shown from the very low values of performance indices (0.18 to 0.33) always obtained under the terminal.

Although increasing the volume of air supply always decreased the level of airborne concentration for any given release rate, the efficiency of the ventilation system in diluting the contamination improved until the ventilation rate reached 15 air changes per hour. After this it decreased and it is likely that the supplied air which was discharged in thick compact jets with an increased throw into the room would entrain less room air and mix less readily with the room air.

In the case of jet air terminal devices, as the ventilation rate was increased from 3 to 15 and then 20 air changes per hour the performance indices increased

when smoke was released at R_{p_1} and decreased when smoke was released at R_{p_2} . Significant layering and restriction of mixing was obtained when smoke was released between the table and the middle exhaust (release position R_{p_2}) for all the ventilation rates (3, 15 and 20 AC/hr) and differential temperatures studied. The much reduced values of PI's obtained (Tables 4.12 and 4.13) when smoke was released at R_{p_2} indicates that there is much less transfer of smoke particles from under the terminal and onto the working table. This effect was more significant at the high ventilation rate (20 AC/hr) due to the greater momentum and throw imparted by the jet terminal device.

Comparison of the results from all the air terminal devices show that the lowest PI's were obtained under the jet terminal device. The much reduced value of PI obtained under the jet (sampling Position No. 1) when smoke was released at R_{p_2} indicate that due to the unidirectional nature of the supplied air and the location of smoke release being some distance away from it there is minimum penetration and entrainment of particles under the jet (Position No. 1). The reduction of average PI (0.64→0.11→0.10) with increased ventilation rates (3→15→20 AC/hr) indicated that less entrainment and mixing is obtained as the volume of supplied air, and hence momentum and throw, is increased. The increase in momentum, along with the unidirectional manner of the jet, reduces the ingress of the contaminated room air into the supply air jet. With this air terminal device, smoke particles liberated at any position in the room were removed very effectively under the jet terminal.

It is worth noting that where jet air terminal devices are installed in cleanrooms, the optimum working place for an operator would be under the terminal, with an exhaust nearby, as the clean supply air will discharge downwards over the person and their work process and sweep away the contamination from the vicinity into the exhaust.

To investigate the parameters having the greatest effect on air mixing, it was necessary to use a statistical technique as there was no true classical relationship among the variables. The statistical technique, namely multiple regression analysis,

relies on empirical evidence to develop relationships among all the studied variables. The analysis was carried out to assess the significance of all the variables measured during the tests with respect to dilution and removal of contamination within the room. The dependent variable was performance index (PI) and the independent variables were as follows:

- (i) Air change rates
- (ii) Type of air terminal devices
- (iii) Location of contaminant source
- (iv) Differential temperature between the supplied air and the room air

The multiple regression analysis (Table 4.14) calculated correlation coefficients from which a prediction equation can be obtained for determining the PI's in terms of the above factors. It was also possible to input the maximum values used in the experiment into the multiple regression equations obtained (Table 4.14) to determine the most important variables affecting mixing at various sampling positions in the room.

The multiple regression analysis was first carried out for all the data obtained. Then the data was divided into smaller sets according to the position of smoke released, type of air terminal device and a combination of these two.

Overall it can be concluded that within the limits of all the variables studied, the parameters having the greatest influence on air mixing *in the centre of the room* in order of significance are:

- (i) location of contaminant source
- (ii) type of air terminal device
- (iii) air supply flow rate

Although for mixing *under the air terminal device*, the most effective variables in order of significance are:

- (i) air supply flow rate
- (ii) type of air terminal device

5.2 Contaminant Dispersion by People and Process Machines

To compute the airborne contaminant concentration in cleanrooms, data on the dispersal of airborne contaminants by people and process machines are required. As discussed in the introduction (section 1.8) no data on the average dispersion rates from people has been published and little good data on machines. It was therefore necessary to carry out experiments to obtain realistic data to use in the computer program.

The link between the airborne contaminant concentration in cleanrooms and contaminant (particles and bacteria-carrying particles) dispersion by people, particularly on the basis of a male/female comparison has not been widely investigated or analysed hitherto. To obtain realistic data 25 male and 30 female volunteers were studied in a dispersal chamber. The observations showed a great variability in contaminant-dispersion rates, particularly in male subjects. This variability is also apparent in the published literature reviewed (section 1.8.2). Although there is no scientific evidence to suggest any factors responsible for this variability, personal observation suggested that the results were affected by some or all of the following factors, and as these factors increased so did the bacteria dispersion rate.

- (i) activity levels
- (ii) skin surface area (including heaviness and obesity)
- (iii) lack of personal hygiene

Comparison of the results from male and female dispersion rates (Tables 4.17 and 4.18) clearly shows significant differences, particularly when indoor clothing is worn. The statistically significant reduction in the ratio of male/female median bacterial dispersion rates (from 5.2 to 1.5) when cleanroom clothing was worn instead of indoor clothing may be explained by the ineffectiveness of the indoor fabrics worn by males. The relatively loosely-woven indoor fabrics worn by the males did very little to prevent the dispersal of contamination into the air. This is because the penetration of airborne particles is most directly related to pore size of the fabric. It is, however, possible that the nylon tights worn by women could

have retained bacteria-carrying particles more effectively due to their high electrical resistance and substantial electrostatic charge.

Lidwell and MacIntosh (1978) reported the results of tests which showed that when surface resistivities exceeded $10^{12} \Omega/\text{cm}$ the residual charges on pieces of fabric after contact with similar material were between 18 and 73 nC. These surface charges are sufficient to substantially reduce contaminant dispersal into the air. They also stated that if skin scales are charged this would accentuate the effects of charges on the fabric in preventing dispersion.

May and Pomeroy (1973) and Hill *et al* (1974) have shown that bacteria-carrying particles are mainly dispersed from the lower part of the body (below the waist). This reinforces the suggestion that the nylon tights worn by females may be the reason for reducing the bacteria dispersed into the air.

As discussed above when cleanroom clothing (ceramic polyester) was worn the ratio of male/female median bacterial dispersion rate reduced to 1.5 as compared to 5.2 when indoor clothing was worn. Furthermore, a substantial reduction of 18.3 fold difference in median bacterial dispersion rate by males was found compared to only 5.4 obtained from females wearing cleanroom clothing. These different reductions between male and female may be explained by the fact that tightly woven ceramic polyester clothing (equivalent pore size about $18\mu\text{m}$) was not as effective in filtering off the particles coming from females as they had already been filtered by nylon tights. An additional reason for this may be that males disperse a different bacterial size distribution to females. If the median size of the skin fragments dispersed from men were, on average, larger than women, the ceramic polyester fabric would be more effective on men than women. Although Mackintosh *et al* (1978) reported the median of the skin fragments dispersed from people to be about $20\mu\text{m}$, there is no published information regarding the difference for males and females.

It is interesting to note that although males disperse more inert particles than females, the ratio of male/female median dispersion rates remains reasonably

constant (2.3 for particles $\geq 0.5\mu\text{m}$ and 1.8 for particles $\geq 5.0\mu\text{m}$) for both types of fabrics (indoor and ceramic polyester). Due to the high variability apparent in the experimental data, the difference in the ratio of male/female bacteria and particulate median dispersion through ceramic polyester coverall is not statistically significant. Also the ratio indoor/cleanroom clothing of median particulate dispersion rate for both males and females remains the same (2 for particles $\geq 0.5\mu\text{m}$ and 5 for particles $\geq 5.0\mu\text{m}$).

The results obtained clearly show significant differences between males and females. These suggest that, where possible, female cleanroom operators should be employed to reduce the level of airborne contamination within the room.

Experiments were also carried out to measure the particle emission from two different makes of vial-filling machines. The average steady-state particles generated varied from 2.6×10^4 to 2×10^6 per minute for particles $\geq 0.5\mu\text{m}$. This 100 fold difference in particle emission rate between the two vial-filling machines show that as the make and model of the machines make an important difference to airborne cleanliness in the cleanroom, information about machine dispersion rates should be supplied by manufacturers.

5.3 Outdoor Airborne Contamination

Experiments to measure the airborne bacteria and particles present in the outdoor atmosphere were carried out in different climatic conditions (wind, sun and rain) and at different locations (urban and rural) to obtain realistic data for incorporation in the airborne contaminant concentration model.

Although there is insufficient data to draw a conclusion on a purely statistical basis, the data obtained indicate that the weather and the location may influence the airborne contaminant concentration.

For all the climatic conditions tested, the airborne contaminant concentration in the urban location was higher than the rural location. Higher bacteria production can be attributed to higher human densities in the urban environment and associated activities such as refuse production and disposal. Similarly, abiotic

particles may be increased in the urban environment by industrial processes, transportation, combustion, etc. Natural climatic dispersal (wind, rain, sunshine) of these higher densities may be retarded by the constraint of building proximities and heights. It was observed that minimum airborne bacterial concentration ($0.45/\text{ft}^3$ or $16/\text{m}^3$) was obtained on a windy day and minimum particulate concentration ($163120/\text{ft}^3$ or $5.8 \times 10^6/\text{m}^3$ $\geq 0.5\mu\text{m}$ and $600/\text{ft}^3$ or $2.1 \times 10^4/\text{m}^3$ $\geq 5\mu\text{m}$) was obtained on a rainy day. These findings suggest that a major element for removing micro-organisms in outdoor air may be the wind and that rain may be a major factor for washing and removing the particles from dusty air.

The mean airborne bacteria concentration of $0.63/\text{ft}^3$ ($22.3/\text{m}^3$) obtained by Whyte (1968) is in good agreement with the results achieved herein. The results of airborne particle concentration obtained by Willike and Whitby (1975) for Los Angeles (smog) and remote areas (clear) illustrate the limits likely to be found in practice ($1 \times 10^8/\text{ft}^3$ or $4 \times 10^9/\text{m}^3$ to $6 \times 10^9/\text{ft}^3$ or $2 \times 10^{11}/\text{m}^3$ for particles $\geq 0.1\mu\text{m}$). Also the results obtained by Liu and Ahn (1986) for airborne particulate concentration ($3 \times 10^5/\text{ft}^3$ or $1.1 \times 10^7/\text{m}^3$ for particles $\geq 0.5\mu\text{m}$) in outdoor air is in good agreement with the results obtained by the author.

5.4 Surface Deposition

The surface deposition rates of airborne particles have been investigated theoretically and experimentally. The ultimate objective was to exclude those deposition mechanisms of little significance in the cumulative airborne contaminant concentration model. As a secondary object, theoretical models were devised which predicted the deposition of particles on surfaces of a room. The accuracy of this model was verified by experiments.

Initially, the deposition models considered gravitational sedimentation, Brownian (molecular) diffusion, turbulent (eddy) diffusion, inertial impaction, electrostatic and thermophoresis. However, due to near proximity of steam pipes, where the petri dishes were stored, the temperature of the agar surface was always hotter than the ambient temperature inside the chamber. As airborne particles move towards

lower temperature locations they move away from the agar surface under the influence of the temperature gradient. Deposition due to thermophoresis would therefore not occur.

As no means were available for measuring the charge carried on the particles formed by spraying, the deposition rate due to electrical forces could not be computed.

The deposition model shows that impaction of particles does not occur until the critical Stokes number is reached. By solving the flow field equations (Chapter 3) it was verified that the minimum Stokes number for finite efficiency of impaction of airborne particles on flat plates is 1/16 and the Stokes number for complete impaction is 1/4. When the computation was carried out for the worst possible case during the experiment (i.e. max. air speed = 1 m/s, diameter of aerosol jet = 5 cm and density of particles = $3.13 \times 10^3 \text{ kg/m}^3$) it became evident that the Stokes number was less than the critical Stokes number and that deposition due to impaction would not occur for particles having diameter less than $18 \mu\text{m}$ and complete impaction would not occur for particles larger than $36 \mu\text{m}$. These sizes were outside the particle size range studied experimentally and in the practical situation in a cleanroom, particles of these sizes will not be present in any significant quantities. Because of these facts, the deposition model was refined to take into account the surface loss rate only caused by (i) gravitational sedimentation, (ii) Brownian (molecular) diffusion and (iii) turbulent (eddy) diffusion for uncharged particles.

The computation for surface deposition was carried out for three nominal ventilation rates (0, 20 and 200 AC/hr) and the variation of the deposition rate with particle size was observed. One feature of the resultant theoretical deposition curves (Figure 4.24) was that all the three curves (0, 20 and 200 AC/hr) gave a size of particle which had a minimum deposition. The values of particle size which gave minimum deposition were found to vary between 0.3 and $0.8 \mu\text{m}$ depending on the stirrer speed and hence eddy diffusion. The particle diameters which gave the minimum deposition became larger as the stirrer speed increased.

The amount of surface deposition obtained indicated that at any fixed flow conditions (still or stir) gravitational sedimentation is the predominant loss mechanisms for particles larger than about $1\mu\text{m}$ while Brownian diffusion, turbulent diffusion and electrostatics are important for particles below about $0.5\mu\text{m}$. In the intermediate size range (0.5 to $1.0\mu\text{m}$) gravitational sedimentation, Brownian diffusion and eddy diffusion were all effective. Furthermore, the computation showed that there was no difference in deposition caused by the air being still or stirred for particles greater than about $1.5\mu\text{m}$ whereas deposition increased for particles below $0.5\mu\text{m}$ as the air change rates were increased. This suggests that turbulent diffusion becomes effective below $0.5\mu\text{m}$ because the motion of particles is affected by the turbulent eddies produced by the air motion.

The above theoretical findings (Table 4.24) were verified by experiment (Table 4.25) where it was found that there was no marked difference between experiments and theoretical results under both still and stirred air for aerodynamic particle diameters of $6.3\mu\text{m}$ and $11.2\mu\text{m}$. The test results demonstrated that the deposition of $0.8\mu\text{m}$ particles increased about 3 fold as the blade was used to agitate the air. This enhanced deposition can be accounted for by the particles in the air stream picking up the turbulent velocity fluctuation in the main part of the flow and in the outer part of the turbulent boundary layer. As a result of this, particles will be conveyed across the mean flow direction with an eddy diffusion coefficient which was very much greater than molecular diffusion coefficient (except very near the surface).

The analysis and resultant deposition curves obtained appear to be very similar to the results obtained by Liu and Ahn (1986) using a heat and mass transfer analogy. They calculated particle deposition velocities onto 125 mm and a 200 mm diameter silicon wafer in a vertical unidirectional flow cleanroom. They found that the deposition velocity decreased with increasing particle size in the diffusion (Brownian) regime, reached a minimum depending on airflow velocity and then increased with increasing particle size when sedimentation became important. Similarly the theoretical deposition curves obtained by Liu and Ahn

(1986) using the heat and mass transfer approach, showed no difference whatsoever in particle deposition for various air flow velocities (100, 50, 25 and 12.5 ft/min or 0.51, 0.25, 0.13 and 0.06 m/s) in sedimentation regime whereas deposition increased with airflow velocity in diffusion regime.

The experimental data obtained for aerodynamic particle diameters of 6.3 μm and 11.2 μm showed that all the particles deposit to the bottom of the chamber, under both still air conditions (0 AC/hr) and stirred air conditions (20 and 200 AC/hr) were as predicted by theory. These findings suggest that as larger particles (6.3 μm and 11.2 μm) fall more rapidly than the small ones (0.8 μm) due to greater density and cross sectional area, the only significant loss mechanism is gravitational sedimentation.

It was found during the experiments that the computational deposition model developed underestimated the deposition rate for aerodynamic particle diameters of 0.8 μm . The reason for this was not immediately clear but by refining the experiment the reason was found to be due to the particles, which were formed by spraying solution and were deposited within a short time after generation, being likely to have carried an appreciable charge. The test results (Table 4.26) indicate these electrical charges dominate the removal rates for particles of 0.8 μm . As there was no measurement of particle charge the surface deposition due to electrical charge could not be predicted. However the deposition velocity obtained by the number of particles deposited show that the particles are very highly charged. Therefore droplets produced by the spinning top generator carried substantial electrical charge which increased particle deposition onto surfaces.

A satisfactory theory for estimating the electrical charge carried by the airborne particles which are formed by spraying solutions, has not been developed. The charging mechanisms responsible for electrification are complicated in that the charging is affected by subtle chemical effects. The amount of charge measured by Chow and Mercer (1971) was about twice that normal charge predicted by electrostatic theory. Similarly, Matteson (1971) reported a large discrepancy between the actual charge carried by the particles formed by spraying solutions and

the theoretical model of electrical charge. He found substantially much larger charge than that predicted. John and Davis (1974) have also reported substantially high electrical charges on latex particles. Reischl *et al* (1977) measured spray charges for various substances from a vibrating-orifice aerosol generator. They found electric charge of $-10,000$ unit charge on $3\mu\text{m}$ diameter dioctylphthalate (DOP) particles. However the vibrating-orifice aerosol generator produces particles much less violently than the spraying top generator. The spray charge from the spinning top generator studied would therefore be much greater.

A comparison of the results obtained when the polarity air ionizer was used show about 50% reduction in deposition (Tables 4.25 and 4.26). This was still 3 times greater than predicted by theory. The degree of neutralization depends on the size of the particles, the initial charge level, the concentration of bipolar ions generated by the ionizer and the time available for neutralization to occur. It may be assumed that although the charged particles have been neutralized to some degree by the ionization device they have not been neutralized completely.

The comparison between the theory and experimental results was therefore generally good, but not perfect for $0.8\ \mu\text{m}$ particles. A more exact agreement between the theory and experimental results in this experimental circumstance is not expected, as the average aerodynamic particle diameter, effective particle density and shape of the particles used in the computational model were doubtful. Variations were also encountered in the number of bacterial colonies from agar plate to agar plate on the surface of the chamber from identical runs and in establishing still conditions where no thermal effects would cause air currents in the chamber to mix the air.

When the computational model was used to predict the deposition of aerodynamic particle diameters of 6.3 and $11.2\ \mu\text{m}$, the experimental results were in good agreement with theoretical predictions. These findings show that the deposition of particles for these sizes ($6.3\ \mu\text{m}$ and $11.2\ \mu\text{m}$) is dominated only by gravitational sedimentation.

When dry particle sizes were examined under the microscope, the particles

were actually smaller (by a factor of 0.83) than when estimated from the wet droplet diameter. This indicated that the wet particle size which was initially multiplied by 0.86 as suggested by May (1966) was not adequate to assess the true wet-drop size. Hence further inspection of the particle sizes under the microscope and comparison of the wet-drop sizes revealed that the wet particle size should have been multiplied by 0.72 to find the true drop size and correctly calculate the dry size.

Overall it can be concluded that, considering the difficulties encountered in carrying out the experiments, the agreement between experiment and prediction is good. Therefore, it can be concluded that gravitational sedimentation is adequate to explain the deposition observed in the chamber.

5.5 Airborne Contaminant Concentration

5.5.1 Theoretical Model

To predict the cumulative airborne contaminant concentration in conventionally ventilated cleanrooms a computer program, as described in Chapter Three, was developed. The computation was based on the assumption of perfect mixing of supplied air with the surrounding contaminated room air. It was verified that the assumption of perfect mixing is reasonable for all types of air terminal devices which entrain room air but less so for air terminal devices in which the air is supplied as a jet.

The input data into the computer program were as follows:

1. Total volumetric flow rate of supplied air
2. Contaminant dispersion rate
3. Final filter penetration
4. Pre-filter penetration
5. Percentage of recirculated air
6. Dimensions of the room
7. Outdoor contaminant concentration

The output results contained (i) cumulative contaminant concentration, (ii) decay

rates and (iii) deposition rate on surfaces or into product containers.

By including realistic distributions of all the variables formulating the model it was possible to predict the cumulative airborne contaminant concentration. A sensitivity analysis (Table 4.31) of the model-to-input parameters was carried out to assess quantitatively the effect of varying each input variable on the airborne contaminant concentration. The analysis was found to be extremely sensitive to changes in dispersion rate and the volumetric flow rate of supplied air. It was found that the airborne contaminant concentration was linearly proportional to the dispersal rate, a 50% increase in dispersion rate being reflected in a 50% increase in airborne contaminant concentration. The analysis also showed that the maximum airborne contaminant concentration corresponds to the peak in the contaminant source size distribution. As discussed in the literature review and earlier in this chapter the human being is normally the most dominant factor, but the manufacturing process can also, in many cases, generate substantial particles.

The sensitivity analysis also indicated that 50% increase of the air-supply volumetric-flow rate decreases the airborne concentration by 33% (in the case of bacteria contamination) and 36% (in the case of particle contamination). The difference in airborne contaminant concentration between bacteria and particles is due to the difference in deposition rate and size distribution of the input data.

It was demonstrated (Table 4.31) that for a given supplied air volume and dispersion rate, the dimensions of the room (or the volume) do not affect the airborne cleanliness to any appreciable degree. The very slight reduction of contaminant concentration with 50% increase in all the dimensions of the room is due to gravitational deposition of airborne particles onto the floor. Therefore the volume of the room has not any bearing on the steady-state airborne contaminant concentration in the room; it is the volumetric flow rate of supplied air which controls and dilutes the airborne contamination within the room. Any specification or guidance should therefore be presented in terms of total volumetric flow rate of supplied air into the room rather than air change rates. This clearly demonstrates the inaccuracy of various standards (Guide to Good Pharmaceutical Manufacturing

Practice, HMSO 1983 and The Rules Governing Medicinal Products in the European Community, EEC 1989) in specifying various grades of microbially controlled environments in terms of air change rates. However, it should be noted, as discussed previously, that the volume of the room can affect the rate of build up as well as the decay rates of airborne contamination in the room.

The analysis showed a substantially higher airborne contaminant concentration in the size range corresponding to the filter's minimum efficiency. This occurred independently of the exact shape of the outdoor or indoor particle size distribution curve. Furthermore, it became clear that nothing is to be gained by the use of highly efficient filters (HEPA or ULPA) as opposed to filters 50% less efficient. This is not surprising, as so few particles pass through the high efficiency filters, that particles from supplied air are only a minor source of airborne contamination in the room.

The Guide to Good Pharmaceutical Manufacturing Practice (HMSO 1983) recommendation on the selection of final filter efficiencies (99.997%, 99.995%, 99.95% against median diameter of about 0.65 μm) to achieve various microbial cleanliness levels (1/A, 1/B, 2) is therefore inappropriate. The document places undue emphasis upon final filter efficiency. The analysis achieved herein demonstrates clearly that nothing is to be gained by using more efficient filters (99.997%) as opposed to less efficient filters (99.995% or 99.95%). This conclusion is not surprising as bacteria are not present in the air as unicellular organisms but are found attached to particles. The micro-organisms contained in outdoor and indoor air are mainly associated with particles larger than 1 μm .

From the bacterial distributions given by Whyte (1968) the median diameter of bacterial particles found in recirculated air is about 6.4 μm and those in outdoor air 16 μm . Today's technology provides final filters that are virtually 100% efficient at 1 μm and larger and ensure that bacteria-free air is supplied into the room. It is not the particles in the supply air that are the source of contamination but particles generated in the room that are the major contribution to the air contamination. This fact suggests a cost advantage of providing

effective cleanroom clothing to reduce airborne contamination rather than increasing and conditioning the supplied air.

The model developed enables one to compute the amount of air necessary for dilution of airborne contaminants to achieve the required airborne cleanliness in the room. It would thus be very useful in sizing the air distribution plant. The computation can be repeated with a wide range of options (e.g. number of people, type of clothing, process machines) to evaluate the effectiveness of different designs and hence find the best way of achieving the desired airborne cleanliness at the most economical cost.

5.5.2 Experimental validation of the model

To evaluate the validity of the airborne contaminant concentration model, predicted values (Table 4.30) were compared with experimental results (Tables 4.28 and 4.29) from two cleanrooms. The 95% confidence limits for upper and lower values of measured airborne contamination were calculated. When comparison was made on the basis of mean airborne contaminant dispersal from people, the computed airborne contaminant concentration was between the lower 95% confidence limit and mean of the averages measured. As discussed previously, the computational airborne contaminant concentration was strongly influenced by the dispersion rate values inserted in the input data file. Therefore, inaccuracy in estimating the contaminant dispersion rate is one of the gravest sources of error in comparing computational and measured airborne contaminant concentration. The slightly higher mean airborne concentration of particles measured during the time period may have corresponded to some higher than normal activity in the room when the measurements were taking place. Precise comparison is difficult due to great variability in the contaminant dispersal values obtained from different volunteers and thus a large difference between the maximum dispersion rate and the mean dispersion rate. The dispersion rate varies greatly by activity and also from day to day, therefore it is difficult to input the exact number of particles that may come from each source into the computer program.

Overall it can be concluded that despite the dynamic and large fluctuations in

the contaminant dispersion rates, the airborne contaminant concentrations can be computed with a good degree of precision from existing information.

REFERENCES

- Adachi, K., Kiriya, S. and Yoshioka, N. (1978). The behaviour of a swarm of particles moving in a viscous fluid. *Chemical Engineering Science*, Vol. 33, p.115.
- Albrecht, F. (1931). Theoretical research concerning the settling of dust from streaming air and its application to the theory of the dust filter. *Physikalische Zeitschrift*, Vol 32., pp. 48-56.
- Alexander, L. G. (1951). Droplet transfer from suspending air to duct walls. *Industrial and Engineering Chemistry*, Vol. 43, pp. 1325-1331.
- Arendt, P. and Kallman, H. (1926). The mechanism of charging dust particles. *Zeitschrift für physik*, Vol. 35, pp. 421-441.
- Austin, P. (1970). Design and operation of clean rooms. Business news publishing company, Birmingham, Michigan, USA.
- Beal, S. K. (1968). Transport of particles in turbulent flow to channel or pipe walls. Bettis Atomic Power Laboratory, Report No. WAPD-TM-765, Westinghouse Electric Co., Pittsburgh, Pa, USA.
- Beeckmans, J. M. (1965). The deposition of aerosols in the respiratory tract. Part I. Mathematical analysis and comparison with experimental data. *Canadian Journal of Physiology and Pharmacology*, Vol. 43, pp. 157-172.
- Bergman, W., Biermann, A., Kuhl, W., Lum, B., Bogdanoff, A., Herbard, M., Hall, M., Banks, D., Mazumder, M. and Johnson, J. (1983). Electric air filtration: Theory, laboratory studies, hardware development and field evaluations. Livermore, CA: Lawrence Livermore Laboratory, University of California, USA, UCID 19952.
- Bethune, D. W., Blowers, R., Parker, M. and Pask, E. A. (1965). Dispersal of *Staphylococcus aureus* by patients and surgical staff. *Lancet*, *i*, pp. 480-483.
- Blowers, R., Crew, B. and Beryl, D. (1960). Ventilation of operating theatres. *Journal of Hygiene*, Cambridge, Vol. 58. pp. 427-448.
- Blowers, R. and McCluskey, M. (1965). Design of operating-room dress for surgeons. *Lancet*, *ii*, pp. 681-683.
- Bourdillon, R. B., Lidwell, O. M. and Lovelock, J. E. (1948). Studies in air hygiene. Medical Research Council Special Report series, No. 262, p. 323.
- BS 3928. (1969). Methods for Sodium flame test for air filters. British Standards Institution.
- BS 5295. (1989). Environmental cleanliness in enclosed spaces. British Standards Institution.
- BS 5958. (1980). Code of practice for control of undesirable static electricity.
- Burgers, J. M. (1942). On the influence of the concentration of a suspension upon the sedimentation velocity. *Proceedings of Koninkhke Nederlandse Akademie van Wetenschappen (Amsterdam)*, Vol. 45, No. 1, p.9 & No. 2, p. 126.
- Chamberlain, A. C. (1967). Deposition of particles to natural surfaces. 17th symposium of the Society for General Microbiology.
- Charnley, J. (1964). Sterile-air operating theatre enclosure. *British Journal of Surgery*, Vol. 51, No. 3, pp. 195-205.

Charnley, J. (1969). Low friction arthroplasty of the hip. Berlin, Heidelberg, New York. Springer-Verlag.

Chirifu, S., Sakata, S., Inove, M., Yoshida, T. and Okada, T. (1987). Study of aerosol deposition on wafer surfaces, Part I: Experimental analysis. Annual Technical Meeting of the Fine Particle Society, Boston, USA.

Chow, H. Y. and Mercer, T. T. (1971). Charges on droplets produced by atomization of solutions. American Industrial Hygiene Association Journal, Vol. 32, pp. 247-255.

Clift, R., Grace, J. R. and Weber, M. E. (1978). Bubbles, Drops and Particles. Academic Press.

Constance, J. D. (1970). Mixing factor is guide to ventilation. Power, February, pp. 56-57.

Cooper, D. W. (1986). Particulate Contamination and Microelectronics Manufacturing: An Introduction. Aerosol Science and Technology, Vol. 5, pp. 287-299.

Cooper, D. W., Miller, R. J. and Wu, J. J. (1988). Deposition of submicron aerosol particles during integrated circuit manufacturing. The 9th International Symposium on Contamination Control, Los Angeles, California, USA.

Corner, J. and Pendlebury, E. D. (1951). The coagulation and deposition of a stirred aerosol. Proceedings of the Physics Society, Vol. B64, pp. 645-654.

Crump, J. G. and Seinfeld, J. H. (1981). Turbulent deposition and gravitational sedimentation of an aerosol in a vessel of arbitrary shape. Journal of Aerosol Science, Vol. 12, No. 5, pp. 405-415.

Crump, J. G., Flagan, R. C. and Seinfeld, J. H. (1983). Particle wall loss rates in vessels. Aerosol Science and Technology, Vol. 2, pp. 303-309.

Cunningham, E. (1910). The Proceedings of the Royal Society, Vol. A83, p. 357.

Dabros, T., and Van de Ven, T. G. M. (1983). A direct method for studying particle deposition onto solid surfaces. Colloid Polymer Science, Vol. 261, pp. 694-707.

Daniel, J. H. and Brackett, F. S. (1951). An electrical method for investigating the nature and behaviour of small airborne charged particles. Journal of Applied Physics, Vol. 22, No. 5, pp. 542-554.

Davies, C. N. and Aylward, M. (1951). The trajectories of heavy, solid particles in a two-dimensional jet of ideal fluid impinging normally upon a plate. The Proceedings of the Physical Society, Section B, Vol. 64, Part 10, pp. 889-911.

Davies, C. N. (1960). Deposition of *Lycopodium* spores upon glass slides exposed in a wind tunnel. British Journal of Applied Physics, Vol. 11, pp. 535-538.

Davies, C. N. (1966). Aerosol Science. Academic Press. New York.

Davies, C. N., Heyder, J. and Subba Ramu, M. C. (1972). Breathing of half-micron aerosols, I: Experimental. Journal of Applied Physiology, Vol. 32, No. 5, pp. 591-600.

Davies, C. N. (1972). Breathing of half micron aerosols, II: Interpretation of experimental results. Journal of Applied Physiology, Vol. 32, No. 5, pp. 601-611.

Davies, C. N., Level, M. J. and Rothenberg, S. J. (1975). 4th International Symposium on Inhaled Particles and Vapour.

Davies, C. N. (1945). The Proceedings of the Physical Society, London, Vol. 57, p. 259.

- Degain, D. D. and Tardos, G. I. (1981). Inertial deposition of small particles on a sphere at intermediate and high Reynolds numbers: A time dependent study. *Journal of Air Pollution Control Association*, Vol. 31, pp. 981-986.
- Doig, C. M. (1972). The effect of clothing on the dissemination of bacteria in operating theatres. *British Journal of Surgery*, Vol. 59, pp. 878-881.
- Drivas, P. J., Simmonds, P. G. and Shair, F. H. (1972). Experimental characterization of ventilation systems in buildings. *Environmental Science & Technology*, Vol. 6, No. 7, pp. 609-614.
- Duguid, J. P. and Wallace, A. T. (1948). Air infection with dust liberated from clothing. *Lancet*, *ii*, pp. 845-849.
- EEC. (1989). The Rules Governing Medicinal Products in the European Community. Guide to Good Manufacturing Practice for Medicinal Products, Commission of the European Communities, Vol. IV.
- Einstein, A. (1905). Investigations on the theory of Brownian motion. Dover, New York, (republished 1956).
- Ensor, D. S., Clayton, A. C. and Donovan, R. P. (1987)*. Particle deposition studies in silicon technology. Annual Technical Meeting of the Fine Particle Society, Boston, USA.
- Ensor, D. S., Donovan, R. P. and Locke, B. R. (1987). Particle size distribution in clean rooms. *The Journal of Environmental Sciences*, Nov/Dec.
- Epstein, P. S. (1924). On the resistance experienced by spheres in their motion through gases. *Physical Review*, Vol. XXIII, pp. 710-733.
- Fairchild, C. I. and Tillery, M. I. (1982). Wind tunnel measurement of the resuspension of ideal particles. *Atmospheric Environment*, Vol. 16, No. 2, pp. 229-238.
- Faith, L. E., Bustany, S. N., Hanson, D. N. and Wilke, C. R. (1967). Particle precipitation by space charge in tubular flow. *Industrial Engineering Chemistry Fundamentals*, Vol. 6, pp. 519-526.
- Farquharson, I. M. C. (1952). Part I: The ventilating air jet. *Journal of the Institution of Heating and Ventilating Engineers*, Vol. 19, p. 449.
- Federal Standard 209D. (1988). Clean room and work station requirements, controlled environment, USA.
- Foord, N. and Lidwell, O. M. (1973). A method for studying air movements in complex occupied buildings such as hospitals: halocarbons as gas tracers using gas chromatography. *Building Services Engineer*, Vol. 41, pp. 93-100.
- Foord, N. and Lidwell, O. M. (1975). Airborne infection in a fully air-conditioned hospital. I. Air transfer between rooms. *Journal of Hygiene, Cambridge*, Vol. 75, pp. 15-30.
- Frean, D. H. and Billington, N. S. (1955). Part II: The ventilating air jet. *Journal of the Institution of Heating and Ventilating Engineers*, Vol. 23, p. 313.
- Friedlander, S. K. (1977). Smoke, dust and haze: Fundamentals of aerosol behaviour. John Wiley, New York.
- Fry, F. A. and Blake, A. (1973). Regional deposition and clearance of particles in the human nose. *Journal of Aerosol Science*, Vol. 4., pp. 113-124.

- Fuchs, N. A. (1964). *The Mechanics of Aerosols*. Pergamon Press, Oxford.
- Fujii, S., Hayakawa, I. and Iwase, K. (1982). Contamination index of various surgical garments by size distribution. 6th International Symposium on Contamination Control, pp. 76-82.
- Fujii, S. and Minamino, O. (1982). Generation of dust from various garments for clean rooms. 6th International Symposium on Contamination Control, pp. 73-76.
- Gallily, I., Schiby, D., Cohen, A. H., Holländer, W., Schlers, D. and Stöber, W. (1986). On the inertial separation of nonspherical aerosol particles from laminar flows. I. The cylindrical case. *Aerosol Science and Technology*, Vol. 5., pp. 267-286.
- Gormley, P. and Kennedy, M. (1949). Diffusion from a stream flowing through a cylindrical tube. *Proceedings of the Royal Irish Academy*, Vol. 52A, pp. 163-169.
- Gregory, P. H. and Stedman, D. J. (1953). Deposition of airborne *Lycopodium* spores on plane surfaces. *Annual of Applied Biology*, Vol. 40, pp. 651-674.
- Hamberg, O. (1982). Particulate fallout predictions for clean rooms. *The Journal of Environmental Sciences*, May/June, pp. 15-20.
- Harrison, A. W. (1979). Quiescent boundary layer thickness in aerosol enclosures under convective stirring conditions. *Journal of Colloid and Interface Science*, Vol. 69, No. 3, pp. 563-570.
- Hemeon, W. C. L. (1955). *The industrial process*. New York.
- HEVAC Association. (1981). *Air diffusion guide*. The Heating, Ventilating and Air Conditioning Association.
- Hidy, G. M. and Brock, J. R. (1970). *The Dynamics of Aerocolloidal Systems*. Pergamon Press, London.
- Hidy, G. M. (1984). *Aerosols: An industrial and environmental science*. Academic Press, Orlando, p. 46.
- Hill, J., Howell, A. and Blowers, R. (1974). Effect of clothing on dispersal of *Staphylococcus aureus* by males and females. *Lancet*, *ii*, pp. 1131-1136.
- Holmes, M. J. and Sachariewicz, E. (1973). The effects of ceiling beams and light fittings on ventilating jets. The Heating & Ventilating Research Association, Laboratory Report No. 79, Bracknell, Berkshire.
- HMSO (1983). *Guide to Good Pharmaceutical Manufacturing Practice*. Her Majesty's Stationery Office, London, England.
- I'Anson, S. J., Irwin, C. and Howarth, A. T. (1982). A multiple tracer gas technique for measuring air-flows in houses. *Building and Environment*, Vol. 17, pp. 245-252.
- Illori, T. A. (1971). Turbulent deposition of aerosol particles inside pipes. Ph.D. Thesis, Mechanical Engineering Department, University of Minnesota, Minneapolis, USA.
- Irwin, C., Edwards, R. E. and Howarth, A. T. (1984). An improved multiple tracer gas technique for the calculation of air movements in buildings. *Air Infiltration Review*, Vol. 5, pp. 4-5.
- Itoh, H., Smaldone, G. C., Swift, D. L. and Wagner, H. N. (1985). Mechanisms of aerosol deposition in a nasal model. *Journal of Aerosol Science*, Vol. 16, No. 6, pp. 529-534.

- Jackman, P. J. (1973). Air movement in rooms with ceiling-mounted diffusers. Heating and Ventilating Research Association, Laboratory Report No. 81, Bracknell, Berkshire.
- Jackman, P.J. (1986). Parameters affecting the selection of air diffusion systems and devices. Expoclima, Brussels.
- Jackson, J. D. (1962). Classical electrodynamics. John Wiley and Sons, Inc., New York.
- Jansen, L. H., Hojyo-Tomoko, M. T. and Kilgman, A. M. (1974). Improved fluorescence staining technique for estimating turnover of the human stratum corneum. British Journal of Dermatology, Vol. 90, pp. 9-12.
- John, W. and Davis, J. W. (1974). The measurement of the charge distribution on monodisperse aerosols. Atmosphere Environment, Vol. 8, pp. 1029-1034.
- John, W. (1980). Generation of aerosols. Ann Arbor Science. Chapter 6: particle charge effects. pp. 141-151.
- Kawamata, T. (1982). More practical calculation method of particle density in clean rooms. The Proceedings of the 6th International Symposium on Contamination Control, Tokyo, Japan, pp. 37-42.
- Kennerad, E. H. (1938). Kinetic theory of gases. McGraw Hill, New York, pp. 327-330.
- Kethley, T. W., Cowan, W. B. and Fincher, E. L. (1962). Bacterial load of air in simulated operating rooms. Progress Report OH-19. Engineering Experiment Station, Georgia Institute of Technology, Atlanta.
- Kirsch, A. A. and Fuchs, N. A. (1967). The fluid flow in a system of parallel cylinders perpendicular to the flow direction at small Reynolds numbers. Journal of the Physical Society of Japan, Vol. 22, pp.1251-1255.
- Koestel, A., Herman, P. and Tuve, G. L. (1952). Comparative studies of ventilating jets from various types of outlets. The American Society of Heating and Ventilating Engineers Transactions, 56, p. 459.
- Kunkel, W. B. (1950). The static electrification of dust particles on dispersion into a cloud. Journal of Applied Physics, Vol. 21, pp. 820-832.
- Kunkel, W. B. (1950). Charge distribution in coarse aerosols as a function of time. Journal of Applied Physics, Vol. 21, pp. 833-837.
- Kuwabara, S. (1959). The forces experienced by randomly distributed parallel circular cylinder or spheres in a viscous flow at small Reynolds numbers. Journal of the Physical Society of Japan, Vol. 14, No. 4, pp. 527-538.
- Lagus, P. and Persily, A. K. (1985). A review of tracer-gas techniques for measuring air flows in buildings. The American Society of Heating, Refrigerating and Air Conditioning Engineers, Transactions 91, HI-85-22, No. 1.
- Langer, G. (1965). Particle deposition and re-entrainment from coniferous trees, Part II: Experiments with individual leaves. Kolloid-Zeitschrift, Vol. 204, pp. 119-124.
- Langstroth, G. O. and Gillespie, T. (1947). Coagulation and surface losses in disperse systems in still and turbulent air. Canadian Journal of Research, Vol. 25, section B, pp. 455-471.

- Lee, K. W. and Liu, B. Y. H. (1982). Theoretical study of aerosol filtration by fibrous filters. *Aerosol Science and Technology*, Vol. 1, pp. 147-161.
- Lidwell, O. M. and Lovelock, J. E. (1946). Some methods of measuring ventilation. *Journal of Hygiene, Cambridge*, Vol. 44, pp.326-332.
- Lidwell, O. M. and Williams, R. E. O. (1960). The ventilation of operating-theatres. *Journal of Hygiene, Cambridge*, Vol. 58, pp. 449-464.
- Lidwell, O. M., Richards, I. D. G. and Polakoff, S. (1967). Comparison of three ventilating systems in an operating room. *Journal of Hygiene, Cambridge*, Vol. 65, pp. 193-205.
- Lidwell, O. M. and MacIntosh, C. A. (1978). The evaluation of fabrics in relation to their use as protective garments in nursing and surgery. Part I: Physical measurements and bench tests. *Journal of Hygiene, Cambridge*, Vol. 81, pp. 433-452.
- Lidwell, O. M., Lowbury, E. J. L., Whyte, W., Blowers, R., Stanley, S. J. and Lowe, D. (1982). Effect of ultraclean air in operating rooms on deep sepsis in the joint after total hip or knee replacement: A randomised study. *British Medical Journal*, Vol. 285, pp. 10-14.
- Lidwell, O. M., Lowbury, E. J. L., Whyte, W., Blowers, R., Stanley, S. J. and Lowe, D. (1983). Airborne contamination of wounds in joint replacement operations: the relation to sepsis rates. *Journal of Hospital Infection*, Vol. 4, pp. 111-131.
- Lidwell, O. M., Lowbury, E. J. L., Whyte, W., Blowers, R., Stanley, S. J. and Lowe, D. (1983). Bacteria isolated from deep joint sepsis after operation for total hip or knee replacement and the sources of the infection with *Staphylococcus aureus*. *Journal of Hospital Infection*, Vol. 4, pp. 19-29.
- Liquin, Z. and Yongnian, L. (1982). Corrections for the theoretical calculating formula of conventional clean rooms. *Proceedings of the 6th International Symposium on Contamination Control*, Tokyo, Japan, pp. 43-47.
- Liu, B. Y. H. and Agarmal, J. K. (1974). Experimental observation of aerosol deposition in turbulent flow. *Journal of Aerosol Science*, Vol. 5, No. 2, pp.145-155.
- Liu, B. Y. H. and Ilori, T. A. (1974). Aerosol deposition in turbulent pipe flow. *Environmental Science & Technology*, Vol. 8, No. 4, pp. 351-356.
- Liu, B. Y. H., Rubow, R. L. and Pui, D. Y. H. (1985). Performance of HEPA and ULPA filters. *Proceedings of the 31st Annual Technical Meeting of the Institute of Environmental Sciences*, Las Vegas, USA, pp. 25-28.
- Liu, B. Y. H. and Ahn, K. H. (1986). Particle deposition on semiconductor wafers. *Mechanical Engineering Department, Particle Technology Laboratory Publication No. 582*, University of Minnesota, Minneapolis, USA.
- Liu, B. Y. H. and Pui, D. Y. H. (1987). Aerosol charging and neutralization and electrostatic discharge in clean rooms. *The Journal of Environmental Sciences*, March/April, pp. 42-46.
- MacIntosh, C. A., Lidwell, O. M., Towers, A. G. and Marples, R. R. (1978). The dimensions of skin fragments dispersed into the air during activity. *Journal of Hygiene, Cambridge*, Vol. 81, pp. 471-479.
- Matteson, M. J. (1971). The separation of charge at the gas-liquid interface by dispersion of various electrolyte solutions. *Journal of Colloid Interface Science*, Vol. 37, pp. 879-890.

- Maxey, M. R. and Riley, J. J. (1983). Equation of motion for a small rigid sphere in a non-uniform flow. *Physics of Fluids*, Vol. 26, pp. 883-889.
- May, K. R. (1945). The cascade impactor: An instrument for sampling coarse aerosols. *Journal of Scientific Instruments*. Vol. 22, pp. 187-195.
- May, K. R. (1949). An improved spinning top homogeneous spray apparatus. *Journal of Applied Physics*, Vol. 20.
- May, K. R. (1966). Spinning-top homogeneous aerosol generator with shock proof mounting. *Journal of Scientific Instruments*, Vol. 43, pp. 841-842.
- May, K. R. and Clifford, R. (1967). The impaction of aerosol particles on cylinders, spheres, ribbons and disks. *Annual of Occupational Hygiene*, Vol. 10, pp. 83-95.
- May, K. R. and Pomeroy, N. P. (1973). Bacterial dispersion from the body surface. *Airborne Transmission and Airborne Infection* (edited by Hers, J. F. and Winkler, K. C.) Utrecht: Oosthoek, pp. 426-432.
- McCready, D. I. (1984). Boundary layer transport of small particles. Ph.D. Thesis, Virginia Polytechnic Institute and State University, Blacksburg, VA, USA.
- McMurray, P. H. and Rader, D. J. (1985). Aerosol wall losses in electrically charged chambers. Particle Technology Laboratory, Department of Mechanical Engineering, University of Minnesota, Minneapolis, USA, publication No. 498.
- Melandri, C., Prodi, V., Tarroni, G., Formignani, M., De Zaiacomo, T., Bompere, G. F. and Maestri, G. (1977). Inhaled particles, W. H. Walton, Ed. Oxford, Pergamon Press, pp. 193-201.
- Montgomery and Corn. (1970). Aerosol deposition in a pipe with turbulent air flow. *Journal of Aerosol Science*, Vol. 1, p. 185.
- Morrison, P. W. (1973). Fundamentals of environmental control. Environmental control in electronics manufacturing, New York: Van Nostrand Reinhold Company, pp. 238-273.
- NASA. (1967). Standards for clean rooms and work stations for the microbially controlled environment. National Aeronautics and Space Administration (USA).
- Natanson, G. L. and Ushakava, E. N. (1961). Theory of charging submicroscopic aerosol particles as a result of capturing of gas ions. *Journal of Physical Chemistry*, Vol. 35, pp. 363.
- Nevins, R. G. (1976). Air diffusion dynamics - Theory, design and application. Business News Publishing Company, Michigan, USA.
- Niemelä, R., Toppila, E. and Tossavainen, A. (1984). The measurement of ventilation parameters by means of tracer gas techniques and a microcomputer. *Annual of Occupational Hygiene*, Vol. 28, pp. 203-210.
- Noble, W. C., Lidwell, O. M. and Kingston, D. (1963). The size distribution of airborne particles carrying micro-organisms. *Journal of Hygiene*, Cambridge, Vol. 66, pp. 385-391.
- Nobuyosin, J. (1986). Study of air flow pattern in the clean rooms for manufacturing semiconductors. Proceedings of the 32nd Annual Technical Meeting of the Institute of Environmental Sciences, USA, pp. 556-564.

- Okuyama, K., Kousaka, Y., Kida, Y. and Toshida, T. (1977). Turbulent coagulation of aerosols in a stirred tank. *Journal of Chemical Engineering Japan*, Vol. 10, No. 2, pp. 142-147.
- Okuyama, K., Kousaka, Y. and Hosokawa, T. (1984). Turbulent and Brownian diffusive deposition and gravitational sedimentation in a stirred tank. *Aerosols*, Liu, Pui and Fissan editors, Elsevier Science Publishing Company, Inc.
- Osborrow, G. S. (1975). Quantitative relationship between airborne viable and total particles. *Health Laboratory Science (USA)*, Vol. 12, p. 48.
- Parkinson, J. T. L. and Billington, N. S. (1957). Part III: The ventilating air jet. *Journal of Heating and Ventilating Engineers*, Vol. 24, p. 415.
- PDA. (1980). Validation of Aseptic Filling for Solution Drug Products. Parenteral Drug Association Inc., Technical Monograph No. 2.
- Peters, M. H., Cooper, D. W. and Miller, R. J. (1988). The effects of electrostatics and inertial forces on the diffusional deposition of small particles onto large disks: stagnation flow approximations. To be published in *Journal of Aerosol Science*.
- Potter, I. N. (1988). Ventilation effectiveness in mechanical ventilation systems. The Building Services Research and Information Association, Technical Note 1.
- Prior, J. J., Littler, J. G. T. and Adlard, M. W. (1983). Development of a multi-tracer gas technique for observing air movement in buildings. *Air Infiltration Review*, Vol. 4, pp. 9-11.
- Pui, D. Y. H., Romay-Novas, F. and Liu, B. Y. H. (1987). Experimental study of particle deposition in bends of circular cross section. *Journal of Aerosol Science and Technology*, Vol. 7, No. 3, pp. 301-315.
- Ranz, W. E. and Wong, J. B. (1952). Impaction of dust and smoke particles. *Industrial and Engineering Chemistry*, Vol. 44, No. 6, pp. 1371-1381.
- Ro, T. and Unno, K. (1986). Experiments on particulate generation from the robot in a clean room. *Proceedings of the 8th International Symposium on Contamination Control*, Milan, Italy, pp. 843-849.
- Rogers, G. G. and Bailey, L. G. (1987). A closed chamber method of measuring particle emissions from process equipment. *Microcontamination Journal (USA)*, Vol. 5, No. 2.
- Rosinski, J. (1957). Efficiency of scavenging devices used in determining fallout. *Armor Research Foundation*, Chicago, No. III.
- Rosinski, J. and Langer, G. (1967). Deposition of aerosol particles on flat surfaces. *Powder Technology*, Vol. 1, pp. 167-173.
- Saffman, P. G. and Turner, J. S. (1956). On the collision of drops in turbulent clouds. *Journal of Fluid Mechanics*, Vol. 1, pp. 16-30.
- Sakata, S., Trone, M., Chimfn, S., Yoshida, T. and Okada, T. (1987). Study of aerosol deposition on wafer surface, part 2: Theoretical analysis. *Annual Technical Meeting of the Fine Particle Society*, Boston, USA.
- Sandberg, M. (1981). What is ventilation efficiency. *Building and Environment*, Vol. 16, No. 2, pp. 123-135.
- Sehmel, G. A. (1968). Aerosol deposition from turbulent airstreams in vertical conduits. *Pacific Northwest Laboratory*, Richland, Washington, USA, No. BNWL-578.
- Reischl, G., John, W. and Devor, W. (1977). Uniform electrical charging of monodisperse aerosols, *Journal of Aerosol Science*, Vol. 8, pp. 55-65.

- Sehmel, G. A. (1970). Particle deposition from turbulent air flow. *Journal of Geophysical Research*, Vol. 75, pp. 1766-1781.
- Sehmel, G. A. (1973). Particle eddy diffusivities and deposition velocities for isothermal flow and smooth surfaces. *Journal of Aerosol Science*, Vol. 4, No. 2, pp. 125-138.
- Slack, G. W. (1963). Sedimentation of compact clusters of uniform spheres. *Nature*, Vol. 200, p. 466.
- Starr, J. R. (1967). Inertial impaction of particulates upon bodies of simple geometry. *Annual of Occupational Hygiene*, Vol. 10, pp. 349-361.
- Stein, R. L., Ryback, W. H. and Sparks, A. W. (1972). Deposition of aerosol in a plastic chamber. *Journal of Colloid and Interface Science*, Vol. 42. No.2.
- Stern, S., Zeller, H. and Schekman, A. (1960). The aerosol efficiency and pressure drop of a fibrous filter at reduced pressure. *Journal of Colloid Science*, Vol. 15, pp. 546-562.
- Stokes, G. G. (1850). *Mathematical and Physical paper*, Vol. III, No. 33. Johnson Reprint Corp. (1966).
- Stowers, I. F. (1984). Aerodynamics of particles. Proceedings on the course of contamination control in clean rooms, Glasgow University, Building Services Research Unit, U.K.
- Stowers, I. F. (1985). Predicting airborne and surface contaminant levels in clean rooms. A paper prepared for submittal to *Microcontamination Journal (USA)*. Livermore National Laboratory, Livermore, California, USA.
- Takahashi, K. and Kasahara, M. (1968). A theoretical study of the equilibrium particle size distribution of aerosols. *Atmospheric Environment*, Vol. 2, pp. 441-453.
- Takahashi, K. and Ito, H. (1976). A computational model for regional deposition of aerosol particles in the human lung. The Institute of Atomic Energy, Kyoto University, Kyoto, Japan, Technical Report, No. 170.
- Thomas, J. W. (1958). Gravity settling of particles in a horizontal tube. *Journal of Air Pollution Control Association*, Vol. 8. pp. 32-34.
- Tuve, G. L. (1953). Air velocities in ventilating jets. *American Society of Heating and Ventilating Engineers, Transactions*. 59, pp. 261-282.
- Van de Vate, J. F. (1972). *Journal of Colloid Interface Science*, Vol. 41, pp. 194-197.
- Van Gunst, E., Erkelens, P. J. and Coenders, W. P. J. (1967). Some results of investigations regarding the supply of cooled air in a test room. *Proceedings of the 4th International Congress of Heating and Air Conditioning*, Paris.
- Viegersma, N. (1980). The bacteriological safety of air movements and air changes in operating theatres. Thesis, Rijksuniversiteit te Groningen. Krips Repro Meppel.
- Wadden, R. and Scheff, P. (1983). Indoor air pollution characterization, prediction and control. John Wiley & Sons.
- Waldmann, L. and Schmitt, K. H. (1966). Thermophoresis and diffusiophoresis of aerosols. *Aerosol science*, Academic Press, New York.
- Walton, W. H. and Prewett, W. C. (1949). The production of sprays and mists of uniform drop size by means of spinning disc sprayers. *Proceedings of the Physical Society*, Vol. B62, pp. 341-350.

- Wedding, J. B., Carlson, R. W., Stukel, J. J. and Bazzaz, F. A. (1975). Aerosol deposition of plant leaves. *Environmental Science & Technology*, Vol. 9, No. 2., pp. 151-153.
- Weibel, E. R. (1963). *Morphometry of the human lung*. Chapter XI, Academic Press.
- Wells, A. C. and Chamberlain, A. C. (1967). Transport of small particles to vertical surfaces. *British Journal of Applied Physics*, Vol. 18, p. 1793.
- Whitby, K. T. and Liu, B. Y. H. (1968). Polystyrene aerosol-electrical charge and residue size distribution. *Atmospheric Environment*, Vol. 2, pp. 103-116.
- Whitfield, W. J. (1962). A new approach to clean room design. Sandia Corporation (USA), Publication No. 4673.
- Whittle, G. E. and Bennett, K. M. (1986). An index for rating the performance of supply air terminal devices used in air conditioning. *Expoclima*, Brussels.
- Whittle, G. E. (1986). Room air distribution: design and evaluation. The Building Services Research & Information Association, Technical Note 4.
- WHO. (1973). Sterility and sterility testing of pharmaceutical preparations and biological substances. World Health Organization, Technical Report Series, No. 530.
- Whyte, W. (1968). Bacteriological aspects of air-conditioning plants. *Journal of Hygiene*, Cambridge, Vol. 66, pp. 567-584.
- Whyte, W., Shaw, B. H. and Barnes, R. (1973). A bacteriological evaluation of laminar-flow systems for orthopaedic surgery. *Journal of Hygiene*, Cambridge, Vol. 71, pp. 559-564.
- Whyte, W. and Shaw, B. H. (1974). The effect of obstructions and thermals in laminar-flow systems. *Journal of Hygiene*, Cambridge, Vol. 72, pp. 415-423.
- Whyte, W., Vesley, D. and Hodgson, R. (1976). Bacterial dispersion in relation to operating room clothing. *Journal of Hygiene*, Cambridge, Vol. 76, pp. 367-378.
- Whyte, W., Hodgson, R. and Bailey, P. V. (1978). An evaluation of the Charnley-Howarth exflow operating-room system. Building Services Research Unit, University of Glasgow Report No. 226.
- Whyte, W., Hodgson, R., Bailey, P. V. and Graham, J. (1978). The reduction of bacteria in the operating room through the use of non-woven clothing. *British Journal of Surgery*, Vol. 65, pp. 469-474.
- Whyte, W., Bailey, P. V., Hamblen, D. L., Fisher, W. D. and Kelly, I. G. (1983). A bacteriologically occlusive clothing system for use in the operating room. *Journal of Bone and Joint Surgery*, Vol. 65, Part B, pp. 502-506.
- Whyte, W. and Bailey, P. V. (1985). Reduction of microbial dispersion by clothing. *Journal of Parenteral Science and Technology*, Vol. 39, pp. 51-60.
- Whyte, W. (1986). Sterility assurance and models for assessing airborne bacterial contamination. *Journal of Parenteral Science & Technology*, Vol. 40, No. 5, pp. 188-197.
- Willeke, K. and Whitby, K. T. (1975). Atmospheric aerosols: size distribution Interpretation. *Journal of the Air Pollution Control Association*, Vol. 25, pp. 529-534.

Willeke, K. (1980). Generation of Aerosols. Ann Arbor Science Publishers, Michigan, USA.

Wilson, I. B. (1947). The deposition of charged particles in tubes, with reference to the retention of therapeutic aerosols in the human lung. Journal of Colloid Science, Vol. 2, pp. 271-276.

Wilson, L. G. and Cavanagh, P. (1967). The relative importance of Brownian diffusion and other factors in aerosol filtration. Atmospheric Environment, Vol. 1, pp. 261-264.

Wilson, L. G. and Cavanagh, P. (1971). The capture of sub-micron aerosol particles by single fine fibres. Atmospheric Environment, Vol. 5, pp. 123-135.

Wong, J. B., Ranz, W. E. and Johnston, H. F. (1956). Collection efficiency of aerosol particles and resistance to flow through fibre mats. Journal of Applied Physics, Vol. 27, pp. 161-168.

Woods, J. E. and Crawford, R. R. (1978). Calculation methods to assess indoor air quality. The American Society of Heating, Refrigerating and Air Conditioning Engineers, Transactions 89, pp. 683-693.

Yu, C. P. (1977). Precipitation of unipolarly charged particles in cylindrical and spherical vessels. Journal of Aerosol Science, Vol. 8, pp. 237-241.

APPENDIX A - Decay Rates

This appendix contains the results of measurements carried out to study decay rates. The experiments as described (section 2.1.2.3) were carried out in a conventionally-ventilated cleanroom being the diagnostic filling area at Organon Pharmaceutical Manufacturing Laboratory at Newhouse near Glasgow.

To study decay rates smoke was released in the room for 10 seconds and the decay of the smoke particles was continuously recorded at three different sampling points. The sampling point locations which were 1m from the floor were:

Position No. 1: Directly below the central air terminal device

Position No. 2: Middle of the room on top of the working table

Position No. 3: Middle side of the room near the middle exhaust.

The experiments were carried out for various air terminal devices (multislot, adjustable vane, dump and jet), ventilation rates and differential temperature. It is reminded that the negative differential temperature indicates supply air hotter than the ambient room air.

The results for each ventilation scheme are presented graphically by plotting the natural logarithm of the smoke concentration remaining at a given time against the time. The effective air change rates (N_{eff}) were estimated by fitting the best straight line through the measured points and evaluating the decay slope. The rate of decay of airborne concentration at different points in the room was then the basis for determining the performance index at the respective sampling points for the given test conditions. Inspection of these gave an insight into the nature of air mixing for various ventilation schemes.

Fig. A1 Decay of airborne particle concentration
 Multislot diffusers
 $N = 2.62$ ac/hr, Mean $N_{eff} = 3.14$ ac/hr, $\Delta T = -1.90K$

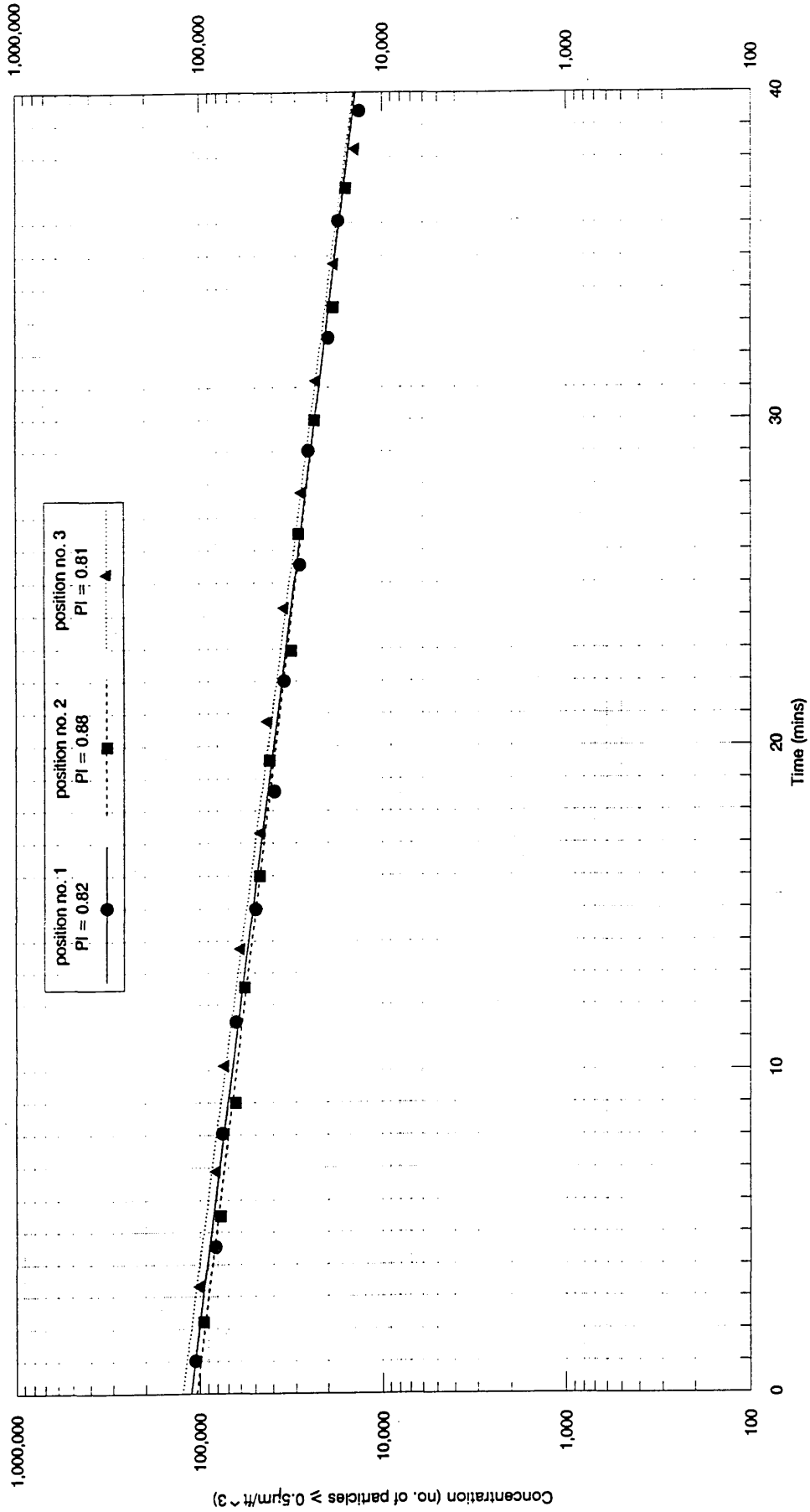


Fig. A2 Decay of airborne particle concentration
 Multislot diffusers
 N = 13.81 ac/hr, Mean Neff = 14.50 ac/hr, $\Delta T = 0K$

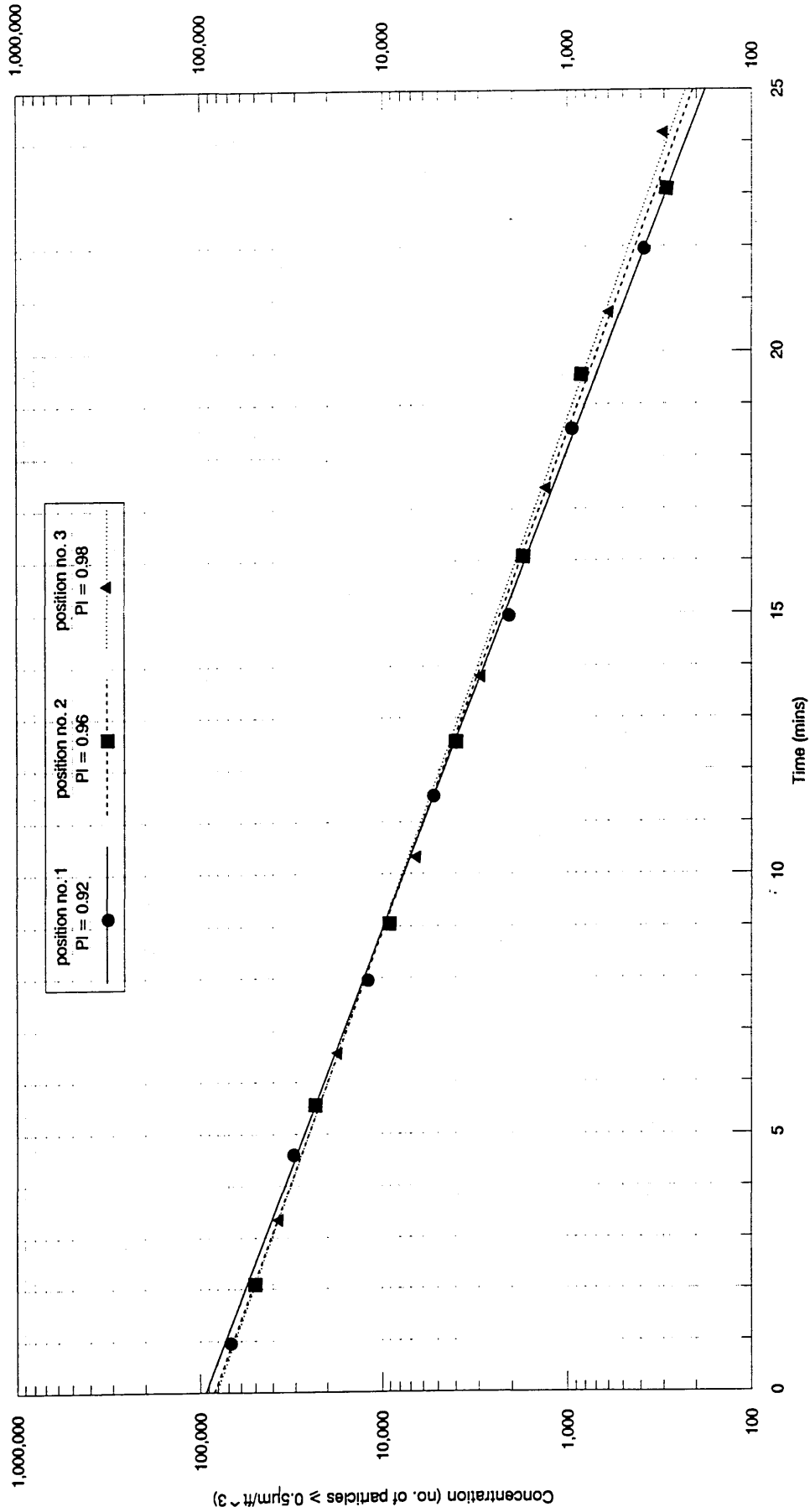


Fig. A3 Decay of airborne particle concentration
 Multislot diffusers
 $N=13.81$ ac/hr, Mean $N_{eff}=13.03$ ac/hr, $\Delta T=+2.12K$

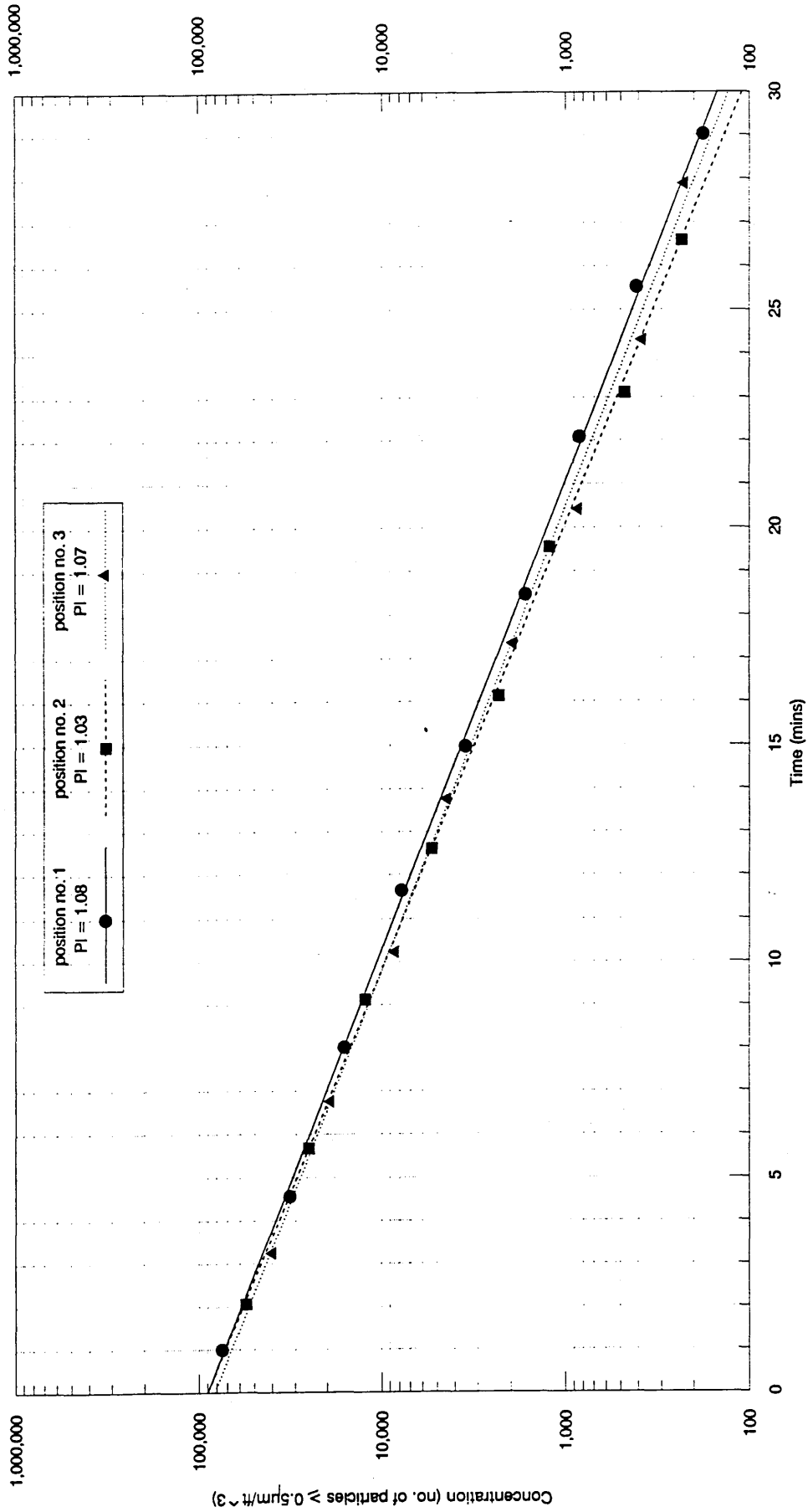


Fig. A4 Decay of airborne particle concentration
 Dump air supply
 $N = 3.59$ ac/hr, Mean $N_{eff} = 3.40$ ac/hr, $\Delta T = -0.10K$

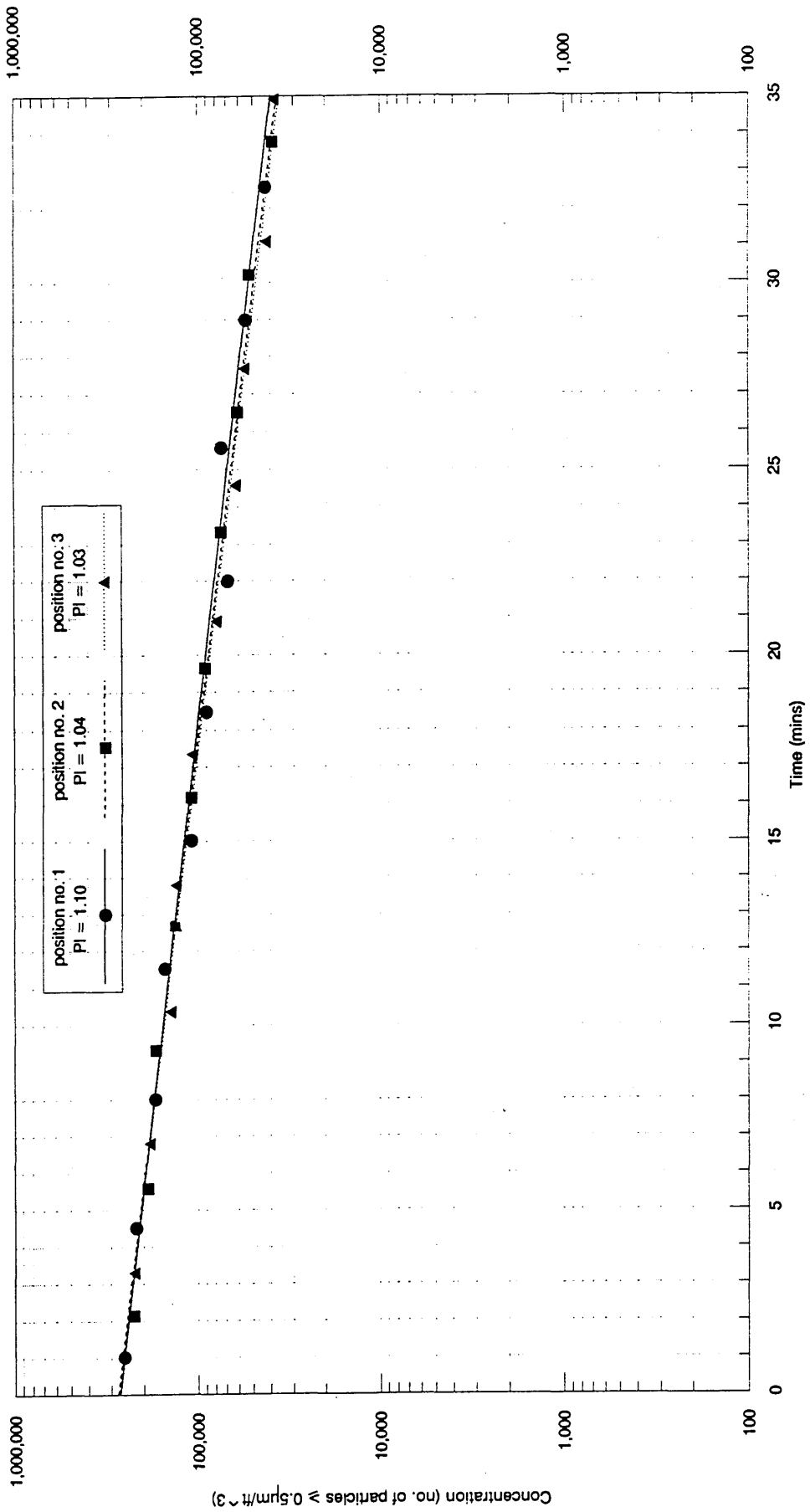


Fig. A5 Decay of airborne particle concentration
 Dump air supply
 $N = 3.59$ ac/hr, Mean $N_{eff} = 4.08$ ac/hr, $\Delta T = -0.40K$

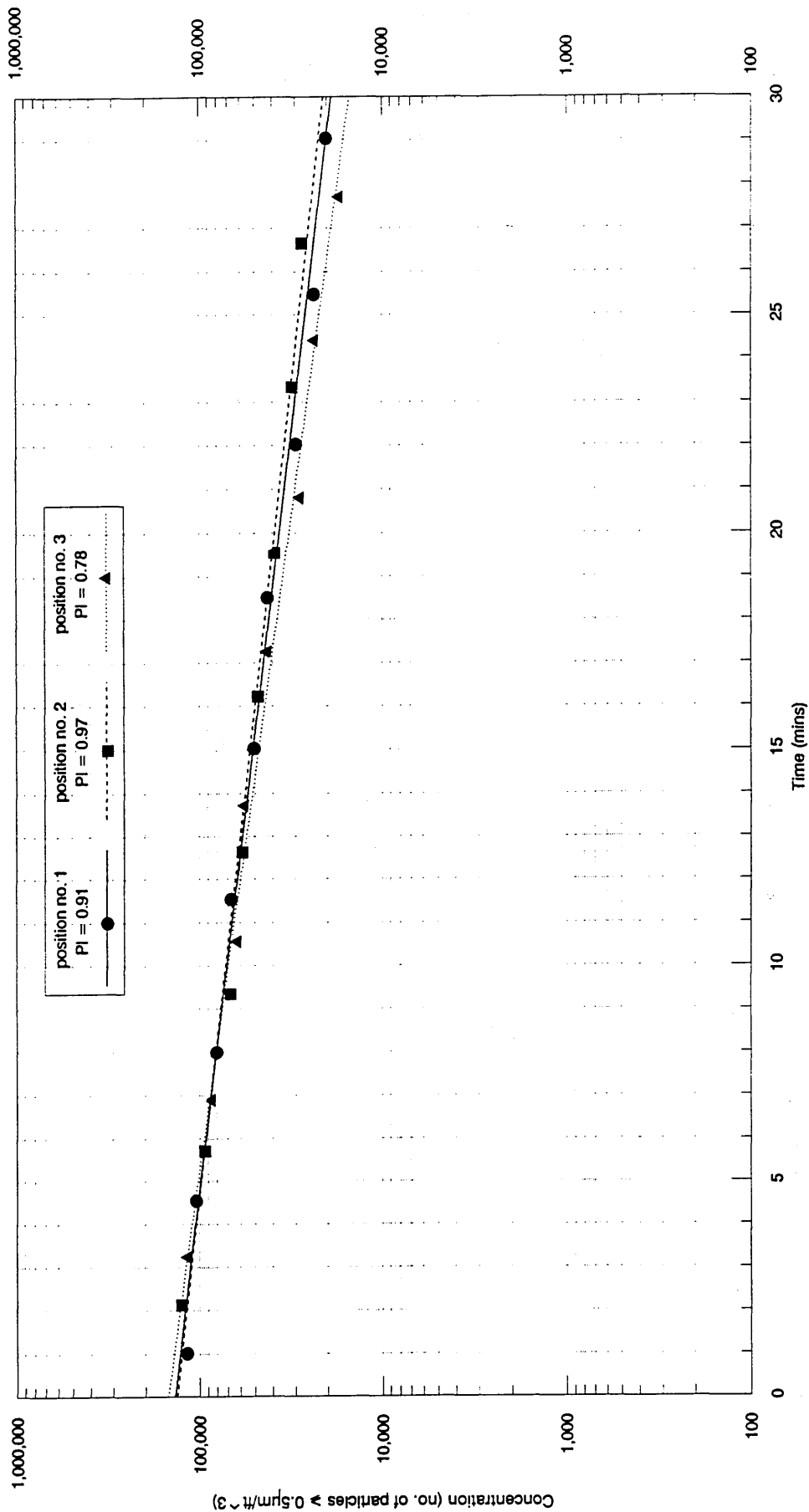


Fig. A6 Decay of airborne particle concentration
 Dump air supply
 $N=16.80$ ac/hr, Mean Neff= 21.00 ac/hr, $\Delta T=+0.15K$

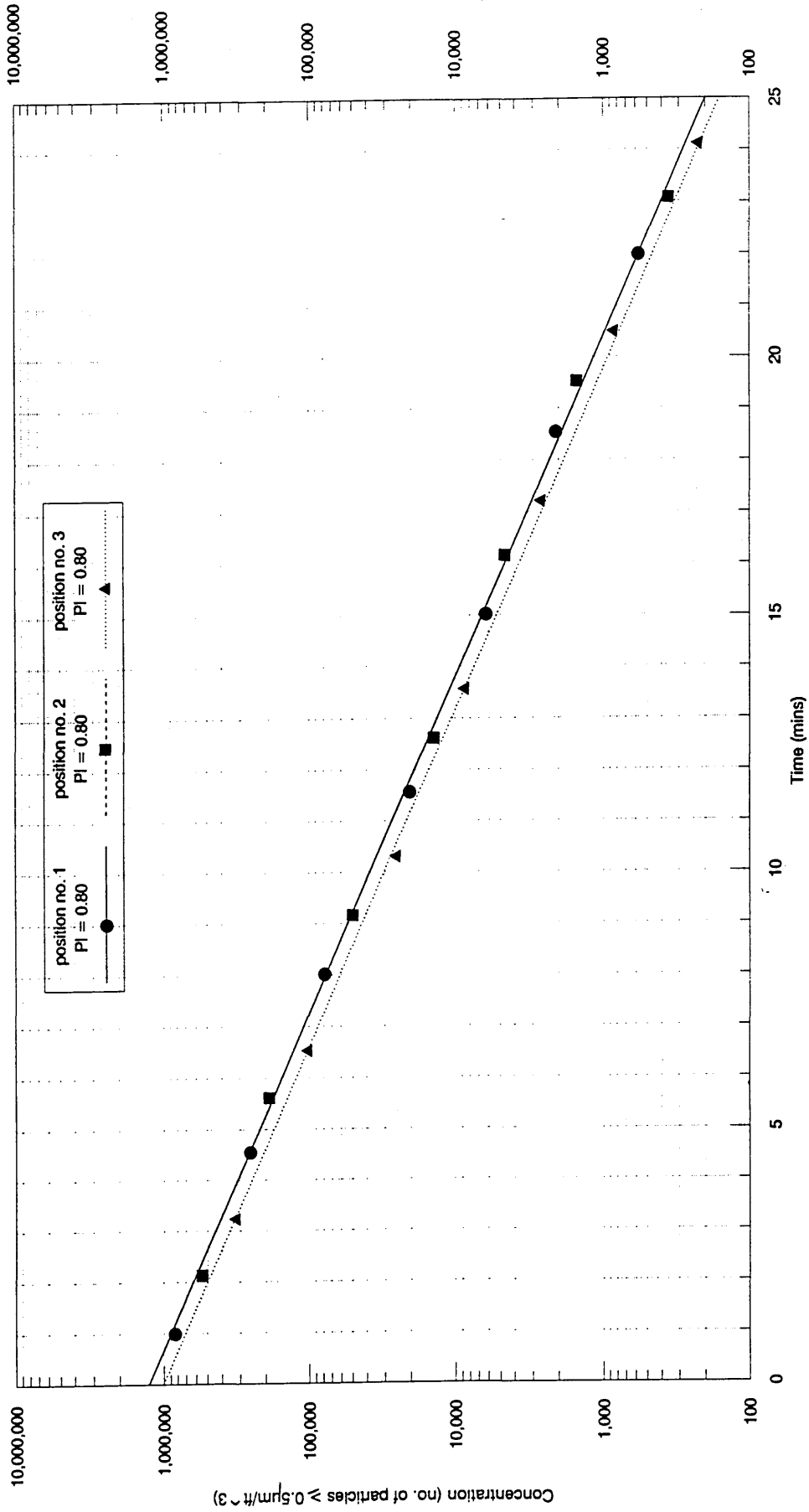


Fig. A7 Decay of airborne particle concentration
 Dump air supply
 $N=13.81$ ac/hr, Mean $N_{eff}=14.70$ ac/hr, $\Delta T=+0.11K$

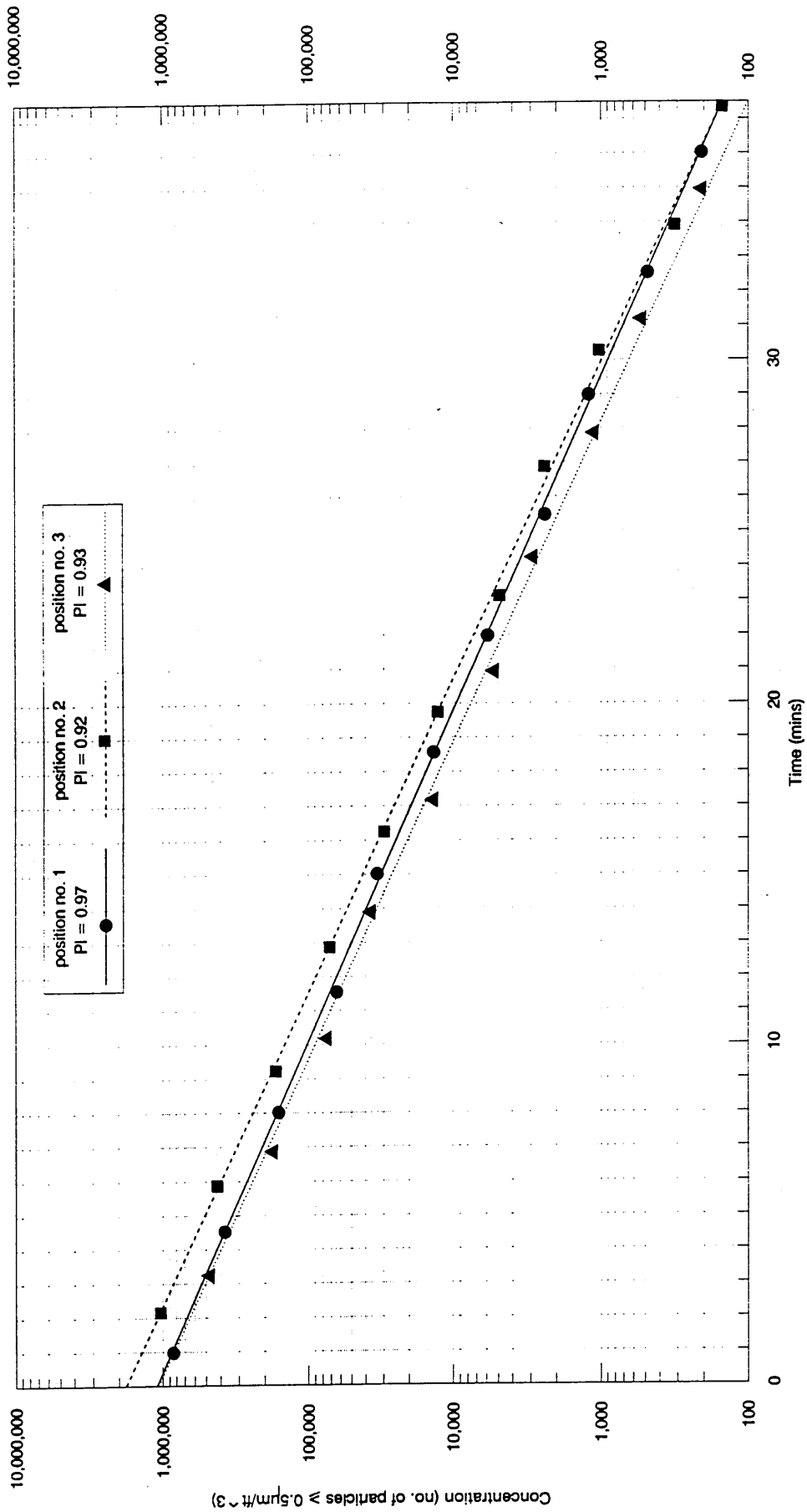


Fig. A8 Decay of airborne particle concentration
 Dump air supply
 $N=13.81$ ac/hr, Mean $N_{eff}=17.41$ ac/hr, $\Delta T=+0.04K$

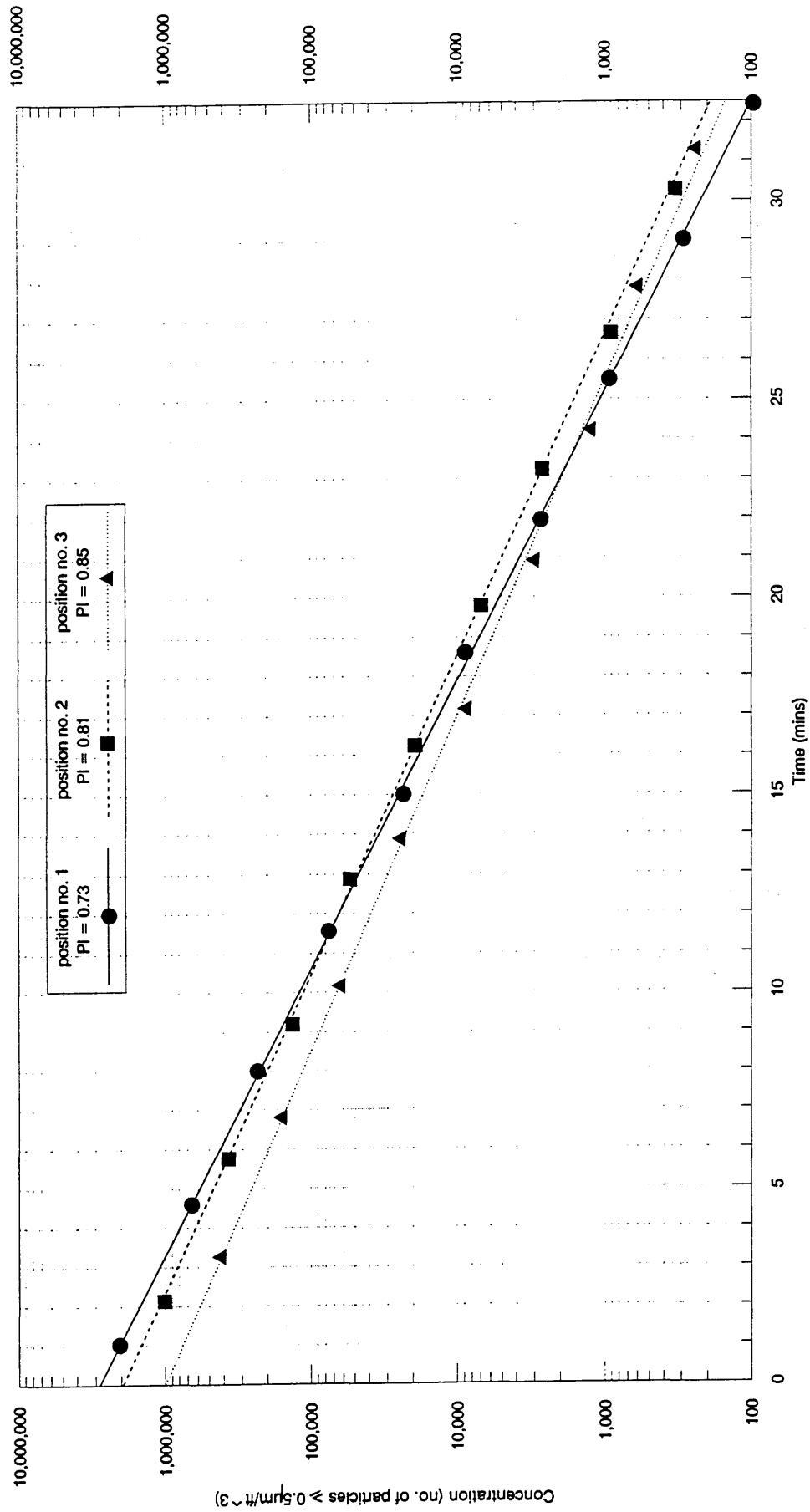


Fig. A9 Decay of airborne particle concentration
 Dump air supply
 $N=13.81$ ac/hr, Mean $N_{eff}=11.33$ ac/hr, $\Delta T=-2.28K$

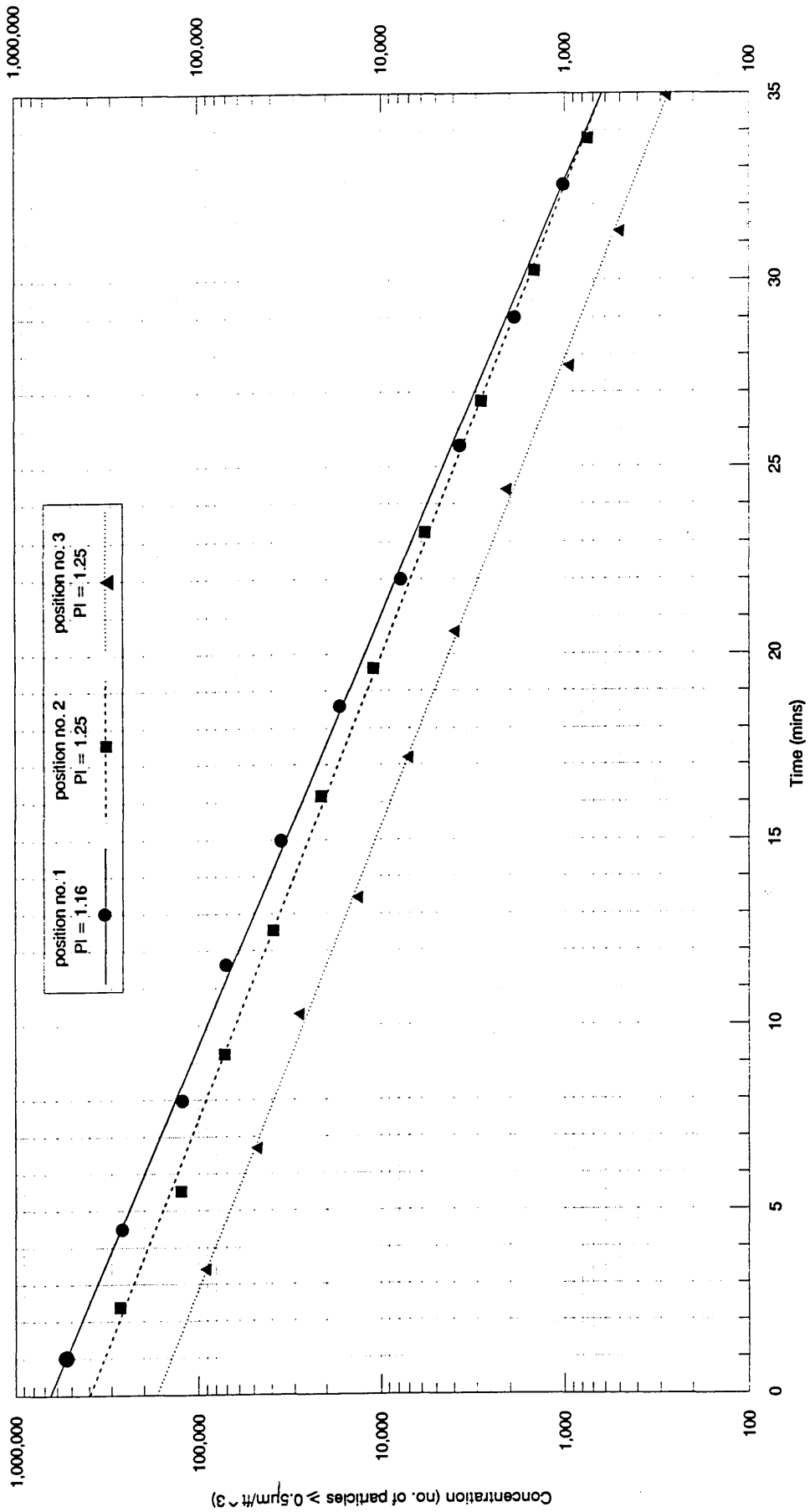


Fig.A10 Decay of airborne particle concentration
 Dump air supply
 $N=13.81$ ac/hr, Mean Neff= 13.75 ac/hr, $\Delta T=-2.23K$

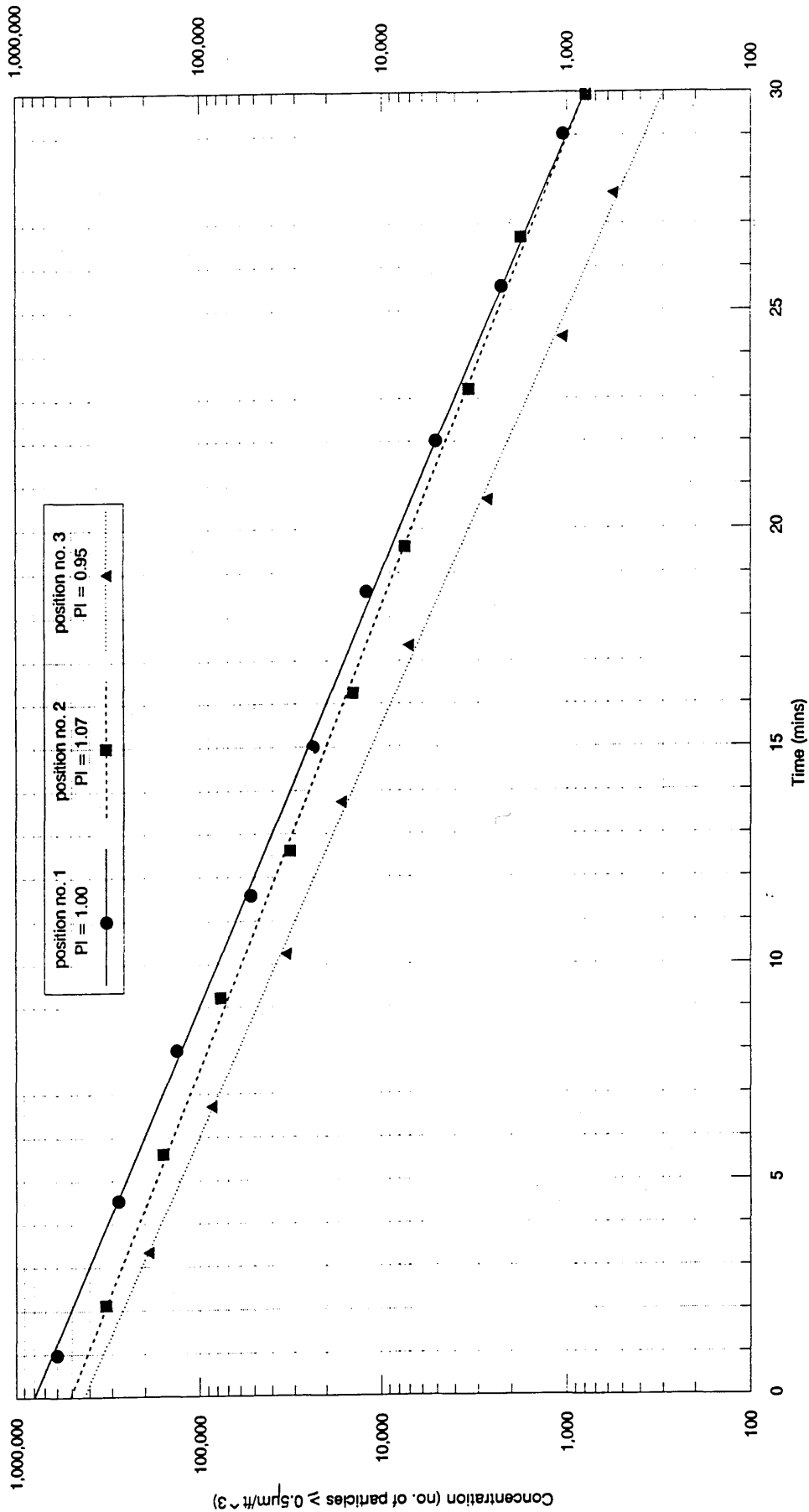


Fig.A11 Decay of airborne particle concentration
 Adjustable vane grilles
 $N = 3.30$ ac/hr, Mean $N_{eff} = 3.14$ ac/hr, $\Delta T = +0.13K$

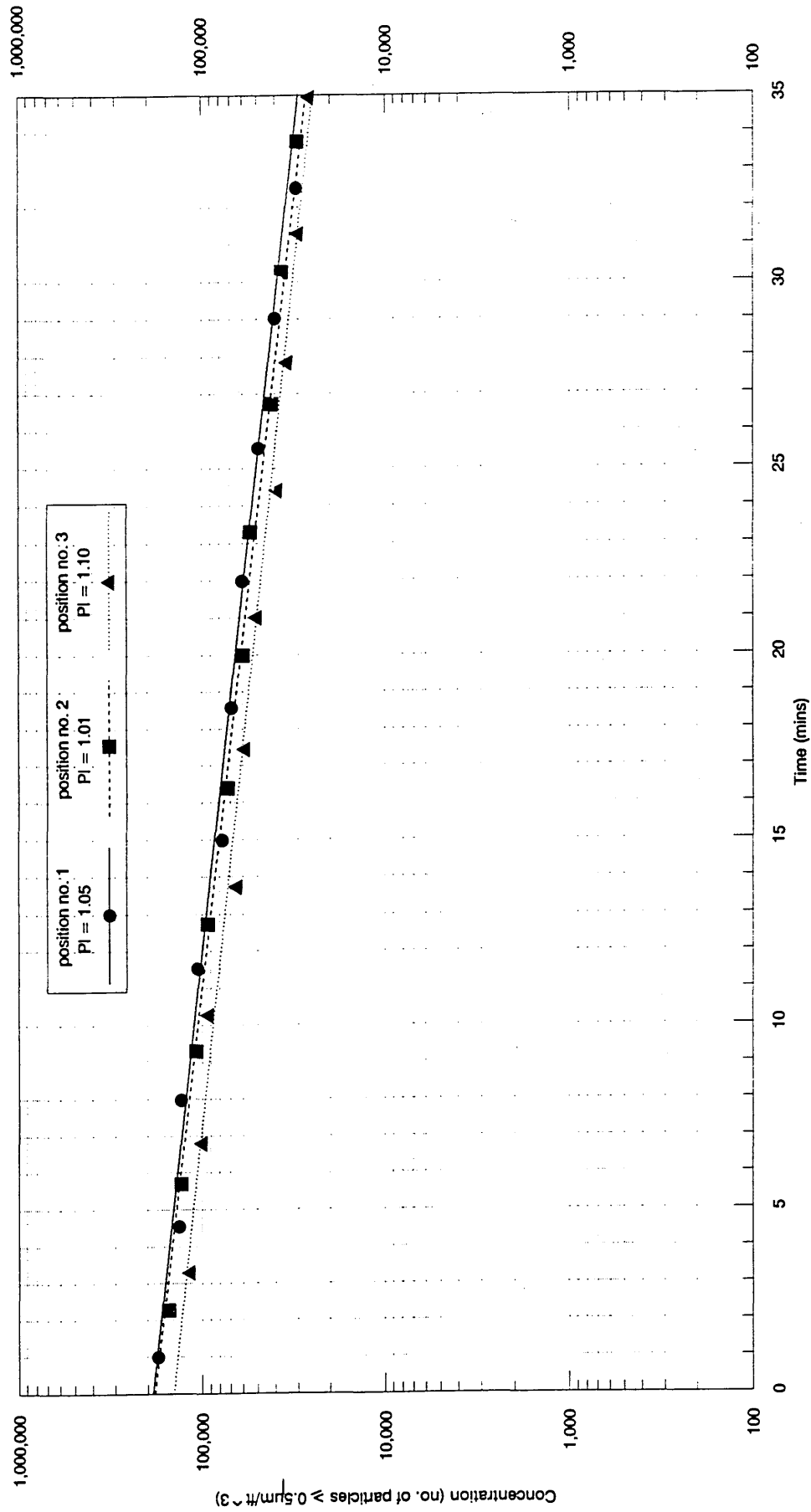


Fig.A12 Decay of airborne particle concentration
Adjustable vane grilles
N = 3.30 ac/hr, Mean Neff = 3.41 ac/hr, $\Delta T = +0.08K$

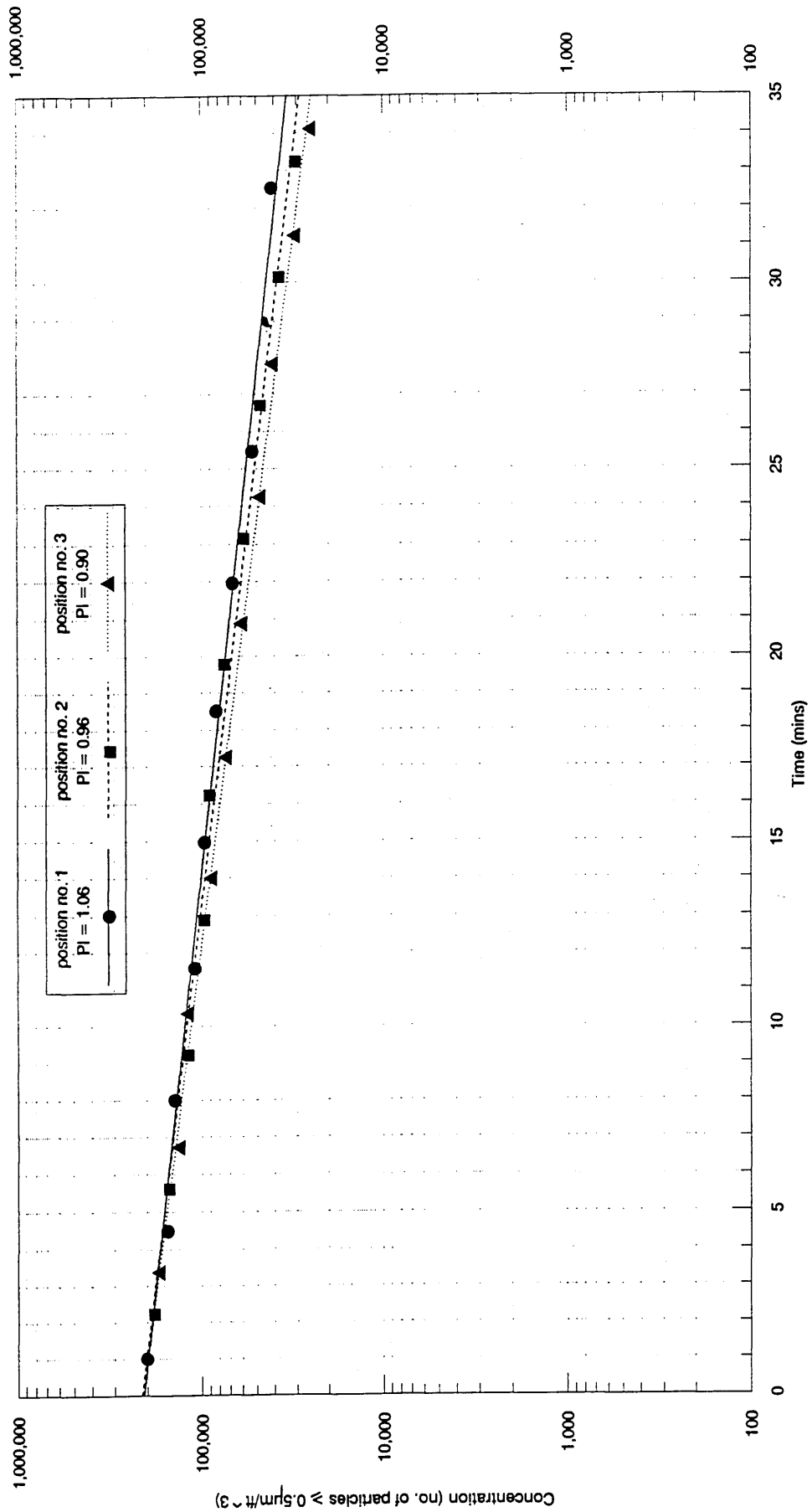


Fig.A13 Decay of airborne particle concentration
Adjustable vane grilles
N=13.81 ac/hr, Mean Neff=14.04 ac/hr, $\Delta T = 0K$

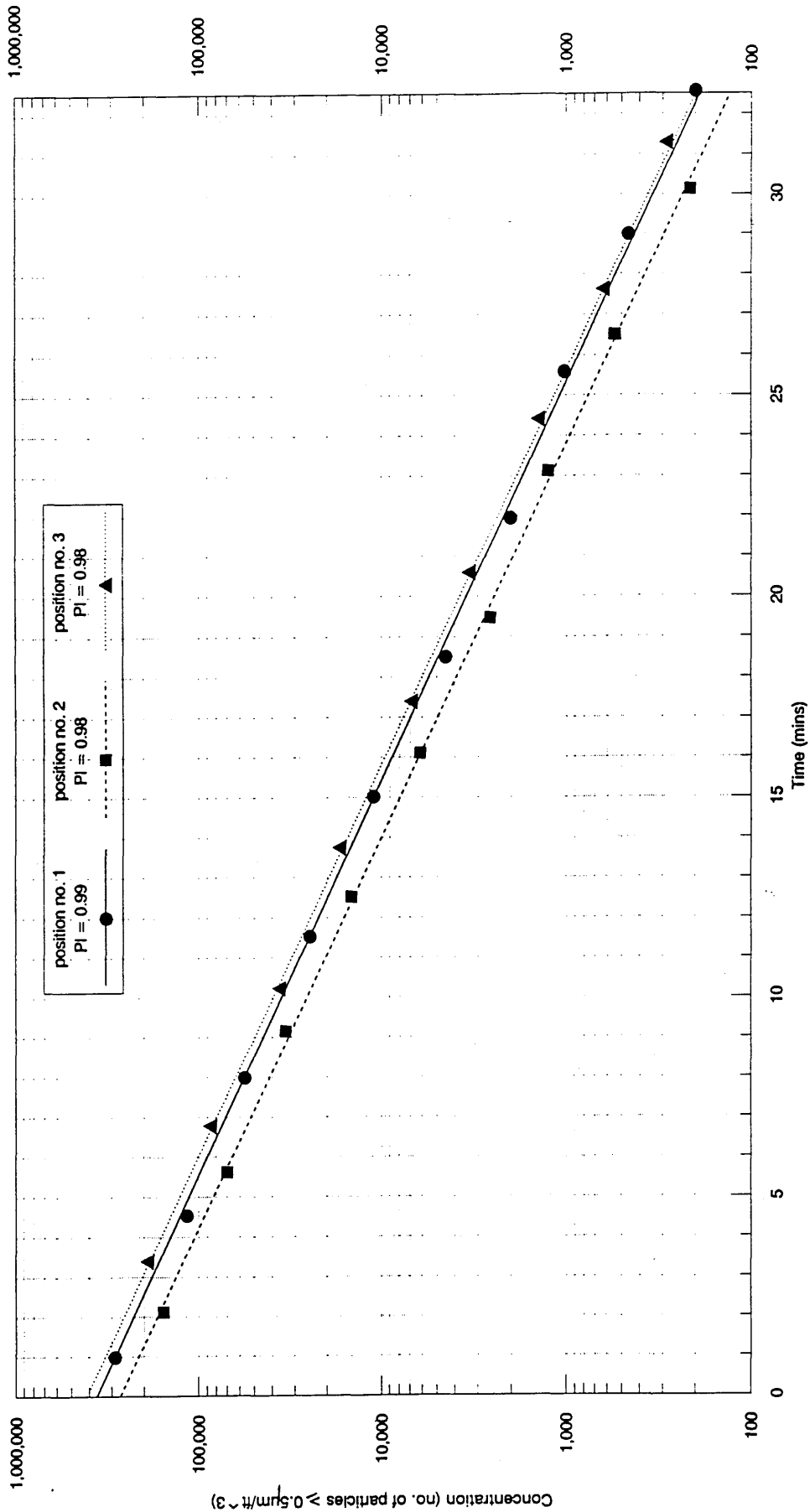


Fig.A14 Decay of airborne particle concentration
Adjustable vane grilles
N=13.81 ac/hr, Mean Neff=14.16 ac/hr, $\Delta T = +1.79K$

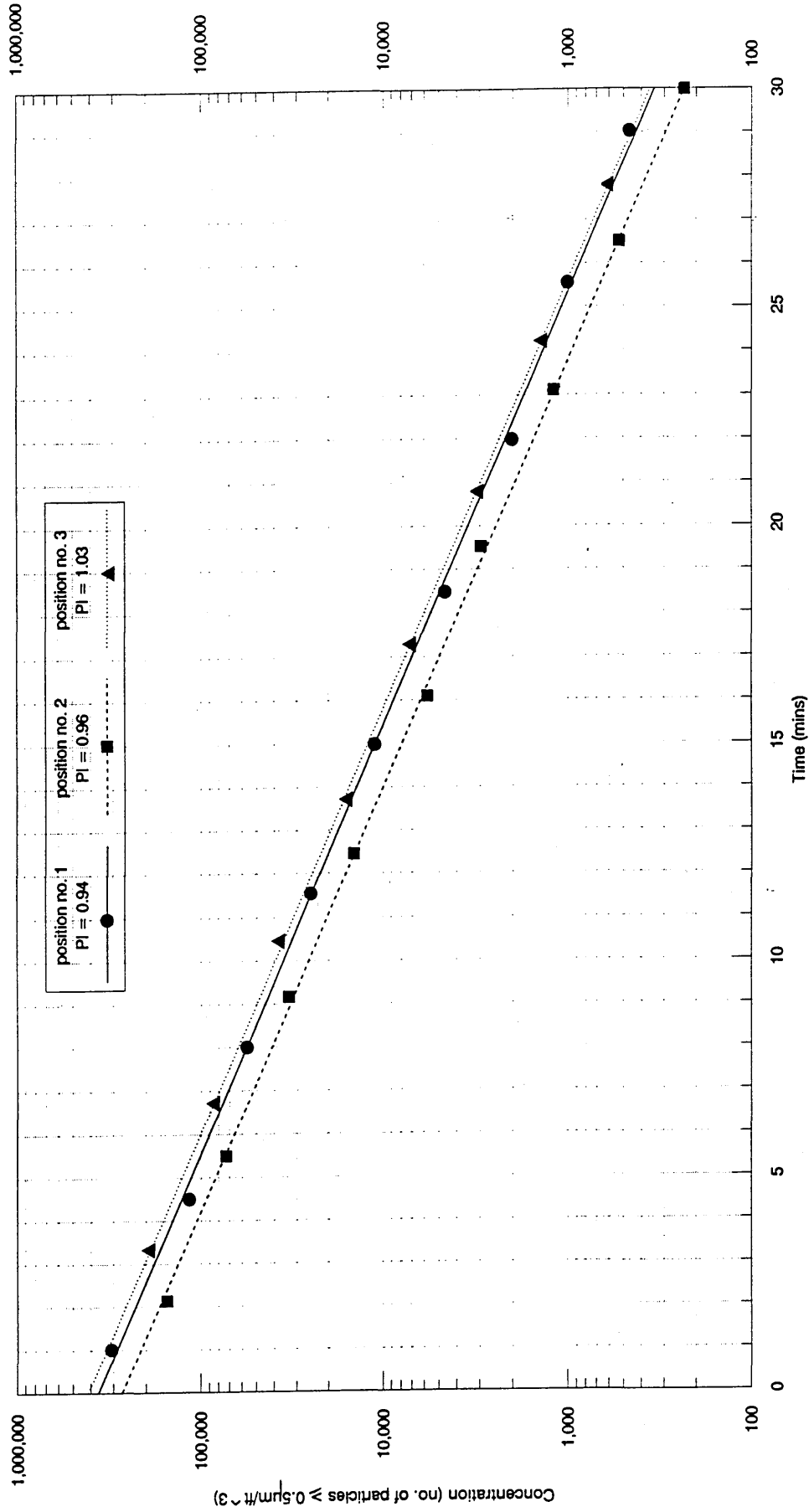


Fig.A15 Decay of airborne particle concentration
 Jet air supply
 $N=14.70$ ac/hr, Mean Neff= 15.34 ac/hr, $\Delta T = +0.15K$

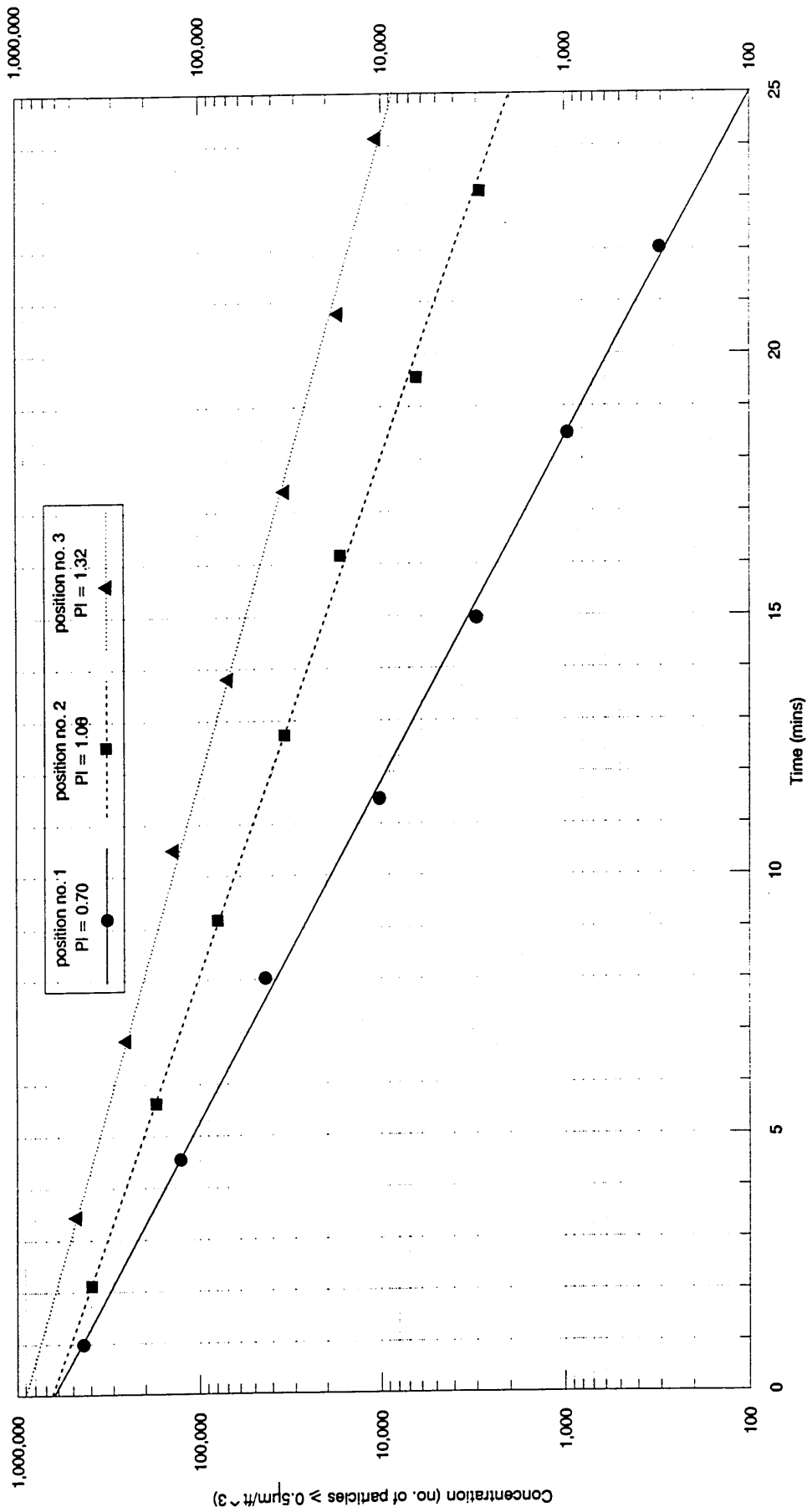


Fig.A16 Decay of airborne particle concentration
 Jet air supply
 $N = 14.70$ ac/hr, Mean $N_{eff} = 16.56$ ac/hr, $\Delta T = +0.13K$

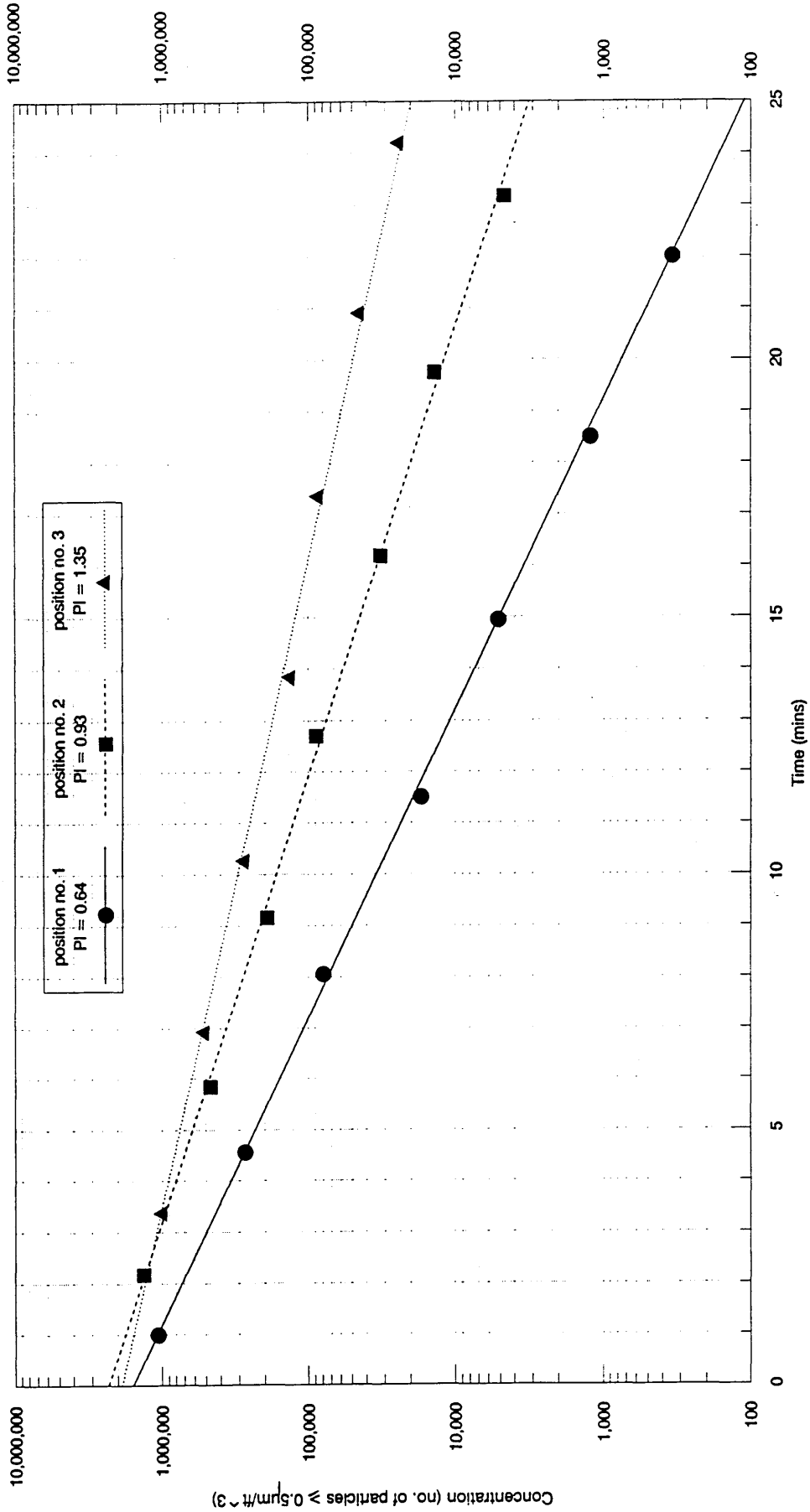


Fig.A17 Decay of airborne particle concentration
 Jet air supply
 $N=14.70$ ac/hr, Mean Neff= 16.51 ac/hr, $\Delta T = +0.17K$

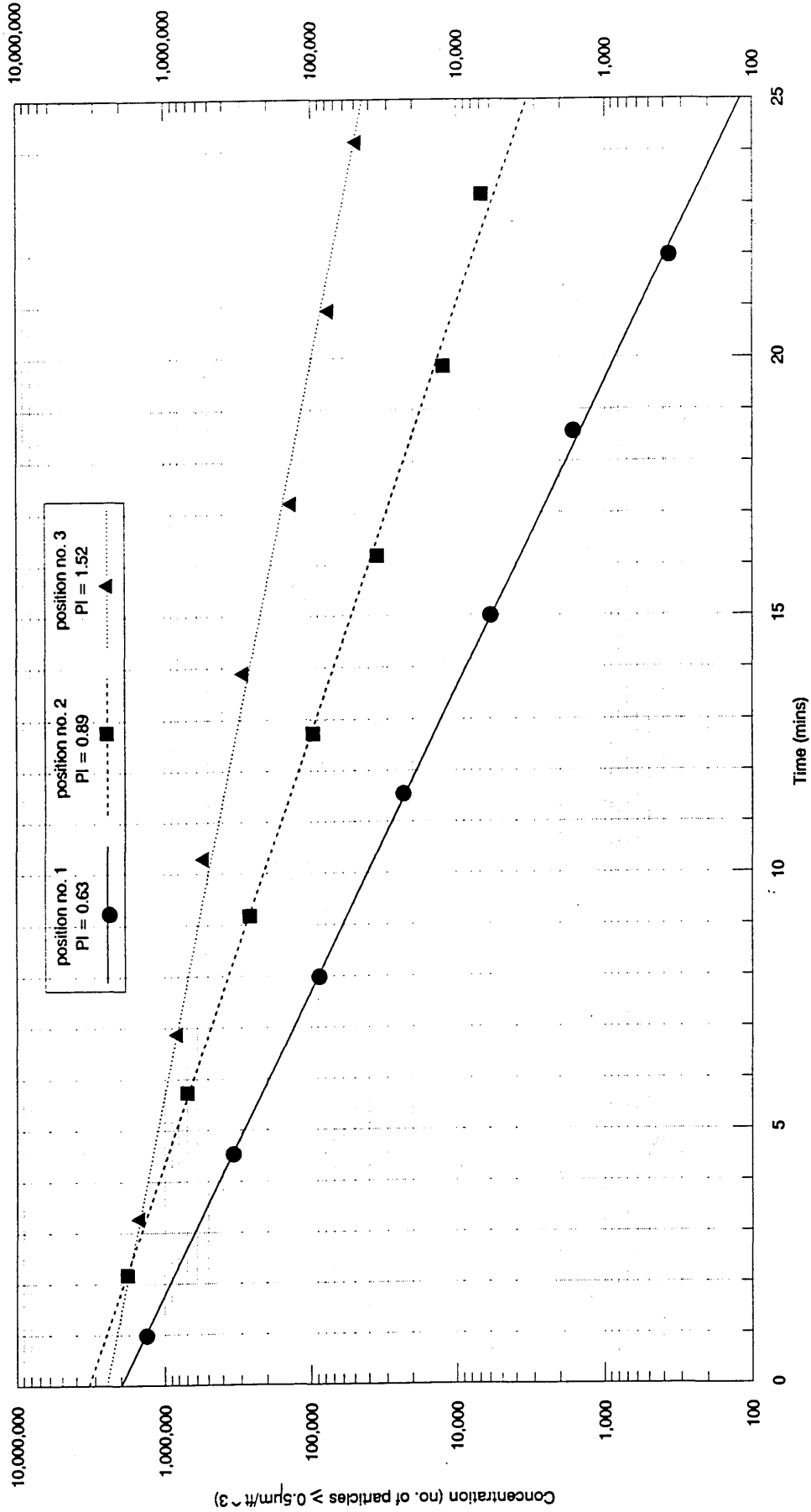


Fig.A18 Decay of airborne particle concentration
 Jet air supply
 $N=14.70$ ac/hr, Mean Neff= 16.37 ac/hr, $\Delta T = -0.06K$

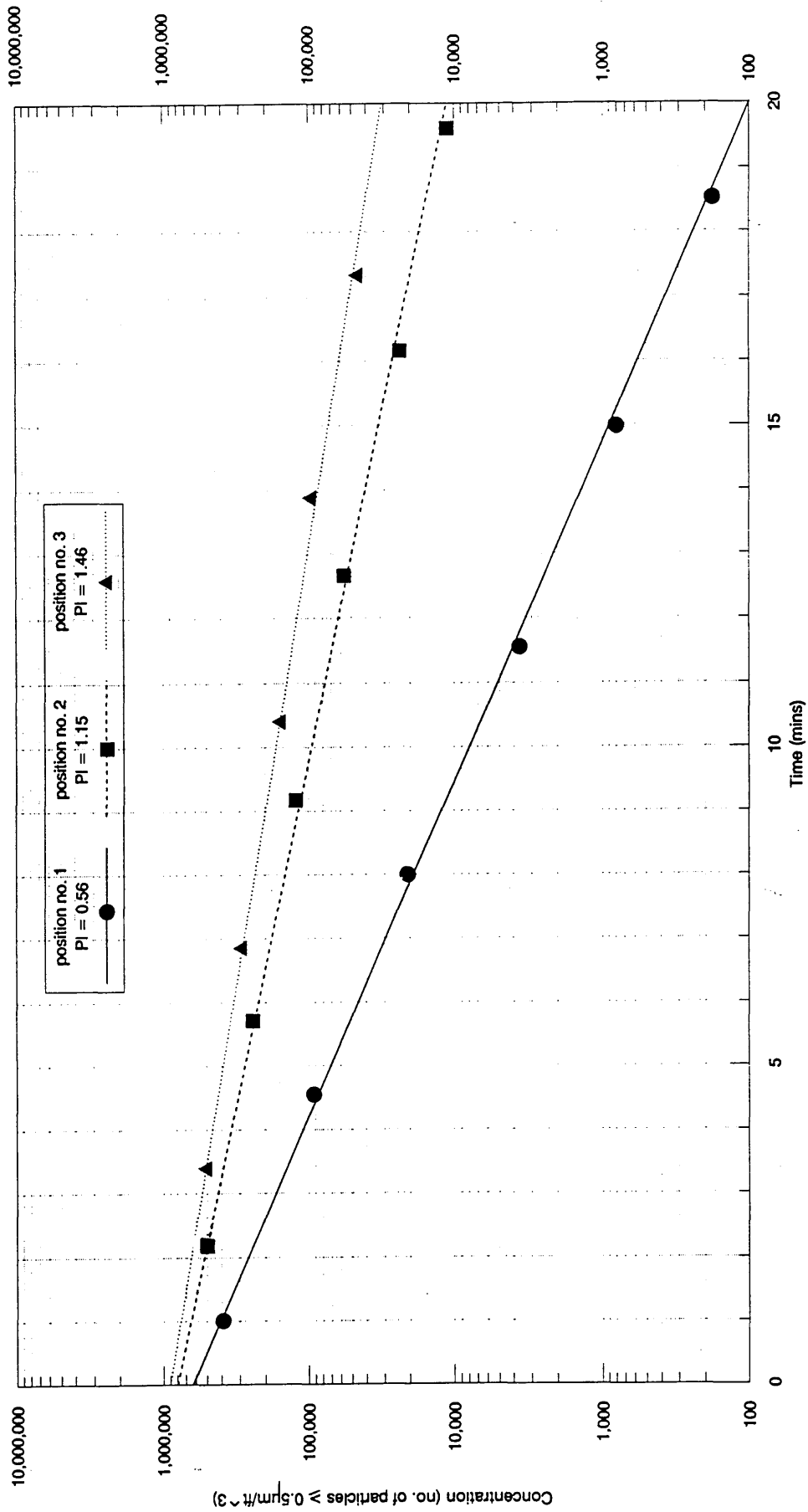


Fig.A19 Decay of airborne particle concentration
 Dump air supply
 $N=13.81$ ac/hr, Mean $N_{eff}=13.56$ ac/hr, $\Delta T = +1.96K$

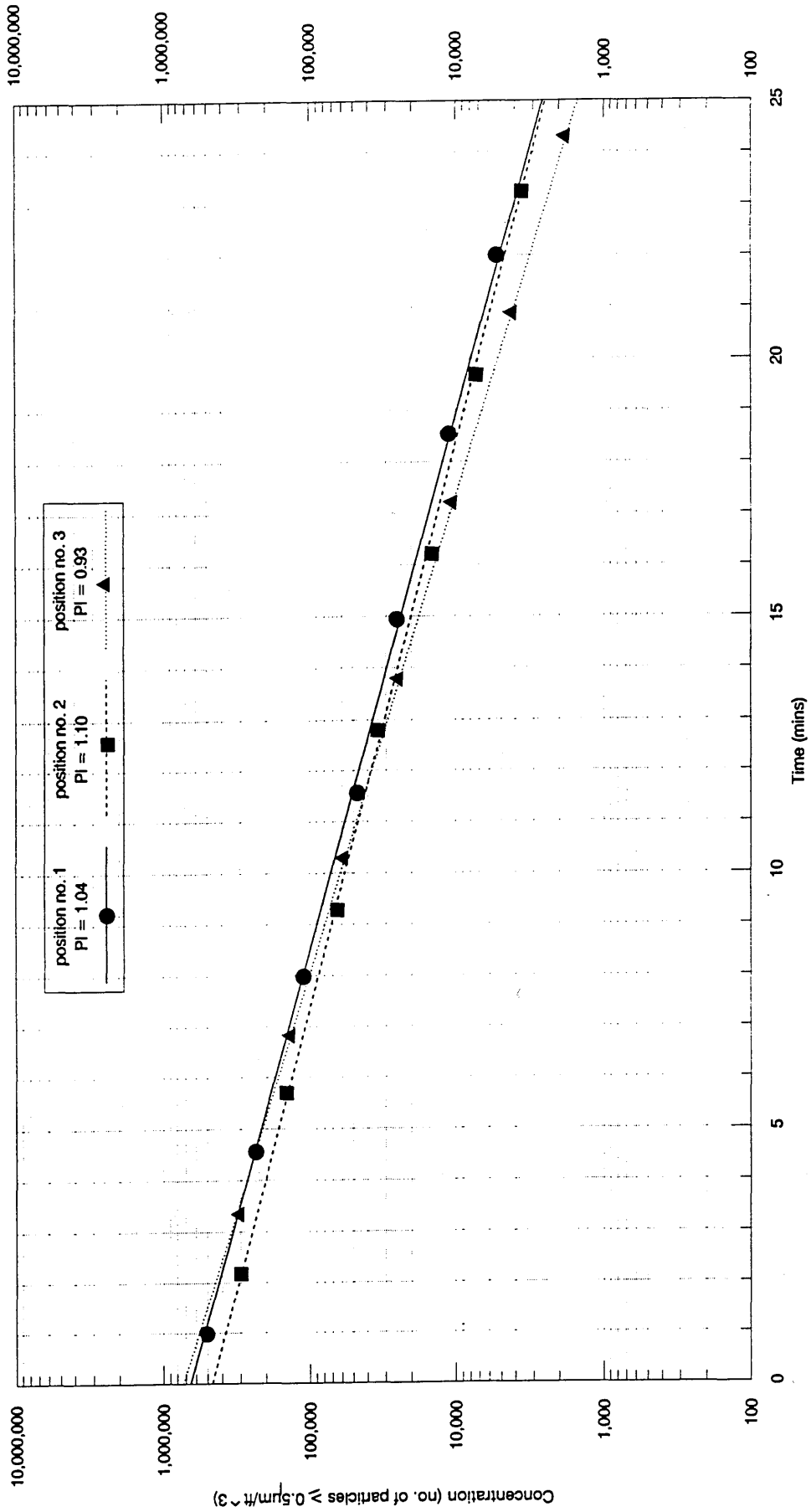


Fig.A20 Decay of airborne particle concentration
 Dump air supply
 $N=13.81$ ac/hr, Mean $N_{eff}=13.49$ ac/hr, $\Delta T = +2.00K$

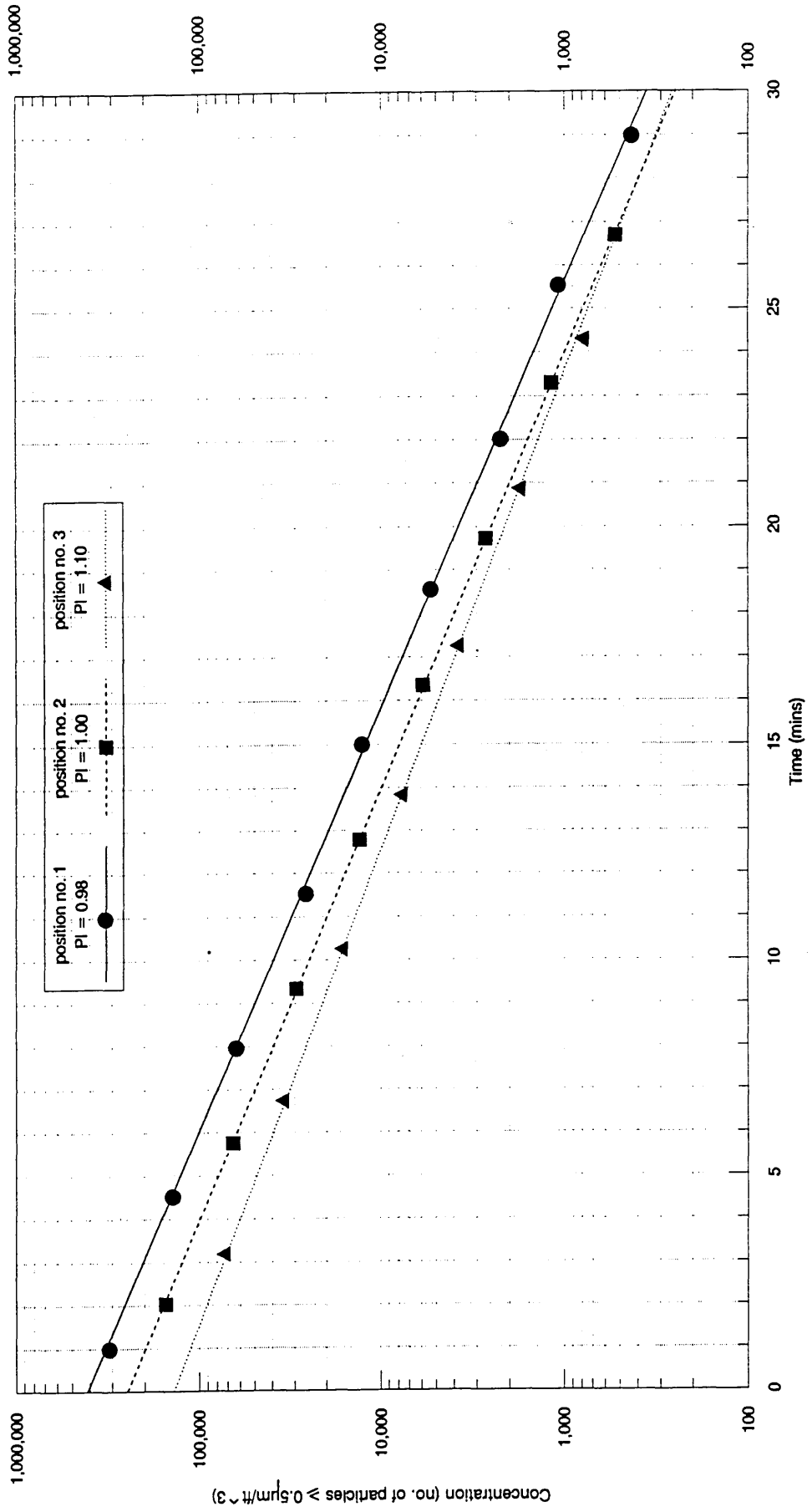
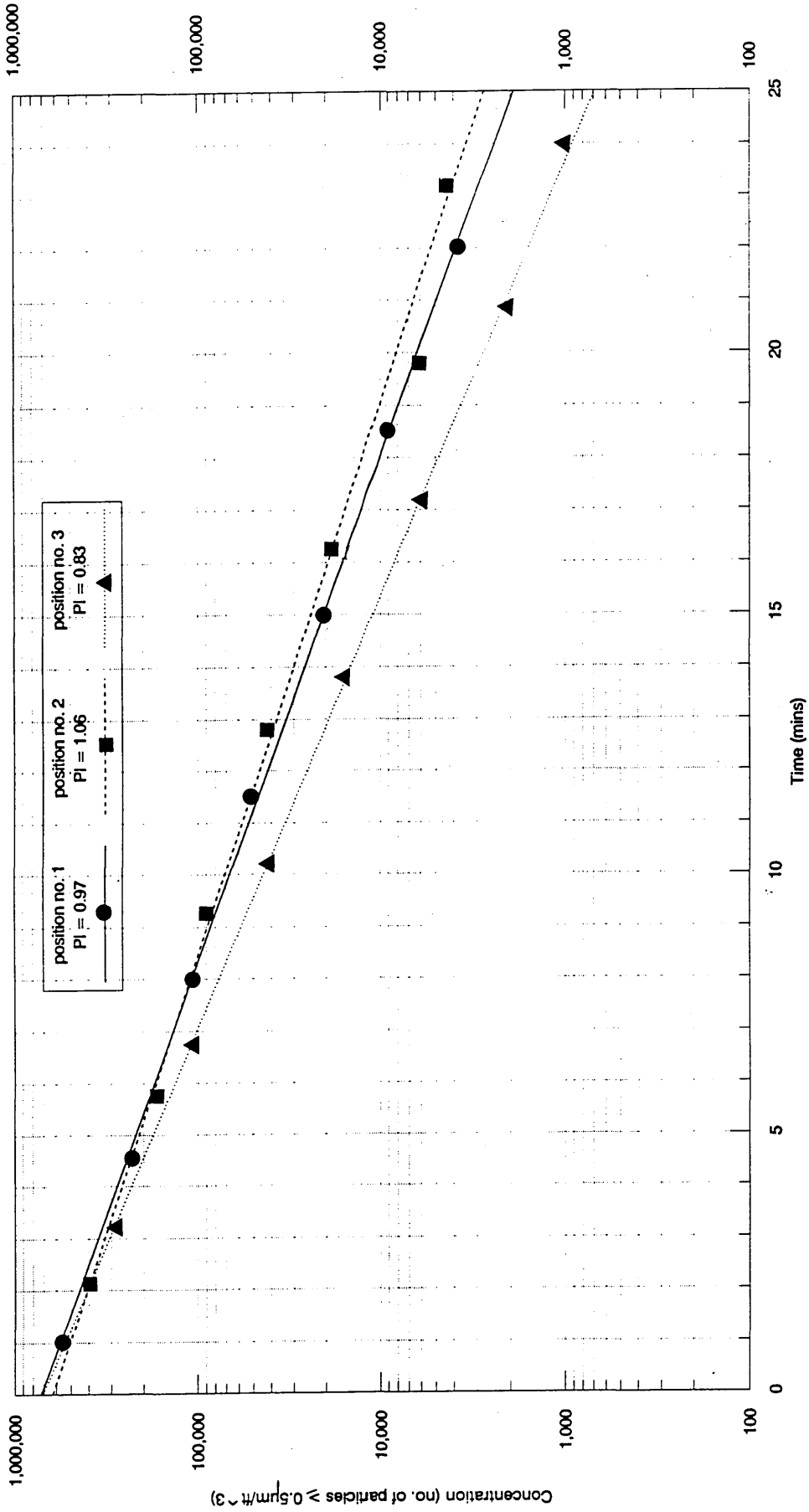


Fig.A21 Decay of airborne particle concentration
 Dump air supply
 $N=13.81$ ac/hr, Mean Neff= 14.64 ac/hr, $\Delta T = +2.10K$



APPENDIX B - Experimental errors

This appendix contains information on the accuracy of the instruments used (see Table B1). Instruments are not guaranteed to give true values of the measurement. There is an uncertainty in the readings taken because of associated errors. A knowledge of the likely error is important so that the results obtained can be properly interpreted.

Manufacturers normally specify the instrument tolerance. The magnitude of the instrument error can be checked by calibration but it can not be fully corrected because there is also an error, albeit it should be small, in the calibration procedure. The minimum instrument error is likely to be the resolution provided by the instrument scale.

When the instrument has a range of scales then there is likely to be a different tolerance for each range setting and different scale graduations. In many cases the tolerance is expressed as percentage of full scale deflection (FSD).

Table B2 is a list of the maximum instrument tolerances recommended in relevant standards. The tolerances recorded in Table B1 for the instruments used are within these limits. The measurements made and figures derived from them, such as the ventilation Performance Index (PI), will therefore be within the normal tolerances in the industry. Any experimental errors will have no significant effect on the overall results and conclusions.

Table B1 Accuracy of the instruments used.

Type of Instrument	Manufacturer/Model	Application	Range	Smallest graduation	Accuracy
Rotating vane anemometer	Airflow Developments Ltd	Air intake or discharge velocity. Grille & diffuser face velocity. Filter face velocity	0 - 30 m/s	0.1 m/s	±2%
Hot wire anemometer [†]	Airflow Developments Ltd TA400	Room air velocity	0 - 30 m/s	0.1 m/s	±2%
Copper-constantan thermocouple	Comark	Room air temperature	0 - 30°C	0.1°C	±0.1°C
Mechanical tachometer	Smith's Industries Ltd	Rotational fan speed	0 - 5000 rpm	5 rpm	±0.05% FSD*

* FSD: Full scale deflection of the maximum scale reading.

† A check calibration in a wind tunnel confirmed the validity of the manufacturer's claimed accuracy.

Table B2 Recommended maximum instrument tolerances
for site measurements.

Instrument Type	Application	Standard	Instrument tolerance
Hot wire anemometer	Room air velocity, V_a	ISO 7726:1985 Thermal environments - instruments and methods for measuring physical quantities.	$\pm(0.05+0.05V_a)$ m/s
Electrical thermometer	Room air temperature	ISO 7726:1985 Thermal environments - instruments and methods for measuring physical quantities.	$\pm 0.5^\circ\text{C}$
Rotating vane anemometer	Supply and exhaust air velocity	ISO 5219:1984 Air distribution and air diffusion - Laboratory aerodynamic testing and rating of air terminal devices.	$\pm 2.5\%$
Mechanical tachometer	Rotational fan speed	BS 848:Part 1:1980 Fans for general purposes. Methods of testing performance.	$\pm 0.25\%$